ICWST 2025

33rd International Conference on Wood Science and Technology

Zagreb, 4th - 5th December 2025

Unleashing the Potential of Wood-Based Materials

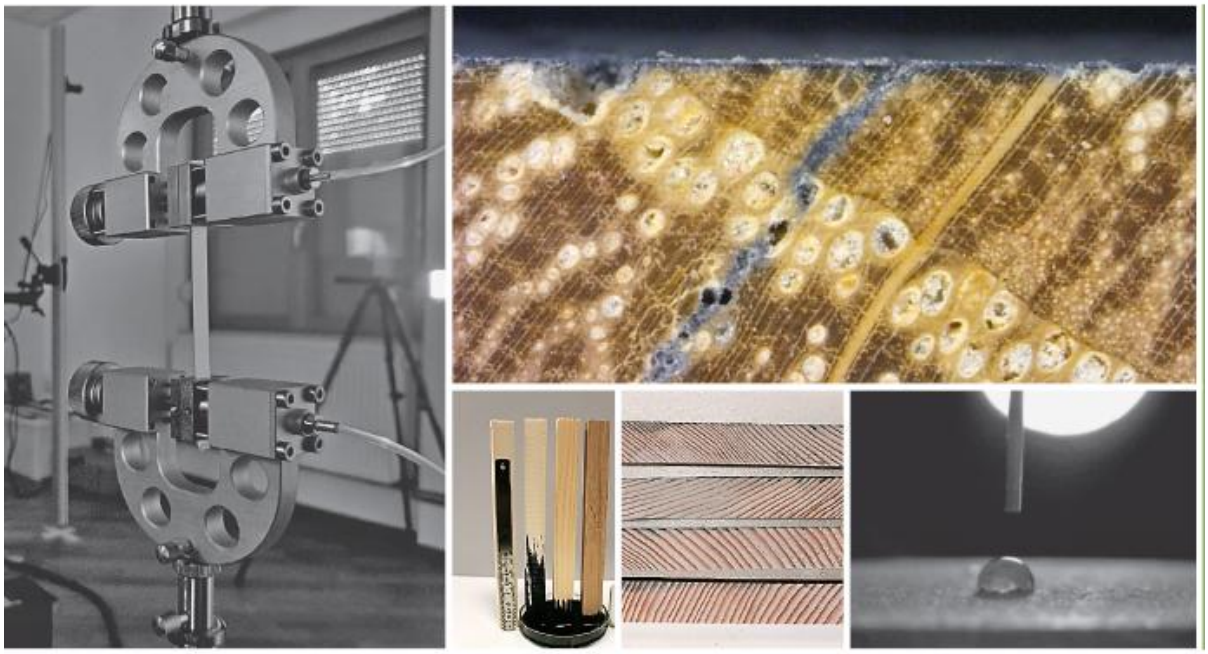

PROCEEDINGS

UNIVERSITY OF LJUBLJANA
BF Biotechnical Faculty
Department of Wood Science and Technology

Innovawood

ORGANISERS

Department of Wood Technology, Faculty of Forestry and Wood Tehnology, University of Zagreb, Croatia

Wood Science and Technology Department, Biotechnical Faculty, University of Ljubljana, Slovenia

Faculty of Forest Industry, University of Forestry, Sofia, Bulgaria

Faculty of Design and Technology of Furniture and Interior, ss. Cyril and Methodius University - Skopje, North Macedonia

InnovaWood, Bruxelles, Belgium

IN COLLABORATION WITH

Academy of Forestry, Croatia

Croatian Forestry Society

Croatian Academy of Sciences and Arts

Croatian Academy of Engineering

Croatian Chamber of Forestry and Wood Technology Engineers

The Croatian Chamber of Economy

Department of Wood Technology, Faculty of Forestry and Wood Tehnology, University of Zagreb, Croatia

Wood Science and Technology Department, Biotechnical Faculty, University of Ljubljana, Slovenia

Faculty of Forest Industry, University of Forestry, Sofia, Bulgaria

Faculty of Design and Technology of Furniture and Interior, ss. Cyril and Methodius University - Skopje, North Macedonia

InnovaWood, Bruxelles, Belgium

33rd International Conference on Wood Science and Technology (ICWST)

UNLEASHING THE POTENTIAL OF WOOD-BASED MATERIALS

PROCEEDINGS

Zagreb, 4th - 5th December 2025

Disclaimer: This proceedings compiles research presented at the 33rd International Conference on Wood Science and Technology (ICWST) ***Unleashing the potential of wood-based materials*** held in Zagreb, Croatia on 4th and 5th December 2025. The opinions expressed within are those of the authors and not necessarily represent those of the host, the editors and or any institution included in organisation of this conference.

Although all reasonable efforts were made by the organising team to ensure the scientific quality of the papers content, the final responsibility for the content therein remains with the respective authors. The editors accept no responsibility for the information contained in the proceedings. The editors are not responsible for the contents of external websites referred to in this publication.

Publisher:
Faculty of Forestry and Wood Technology, University of Zagreb, Croatia

Organizers:
Department of Wood Technology, Faculty of Forestry and Wood Tehnology, University of Zagreb, Croatia
Wood Science and Technology Department, Biotechnical Faculty, University of Ljubljana, Slovenia
Faculty of Forest Industry, University of Forestry, Sofia, Bulgaria
Faculty of Design and Technology of Furniture and Interior, ss. Cyril and Methodius University - Skopje, North Macedonia
InnovaWood, Bruxelles, Belgium

In Collaboration with:
Academy of Forestry, Croatia
Croatian Forestry Society
Croatian Academy of Sciences and Arts
Croatian Academy of Engineering
Croatian Chamber of Forestry and Wood Technology Engineers, Croatia
The Croatian Chamber of Economy

Editors:
Josip Miklečić
Nikola Španić
Miljenko Klarić

Online edition

ISBN: 978-953-292-094-9

FOREWORD

Welcome to the 33rd International Conference on Wood Science and Technology – ICWST 2025, themed "Unleashing the Potential of Wood-Based Materials." It is with great excitement that we delve into a rich tradition that has evolved over the years, connecting experts, researchers, and enthusiasts in the field of wood science and technology. Building upon the success of previous conferences, ICWST 2025 is set to be a catalyst for innovative discussions, collaborations, and breakthroughs in the everexpanding realm of wood science.

Our conference is honoured to be hosted by esteemed institutions such as the Faculty of Forestry, University of Zagreb; Biotechnical Faculty, University of Ljubljana; Faculty of Design and Technology of Furniture and Interior, ss. Cyril and Methodius University - Skopje; Faculty of Forest Industry, University of Forestry - Sofia, and InnovaWood. This collaborative effort reflects the commitment of diverse scientific communities to the advancement of wood science and its applications.

In the spirit of tradition and progress, ICWST 2025 seeks to create a multidisciplinary platform where the exchange of ideas transcends borders. We anticipate the convergence of scientists and researchers from a variety of backgrounds, fostering an environment conducive to scientific novelty, industrial applicability, and comprehensive syntheses of high-impact subjects.

As we reflect on the achievements of the past, present, and future, ICWST 2025 is proud to unveil a program that encapsulates the essence of wood science. Distinguished speakers will explore a wide range of topics. We are honoured to host renowned experts who will share their insights, contributing to the rich tapestry of wood science discourse.

This year's conference aims to go beyond the realms of wood science and technology, touching upon interconnected topics such as materials, technologies, design, and more. We aspire to raise awareness about the vital role of wood as a natural resource in the bioeconomy, advocating for its use as a green building material in the fight against climate change.

We look forward to a conference filled with intellectual exchange, collaboration, and the exploration of the untapped potential within wood-based materials. May ICWST 2025 be a stepping stone towards a future where the sustainable utilization of wood contributes to the betterment of our world.

Editors

Contents

Driftwood as a Material for Making Unique Furniture

Bego, Margarita[1*]; Martinović, Sandra[2]; Lobaš Kukavičić, Iris[1]; Šenjug, Luka[1]

[1] Department of Art and Restoration, University of Dubrovnik, Dubrovnik, Croatia
[2] Department of Wood Technology, Mechanical Engineering Faculty, University of Sarajevo, Bosnia and Herzegovina
*Corresponding author:margarita.bego@unidu.hr

ABSTRACT

This paper explores the potential of using driftwood, collected from the Dubrovnik area (Republic of Croatia), as a sustainable material for furniture design. Building on previous research into its mechanical properties: compressive strength parallel to the grain, bending strength, and modulus of elasticity, this study highlights the reduced processing quality of driftwood due to prolonged exposure to external influences. Within the framework of the "Days of Cultural and Creative Industries" 2024, a unique coffee table was designed and produced at the Department of Art and Restoration, University of Dubrovnik. Special attention was given to aesthetic qualities, particularly the characteristic color changes of driftwood, which were enhanced through surface treatment. The project demonstrates how recycled wood can be carefully selected and applied in modular furniture design, contributing both to sustainable practices and innovative artistic expression.

Key words: driftwood, sustainable materials, furniture design, modular furniture

1. INTRODUCTION

Driftwood, a wood shaped and naturally modified by the long-term action of the sea, represents a valuable example of natural recycling of materials.

Exposed to the time and the influence of the sea, the wood undergoes physical and aesthetic methamorphosis. Through processing and the combination of different fragments, a new object emerges, one that simultaneously tells a story of decay and renewal.

The aim of this research was to explore the potential use of driftwood, collected along the Dubrovnik coastline, in contemporary and sustainable furniture design. Using driftwood and discared wooden pices, a table was created that merges natural irregularity of the material with a clear, contemporary form.

2. MATERIALS AND METHODS

The work process began with collecting driftwood along the seashore, followed by cutting, joining, sanding and coloring of the elements according to the table sketch, that was conducted at the Department of Art and Restoration, University of Dubrovnik.

Mechanical properties of collected driftwood samples were tested at the Department of Wood Technology, University of Sarajevo, Mechanical Engineering Faculty, Bosnia and Herzegovina. The compressive strength parallel to the grain, the bending strength, and modulus of elasticity of driftwood were determined according to ISO 13061-17 (2017), ISO 13061-3

(2014), and ISO 13061-4 (2017), respectively. The testing was performed on universal testing machine Zwick 1282.

An assessment of the wood´s workability and surface quality was carried out after prolonged exposure to environmental factors and the experimental design and production of the coffee table prototype were realized within the framework of the project ″Days of Cultural and Creative Industries 2024.″

3. RESULTS AND DISCUSSION

A unique coffee table, an artistically designed piece, made from marine driftwood, was created, demonstrating the entire process of making. The physical and mechanical properties of the driftwood were tested beforehand, in order to confirm its suitability for use in sustainable furniture design.

Based on the macrostructure and microstructure analysis of the driftwood cross-section, the wood type was identified as poplar wood (Populus spp.) The test samples for compressive strength testing were divided into clear wood specimens and specimens of wood with defects. The results of compressive strength of driftwood samples are given in Table 1. The results showed that the compressive strength parallel to the grain of clear wood specimens is 39.1 % higher than the same strength of wood with defects. The obtained experimental results of compressive strength parallel to the grain of clear wood specimens agree with the literature data of 38 MPa for poplar wood (Forest Products Laboratory, 2021).

Table 1. Compressive strength of clear wood specimens and specimens with wood defects (Laboratory conditions: T=20 °C, RH=65 %)

Compressive strength, MPa	Clear wood specimens of poplar (W=13.41 %)	Specimens of poplar with wood defects (W=13.77 %)
Mean	41.86	30.08
Stan. dev.	1.70	8.64
Range	4.51	20.95

The test samples for the bending strength and the modulus of elasticity testing were not divided into clear wood and defective wood specimens. The results of the bending strength and the modulus of elasticity of the driftwood samples are given in Table 2. The test results showed that the mean value of bending strength is 45.10 MPa, and it is lower than the literature value of bending strength of 70 MPa (Forest Products Laboratory, 2021). The mean value of modulus of elasticity is 6.07 GPa, and it is lower than the literature value of 10.90 GPa (Forest Products Laboratory, 2021), but the maximal value of modulus of elasticity of 10.47 GPa agree with the literature data of modulus of elasticity for poplar wood.

Figure 1. shows the curves of force-displacement diagrams of the bending strength of the tested driftwood specimens. The high standard deviation and the range of the bending strength and modulus of elasticity indicate the significant effect of wood defects on the analysed mechanical properties of driftwood (Bego *et al*., 2023).

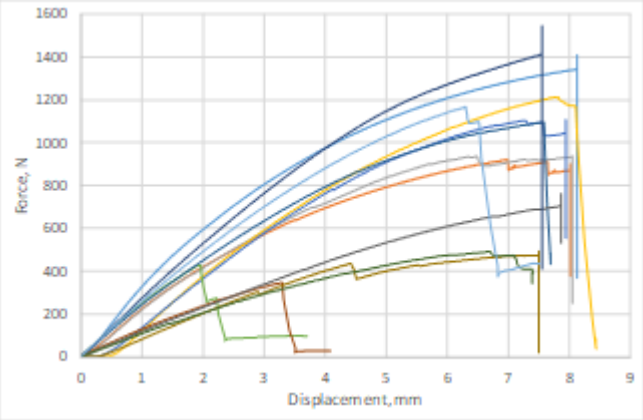

Figure 1. Testing of bending strength: force-displacement curves

Table 2. Bending strength and modulus of elasticity of the driftwood samples (Laboratory conditions: T=20 °C, RH=65 %)

Wood specimens of poplar	Bending strength, MPa	E modulus, GPa
Mean	45.10	6.07
Stan. dev.	18.53	2.50
Range	57.73	8.22

Based on the analysis of mechanical properties of driftwood samples it can be concluded that properties of driftwood vary and are dependent on wood defects, as a result of exposure to external influences.

Figure 2. Driftwood from the sea (left), joining of driftwood elements (right)

The results show that clear poplar driftwood can be used for wooden constructions of wooden furniture. Therefore, with a careful selection of wood, it is possible to create objects of functional quality. Figure 2. shows selected driftwood material collected from the seashore that can be used for furniture making. Figure 3. shows the assembly of driftwood elements in the process of creating a unique coffee table.

Figure 3. Driftwood elements that can be modeled differently and change shape

The surface treatment further emphasized the natural variations in a color and texture of the wood. Through the combination of recycled materials and contemporary design, a modular and aesthetically valuable piece of furniture was created (Figure 4).

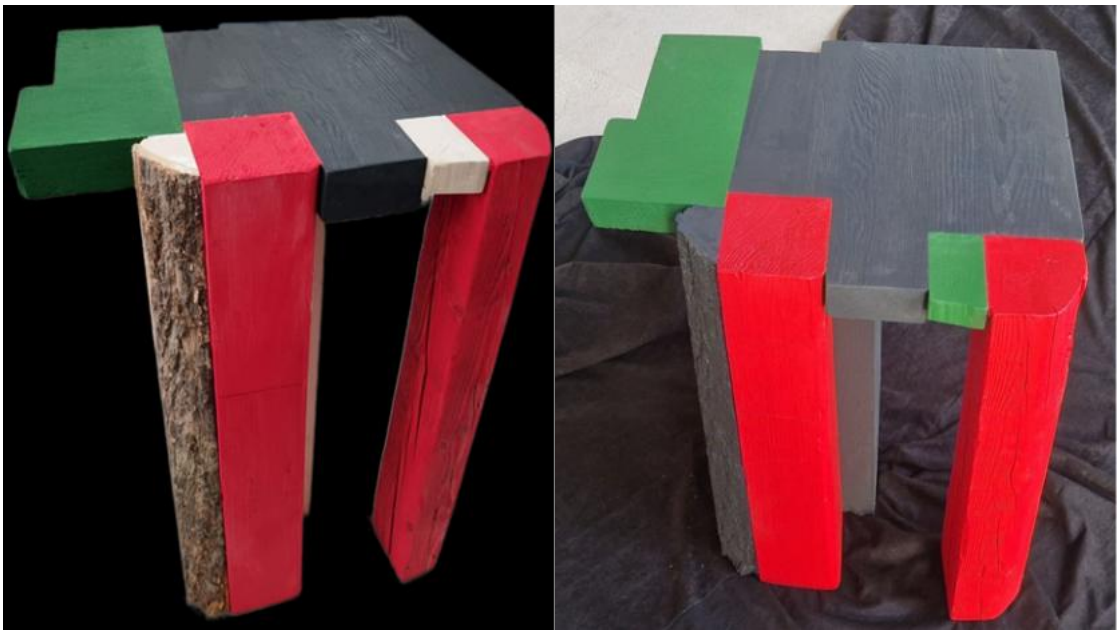

Figure 4. Caffee table after painting (left), and as an exibition artifact (right)

4. CONCLUSIONS

The paper demonstrates how driftwood can be successfully utilized in furniture design. Mechanical properties testing showed strong effect of wood defects on mechanical properties of driftwood. Therefore, in order to be used in furniture design, collected driftwood material firstly needs to be scanned and sorted, based on the quality, before deciding which pieces can be used for furniture design. Only high-value driftwood pieces can be used for furniture making.

By using driftwood waste in coffee table design, eco-friendly product was created, which promotes sustainable practices, while simultaneously fostering artistic expression within the context of contemporary culture and ecology.

5. REFERENCES:

Bego, M.; Lobaš Kukavičić, I.; Martinović, S.; Hajdarević, S.; Obučina, M., 2023: Basic Physical and Mechanical Properties of Driftwood Used for Art Installations. In: Proceeding of the 32nd International Conference on Wood Science and Technology (ICWST), Zagreb: Faculty of Forestry and Wood Technology, pp. 27-34.

***Forest Products Laboratory, 2021: Wood handbook wood as an engineering material. General Technical Report FPL-GTR-282. Madison, WI: U.S. Department of Agriculture, Forest Service, Forest Products Laboratory. p. 543.

***ISO 13061-17, 2017: Physical and mechanical properties of wood - Test methods for small clear wood specimens. Part 17: Determination of ultimate stress in compression parallel to grain.

***ISO 13061-3, 2014: Physical and mechanical properties of wood - Test methods for small clear wood specimens. Part 2: Determination of ultimate strength in static bending.

***ISO 13061-4, 2017: Physical and mechanical properties of wood - Test methods for small clear wood specimens. Part 2: Determination of modulus elasticity in static bending.

Conservation and Restoration of the Writing Desk of August Šenoa

Bego, Margarita[1]; Čavara, Pero[2]

[1] Department of Art and Restoration, University of Dubrovnik, Dubrovnik, Croatia
[2] Škola drvne tehnologije i šumarstva, Zagreb, Croatia
*Corresponding author: margarita.bego@unidu.hr

ABSTRACT

This paper presents the conservation and restoration of the writing desk of August Šenoa, dating from around 1870, crafted by an unknown master and preserved in a private collection. Structural instability was detected during the condition assessment, requiring the dismantling of critical parts. Surface cleaning was followed by the reconstruction of missing wooden elements using the same wood species, identified by comparison with a veneer atlas. Damaged veneer was replaced with matching material, while the final surface treatment consisted of shellac polish, restoring both protective and aesthetic values. The intervention successfully halted deterioration and ensured the valorization of the object for future public presentation within the Šenoa family collection. This case study illustrates the importance of conservation in safeguarding cultural heritage and emphasizes the role of responsible material use in line with circular economy principles.

Key words: conservation, restoration, furniture, August Šenoa, cultural heritage, circular economy

1. INTRODUCTION

The preservation of cultural heritage ensures the promotion and contribution to sustainable development through heritage as a component of quality of life (Grazulevičiüte,2006). Sustainable management of cultural heritage implies a balance between the preservation of authenticity and adaptation to the contemporary needs of society, whereby cultural objects are not treated merely as material remnants of the past but as active bearers of cultural identity and collective memory (Lowenthal, 1998).For this reason, conservation-restoration practice occupies a key position in ensuring the continuity of cultural value through physical stabilization, aesthetic renewal, long-term protection, documentation and interpretation of objects within their original context.

The conservation-restoration process is viewed as a scientifically based procedure that integrates historical research, technological material analysis, and practical skills of treatment and reconstruction (Halbertsma, 1999). According to Matero (2000), the contemporary conservator – restorer operates at the intersection of science, art and ethics, where every intervention decision must be professionally justified, documented and aligned with international principles.

The importance of adhering to the principles of minimal intervention, reversibility and distinguishability of new additions – as defined by international documents such as the Venice Charter (ICOMOS, 1964. And E.C.C.O. Code of Ethics (2003) – forms the foundation of modern restoration practice. Such an approach enables the preservation not only of the physical integrity of the object but also of its intangible values – cultural identity, historical continuity and symbolic meaning (Clavir, 2008).

In this context, conservation – restoration interventions are not viewed solely as technical processes of material renewal but also as a contribution to the preservation of cultural memory and the interpretation of historical layers that testify to the social, aesthetic and personal dimensions of the past.

The subject of this paper is the conservation – restoration of the writing desk of August Šenoa, one of the most prominent Croatian writers of the 19 Century.

The desk made around 1870 by an unknown craftsman, is part of private family collection and represents a valuable example of historicist furniture from that period. Is restoration preserves not only a material object but also a symbol of the cultural heritage of Croatian literature – a testimony to the time and environment in which Šenoa created.

2. MATERIALS AND METHODS

The restoration of August Šenoa´s writing desk required an interdisciplinary approach combining art – historical research, material analysis, application of conservation technologies and an understanding of aesthetic and ethical principles of the profession. The procedures were based on the principles of minimal intervention, reversibility and distinguishability of new additions (E.C.C.O., 2003; ICOMOS, 1964), with continuous documentation of all work phases. The entire process included research, damage diagnostics, material testing, selection of appropriate cleaning and consolidation methods, and final protection and presentation of the object.

The result of the intervention was not only the physical preservation of the object but also its valorization and preparation for future public presentation within the Šenoa family collection. This fulfils one of the fundamental goals of conservation work – to ensure lasting accessibility and understanding of cultural heritage for future generations.

2.1. Object data and location

The Šenoa House in Zagreb, Mallinova 27, preserves the valuable Šenoa family Collection, which has been designed a cultural property by the Ministry of Republic of Croatia under number Z-4742. The building itself is also a protected cultural, listed under number Z-730.

August Šenoa´s writing desk was made around 1870 from walnut wood (*Juglans*), walnut veneer and spruce wood (*Picea*) as the substrate for veneering with a leather central section on the tabletop. The desk belongs to the historicist style of furniture typical of the second half of the19th Century and reflects the cultural status and aesthetic preferences of the bourgeois class of the time. Understanding the cultural and historical context of the desk is essential for planning interventions and selecting appropriate restoration methods.

Figure1. Front view of the desk in its initial condition, photo by P. Čavara, 2021.

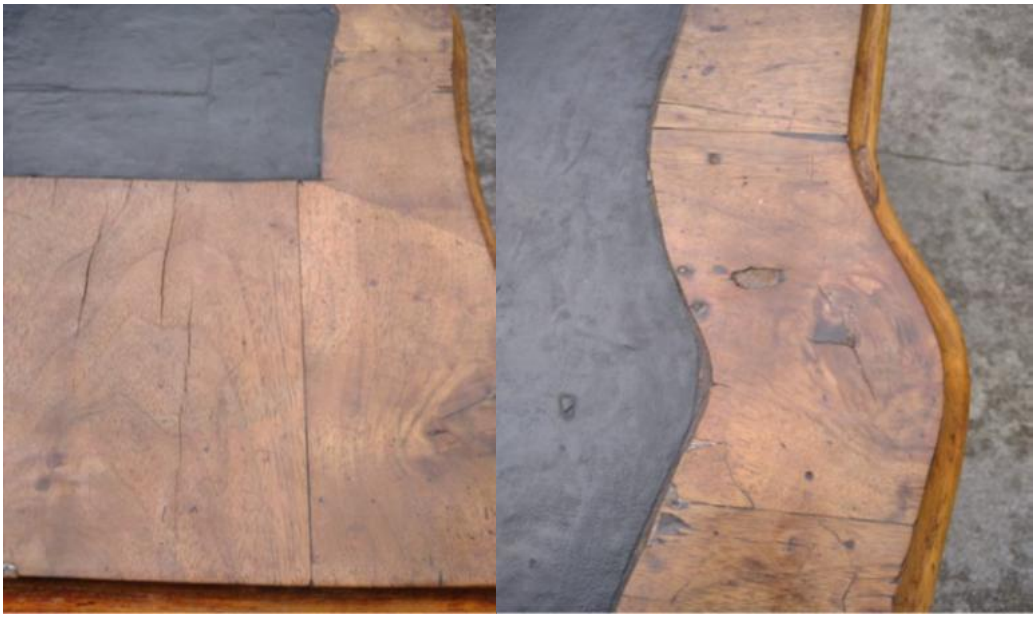

a) *b)*

Figure 2a, 2b.. Cracks and damage to walnut veneer before restoration, photo by P. Čavara, 2021.

Figure 3. Carved decoration before restoration, photo by P.Čavara, 2021.

2.2. Damage assessment and restoration plan

Detailed documentation of the desk´s damage was crucial for selecting appropriate conservation procedures, ensuring that the intervention remained targeted and minimally invasive.

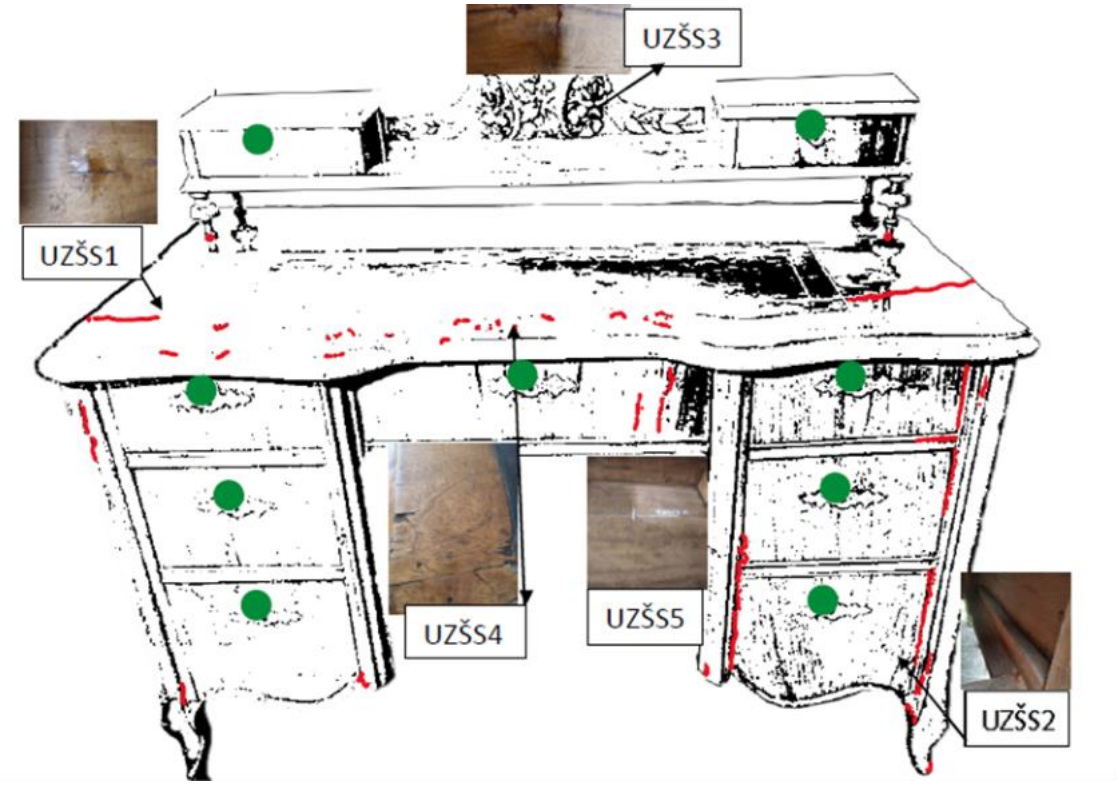

Graphic1.Marked areas indicate probe sites: chemical damage caused by corrosion products (green); mechanical damage and loosened joins (red). Front side of the writing desk, photo by P. Čavara, 2021.

2.3. Layer probing

Before restoration, layer probing was carried put to determine the structure and composition of the wooden, veneered and finishing layers of the desk and to select the most effective and safest cleaning and consolidation methods. Tests were performed on samples labelled UZŠS1 – UZŠS5, each used for specific analyses:

- macroscopic wood species identification- UZŠS1, UZŠS2
- surface dirt cleaning tests - UZŠS2, UZŠS5
- solubility tests of the painted layer – UZŠS1, UZŠS3
- FTIR analysis of the finishing layer – UZŠS4

2.3.1. Macroscopic identification of wood species

Wood identification enables the selection of compatible materials for consolidation and retouching, ensuring the long-term stability and preservation of the desk´s original appearance.

Figure 4. Comparison of walnut wood (Juglans) texture with INTKEY 5 Atlas – DELTA (Dallwitz et al., 2002)

Figure 5. Comparison of desk support wood (silver fir-Picea), source: https://www.mmm-vukelic.hr/drvo/jela/smreka/

2.3.2. Cleaning of wood, leather and metal fittings

Prior to cleaning, solubility tests were performed to determine the safest and most effective cleaning method for the wooden surface (Bešvir, 1998).Tests with organic solvents – distilled water, ethanol and acetone – showed that a citric acid solution was most suitable for removing dirt from selected surface areas.

Preparation of solution:

100 ml distilled water

0.5 g citric acid

few drops of triethanolamine (TEA)

The initial water – citric acid mixture had a pH of 2.5; TEA was gradually add under constant stirring until pH stabilized at 6.5 – optimal for safe wood cleaning.

For cleaning the leather surface, the product Erdal (leather milk with beeswax)was used, applied carefully with a sponge in thin layers to preserve the natural texture and color of the leather.

Metal parts, including keyhole escutcheons, were cleaned with 96 % ethanol to remove old shellac coating and surface dirt, while preserving the patina that contributes to the object´s historical and aesthetic value.

a) b)

Figure 6. Presence of shellac, dirt and patina (a); keyhole escutcheons after cleaning (b), photo by P. Čavara, 2021

2.3.3. Solubility tests and trial cleaning of shellac layer

The goal of the solubility tests and trial cleaning was to selecta method that removes dirt without damaging the original layers and patina, in accordance with the principles of minimal intervention and reversibility.

Tests were performed with acetone and 96 % ethanol. Results showed that ethanol provided the most effective and safest cleaning of the shellac surface.

During the actual cleaning a thickened ethanol gel was used -ethanol with 5% Klucel G – which allowed precise control of solvent application and minimized the risk of damaging the finish (Unger, 2001).

Figure 7. Comparison of uncleaned and clean surface, photo by P. Čavara, 2021

Figure 8. Carved section before cleaning, photo by P. Čavara, 2021

Figure 9. Carved section after cleaning, photo by P. Čavara, 2021

3. RESULTS

Instrumental analysis was subsequently carried out to confirm previous findings, specifically the presence of shellac in sample UZPŠS4. The analysis also identified the pigment within the shellac layer: Van Dyke Brown – a bitumen -Based pigment (carbon)with added black iron oxide) Fe^3O4, magnetite).

FTIR spectra of the finishing layer were analyzed at the Department of Conservation and Restoration of Works of Art, Academy of Fine Arts, Zamenhofova 14, Zagreb.

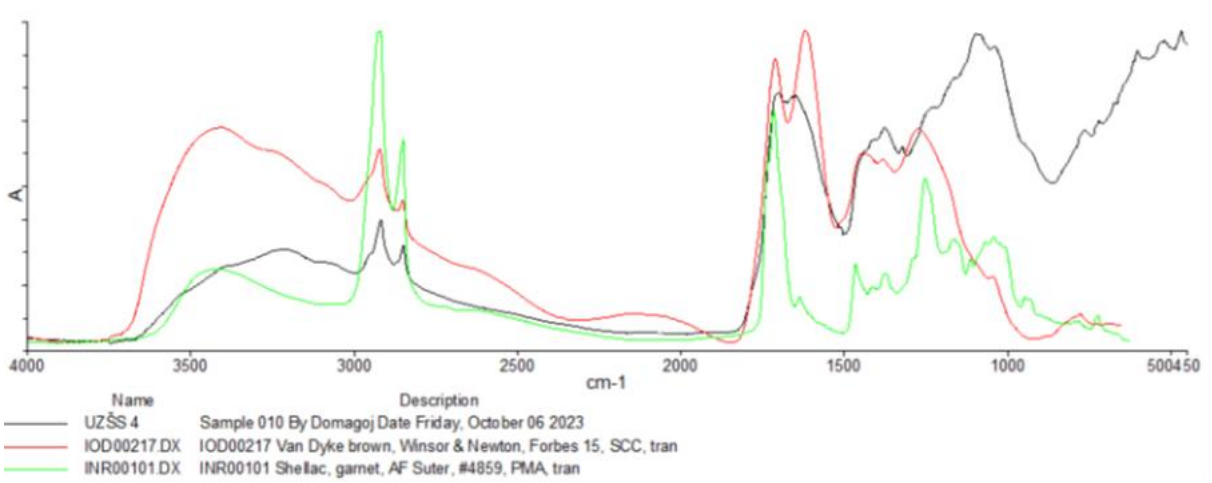

Sample ID	Sampling location	Sampling image	Results
UZŠS4	Tabletop, front right-center		-Presence of shellac -Bitumen-based pigmet(carbon) with added black iron oxideFe3O4(magnetite)

Figure 10. FTIR analysis results

The image document the sample´s condition before and after cleaning, demonstrating preservation of the finishing layer and identified materials. The results confirm that both shellac and original pigment were preserved and that the applied cleaning and consolidation methods did not negatively affect the finish. These finding provide a foundation for interpretation and further valorization of the object within the Šenoa House Collection.

Figure11. Detail of carved section after restoration, photo by P. Čavara 2021

Figure 12. Restored writing desk of August Šenoa,1870, photo by P. Čavara 2021

4. CONCLUSION

The Šenoa House in Zagreb, Mallinova 27preserves the Šenoa Family Collection, designated a cultural property by the Ministry of Culture of the Republic of Croatia and registered under number Z.4742. The building itself is also a protected cultural monument Z-730.

This paper presented the art-historical context of August Šenoa´s writing desk and detailed overview of the conservation – restoration process. All investigative procedures, instrumental analyses and interpreted results were explained, forming the basis for defining the restoration concept. The materials used and technical decisions were documented, adhering to the principles od minimal intervention, reversibility and distinguishability of the new additions.

The conservation- restoration work ensured the preservation of the desk´s integrity and aesthetic value, applying reversible materials and traditional techniques consistent with professional standards. The intervention provided long- term protection, preserved the original appearance and completeness of the object and enable its valorization for future generations and potential public display within the Šenoa House Collection.

5. REFERENCES

Bešvir, D., 1998: Zaštita i restauracija drvenih artefakata s posebnim osvrtom na suzbijanje drvnih štetočina, mikroorganizama i biogenih štetnih procesa. Vol. 7, Ludbreg Restauration Centre. p. 207 – 219.

Clavir, M., 2002: Preserving What Is Valued: Museums, Conservation, and First Nations. UBC Press.

Dallwitz, M. J.; Paine, T.A.; Zurcher, E.J., 2002: INTKEY5 – DELTA (The Delta System, Description Language for Taxonomy).

Matero, F., 2000: Ethics and Policy in Conservation. Journal of the American Institute for Conservation.

Grazuleviciute-Vileniske, I., 2006: Cultural Heritage in the Context of Sustainable Development, Kaunas University of Technology.

Halbertsma, H., 1999: The complete encyclopedia of antiques: covers antiques from the Middle Ages until the early 20th century, Rebo International b.v., Lisse, The Netherlands.

Lowenthal, D., 1998: The Heritage Crusade and the Spoils of History. Cambridge University Press.

Unger, A.; Schniewingd, A. P.; Unger, W., 2001: Conservation of wood artifacts, A Handbook, Springer, Berlin

International Charter for the Conservation and Restoration of Monuments and Sites, "Venice Charter", 1964.

***E.C.C.O., 2003: Professional Guidelines and Code of Ethics.

Possibilities for Using Waste and Mycelium-Based Composites in Furniture Design, with a Focus on Outdoor and Temporary Furniture

Markéta Daňková[1*], Ján Iždinský[2], Miroslav Jozífek[3], Monika Sarvašová Kvietková[1], Ondřej Dvořák[1], Miroslav Gašparik[1]

[1] Department of Wood Processing and Biomaterials, Faculty of Forestry and Wood Sciences, Czech University of Life Sciences Prague, Prague, Czech Republic;
[2] Department of Wood Technology, Faculty of Wood Sciences and Technology, Technical University in Zvolen, Zvolen, Slovakia;
[3] Department of Horticulture, Faculty of Agrobiology, Food and Natural Resources, Czech University of Life Sciences Prague, Prague, Czech Republic
*Corresponding author: dankovam@fld.czu.cz

ABSTRACT

This study investigates three structural configurations of MBC panels made from beech and spruce wood shavings colonized by Ganoderma sessile: (A1) a monolithic panel; (A2) a sandwich formed by fusing two preforms; and (A3) a sandwich incorporating three layers of linen fabric (face–core–face). All samples were stabilized via wet pressing (180 °C, ≤ 8 MPa, 20 min) and subsequently dried (≈ 101–103 °C for 2 h). Evaluated properties included density, water absorption (2 h/24 h), and thickness swelling (2 h/24 h). Pressing improved material cohesion and surface smoothness. The sandwich architecture and linen reinforcement further enhanced planar integrity, cohesion, and handling during growth and post-processing. Despite these improvements, mechanical properties remain below those of particleboards of comparable thickness, and MBCs exhibit higher water uptake and swelling. Nevertheless, the panels retain their shape after re-drying with minimal deformation. The textile surface also enables new aesthetic treatments (dyeing, coatings) without direct contact with the fungal skin. Based on these findings, a design proposal was developed for elements to be used in small furniture (e.g., stools, partitions, flowerpots, bins), where biodegradability is a functional advantage rather than a limitation. After seasonal use, they can naturally decompose into substrate.

Key words: mycelium-based composites, design, density, water absorption, outdoor furniture

1. INTRODUCTION

The increasing demand for comfort, rapid product turnover, and low-cost solutions is reshaping furniture design and the broader category of short-lifespan consumer goods. Notable examples include children's furniture, seasonal outdoor furnishings and exhibition setups. These products often result in waste streams composed of plastics and agglomerated materials that are difficult to recycle. Mycelium-based composites (MBCs) offer a promising route for upcycling lignocellulosic and textile residues into fully biodegradable alternatives to synthetic composites. However, their wider use is hampered by limited mechanical performance, moisture sensitivity, and low aesthetic appeal of fungal bark, which is typically brittle, inconsistent, and difficult to process (Islam *et al*., 2018; Bonenberg *et al*., 2023). In MBCs, conventional binders are replaced by a three-dimensional network of fungal hyphae that mechanically interconnect substrate particles and form a compact surface layer known as the "fungal skin" (Sun *et al*., 2020). Review papers consistently emphasize the environmental

benefits and broad application potential of MBCs, ranging from packaging materials (Jones *et al*., 2020) and acoustic panels (Appels *et al*., 2019) to architectural installations (Elsacker *et al*., 2021). Recent studies have explored MBCs as biomimetic leather alternatives (Lewandowska *et al*., 2024) and investigated hybridization strategies to improve mechanical strength and aesthetic qualities (Yang *et al*., 2021). Methodological inconsistencies across publications complicate data comparison and hinder practical implementation (Attias *et al*., 2020). Post-growth interventions can significantly modify MBC properties. Pressing—both cold and hot—is currently the most effective stabilization method, enhancing strength and stiffness, though it may reduce insulation performance and cause steam cracks or delamination under wet conditions (Nussbaumer *et al*., 2023; Alaneme *et al*., 2023). Hybridization, involving reinforcement layers such as veneers, fibers, meshes, or nanocellulose, improves shear transfer, edge durability, and dimensional stability. Mechanical improvements have been demonstrated with grid and sandwich reinforcements using wood veneer combined with compression (Ozdemir *et al*., 2022). Fungal species selection is critical. For panel-type MBCs, wood-decaying fungi with trimitic hyphal systems are preferred due to their rigid, spatially connected networks (Yang *et al*., 2021). In addition to the widely studied Ganoderma lucidum, Ganoderma sessile has shown high yield, contamination resistance, and rapid growth (Stamets, 2006), confirmed by cultivation. Its reputation as a medicinal "reishi" mushroom may further support user acceptance (Sun *et al*., 2019). One persistent issue is the brittleness of the fungal skin after drying. Literature recommends combining hot pressing with plasticization and biocoatings—e.g., 20–40 % glycerol to stabilize the chitin–glucan matrix, increase flexibility, and reduce fracture brittleness; or soy wax coatings reheated in the press to form compact, water-repellent layers (Haneef *et al*., 2017). Beyond physical properties, user acceptance—especially aesthetic perception—is vital. The natural fungal surface is often associated with mold. Studies with architects and users show that homogeneous textures and readable surfaces improve acceptance for interior use (Vandelook *et al*., 2021; Karana *et al*., 2018). Against this backdrop, our study systematically compares three panel architectures made from spruce and beech shavings colonized by G. sessile under standardized cultivation and stabilization conditions:

S,B 1-3: monolithic panel (80 mm thick, without fabric)

S,B 4-6: in-growth sandwich (two 40 mm boards to a total board thickness of 80 mm)

S,B 7-9: sandwich with three layers of linen fabric (surface–core–surface, 80 mm thick). All variants were wet-pressed (≈180 °C, ≤ 8 MPa, 20 min) and dried (≈101–103 °C).

This study aims to verify:

- the possibility of increasing the fiber density in the core layer of MBC boards by laminating the boards during growth.

- usability in design based on the resulting properties, to design furniture elements intended for outdoor or temporary furniture, where biodegradability is considered a functional advantage.

2. MATERIALS AND METHODS

2.1. Raw materials, inoculation, and cultivation

The substrate was prepared from wood chips of two commonly used wood species – Norway spruce (*Picea abies* (L.) H. Karst.) and European beech (*Fagus sylvatica* L.) – originating from the carpentry workshop of the university (Czech University of Life Sciences), with an initial moisture content of 9–11 %. The substrate was hydrated to a target moisture content of approximately 59 % using boiled water (≈90 °C) and packed into autoclavable Microsac filter bags with HEPA filters ($SACO_2$). Then pasteurized in an autoclave at 122 °C for 3 hours. Autoclave Sanyo, model MLS-3750-SV. After was exposed to UV radiation for 24 hours to reduce microbial contamination. Linen fabric (100 %, plain weave, waste) was pasteurized using the same procedure. The process is shown in Figure 1.

a) **b)** **c)**

Figure 1. Proces of preparing substrate a) wood chips b) hydratation c) substrates in $SACO_2$, after autoclaving in flowbox

2.1.1. Type and source of mycelium

For the production of composite panels, mycelium of *Ganoderma sessile* (collection FŽP CZU – strain no. 122) was used. Grain-based spawn served as the inoculum. Wheat grains supplemented with gypsum were hydrated to a moisture content of (47 ± 2) %, sterilized, and inoculated with fungal cultures. The inoculum was incubated for 12 days in glass flasks at a constant temperature of 24 °C.

2.1.2. Inoculation procedure, cultivation conditions

Under sterile conditions in a laminar box, the substrates were inoculated and resealed in bags with HEPA filters, then mixed by hand. The inoculation rate was 10 % (wet weight/wet weight). The inoculated substrates were incubated at 24 °C and 95 % relative humidity (RH). After 14 days, the substrates were completely colonized by the fungus. They were manually crushed and packed into standardized molds (270 mm × 350 mm × 80 mm) made of fiberboard lined with disinfected plastic film. The molds were placed in specially made growth boxes of TBA plastic crates (600 mm × 400 mm × 185 mm) with modified lids. The ventilation openings were fitted with heat-sealed HEPA filters to ensure sterile gas exchange during mycelium

growth. Before molding, the substrate moisture content was measured again and, if necessary, adjusted with distilled water to ensure uniform moisture content (W ≈ 59 %).

2.2. Desks architecture and in-growth fusion

In the molds, the boards were marked according to the planned composition (architecture) S (spruce) - 1-3 thickness 80 mm, 4-9 a,b thickness 40 mm and B (beech) 1-3 thickness 80 mm, 4-9 a,b thickness 40 mm. The composites were cultivated in the molds for 6 days. After this period, the samples were removed and the plastic film was removed. Our previous experiments showed that completely sealing the films poses a risk due to limited air exchange. The plates 1-3 (S,B) were only turned, samples 4-6 (S,B) joined together always plates a + b. Plates 7-9 were joined a+b with a layer of fabric. The modified samples continued to grow in boxes with HEPA filters under the same conditions for another 5 days, after which the temperature was reduced to 15 °C to slow down growth (showed in Figure 2).

a) **b)**

Figure 2. a) substrat in molds in TBA plastic box with hepafilers on the sides, b) plates colonized with mycelium

2.3. Pressing and drying process

All samples were found to be suitable for pressing. The average sample weight was approximately 1300 g with a moisture content of 59 %. The target thickness of the final pressed panels was calculated to be 0.98 mm. Each sample was weighed and measured on baking paper. Cold pre-pressing was performed using a manual press to a thickness of 20 mm for 20 seconds (Figure 3). During this step, a minimal amount of water was removed. After release from the press, all samples returned to a thickness of approximately 40 mm.

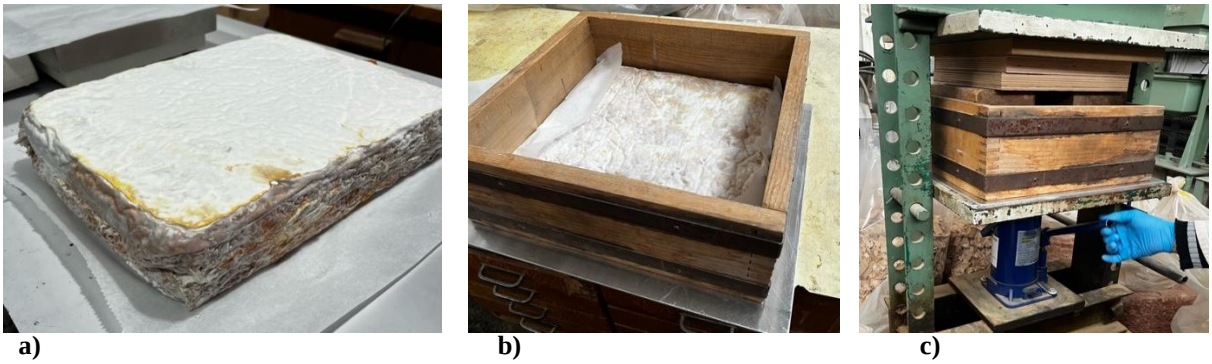

a) **b)** **c)**

Figure 3. Prepare samples a) fully colonizated sample b) in cold pressing mold c) cold pressing

a) **b)** **c)**

Figure 4. Samples pressing) Hydraulic pressing machine DS-C8J-100 in TUZVO, b) pressing c) final plates

The samples were then subjected to final pressing for 20 minutes. Each sample was placed between two stainless steel plates and pressed at a temperature of 180 °C for 20 minutes. Hydraulic pressing machine DS-C8J-100 in TUZVO, Zvolen, SK (Figure 4). The pressure used reached up to 8 MPa, and pressing was followed by drying at a temperature of 103 °C for 2 hours. All procedures and evaluation methods were conducted in accordance with the standards.

2.4. Density measurement, water absorption, and swelling

For measurement purposes, 12 samples measuring 50 mm × 50 mm were cut from each B1-9 and S1-9 plate, which were marked and supplemented with a number after a slash indicating the position on the given plate. The S7a9 plates were excluded from the measurement. The samples were measured using a Mahr 40 ewr sliding digital micrometer and weighed on a G&G1200 digital scale. The density was calculated for each sample. To determine water absorption, the samples were dried, weighed, and immersed in water. After 2 and 24 hours, they were measured and weighed. They were then dried again.

a) **b)** **c)**

Figure 5. Final samples a) samples b) detail foto of samples c) samples after 24 hours of soaking

2.5. Design furniture prototypes

Based on the identified properties, a concept of designs usable as temporary or outdoor elements was proposed. Variable flowerpots, stools, tables, and dividing elements. The design worked with the possibility of natural fusion of MBCs or binding of attached textiles. SketchUp 2022 was used for the design.

3. RESULTS AND DISCUSSION

For a clearer presentation results were divided into several chapters.

3.1. Mycelial growth and colonization

The mycelium growth process was a key phase for further processing and design. After 6 days of growth, the MBCs achieved sufficient structural integrity to be shaped or bent without breaking. A continuous layer of mycelium formed on the surface, ensuring the cohesion of the material and allowing individual parts to be joined together through „fusion by growth“. This property is essential for creating larger units without the need for adhesives or fasteners. Differences in the degree of colonization were observed between species. Beech (Fagus sylvatica) substrates showed a denser mycelial network than spruce (Picea abies). This difference can be attributed to the different chemical composition of the wood, in particular the content of extractive substances, which can influence the growth conditions of the mycelium.

3.2. Plates shaping and structure

During growth, panels 4-6a,b were joined together. After assembly, the mycelium layer bonded the boards into a single unit. This phenomenon allows two or more parts to be joined without the use of adhesives and increases the integrity of the board right at its core. The result was a higher-density material that shows potential for multi-layer bonding into a thick board and product shaping during the growth phase. Samples 7-9 a,b were joined using mycelium with a textile layer. This phenomenon will allow further shaping into endless boards or folded structures without the use of metal or chemically bonded joints.

3.3. Stabilization, compression, density, and absorbency

After cold pressing, the board sprang back by 40 mm. Wet pressing led to significant water and steam leakage. After pressing, the boards were smooth and firm, the surface of the mycelium skin on the boards with a layer of fabric smoothed out and the impression of mold disappeared. During pressing, some boards cracked inside due to steam pressure. The entire process was carried out in accordance with technical standards, which ensures the repeatability and comparability of results. In figure 7 are showed the results of density.

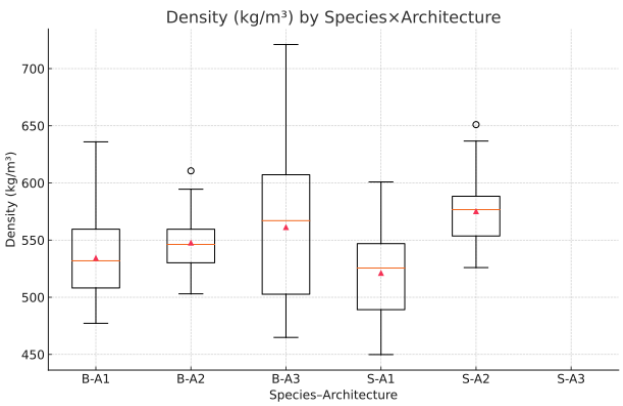

Figure 6. Samples density

B-A1, S-A1 samples without layering, B-A2, S-A2 - connection in the growth phase, B-A3 - connection with fabric. S-A3 were excluded from the measurement due to an insufficient number without cracks. The figure clearly shows that the density of the samples increased due to the bonding of the layers (except samples S-A3).

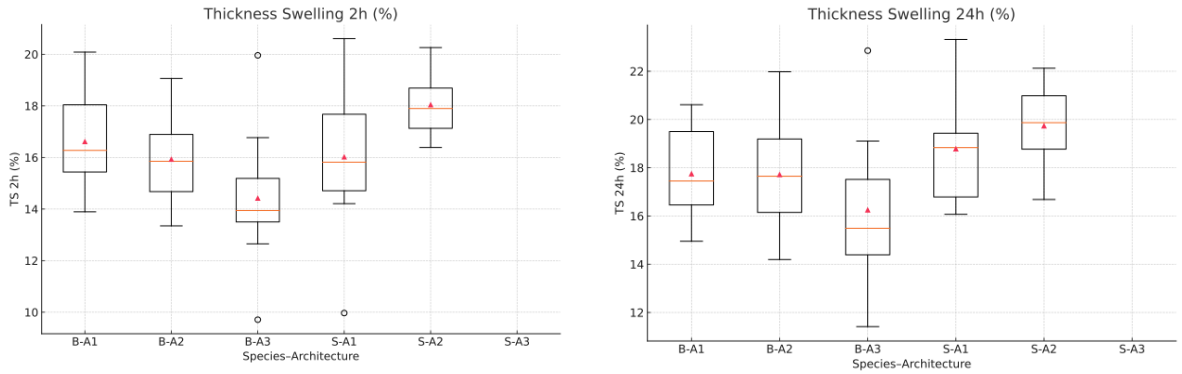

a) **b)**

Figure 7. Tickness swelling of samples after a) 2 hours, b) 24 hours

Figure 7 shows changes in size due to swelling, and Figure 8 shows water absorption. The measurements show that the greatest increase in swelling occurred at the beginning. This is because the mycelium itself can absorb water, and also because it grows through the wood chips, opening up pathways for water. After 24 hours, the increase was no longer as noticeable.

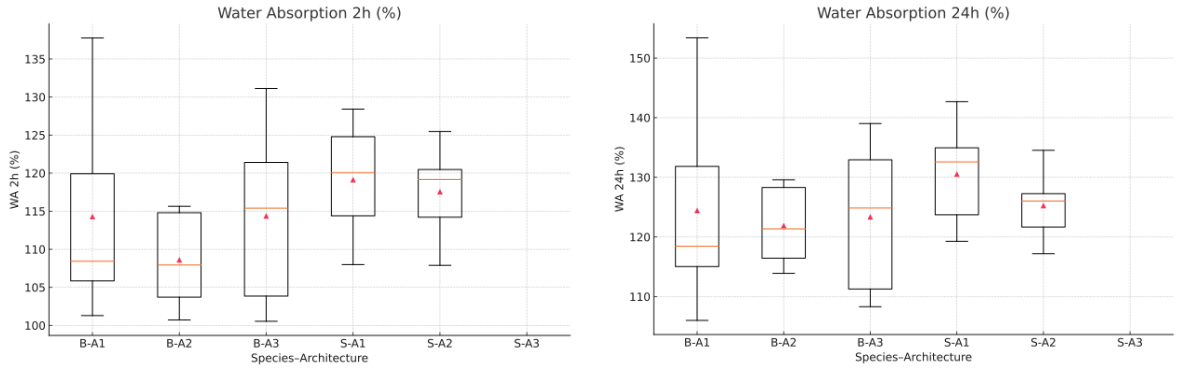

a) **b)**

Figure 8. Water absorpcion a) after 2 hours, b) after 24 hours

3.4. Design

Based on findings, the first design prototypes were developed, demonstrating the potential of this material in the field of sustainable design. Mycelium enabled the connection of individual parts without the use of adhesives, which contributes to the overall ecological value of the product. In some variants, linen fabric was integrated into the panels, allowing for connection/sewing after the pressing process. The fabric also contributed to the visual appeal of the products by reducing the moldy appearance of the mycelium bark. The resulting products

(Figure 9) are suitable for temporary or outdoor use, such as flower pots in parks and greenhouses, where biological decomposition is automatically expected. Elements using the natural growth method. Dividing elements and tables with the possibility of planting small seedlings. The roots will gradually absorb the MBC and the design will decompose naturally.

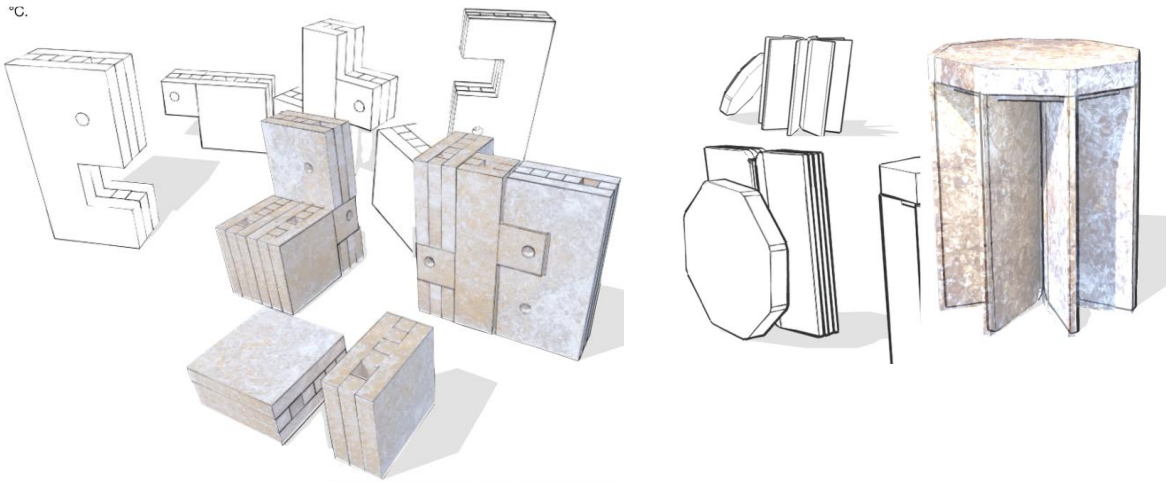

a) **b)**

Figure 9. Final products a) Design of a "myco-playground" b) "Sewn Stool" Design - Stool design using the method of sewing together pieces of grown fabric.

4. CONCLUSIONS

The experimental results confirmed that mycelial composites represent a promising material for sustainable design due to their natural biodegradability and the possibility of forming joints. The main advantage is degradability and disposal of textile or carpentry waste. The disadvantages are insufficient mechanical properties and high water absorption.

Acknowledgements: We would like to thank you for the materials, equipment of the laboratory and pressing machines to Faculty of Agrobiology, Food and Natural Resources, Czech University of Life Sciences and Faculty of Wood Sciences and Technology, Technical University in Zvolen.

5. REFERENCES

Alaneme, K. K.; Anaele, J. U.; Oke, T. M.; Kareem, S.; Adediran, M.; Ajibuwa, O. A.; Anabaranze, Y. O., 2023: Mycelium based composites: A review of their bio-fabrication procedures, material properties and potential for green building and construction applications. Alexandria Engineering Journal, 83: 234-250. https://doi.org/10.1016/j.aej.2023.10.012

Appels, F. V. W.; Camere, S.; Montalti, M.; Karana, E.; Jansen, K. M. B.; Dijksterhuis, J.; Krijgsheld, P.; Wösten, H. A. B., 2019: Fabrication factors influencing mechanical, moisture- and water-related properties of mycelium-based composites. Materials & Design, 161: 64-71. https://doi.org/10.1016/j.matdes.2018.11.027

Attias, N.; Danai, O.; Abitbol, T.; Tarazi, E.; Ezov, N.; Pereman, I.; Grobman, Y. J., 2020: Mycelium bio-composites in industrial design and architecture: Comparative review and experimental analysis. Journal of Cleaner Production, 246: 119037. https://doi.org/10.1016/j.jclepro.2019.119037

Bonenberg, A.; Sydor, M.; Cofta, G.; Doczekalska, B.; Grygorowicz-Kosakowska, K., 2023: Mycelium-Based Composite Materials: Study of Acceptance. Materials, 16: 2164. https://doi.org/10.3390/ma16062164

Elsacker, E.; Vandelook, S.; Damsin, B.; Van Wylick, A.; Peeters, E.; De Laet, L., 2021: Mechanical characteristics of bacterial cellulose-reinforced mycelium composite materials. Fungal Biology and Biotechnology, 8: 18. https://doi.org/10.1186/s40694-021-00125-4

Haneef, M.; Ceseracciu, L.; Canale, C.; Bayer, I. S.; Heredia-Guerrero, J. A.; Athanassiou, A., 2017: Advanced materials from fungal mycelium: fabrication and tuning of physical properties. Scientific Reports, 7: 41292. https://doi.org/10.1038/srep41292

Islam, M. R.; Tudryn, G.; Bucinell, R.; Schadler, L.; Picu, R. C., 2018: Mechanical behavior of mycelium-based particulate composites. Journal of Materials Science, 53: 16371-16382. https://doi.org/10.1007/s10853-018-2797-z

Jones, M.; Mautner, A.; Luenco, S.; Bismarck, A.; John, S., 2020: Engineered mycelium composite construction materials from fungal biorefineries: A critical review. Materials & Design, 187: 108397. https://doi.org/10.1016/j.matdes.2019.108397

Lewandowska, A.; Bonenberg, A.; Sydor, M., 2024: Mycelium-Based Composites: Surveying Their Acceptance by Professional Architects. Biomimetics, 9 (6): 333. https://doi.org/10.3390/biomimetics9060333

Nussbaumer, M.; Van Opdenbosch, D.; Engelhardt, M.; Briesen, H.; Benz, J. P.; Karl, T., 2023: Material characterization of pressed and unpressed wood–mycelium composites derived from two *Trametes* species. Environmental Technology & Innovation, 30: 103063. https://doi.org/10.1016/j.eti.2023.103063

Özdemir, E.; Saeidi, N.; Javadian, A.; Rossi, A.; Nolte, N.; Ren, S.; Dwan, A.; Acosta, I.; Hebel, D.E.; Wurm, J.; Eversmann, F., 2022: Wood-Veneer-Reinforced Mycelium Composites for Sustainable Building Components. Biomimetics, 7 (2): 39. https://doi.org 10.3390/biomimetics7020039

Stamets, P., 2006: Can mushrooms help save the world? Explore, 2: 152-161. https://doi.org/10.1016/j.explore.2005.12.011

Sun, W.; Tajvidi, M.; Howell, C.; Hunt, C. G., 2020: Functionality of surface mycelium interfaces in wood bonding. ACS Applied Materials & Interfaces, 12: 57431-57440. https://doi.org/10.1021/acsami.0c18165

Sun, W.; Tajvidi, M.; Hunt, C. G.; McIntyre, G.; Gardner, D. J., 2019: Fully bio-based hybrid composites made of wood, fungal mycelium and cellulose nanofibrils. Scientific Reports, 9: 3766. https://doi.org/10.1038/s41598-019-40442-8

Vandelook, S.; Elsacker, E.; Van Wylick, A.; De Laet, L.; Peeters, E., 2021: Current state and future prospects of pure mycelium materials. Fungal Biology and Biotechnology, 8: 20. https://doi.org/10.1186/s40694-021-00128-1

Yang, L.; Park, D.; Qin, Z., 2021: Material function of mycelium-based bio-composite: A review. Frontiers in Materials, 8: 737377. https://doi.org/10.3389/fmats.2021.737377

***ČSN EN 310, 1995: Desky ze dřeva – Stanovení modulu pružnosti v ohybu a pevnosti v ohybu. Praha: ÚNMZ.

***ČSN 49 0104, 1988: Skúšky vlastností rasteného dreva – Metóda zisťovania nasiakavosti a navlhavosti. Praha: ÚNMZ.

***ČSN 49 0108, 1993: Drevo – Zisťovanie hustoty. Praha: ÚNMZ.

***ČSN 49 0126, 1983: Skúšky vlastností rastlého dreva – Metóda zisťovania napúčavosti. Praha: ÚNMZ.

Design of a Wooden Portable Office for Engineering Field Work

Domljan, Danijela*; Grabić, Tomislav[1]

[1] Department of Furniture and Wood in Construction, Faculty of Forestry and Wood Technology, University of Zagreb, Zagreb, Croatia
*Corresponding author: ddomljan@sumfak.unizg.hr

ABSTRACT

The topic of this paper is the design and construction of a portable office for field work by users such as wood technologists, builders, architects, technicians, and others. This office would facilitate and accelerate field work while also preventing potential physical discomfort among engineers. The needs of the target group were researched through an online survey in order to propose an innovative design of a portable office that would help these professionals perform their tasks more easily and protect their health. The paper outlines the concept development process, including research into the use of wood in product design and construction.

Key words: body posture, design, engineering field work, musculoskeletal disorders, portable office, wooden materials

1. INTRODUCTION

Field work has been practised since ancient times in certain engineering professions, such as civil engineering, architecture, surveying, wood technology, carpentry, forestry, and others. Employees often carry out field measurements, record observed and characteristic details on objectsor field samples, inspect or measure the current condition, collect data from new objects or samples, complete forms, take photographs, make sketches, record dimensions, and perform other tasks. Field work is not physically easy, both because of all the necessary tools and measuring instruments required, and due to the physical conditions of the environment (rain, sun, hazardous conditions on construction sites, etc.). Such working conditions are often non-ergonomic, and suitable work equipment is often lacking.

The topic of this paper was prompted by the sudden earthquakes that struck the City of Zagreb and Banovina in the Republic of Croatia in 2020, during which civil engineers, surveyors, wood technologists, architects, doctors, and emergency services worked intensively in the affected areas. It was observed that a suitable modern solution for the storage and disposal of various tools, measuring instruments, modern devices, and other essential equipment used in safe field work had not yet been developed – one that would also meet ergonomic requirements and ensure the availability of measuring instruments and other equipment to improve work efficiency.

There was a lack of a suitable portable “mobile office” to prevent difficulties such as back, neck and shoulder pain, fatigue, and other symptoms associated with uncomfortable or incorrect body posture during work (Grandjean, 1988; Scheer and Mital, 1997; Kroemer and Kroemer, 2017), as well as to increase efficiency in performing field work.

1.1. Aim of the paper

In this paper, "field work" refers to tasks requiring employees to visit construction and architectural sites to measure interior spaces within buildings, using specific equipment such as laptops, pencils, measuring tapes or similar. The paper aims to use an online questionnaire to investigate users' needs regarding work equipment during field work and to propose a portable office design that will enable professionals to perform necessary tasks more easily and efficiently, thereby protecting their health while working in the field.

This paper presents proposals for conceptual solutions for a portable office for field work.

2. WORKING CONDITIONS CHARACTERISTIC OF FIELD WORK

Fieldwork on buildings and interiors is most often carried out by architects, designers, constructors, wood technologists, and related professions. Working in environments where workers stand, lift loads, or perform tasks requiring bending, squatting, or kneeling increases the likelihood of developing neck and back pain (Grandjean, 1988). Significant ergonomic problems arise particularly in tasks where the arms and legs are used in extreme positions, and back and musculoskeletal pain are reported more frequently than average (Tissot *et al*., 2009; Piznke and Lavesson, 2018).

In addition to bending, squatting, and kneeling, forward neck bending also occurs when sketching or recording measurements if no surfaces are available on which to place a notebook or tablet. Localised muscle fatigue in the neck may indicate more serious chronic musculoskeletal disorders. According to Grandjean (1988), the neck angle should not exceed 30° and should not be maintained for extended periods, especially when using tablets and smartphones, to avoid the so-called "text neck" syndrome (Fercho *et al*., 2023).

To prevent cervical spine problems, it is necessary to provide a surface for placing a notebook or tablet, with the recommendation that the equipment be positioned at eye level and on a surface angled at 45° (Tomita *et al*., 2022).

3. METHODS AND MATERIALS

3.1. Research methods

For the research, online questionnaire methods were used. The results provided guidelines for the design, where the Cyclic method of the creative process was applied. The online survey was conducted in spring 2023 using the Google Forms application. The questionnaire was compiled to identify users' needs, which were then set as requirements for the final product. The structure of the questions is shown in Table 1.

Table 1. The structure of the Questionnaire

Section	Topics	Number of Questions
O	Survey description	-
A	General questions	4
B	Your work in the field - the equipment you use	1
C	Your body positions on the field and pain	4
D	Instructions for designing your mobile office	10
E	Additional comments	
Sum		19

3.2. The respondents

The respondents in the survey were selected based on their professions, specifically the profession most closely related to the work performed in the field. When selecting respondents, healthy individuals of both sexes, aged between 25 and 60 years, were included, and it was important that they did not suffer from any chronic diseases.

As the research involved working with people, approval for the implementation of the survey was obtained from the Ethics Committee of the Faculty of Forestry and Wood Technology, number EP09-22/23.

3.3. Software tools for designing solutions

The software tools Inventor, Woodwork for Inventor, and WoodWOP were used in creating the conceptual solution and the final product. With Inventor and Woodwork for Inventor, it is possible to fully design, construct the product, and prepare it for production. After designing, CNC programmes are generated in the software tool for programming and managing the CNC machining centre of the Homag group, called WoodWOP.

4. RESULTS AND DISCUSSION

4.1. Results of the questionnaire

The aim of the questionnaire was to gain insight into the need for a product such as a portable office intended for fieldwork, its desired appearance, and the requirements of people working in the field.

Answers to general questions (A):

A total of 51 people responded to the questionnaire. During processing, one questionnaire was marked as invalid. Female respondents comprised 47.1 % of participants, while male respondents accounted for 52.9 %. The majority of respondents were in the 25–30 age group, representing 45.1 %. The three most common professions among respondents were wood technology (51 %), design (15.7 %), and architecture (11.8 %). 60 % of respondents held a university degree.

Answers to the equipment used and fieldwork (B):

Of the offered equipment and equipment used in fieldwork, respondents noted the greatest use of the following equipment: paper/notebook/pad (90.2 %); pencil/pen (86.3 %); mobile phone for taking pictures of the area (82.4 %); meter (72.5 %); hand-held laser (66.7 %); backpack (62.7 %); laptop (43.1 %); tablet (23.5 %); bag (21.6 %); cross laser (19.6 %); square (17.6 %); safety helmet (13.7 %); professional camera (11.8 %); gloves (5.9 %); string (2 %); BIM camera and accessories (2 %). Accessories not included among the offered answers but listed by respondents themselves include a tablet with a Windows programme and a 3D BIM scanner, a digital protractor, a spirit level, and assembly tools.

Answers regarding body positions in the field and pain (C):

According to the frequency of body positions during fieldwork, standing with head and neck rotation is the most frequently used body position during work (Table 2).

Table 2. Most commonly used body positions during fieldwork (5 = most frequently, 0 = least frequently)

Body posture	Mark
Standing	5
Head and neck rotation	5
Body rotation left-right	4
Bending	3
Raising arms above head	3
Squatting or kneeling	2 and 3
Sitting	3
Lying	0

Regarding pain during work, 60 % of respondents sometimes experience pain in their bodies during fieldwork, while 30 % do not experience it at all. Ten percent of respondents always feel pain during fieldwork. Respondents state that the squatting position causes the most problems and is the most difficult to tolerate.

Respondents' suggestions for designing a mobile office (D):

When asked whether they need a product such as a portable office to facilitate work in the field, 31.4 % of respondents confirmed that a portable office would speed up and facilitate fieldwork, 56.9 % answered that it would sometimes do so, while 11.8% remained neutral. Additionally, 74.5 % stated that they need to put away items such as a jacket, purse, or bottle during fieldwork, 19.6% sometimes have this need, and 5.9 % do not have this need at all.

A portable writing surface is needed by 72.5 % of respondents, while 9.8 % sometimes need one and 17.6 % do not need one at all.

A total of 62.7 % of respondents always need to put down their laptop or tablet while working, 21.6 % need to do so sometimes, and 15.7 % do not need to put down their laptop or tablet at all.

The respondents identified the following as the most necessary elements for fieldwork: a surface for storing paper, notebook, and pen (writing) (82.4 %); a surface for storing a tablet or computer (computer work) (64.7 %); a space for storing a pen or pencil (64.7 %); a space for storing a meter or laser (51 %); a space for storing a backpack or purse (51 %); a surface for storing a mobile phone (47.1 %); a space for batteriesor adapters for charging tablets, laptops, or mobile phones (37.3 %); and a space for storing cables, wires, or strings (17.6 %).

According to the respondents, a product that would make field work easier should be carried on the back (29.4 %), by pulling or pushing on the ground using wheels (27.5 %), or by holding it on the shoulder (19.6 %).

The materials that are most desirable for making a portable office according to the respondents are: plastic (62 %); fabric (46 %); wood composites (44 %); wood panels (26 %); metal rods/tubes (26 %); solid wood (16 %); twine (16 %); glass (1 %); and materials that were supplemented by the respondents, carbon fiber and leather.

In terms of product construction, the ideal product should be foldable or dismantled (58.8 %), or a combination of foldable and non-dismantled components (33.3 %). Only 2 % of respondents stated that the product should be non-foldableand non-dismantled, while 5.9 % of respondents do not know what their ideal field product should be.

At the end of the questionnaire, respondents had the opportunity to provide ideas, suggestions, or ask further questions. Some interesting reflections are below:

Respondent A: "For sketching or drawing on the move, a flat board worn under the chest with shoulder straps and ergonomic support, so it does not press into the chest, would be useful. The straps should be removable, and the board should fold in half to fit in a backpack."

Respondent B: "Perhaps a good question would be: 'How do you travel to the field? By car, train, or plane?' I always wondered where or how I would carry an 'extra suitcase' with me. I usually travel by plane to the field, and in fact, I need a pad for working on my laptop the most."

4.2. Project task

The project task was to design a product aimed at facilitating field trips, including visits to construction sites and taking interior measurements. The product should incorporate several functions, such as a writing surface, a compartment for carrying equipment, and storage for additional items like a jacket or bottle. By combining different materials, it is necessary to create a lightweight, foldable, and easily portable product that is fully dimensioned to suit the future user. Ideally, the product should be made from fabric, plastic, and wood composites, and include elements such as a writing surface for computer work, as well as storage for a tape measure, laser, and other essential equipment. In addition to measuring tools, there should be space to store other items such as a jacket, bottle, handbag, or backpack.

4.3. Product requirements

To develop conceptual solutions and design a quality product, it is necessary, in addition to the guidelines obtained from respondents, to consider various requirements, limitations, standards, and regulations for designing this type of product as listed in the studied literature.

Ultimately, the product requirements were defined as follows: the product must be lightweight (using materials such as aluminium, lightweight wood, and recycled plastics (Jambreković, 2004; Skejić *et al*., 2015; Tümer *et al*., 2021)); foldable; easily portable; adjustable to the user's height (Panero and Zelnik, 1987); provide seating; include a writing surface; offer storage for tablets and laptops; provide space for equipment, bottles, jackets, handbags, etc.; be intended for architects and wood technologists; be suitable for both male and female users aged 18 to 65; and ensure harmony of dimensions and materials.

4.4. Conceptual solutions

The following sketches (Table 3) represent the phase of developing conceptual solutions within the Cyclic method of the creative process.

Table 3. Proposed conceptual solutions for a mobile office.

No	Functional Concept Drawing
I	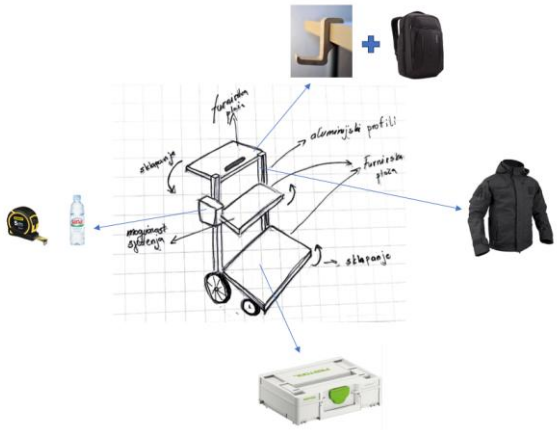
II	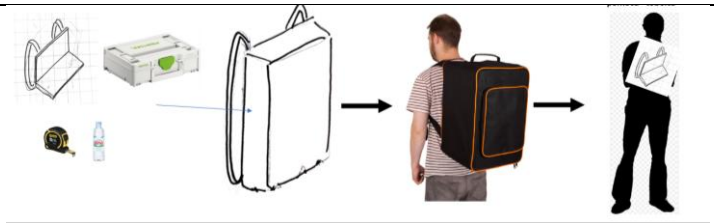
III	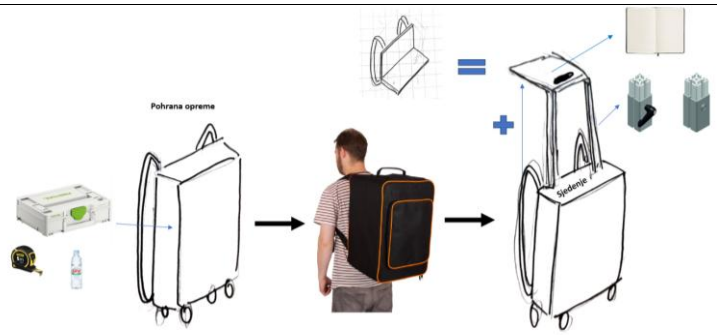

Concept I is designed as a mobile cart for transporting measuring equipment and other necessary items. The product includes storage for larger items (e.g. a box for a cross laser), compartments for smaller items (such as a meter, laser, water bottle, etc.), a place to hang a jacket and backpack, and a seat. The product is foldable to occupy less space during transport and is moved by pushing it on wheels.

The Concept II is a backpack with larger dimensions, designed to store measuring equipment and other necessary items. Unlike the Concept I, this product is carried on the back and does not have a fixed surface for writing or storing a notebook, tablet, or laptop. Instead, it features a panel with straps that rests under the user's chest. In this way, it serves as a "quiver" for sketching spaces and recording measurements on the way.

Concept III combines the first and second concepts. It features a backpack with larger dimensions to store measuring equipment and other necessary items. The product can be carried on the back or pushed using wheels. It includes a removable surface for writing and storing a notebook, tablet, or laptop, which attaches to the backpack straps with buckles. This surface can be detached as needed, transforming into a "quiver" that allows users to sketch and record measurements on a hard surface while on the move.

4.5. Final conceptual proposal

The final optimised conceptual product proposal (Figure 1) for fieldwork has a folded size of 452 mm × 280 mm × 700 mm (width × depth × height), to facilitate transport to and movement within the facility.

The main components of the final portable office proposal are:

(a) a body section that serves as storage for necessary equipment and as a seat;

(b) two telescopic aluminium profiles attached to the body and connected transversely by a wooden support; and

(c) a writing and computer work surface that enables sketching and recording measurements on the go or when securely attached to the wooden support of the portable office.

Figure 1. Visualisation of the final concept for the mobile office. Drawing: Grabić, 2023

5. CONCLUSION

Fieldwork is a common task for wood technologists and architects, where employees take measurements, record observed and characteristic details on objects, take photographs, and note dimensions, often "on the fly". Such work is challenging, both due to the transportation of necessary equipment and the varying conditions at different sites. Fieldwork inevitably involves body positions such as standing, bending, squatting, and kneeling. The parts of the body where pain most frequently occurs during fieldwork are the spine, neck, and feet.

This paper proposes an innovative conceptual solution for a portable office called POFF (Portable OFFice). The solution is based on the results of a survey that confirmed the need for a product such as a portable office. The requirements for this product were primarily determined by the responses to the survey questionnaire, reflecting the respondents' needs, and by additional literature review.

A product such as a portable office makes it easier to travel to and work in the field. Easier transport and transfer of equipment, along with adjustable work surface height, reduce uncomfortable and incorrect postures that contribute to pain in the spine, neck, and shoulders, as well as fatigue. The option to sit also reduces pain in the legs and feet.

To confirm that this concept addresses the above problems, further research is required.

Acknowledgements: We thank the participants who voluntarily took part in the survey and whose responses helped guide the design of the conceptual solution.

6. REFERENCES

Fercho, J.; Krakowaik, M; Yuser, R.; Szmuda, T.; Zieliński, P.; Sazrek, D.; Miekisiak, G., 2023: Kinematic Analysis of the forward Head Posture Associated with Smartphone Use, Symmetry 15:667.

Grandjean, E., 1988: Fitting the task to the Man. Taylor & Francis, London, New York, Philadelphia.

Jambreković, V., 2004: Drvne ploče i emisija formaldehida. Šumarski fakultet Sveučilišta u Zagrebu.

Kroemer, K.; Kroemer A., 2017: Office ergonomics, Ease and efficiency at Work. CRC press, New York.

Panero, J.; Zelnik, M., 1987: Antropološke mere i interijer, IRO Građevinska knjiga, Beograd.

Pinzke, S.; Lavesson, L., 2018: Ergonomic conditions in manual harvesting in Swedish outdoor cultivation, Swedish University of Agricultural Sciencis (SLU), AEM.

Scheer, S. J.; Mital, A., 1997: Ergonomics. Archives of Physical Medicine and Rehabilitation, 78 (3): 36-45.

Skejić, D.; Boko, I.; Torić, N., 2015: Aluminij kao materijal suvremene konstrukcije. Građevinar, 11/2015. https://doi.org/10.14256/JCE.1395.2015

Tissot, F.; Messing, K.; Stock, S., 2009: Studying the relationship between low back pain and working postures among those who stand and those who sit most of the working day. Ergonomics, 52 (11): 1402-1418.

Tomita, Y.; Suzuki, Y.; Shibagaki, A.; Takahashi, S.; Matsuka, Y., 2022: Physical Load While Using a Tablet at Different Tilt Angles during Sitting and Standing. Sensors, 22: 8237.

Tümer, E. H.; Erbil, H. Y., 2021: Extrusion-Based 3D Printing Applications of PLA Composites: A Review. Coatings, 11: 390.

Research on Sleep Habits and Influencing Factors

Drača, Maja*; Vlaović, Zoran[1]

[1] Institute of Furniture and Wood in Construction, University of Zagreb Faculty of Forestry and Wood Technology, Zagreb, Croatia
*Corresponding author: majadraca24@gmail.com

ABSTRACT

Sleep quality is shaped by the interaction of multiple factors, with the mattress playing a particularly important role in providing comfort and ergonomic support to the body. Its construction and materials directly affect pressure distribution, spinal alignment, and the subjective feeling of rest. This paper discusses contemporary mattress design solutions and their relationship to ergonomics and health outcomes, while also considering additional elements such as sleep routines and environmental conditions (temperature, light, noise). By analyzing selected scientific literature, the study presents findings on how the combination of mattress ergonomic properties and adapted lifestyle habits can contribute to healthier and higher-quality sleep. The results indicate that the mattress represents a fundamental link between furniture products and user well-being, while routines and environmental factors act as supporting elements. The conclusions emphasize the importance of an interdisciplinary approach and highlight the need to develop objective methods for evaluating mattress comfort in the context of product design, ergonomics, and sleep research.

Key words: comfort, environmental factors, ergonomics, mattress, sleep

1. INTRODUCTION

Sleep is one of the body's essential physiological needs, crucial for physical restoration, energy renewal and mental well-being. Key regulatory processes that support brain function, immune activity and emotional stability occur during sleep, and since people spend roughly one-third of their lives sleeping, identifying factors that influence sleep quality is increasingly important (Kushida, 2013). Modern lifestyle demands, stress and frequent technology use have contributed to more common sleep disturbances, particularly among younger individuals, who often experience delayed sleep onset, shallow sleep and morning fatigue (Grandner, 2019). Sleep quality is shaped by pre-sleep habits, environmental conditions and the physical surface on which a person rests. The mattress affects spinal alignment, pressure distribution and comfort, and when poorly adapted, it may cause discomfort and disrupt sleep continuity (Caggiari *et al*., 2021). Sleep should therefore be viewed holistically, as an outcome of continuous interaction between the individual, their environment and the products they use, and this paper examines these interconnected factors to better understand how mattresses, everyday habits and environmental conditions contribute to high quality sleep.

2. MAIN FACTORS FOR SLEEP QUALITY

Sleep does not depend on a single element but results from the interaction of several key factors that shape both physical and psychological comfort during the night. Among these, the

characteristics of the mattress, personal routines before sleep, and environmental conditions in the bedroom stand out as the most influential. Each of these factors affects different aspects of sleep, from maintaining proper spinal support, to regulating sleep onset and preserving sleep continuity. As illustrated in Figure 1, sleep quality is determined by multiple interrelated domains including physiological, behavioral, environmental, and health-related influences. The following sections provide an overview of how these elements contribute to sleep quality and why their combined influence must be considered when seeking better and more restorative sleep.

Figure 1. Multifactorial determinants of sleep quality (Adapted from Wei et al. Copyright 2022 Taylor & Francis)

2.1. The role of mattress

Mattresses have evolved from simple natural surfaces used in ancient civilizations to highly engineered systems designed to enhance comfort and support. Modern mattress development focuses on ergonomics, material performance and personalization. The primary function of a mattress is to maintain spinal alignment and distribute body weight evenly across load-bearing regions. When a mattress provides insufficient support, spinal deviation may occur, leading to discomfort, pain and poor sleep continuity (Verhaert *et al*., 2012; Hong *et al*., 2023). Different sleeping positions require different ergonomic demands; while side sleeping may reduce pressure-related symptoms, it is not ideal for everyone, and prone sleeping often increases neck and lower-back strain. Material characteristics directly affect comfort and pressure relief. Viscoelastic foam conforms to the body and reduces motion transfer, making it beneficial for individuals with back pain or for partners sharing a bed (Hong et al., 2023). Natural latex is valued for elasticity, durability and ventilation, contributing to reduced pressure in the torso

and hip area (Low *et al*., 2017). Ergonomic performance is further improved by zoning varying firmness along the mattress to support different anatomical areas. Zoned systems allow shoulders and hips to sink slightly while stabilising the lumbar region, promoting a more neutral spinal posture (Wong *et al*., 2019). Individual perception remains an important consideration, but when mattress structure reduces pressure peaks and supports posture, sleep becomes less fragmented and more restorative (Grandner, 2019).

2.1. Pre-sleep routines and sleep hygiene

Sleep related routines are an essential determinant of sleep quality. The way individuals prepare for bedtime, together with their lifestyle habits, influences whether sleep will be restorative or disrupted. Sleep consists of cyclical transitions through light, deep and REM phases, each supporting physical and cognitive recovery. Disruptions in these cycles may reduce both the restorative function of deep sleep and the emotional processing associated with REM (Grandner, 2019). Psychological factors also play a significant role. Stress, anxiety and worry commonly prolong sleep onset and increase nighttime awakenings. This interaction is bidirectional: insufficient sleep exacerbates psychological strain, while emotional tension weakens sleep continuity (Grandner, 2019). The effects are often more pronounced in adolescents and young adults due to academic and social pressures.

Good sleep hygiene refers to behaviours that promote a stable nightly rhythm. Consistent bedtimes, limiting caffeine and screen exposure before sleep and maintaining a calm mental state help regulate the circadian system and ease the transition into deeper sleep (Irish *et al*., 2015). Excessive evening screen use is particularly disruptive because blue light suppresses melatonin production, delaying sleep onset and reducing total sleep duration. Physical activity further contributes to sleep quality by lowering stress levels and promoting deeper sleep. However, high-intensity exercise shortly before bedtime may elevate alertness temporarily and make falling asleep more difficult, whereas moderate exercise earlier in the evening does not show such negative effects (Kim *et al*., 2023). Maintaining a regular sleep schedule is especially beneficial for students, who are prone to variable bedtimes and associated daytime fatigue. Taken together, these findings highlight that pre-sleep routines and psychological well-being are closely associated with perceived sleep quality, especially in younger populations, which supports the focus of the present study on bedtime behaviours and lifestyle patterns among students.

2.3. Environmental conditions during sleep

Environmental factors strongly contribute to whether sleep will be continuous and restorative. When the sleeping environment is suboptimal, nighttime awakenings become more frequent, leading to reduced sleep quality (Verhaert *et al*., 2011; Grandner, 2019). Thermal comfort is especially important, as the body needs to cool down before falling asleep. Excessive heat disrupts REM sleep, while cold conditions prolong wakefulness (Grandner, 2019). The microclimate of the bed itself may also influence comfort, since materials that retain too much heat can increase sleep disturbances (Lee *et al*., 2022). Noise often causes brief arousals that are not remembered but still fragment sleep and reduce morning alertness (Exelmans & Van

den Bulck, 2016). Light exposure particularly from electronic devices delays melatonin release and disrupts circadian rhythms, resulting in delayed sleep onset (Chang *et al*., 2015).

3. SLEEP HABITS AND INFLUENCING FACTORS

This section presents the key findings related to sleep quality, focusing on the interaction between mattress characteristics, sleep routines and environmental conditions. The results are interpreted in the context of previously discussed theoretical concepts and relevant scientific literature. Particular emphasis is placed on identifying practical and ergonomic factors that can support healthier and more restorative sleep. Each analysed element is considered both individually and as part of a comprehensive sleep system, which includes the physical sleeping surface, behavioural habits before bedtime and the surrounding sleep environment.

3.1. Influence of mattress design on sleep comfort

Mattress design strongly affects spinal alignment, pressure distribution and sleep continuity. Hu *et al*. (2025) found that medium-firm mattresses provide adequate support for the spine while reducing sleep onset latency and nighttime awakenings. The replacement of an old mattress with a medium-firm model can significantly reduce perceived back pain over the first weeks of use. Jacobson *et al*. (2009) reported a rapid decrease in back pain ratings from baseline to the first week, followed by stabilisation of pain levels over the intervention period. These findings support the role of balanced support and adequate spinal alignment in reducing sleep-related discomfort and improving restorative sleep.

Material behaviour is another essential component of comfort. Low *et al*. (2017) demonstrated that elastic materials such as natural latex better distribute pressure across the body, especially in the shoulder and hip areas. Their measurements showed significantly lower peak pressures on latex than on standard polyurethane foam, which reduces discomfort and the likelihood of micro-arousals during sleep. Durability plays a key role in long-term satisfaction. Vlaović *et al*. (2024) reported that mattresses made entirely from PUR foam demonstrate good durability and stable mechanical performance after an initial break-in period. The changes that occur over time are further illustrated in Figure 2, which shows the indentation load deflection behaviour of PUR foam at the beginning of use compared to after 90,000 loading cycles. Although the material still retains support, a visible flattening of the curve indicates gradual softening and reduced resistance to deformation. This suggests that foam only constructions may experience a decline in firmness with prolonged usage.

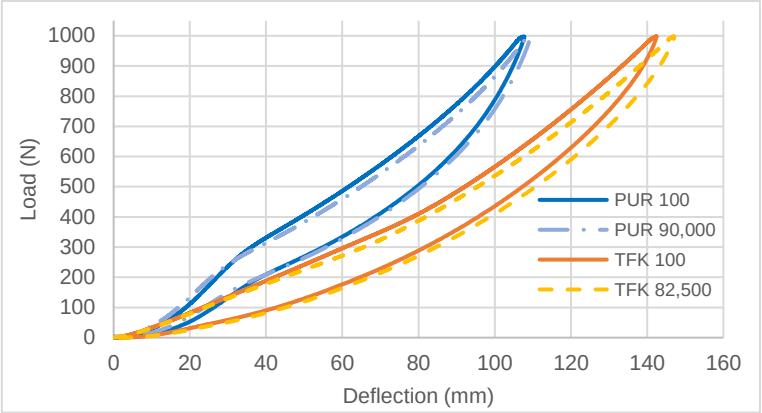

Figure 2. Indentation load deflection (ILD) characteristics of a polyurethane (PUR) foam and pocket-spring (TFK) mattress (Adapted from Vlaović et al., 2024)

In contrast, pocket-spring (TFK) systems generally maintain more stable firmness and mechanical integrity throughout their lifespan. As shown in Figure 2, the ILD curve for a mattress with a spring core exhibits minimal deviation over repeated cycles, indicating better long-term stability and greater resistance to structural fatigue. This confirms that spring-based systems can provide long-lasting support compared to foam-only structures, particularly when subject to repeated body loading during everyday use.

Mattresses that incorporate zoned firmness provide more localised pressure relief in areas exposed to greater loading, while simultaneously ensuring increased stability in the lumbar region. Caggiari *et al*. (2021) highlight that such constructions are especially beneficial for side sleepers or those experiencing chronic back pain, because they better preserve the natural curvature of the spine. Although research provides clear performance indicators, comfort remains partly subjective. Grandner (2019) notes that sleep experience depends on individual preferences, body characteristics and sleeping posture. For that reason, a mattress must be evaluated not only by its biomechanical results, but also by personal perception and adaptation through time. Verhaert *et al*. (2012) emphasize that support quality also depends on the compatibility between the mattress and its bed base, meaning that the entire sleep system should function as a biomechanical unit.

Overall, the evidence suggests that medium-firm surfaces with pressure-relieving materials and durable support structures offer the most consistent benefits for sleep quality. However, selecting a mattress should always account for the user's physical needs, preferred sleep position and total sleeping environment.

3.2. Influence of sleep routines and behaviour on sleep quality

Sleep behaviour plays a crucial role in shaping both the structure and the restorative quality of sleep. Grandner (2019) explains that sleep is organised into repeated cycles consisting of light sleep, deep sleep and REM phases, each supporting specific physiological and cognitive functions. When these cycles are interrupted, the benefits of sleep are reduced, even if the total duration appears sufficient.Psychological factors are among the most frequent causes of sleep disruption. Stress, anxiety and emotional tension can prolong the process of falling asleep and cause more frequent awakenings during the night, while insufficient sleep further intensifies psychological strain, creating a negative feedback loop that affects daily well-being (Grandner,

2019). Sleep hygiene refers to behaviours and environmental adjustments that support consistent and high-quality sleep. Irish *et al*. (2015) highlight the importance of maintaining a regular bedtime, limiting stimulant consumption in the evening and reducing screen use before sleep, since blue light delays melatonin secretion. Individuals who frequently use digital devices late at night tend to report lower sleep satisfaction and reduced deep sleep. Daily routines also influence levels of daytime alertness. Alanazi *et al*. (2023) compared individuals with good and poor sleep hygiene and found significantly higher daytime sleepiness among those with irregular routines and excessive evening screen exposure. These findings are illustrated in Figure 3, which shows the difference in subjective alertness between the two groups.

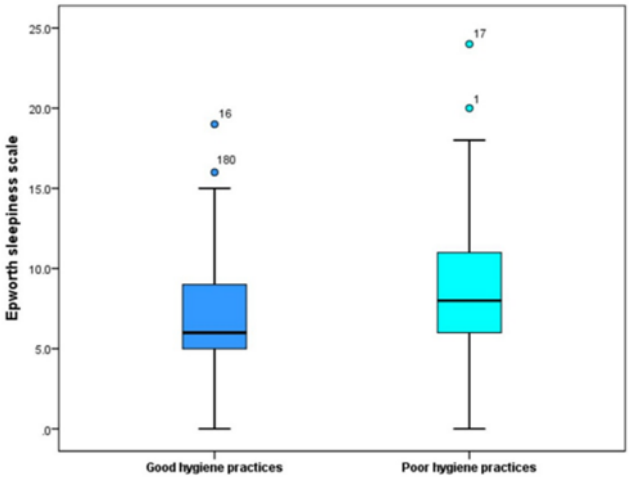

Figure 3. Differences in daytime sleepiness between students with good and poor sleep hygiene (Alanazi et al., 2023)

Taken together, these results confirm that behavioural factors represent one of the most accessible targets for improving sleep quality. Even small changes, such as reducing evening screen time or maintaining a consistent sleep schedule, can lead to more restful and continuous sleep.

3.3. Environmental conditions and sleep quality

Environmental factors create the physical context in which sleep occurs, influencing both its continuity and restorative value. Verhaert *et al*. (2011) underline that the environment must align with an individual's comfort needs, as otherwise even mild discomfort can disrupt sleep. Temperature shows a particularly strong effect: Okamoto-Mizuno and Mizuno (2012) found that even moderate nighttime warming increases body temperature and leads to lighter, more fragmented sleep a situation common in poorly ventilated rooms or during heat waves. Humidity additionally shapes thermal comfort. Basner *et al*. (2025) noted that higher humidity reduces total sleep duration, even if sleep efficiency remains unchanged. Noise also acts as a major disruptor, increasing wakefulness after sleep onset through micro-arousals that often go unnoticed. Lighting conditions also contribute to sleep quality. Grandner (2019) points out that evening exposure to artificial light, especially from electronic devices, delays melatonin release and interferes with the natural circadian rhythm. As a result, sleep onset is delayed and REM

sleep is reduced, often creating a cycle of late bedtimes and morning tiredness. Environmental factors affect sleep in different ways: temperature and humidity influence physical comfort, noise disrupts continuity and light regulates the timing of sleep onset. Even small deviations in these conditions can measurably alter sleep structure and next-day alertness. Since these influences often appear together, future research should focus on settings that better reflect real-life sleeping environments.

4. DISCUSSION AND CONCLUSION

Sleep quality develops through the combined action of several important influences that work together during the night. None of these factors can ensure good and restorative sleep on their own. A comfortable and well-designed mattress will not be enough if sleep habits are irregular, just as a quiet and pleasant bedroom cannot completely make up for poor support or discomfort caused by the mattress. Studies show that medium firm mattresses made from materials that evenly distribute pressure, such as viscoelastic foam and latex, help maintain proper spinal alignment and reduce the points of highest pressure on the body. This supports deeper and more restful sleep. Still, the feeling of comfort remains individual and depends on body weight, body shape and preferred sleep position. Daily routines strongly influence how easily sleep begins and how restorative it becomes. When sleep and wake times are inconsistent, when screens are used late at night or when stress is high, the body has more difficulty transitioning into the deeper phases of sleep. Environmental conditions then play a role in keeping sleep continuous. Even small changes in temperature, humidity or surrounding noise can interrupt sleep and reduce its quality, especially outside laboratory conditions where everything is controlled. Because of these combined effects, sleep should be understood as a process shaped by multiple factors that are closely connected. The mattress provides physical support, daily habits guide the body into sleep and the environment ensures that sleep is not disturbed. Improving sleep comfort therefore often requires changes in more than just one of these areas. The best results occur when ergonomic mattress features are matched with healthy routines and a well-adjusted sleeping environment. Future research that connects material design for mattresses with lifestyle habits and real conditions in bedrooms could lead to even more personalised and effective solutions for better sleep and long-term well being.

5. REFERENCES

Alanazi, Y.; Moussa, M.; Alzahrani, A.; Alghamdi, A., 2023: Bedtime habits and daytime sleepiness: The impact of sleep hygiene on university students. Journal of Sleep Health, 9 (2): 55-63.

Basner, M.; Smith, M. G.; Jones, C. W.; Ecker, A. J.; Howard, K.; Schneller, V.; Cordoza, M.; Kaizi-Lutu, M.; Park-Chavar, S.; Stahn, A. C.; Dinges, D. F.; Shou, H.; Mitchell, J. A.; Bhatnagar, A.; Smith, T.; Smith, A. E.; Stopforth, C. K.; Yeager, R.; Keith, R. J., 2025: Impact of PM2.5, relative humidity, and temperature on sleep architecture and arousals. Environmental Health Perspectives, 133 (2): 27002.

Chang, A.-M.; Aeschbach, D.; Duffy, J. F.; Czeisler, C. A., 2015: Evening use of light-emitting eReaders negatively affects sleep, circadian timing, and next-morning alertness. Proceedings of the National Academy of Sciences, 112 (4): 1232-1237.

D'Arienzo, M.; Picone, A.; Di Lorenzo, S., 2022: Aging behaviour of polyurethane foams with bio-based components. Polymer Testing, 105: 107-126.

Exelmans, L.; Van den Bulck, J., 2016: Bedtime mobile phone use and sleep disturbance in adolescents. Journal of Youth & Adolescence, 45 (1): 93-103.

Grandner, M. A., 2019: Sleep, health, and society: An introduction to social and behavioral sleep science. Oxford University Press.

Hu, L.; Zhang, X.; Wei, Y., 2025: Mattress firmness and polysomnographic sleep outcomes: A controlled laboratory trial. Sleep Science, 14 (1): 45-54.

Hong, C.-H.; Lin, Y.-C.; Wang, Y.-T., 2023: The influence of mattress stiffness on spinal curvature and comfort during sleep: A biomechanical evaluation. Journal of Healthcare Engineering, 2023: 6668123.

Irish, L. A.; Kline, C. E.; Gunn, H. E.; Buysse, D. J.; Hall, M. H., 2015: The role of sleep hygiene in promoting public health: A review of empirical evidence. Sleep Medicine Reviews, 22: 23-36.

Jacobson, B. H.; Gemmell, H. A.; Hayes, B. M.; Altena, T., 2009: Effectiveness of a selected bedding system on sleep quality and low back pain. Journal of Chiropractic Medicine, 8: 1-8

Kim, J.; Lee, H.; Park, S., 2023: Evening exercise and sleep: Timing matters. Journal of Sports Medicine & Physical Fitness, 63 (4): 612-620.

Kushida, C. A., 2013: Encyclopedia of sleep (Vols. 1–4). Academic Press.

Lee, H.; Moon, J.; Seo, K., 2022: Thermal comfort of mattress materials and its influence on sleep outcomes. Building and Environment, 226: 109-124.

Low, F.-Z.; Chua, M. C.-H.; Lim, P.-Y.; Yeow, C.-H., 2017: Effects of mattress material on body pressure profiles in different sleeping postures. Journal of Chiropractic Medicine, 16 (1): 1-9.

Okamoto-Mizuno, K.; Mizuno, K., 2012: Effects of thermal environment on sleep and circadian rhythm. Journal of Physiological Anthropology, 31 (1): 14-21.

Verhaert, V.; Haex, B.; De Wilde, T.; Berckmans, D., 2011: Sleep comfort and the design of bedding systems: Sleep posture and micro-environment. Applied Ergonomics, 42 (1): 66-75.

Vlaović, Z.; Klarić, N.; Domljan, D., 2024: Investigating the impact of long-term use on mattress firmness and sleep quality – Preliminary results. Applied Sciences, 14 (21): 10016.

Wei, Y.; Xu, J.; Miao, S.; Wei, K.; Peng, L.; Wang, Y.; Wei, X., 2022: Recent advances in the utilization of tea active ingredients to regulate sleep through neuroendocrine pathway, immune system and intestinal microbiota. Critical Reviews in Food Science and Nutrition, 63 (25): 7598-7626.

Wong, D. W.-C.; Fong, D. T.-P.; Li, W.-C., 2019: Ergonomic mattress design and spinal biomechanics: A review. Spine Journal, 19 (11): 1951-1963.

Evaluating Density Homogeneity in Beech Wood (*Fagus sylvatica* L.) Using Semi-Non-Destructive Resistance Drilling

Gačo Jež, Amina*; Humar, Miha[1]

[1] Department of Wood Science and Technology, Biotechnical Faculty, University of Ljubljana, Ljubljana, Slovenia
*Corresponding author: amina.gaco.jez@bf.uni-lj.si

ABSTRACT

Wood is one of the most important materials and its quality is of central importance for based industries. Choosing the right wood for specific purposes requires a thorough evaluation of its technological, physical and aesthetic properties. Among the physical properties, wood density is particularly important as it reflects the ratio of mass to volume at a given wood moisture content and strongly influences the properties of wood. Various non-destructive and semi-non-destructive methods have been developed to assess wood quality, including the resistant drilling (resistographic) method. With this method, we can quickly assess the density of the wood and detect internal defects. In this study, we focused on European beech (*Fagus sylvatica* L.), an economically important tree species in Slovenia and the wider region. The research aimed to determine whether there are statistically significant differences in wood density between measurement heights along the trunk and whether the resistograph can effectively detect internal structural defects. The results showed a trend towards increasing density with height, although the differences were not statistically significant, probably due to the small sample size. Nevertheless, the resistograph proved to be a reliable tool for the rapid and minimally invasive detection of density changes and possible internal trunk damage.

Key words: beech, density, *Fagus sylvatica* L., rezistograph

1. INTRODUCTION

Wood and wood-based materials have always been versatile materials used in many industries, from construction to furniture manufacturing and art (Ghorbanian Far *et al*., 2024). In Slovenia forests plays very important role. Forests cover 58.1 % of total area, making it the third most forested country in the EU (ZGS, 2025; EU, 2025). One of the most essential deciduous trees in European forests and the most widespread deciduous tree in Slovenia is the European beech (*Fagus sylvatica* L.) (Brus, 2012a). It plays an important role both for the wood-processing industry and for ecosystem services. Due to its mechanical properties, aesthetic appearance and processing properties, it is in high demand for the production of furniture, kitchen equipment, plywood, veneers, railway ties and other high-quality solid wood products (Brus, 2012b; Čufar, 2006). In the recent years even the composites for construction applications were developed, such as LVL. For this very reason, an accurate assessment of the quality of beech wood is crucial, not only in terms of commercial value, but also for the optimal utilization of the wood. The traditional categorization of logs into quality classes is mainly based on external assessment. Such an assessment includes the shape of the log, the presence of knots, color changes or other visible defects (Čufar, 2006). However, defects are not only found on the outside of the trunk. Many defects are found on the central part of the trunk, such

as rot, cracks, cavities or other types of degradation that remain hidden inside the trunk. Such damage significantly reduces the mechanical properties of the wood and limits further use (Čufar, 2006; Schwarze *et al*., 2000). For these reasons, it is becoming increasingly important to develop a methodology for quality assessment, based on non-destructive and semi-non-destructive methods that allow an insight into the internal structure of the wood during clasification. Wood density is one of the most important characteristics of wood (Rinn *et al*., 1996).

The method we use today, as a non-destructive and semi-non-destructive method to assess density is the resistograph method based on the resistance drilling. With the help of the resistograph, we can easily see the distribution of wood density through the cross-section of the trunk. There are several commercial applications of resistance drilling available, such as analysis of the density of layers, ring widths, estimating tree age, estimating wood density, estimating tree decay, and assessing the condition of structural wood (Johnstone *et al*., 2007; Schimleck *et al*., 2019; Yao *et al*., 2023). It is based on a simple and effective operating principle in which a thin steel drill bit is drilled into the wood. During drilling, the device records the exact energy required to penetrate the material, which is reflected as the resistance value of the wood. This data is closely related to the density and hardness of the wood and clearly shows the uniformity or defects in the internal structure of the wood (Rinn *et al*., 1996). Due to its accuracy, speed and minimal invasiveness, the method is used in forestry, wood processing, heritage science, construction industry and tree care to assess the quality and safety of wood.

The objective of the respective work is to describe the suitability of the respective method to asses the density variation at beech. Till now, the method has been predominantly applied to the conifers, like Norway spruce and Radiata pine, while this is up to our best knowledge, the first attempt to apply this method on beech wood.

2. MATERIALS AND METHODS

2.1. Description of the study area

In our study, we wanted to show whether there are large differences in the wood density measured with a resistograph at different log heights. The sample we used for our study was a log of European beech (*Fagus sylvatica* L.) with a length of 1.40 m and a diameter of 36 cm. There were no visible defects on the outside. However, a red heart was visible on the inside of the cross-section. After felling, the log was air-dried in a natural environment under a roofin March 2025 for 14 days. The average daily temperature was 8.6 °C, the average maximum temperature was 14.4 °C and the average minimum temperature was 4.2 °C. The total amount of precipitation during the 14-day dry period was 177 mm (ARSO, 2025). However, it should be considered, that the wood was not exposed to precipitations.

2.2. Resistograph analysis

The drilling resistance method is a non-destructive and semi-destructive method. It is suitable for detecting internal wood damage such as cracks, rot and other internal changes in

the wood structure. Healthy wood has significantly higher drilling resistance values (higher density profile) than the values measured in damaged wood.

The resistographic method was used to analyse changes in density and internal wood structure. The analysis with the resistograph was carried out on a European beech wood according to the instructions for use supplied with the device. Two boreholes were drilled at three heights of the wood. Thus, 6 analyses were carried out with a resistograph at each height. We used IML-RESI PowerDrill 500 device. The holes were drilled at three different heights along the wood, at 30, 60 and 120 cm, each in a horizontal direction at an angle of 90°. Two repetitions were carried out at each height. The device used a steel needle with a diameter of 1.5 mm, a constant speed of 1500 min^{-1} and a feed rate of 40 cm/min. The drilling depth was set to 300 mm. The free platform ResiProcessor (GeofgDownes, 2025) was used to collect data from the resistograph (GeofgDownes, 2025).

Figure 1. Resistograph method of beech (Fagus sylvatica L.)

3. RESULTS

3.1. Data analysis

The data analysis was carried out with the statistical program JASP 0.19.3.0. Data from the ResiProcesor program (OWDensity) obtained with a resistograph were used. We had two replicates per height. Descriptive statistical analysis of wood density measurements at different heights (30 cm, 60 cm and 120 cm) showed differences in median values and variability between groups. At a height of 30 cm, the median density value was 527.65 kg/m³ with a very low standard deviation (2.33), indicating a high degree of homogeneity in the measurements. The interquartile range was also narrow, which further confirms the low dispersion of the data.

At a height of 60 cm, the median was slightly higher (529.05 kg/m³), while the variability of the results also increased (standard deviation 7.00). The interquartile range increased, indicating a greater diversity of wood density at this height.

The highest density values were measured at a height of 120 cm, where the median was 550.75 kg/m³. This height differs significantly from the other two, as it not only has a higher average density, but also much greater variability between measurements (standard deviation

20.15). The interquartile range was the largest, indicating a wider range of density values, probably due to the greater influence of anatomical differences in wood structure.

Table 1. Descriptive statistic of wood density for three different height

Height, cm	30	60	120
Valid measurements	2	2	2
Median	527.65	529.05	550.75
Standard deviation	2.33	7.000	20.153

We conducted an additional post-hoc test to analyse the differences between the samples and did not confirm them as statistically significant. On this basis, we have no evidence that any of the groups differ from each other.

Table 2. Post Hock test for wood density for three different height

		Mean difference	SE	df	t	p_{tukey}
30	60	-1.400	12.391	3	-0.113	0.993
	120	-23.100	12.391	3	-1.864	0.292
60	120	-21.700	12.391	3	-1.751	0.324

The results are also graphically presented using a boxplot diagram (Figure 2), which clearly illustrates the increase in median density with increasing measurement point on the trunk. The boxes with whiskers at 30 cm and 60 cm are quite narrow, confirming low variability, while at 120 cm they are significantly wider, corresponding to the high dispersion of the measured values. It is also evident that the density values increase systematically with height, which may indicate changes in the structure of the wood along the trunk or the presence of specific anatomical changes.

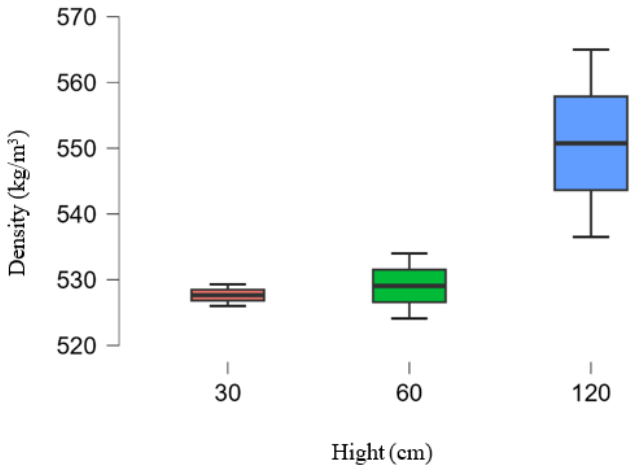

Figure 3. Box plot analysis of density obtained at three different heights using a resistograph

The values obtained in this study align closely with published basic density values for European beech, which typically average around 575 kg/m³. By contrast, air-dry density at 12%

moisture content is generally reported between 700 and 780 kg/m³ (Pretzsch *et al*., 2018). Oven dry density corresponds rather well to resistograph assesed density.

Resistographic methods have been shown to correlate strongly with gravimetric density, but intra-stem variations and instrument-specific factors influence absolute values . Furthermore, literature on vertical density trends in beech suggests that density often decreases with stem height, although site conditions and tree age can reverse this pattern . The observed higher median density at 120 cm, together with increased variability, fits within this known variability and may reflect localized anatomical transitions (Arnič *et al*., 2021).

The resistographic results demonstrate that beech wood density in the lower stem is relatively homogeneous, while upper sections show greater heterogeneity. The absolute values obtained are consistent with reported basic density ranges, confirming the suitability of resistography for non-destructive density profiling. Comparison with literature highlights the importance of calibration and contextual interpretation, particularly when relating resistograph data to air-dry density values commonly reported for beech.

3.2. Resistograph data analysis

The following section shows the profiles of the resistograph versus rotation and wood density at different height. The resistograph (Figures 3, 4 and 5) shows a graphical representation of the energy consumed by the electric motor when producing a sample with a drill at constant speed. Given the internal composition of the wood, it is thus possible to determine a series of variables that relate the properties of the material to the amount of energy consumed at a given time. The rest of this article shows the drilling resistance profiles and the density of the resistograph at different heights of the log.

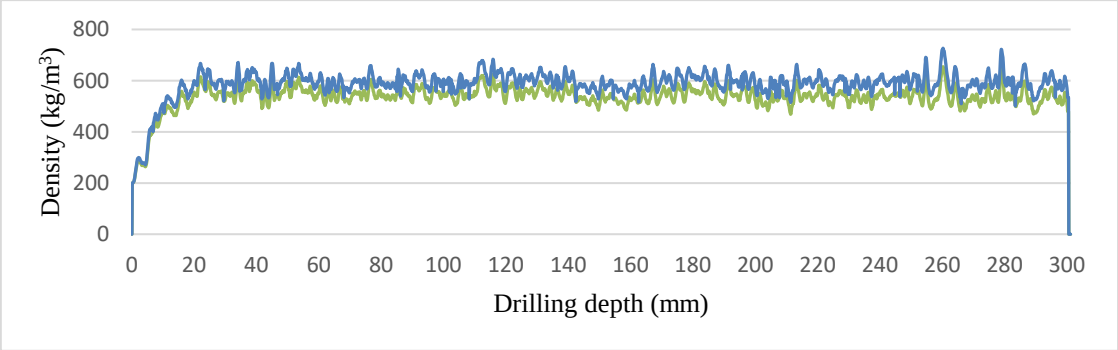

Figure 4. Density analysis obtained at a height of 30 cm using a resistograph

The drilling results at a height of 30 cm are shown in Figure 3. The drilling resistance curve and the displacement curve show no signs of error. After drilling to a depth of 30 cm, the needle leaves the tree and both curves drop. The highest density (654.36 kg/m^3) is found at a depth of 26 cm. The lowest density is expected in the bark area.

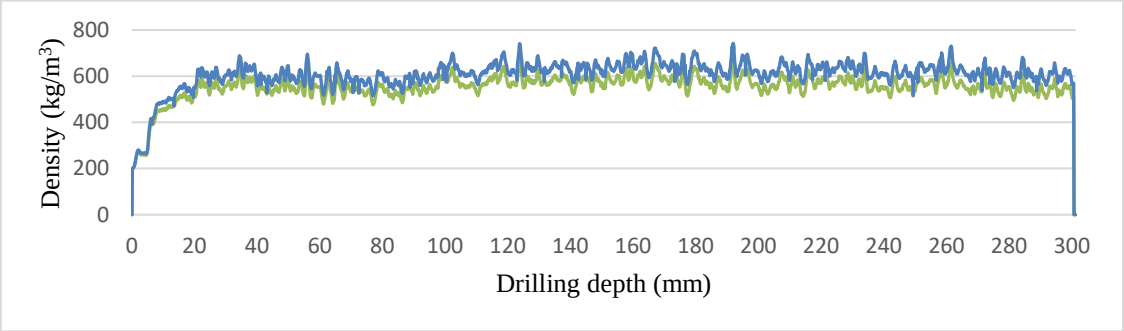

Figure 5. Density analysis obtained at a height of 60 cm using a resistograph

The drilling results at a height of 60 cm are shown in Figure 4. The drilling resistance curve and the displacement curve show no signs of error. After drilling to a depth of 30 cm, the needle leaves the tree and both curves drop. The highest density (674.28 kg/m^3) is found at a depth of 12 cm. The lowest density is expected in the bark area.

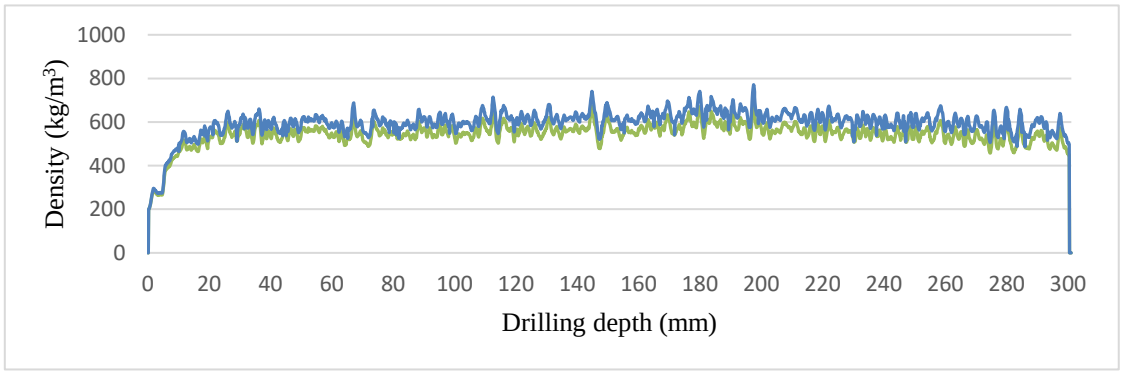

Figure 6. Density analysis obtained at a height of 120 cm using a resistograph

The drilling results at a height of 120 cm are shown in Figure 5. The drilling resistance curve and the displacement curve show no signs of error. After drilling to a depth of 30 cm, the needle leaves the tree and both curves drop. The highest density (697.23 kg/m^3) is found at a depth of 19 cm. As expected, the lowest density is found in the bark area.

4. CONCLUSION

The non-destructive and semi-non-destructive method with the resistograph can be used to estimate the wood density and to monitor the internal properties of the wood. The results of this study show that the densities do not vary greatly depending on the measurement height. It should also be noted that the sample size of the study is small. A larger number of samples should be taken in future investigations.

Acknowledgements: We The Slovenian research and Innovation Agency (ARIS) 's financial support within the research programme P4-0015 (Wood and lignocellulosic composites), research project J7-50231 (GROWTH), and the Infrastructure Centre (IC LES

PST 0481-09) is accredited. This work was supported by the WoodInnovate project, implemented within the farmwork of Interreg V-A Italy-Slovenia cooperation programme and co-financed by the European Community.

5. REFERENCES

Arnič, D.; Humar, M.; Kržišnik, D., Krajnc, L.; Prislan, P., 2021: Gostota lesa—Metode določanja in pomen pri razvoju gozdno lesnega biogospodarstva. Acta Silvae et Ligni, 124, 1-11. https://doi.org/10.20315/ASetL.124.1

Čufar, K., 2006: Anatomija lesa: [Univerzitetni učbenik]. Biotehniška fakulteta, Oddelek za lesarstvo, Ljubljana, 185.

Ghorbanian Far, M.; Najafian Ashrafi, M.; Shaabani Asrami, H.; Amiri Moghadam, Y.; Bari, E., Niemz, P.; Hosseinpourpia, R.; Ribera, J., 2024: Physical and mechanical properties of different beech wood species grown at various climate conditions. Holzforschung, 78 (7): 377-386. https://doi.org/10.1515/hf-2023-0117

Johnstone, D. M.; Ades, P. K.; Moore, G. M.; Smith, I. W., 2007: Predicting Wood Decay in Eucalypts Using an Expert System and the IML-Resistograph Drill. Arboriculture & Urban Forestry (AUF), 33 (2): 76-82. https://doi.org/10.48044/jauf.2007.009

Pretzsch, H.; Biber, P.; Schütze, G.; Kemmerer, J.; Uhl, E., 2018: Wood density reduced while wood volume growth accelerated in Central European forests since 1870. Forest Ecology and Management, 429: 589-616. https://doi.org/10.1016/j.foreco.2018.07.045

Rinn, F.; Schweingruber, F.-H.; Schär, E., 1996: RESISTOGRAPH and X-Ray Density Charts of Wood. Comparative Evaluation of Drill Resistance Profiles and X-ray Density Charts of Different Wood Species. Holzforschung, 50 (4): 303-311. https://doi.org/10.1515/hfsg.1996.50.4.303

Schimleck, L.; Dahlen, J.; Apiolaza, L. A.; Downes, G.; Emms, G.; Evans, R.; Moore, J.; Pâques, L.; Van den Bulcke, J.; Wang, X., 2019: Non-Destructive Evaluation Techniques and What They Tell Us about Wood Property Variation. Forests, 10 (9): 9. https://doi.org/10.3390/f10090728

Schwarze, F. W. M. R.; Engels, J.; Mattheck, C., 2000: Fungal strategies of wood decay in trees. Springer.

Yao, J.; Wu, Z.; Zheng, Y.; Rao, B.; Li, Z.; Hu. Y.; Nie, B., 2023: Design of a Tree Micro Drill Instrument to Improve the Accuracy of Wood Density Estimation. Forests, 14 (10): 10. https://doi.org/10.3390/f14102071

***ARSO, 2025: ARHIV-opazovani in merjeni meteorološki podatki po Sloveniji. https://meteo.arso.gov.si/met/sl/weather/

***EU, 2025, March 31: The European Union and forests | Fact Sheets on the European Union | European Parliament. https://www.europarl.europa.eu/factsheets/en/sheet/105/the-european-union-and- forests

***Zavod za gozdove Slovenije, 2025. Gozdovi Slovenije—Zavod za gozdove Slovenije. Retrieved July 14, 2025. https://www.zgs.si/gozdovi-slovenije/

Prediction of Fatigue Life in Spruce Wood using Resonance Frequency Analysis

Gaberšček Tuta, Gregor*; Fajdiga, Gorazd; Straže, Aleš[1]

[1] Department of Wood Science and Technology, Biotechnical Faculty, University of Ljubljana, Ljubljana, Slovenia
*Corresponding author: gregor.gaberscektuta@bf.uni-lj.si

ABSTRACT

An alternative method for predicting the fatigue life of wood was investigated due to the low accuracy of conventional prediction techniques. Damaged material invariably exhibits a lower resonance frequency than undamaged material because of its reduced stiffness. We conducted a low-cycle fatigue test on a single spruce wood specimen and monitored its resonance frequency. The collected data were used to predict fatigue life using between 40 % and 100 % of the monitored data. A Weibull cycle density distribution was applied to the predictions. Consequently, the predicted number of cycles with the highest probability was selected. The measured stiffness reduction in spruce wood was 35 Hz, or 6%, which is lower than that observed in similar materials. The prediction error decreased monotonically with the amount of resonance frequency data used for fatigue life prediction, reaching its lowest value of 1% when the full monitored dataset was employed. The proposed fatigue life prediction method demonstrated potential as an alternative to conventional methods. However, it should be further validated with a larger sample size, as fatigue is inherently a statistical phenomenon.

Key words: spruce wood, fatigue life prediction, resonance frequency, Weibull distribution

1. INTRODUCTION

The properties of undamaged and damaged materials in terms of resonance frequency have been extensively researched through review (Caicedo *et al*., 2021) beam damage assessments (Gillich *et al*., 2022), damage identification studies (Dubey *et al*., 2020), evaluations of mechanical properties (Kouroussis *et al*., 2017) and investigations of resonance frequency changes (De Paz *et al*., 2019; Horta-Rangel *et al*., 2008; Negru *et al*., 2015). A common finding is that undamaged materials exhibit higher resonance frequencies than damaged materials due to their greater stiffness. Material fatigue, resulting from the accumulation of damage, leads to a progressive reduction in stiffness and ultimately to failure. Consequently, the resonance frequency of a material is frequently used as a key parameter for monitoring its condition and predicting the development of fatigue damage. Modal analysis has already demonstrated its utility in studying the fatigue of steel (Shang, 2003; Shang, 2009; Wang *et al*., 2009), aluminium alloys (Banks and Emeric, 1998) and composite materials (Kessler *et al*., 2002; Liang *et al*., 2024; Wu *et al*., 2020); however, research in this area is less developed for wood.

For wood exhibiting complex anisotropic properties, predicting the time to failure using conventional methods is less successful, as noted by (Šraml *et al*., 2019) in a review of wood fatigue life models. Multiple studies by Klemenc (2022; 2023) indicate low predictive success due to small test populations. Others have highlighted a lack of generalisation in current wood

fatigue life prediction models (Clorius *et al*., 2009; Kolesnikov and Nazarev, 2023). Previous research has demonstrated that cracks and lower density in wood affect resonance frequency and damping (Negru *et al*., 2015; Shah *et al*., 2020). Modal analysis has been successfully employed to predict the development of fatigue damage in glued joints (Khoshmanesh *et al*., 2020) and polymer composites (Bedewi and Kung, 1997), suggesting the potential of this approach for studying wood. While the Weibull distribution has been used to model fatigue in metallic and composite systems (Barraza-Contreras *et al*., 2020), its application in resonance-based fatigue monitoring for wood has not yet been reported.

Existing studies have focused on changes in modal parameters during the fatigue of materials such as concrete, metals, and composites (Ibrahim, 1977; Z. Wang *et al*., 2012). These studies have found that a decrease in resonance frequency correlates with the accumulation of damage and the growth of cracks, enabling real-time monitoring of material condition. For example, the study by Bedewi (1997) demonstrated that resonance frequency is a reliable indicator of crack growth in polymer composites; however, similar studies are scarce for wood-based materials.

The aim of this study was to develop a method for monitoring the dynamic properties of spruce wood under low-cycle fatigue and to evaluate the usefulness of modal parameters in predicting fatigue life. By investigating changes in resonance frequency, we sought to determine whether it is possible to accurately predict the number of cycles to failure based on early measurements. This approach could make a significant contribution to the development of methods for monitoring the condition of timber structures and enhancing their safety and durability under real-world conditions.

2. MATERIALS AND METHODS

We used clear spruce (*P. abies*) wood samples measuring 380 mm in length with a cross-section of 15 mm × 15 mm. Four specimens were employed to determine the static bending strength while one specimen was used as an example for the fatigue life prediction method proposed in this study. The specimens for both static and dynamic tests were stored for one month under standard conditions at 20 °C and 65 % relative humidity. The mean moisture content of all specimens was 12.8 % with a coefficient of variation of 3.5 %. The moisture content of the fatigue specimen was 13 %. These values comply with the standard conditioning procedures outlined in ISO 3129 (ISO Standards, 2019). The mean density of all specimens was 416.4 kg/m^3 and 430.5 kg/m^3 for the fatigue specimen. The coefficient of variation of density was 9.3 %. The test was conducted using a Zwick 1464 mechanical universal testing machine (ZwickRoell GmbH, Ulm, Germany). It was adapted for fatigue testing by incorporating a unit to control the dynamic mechanical excitation (PCI-6024E; National Instruments, Austin, USA) and to record the response signal (PCB-130E20; PCB Piezotronics, Walden, USA). The loading cycle, mechanical excitation, and response signal recording were automated to ensure the most consistent test conditions possible. The data obtained on resonance frequencies and number of cycles were used to predict fatigue life.

2.1. Experiment setup

The distance between the supports was adjusted according to the length of the specimen. The first vibration mode was determined using the expression $k_1L = 4.73$, which was used to calculate the distance between the supports as 210 mm according to (Gaberšček Tuta *et al*., 2025). A schematic of the experimental setup is shown in (Figure 1*)*.

Cyclic loading with a dynamic load ratio of 0 was applied using a universal testing machine. For each loading cycle, once the loading tool had reached the starting position and the specimen was unloaded, mechanical excitation was applied to the specimen's free end. A small wooden hammer, driven by an electromagnet, was used for this purpose. Simultaneously, the response signal was recorded using a microphone attached to the opposite end of the specimen. The response signal was recorded for 1.1 seconds and was used to determine the resonance frequency of the specimen's first vibration mode via fast Fourier transformation. The subsequent loading cycle then commenced.

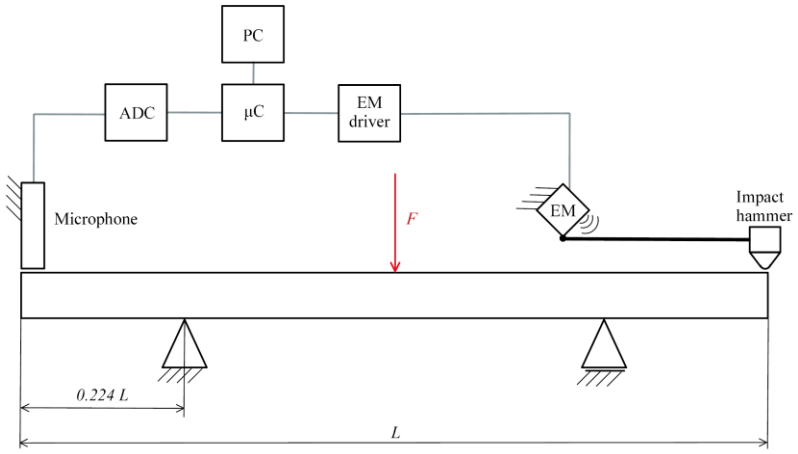

Figure 1. Test setup for static fatigue bending tests and vibration resonance analysis: specimen, microphone, analogue-to-digital converter (ADC), microcontroller (µC), personal computer (PC), hammer, electromagnet (EM), and electromagnet driver.

Prior to conducting the cyclic fatigue test, static bending tests were performed to determine the specimens' static bending strength. The mean static bending strength was 82.5, MPa with a coefficient of variation of 10.6 %. For the low-cycle fatigue tests, the maximum force was set to 800 N, corresponding to 90 % of the mean static bending strength. The value of 90 % was selected based on preliminary tests to ensure low-cycle fatigue behaviour, as described in the literature on the fracture of brittle wood during cyclic bending (Klemenc and Fajdiga, 2022; Šraml *et al*., 2019) and on stiffness changes during fatigue loading (Ogawa et al., 2017). The force sensor was calibrated and the starting position was set to approximately 1 mm above the specimen. The microphone and hammer were positioned at an appropriate distance from the specimen surface, as illustrated in (Figure 2*)*.

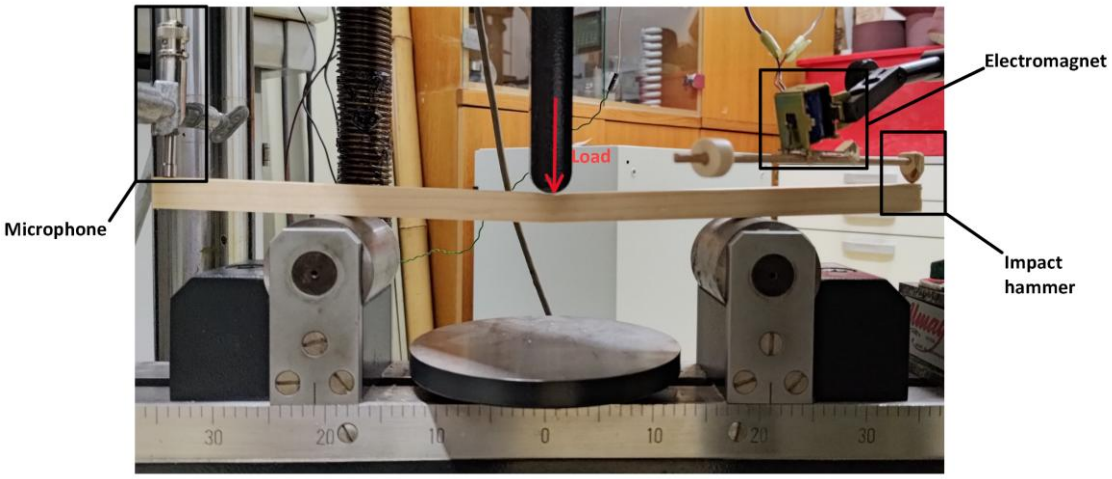

Figure 2. Experiment setup.

The cyclic loading was conducted at a rate of 10 mm/min or at a frequency of 0.015 Hz. The test concluded when the specimen's strength had diminished to the point that it could no longer withstand the specified load and failed completely.

2.2. Data Analysis

We predicted fatigue life using a linear approximation for each segment of the resonance frequency data. We began with the first three values and calculated the predicted number of cycles based on the slope of the linear approximation, the initial values, and the limit values. With each additional data point, both the slope of the approximation and the predicted fatigue life were updated. For the limit values, we selected the lowest values of the resonance frequency derived from the linear approximation. We used the predicted number of cycles at various points in the data to predict the specimen's fatigue life. Three different approaches were employed: in the first, simpler method, the slope of the linear approximation was used for a specific data portion; in the second simple method, the mean value of the predicted number of cycles was calculated; in the third method, we analysed the predicted number of cycles using the Weibull cycle density distribution.

2.2.1. Weibull cycle density distribution

From all the predicted numbers of cycles to failure, we predicted the fatigue life of the tested specimen using only a portion of the data, applying the Weibull cycle density distribution. The objective was to determine the number of cycles to failure as accurately as possible from minimal data or cycles. After each new cycle, we obtained a new prediction based on the drop in frequency; these predictions were then statistically analysed using the Weibull cycle distribution density (c.d.d.) as described in Equation (1) (Weibull, 1939). The parameters θ and β of the Weibull c.d.d. were determined using Benard's approximation (Benard and Bos-Levenbach, 1955). For this approximation, it is necessary to index the predicted number of cycles with the index i and calculate the median rank P_i according to Equation (2). In this equation, n_i represents the total number of predictions. The predicted values must be sorted from the smallest to the largest value N_s, and then a linear regression must be performed to find the linear curve that best fits the data. The points X and Y are calculated according to Equations

(3) and (4). The parameters of the linear curve equation k and n are used to determine the parameters of the Weibull c.d.d. θ and β according to Equations (5) and (6).

$$f(N) = \frac{\beta}{\theta}\left(\frac{N}{\beta}\right)^{\beta-1} e^{-\left(\frac{N}{\beta}\right)^{\beta}} \quad (1)$$

$$P_i = \frac{i-0.3}{n_i+0.4} \quad (2)$$

$$X = \ln\left(-\ln(1-P_i)\right) \quad (3)$$

$$Y = \ln(N_s) \quad (4)$$

$$\beta = k \quad (5)$$

$$\theta = e^{-\frac{n}{k}} \quad (6)$$

3. RESULTS AND DISCUSION

3.1. Fatigue life prediction

We compared linear and cubic approximation of the resonance frequency data as shown on (Figure 3*)*. The decrease in resonance frequency from the start to the end of fatigue is approximately 35 Hz, or 6 %. Relative difference between goodness of fit for linear and cubic approximations is 0.35 %. We used only linear approximations for fatigue life prediction because they are more stable when working with a smaller dataset. Cubic approximations were not employed, as the difference in data deviation between linear and cubic methods is negligible.

The variable employed in the fatigue life prediction methods was resonance frequency (ω). The results of all three methods, along with the corresponding errors, are presented in Table 1. According to the first method, the best prediction, based on 40 % of the data, is from ω, but it is not conservative. The second fatigue life prediction method yields the lowest relative error (Err_{avg}) when ω is used and is also conservative. In the third and more complex method for predicting fatigue life, it was necessary to determine the number of cycles at which the theoretical distribution attains its maximum value.

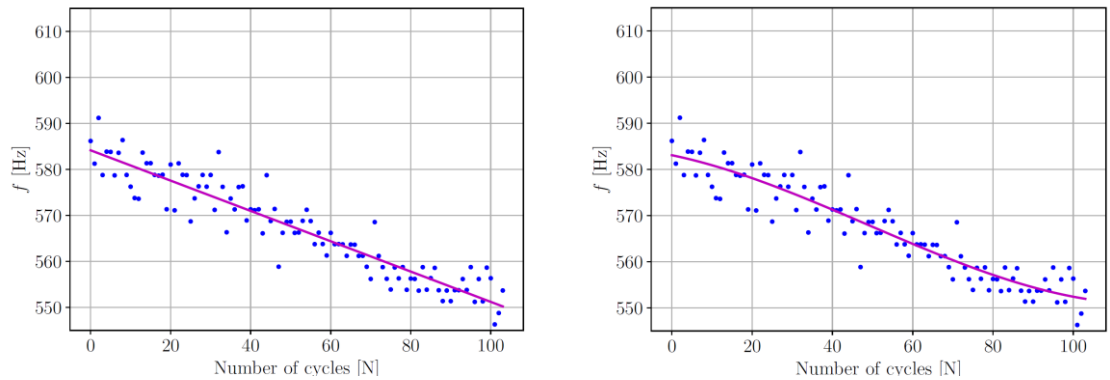

Figure 3. Approximation of resonance frequency. (a) Linear approximation, (b) cubic approximation.

Table 1 presents the parameters of the Weibull c.d.d. equation - namely θ_{40}, β_{40}, for 40 % of the data, and θ_{100}, β_{100}, for 100 % of the data - along with the predicted number of cycles and the corresponding relative errors (Err_{w40}, Err_{w100}). The theoretical distribution of the predicted number of cycles, derived from ω at 40 % and 100 % of the data, resembles an approximately Gaussian curve, as illustrated in (Figure 4*)*. The prediction is conservative for both data portions and is the most accurate when using the full dataset. However, with a smaller portion of data, the prediction is less accurate than that obtained by the first method.

Table 1. Fatigue life prediction using 40 % and 100 % of the data with the Weibull c.d.d. (N_{w40}, N_{w100}), using slope method, (N_{40}) and using an average value from all data (N_{avg}).

	θ_{40}	β_{40}	N_{w40}	Err_{w40}	N_{40}	Err_{40}	θ_{100}	β_{100}	N_{w100}	Err_{w100}	N_{avg}	Err_{avg}
ω	101.9	3.18	90	15.1	118	11.3	110.3	4.4	105	0.94	99	6.6

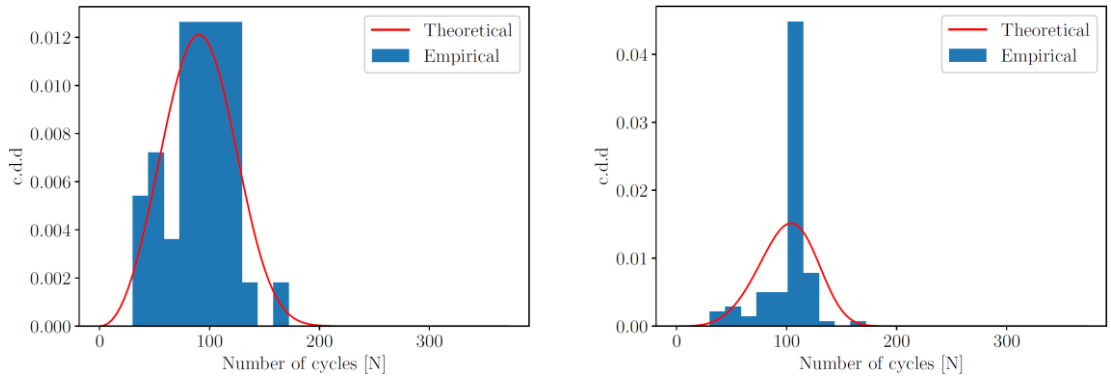

Figure 4. Weibull c.d.d of the predicted number of cycles based on resonance frequency data. (a) 40 % of data, (b) full dataset.

The adequacy of the third prediction method was assessed by monitoring the relative error across various data portions employed for the prediction. (Figure 5*)* illustrates the relative error as a function of the portion of data used for fatigue life prediction. The error as a function of the data portion remains relatively small and decreases monotonically. Although the error is not the smallest for a medium portion of the data, ω is a suitable data type for predicting fatigue life.

The results of this study highlight the importance of monitoring the dynamic properties of wood, such as resonance frequency, to understand the fatigue process and predict the material's fatigue life. We found that resonance frequency is sensitive and reliable parameter for monitoring the fatigue of wood. The linear decrease in resonance frequency with an increasing number of cycles confirms its utility as an indicator of the material's stiffness reduction. This trend aligns with the findings of Bedewi (1997), who also observed a 25 % decrease in resonance frequency in polymer composites. Similar decreases in resonance frequency have been reported for other composites (Abo-Elkhier *et al.*, 2014; Wu *et al.*, 2020). For wood, the relative decrease in resonance frequency (6 %) was lower than that observed in some other materials, indicating reduced sensitivity to cyclic loading. In spot-welded steel plates, (Wang *et al.*, 2009) also reported a decrease in resonance frequency of approximately 6 %.

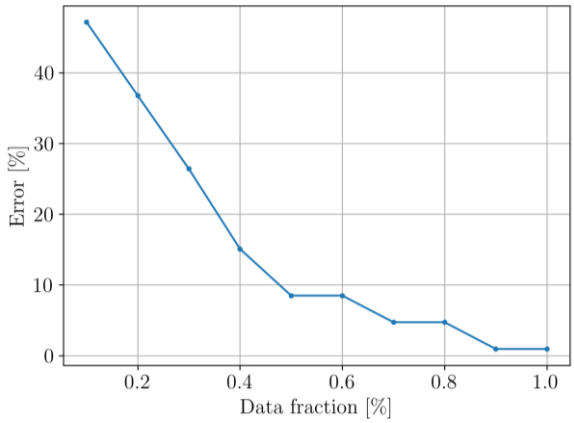

Figure 5. Relative error in correlation with data fraction used for fatigue life prediction using Weibull c.d.d.

The analysis using the Weibull cycle density distribution demonstrated that this method enables efficient and accurate prediction of the fatigue life of wood. The possibility of predicting fatigue life by monitoring resonance frequency during fatigue was described by (Wang *et al*., 2009). The Weibull distribution has also been employed to model the statistical distribution of the number of cycles, as reported by (Barraza-Contreras *et al*., 2020). To our knowledge, the combination of resonance frequency monitoring and the Weibull distribution has not yet been applied to fatigue life prediction of wood. Our investigations have shown that the prediction error is less than 1 % when the entire dataset is utilised. Using an example, we demonstrate that the proposed method has the potential to be one of the most accurate approaches for predicting the fatigue life of wood.

One of the primary limitations of this study is the small number of test samples, which may affect the generalisability of the results. Extending the investigation to include other wood species and a larger number of specimens would allow for better validation of the proposed method, as also noted by (Wang *et al*., 2012), who investigated the fatigue life of wood composites. It would also be beneficial to examine the effects of different types of loading and environmental factors, such as humidity and temperature, on the dynamic properties of wood. The results demonstrate significant potential for the practical application of modal analysis in monitoring the structural health of timber structures. Real-time monitoring of resonance frequency, as proposed by (Omar *et al*., 2023), could enable early detection of damage and help prevent critical failures. However, in practice, structural timber often contains natural defects such as knots and cracks that affect its physical and mechanical properties. Further investigation of the proposed method is required to confirm its practical utility. It is important to emphasise that the proposed method has currently only been validated for homogeneous, clear spruce wood samples. Its applicability to more heterogeneous or defective wood species - where wave propagation behaviour may vary due to local density changes or structural discontinuities - remains to be explored. Therefore, the method should presently be considered case-specific rather than universal.

4. CONCLUSION

Research has shown that modal analysis, particularly resonance frequency monitoring, can be a reliable method for predicting the fatigue life of wood under low-cycle fatigue. Resonance frequency has been identified as a reliable parameter as its linear decrease accurately reflects the reduction in material stiffness. The Weibull cycle density distribution provided accurate predictions with an error of less than 1 %, confirming the effectiveness of this approach.

Modal analysis holds significant potential for monitoring the mechanical condition of timber structures, as it facilitates non-destructive, real-time assessment of material integrity. A limitation of this study is the use of a single fatigue specimen, which restricts the statistical generalisability of the results. Further research should incorporate a larger number of samples, various wood species, and an examination of the effects of environmental factors. This approach offers a promising solution for enhancing the monitoring of fatigue life and the safety of timber structures.

Acknowledgements: This research was funded by the Slovenian Research Agency "ARRS" in the framework of the Research Programs "Development Evaluation P2-0182" and "Forest-wood value chain and climate change: transition to circular bioeconomy P4-0430."

5. REFERENCES

Abo-Elkhier, M.; Hamada, A. A.; Bahei El-Deen, A., 2014: Prediction of fatigue life of glass fiber reinforced polyester composites using modal testing. International Journal of Fatigue, 69: 28-35. https://doi.org/10.1016/j.ijfatigue.2012.10.002

Banks, H. T.; Emeric, P. R., 1998: Detection of Non-Symmetrical Damage in Smart Plate-Like Structures. Journal of Intelligent Material Systems and Structures, 9 (10): 818-828. https://doi.org/10.1177/1045389X9800901005

Barraza-Contreras, J. M.; Piña-Monarrez, M. R.; Molina, A., 2020: Fatigue-Life Prediction of Mechanical Element by Using the Weibull Distribution. Applied Sciences, 10 (18): 6384. https://doi.org/10.3390/app10186384

Bedewi, N. E.; Kung, D. N., 1997: Effect of fatigue loading on the modal properties of composite structures and its utilization for prediction of residual life. Composite Structures, 37 (3-4): 357-371. https://doi.org/10.1016/S0263-8223(97)00028-7

Benard, A.; Bos-Levenbach, E. C., 1955: The Plotting of Observations on Probability-paper. Stichting Mathematisch Centrum. Statistische Afdeling.

Caicedo, D.; Lara-Valencia, L. A.; Brito, J., 2021: Frequency-based methods for the detection of damage in structures: A chronological review. DYNA, 88 (218): 203-211.

Clorius, C. O.; Pedersen, M. U.; Hoffmeyer, P.; Damkilde, L., 2009: An experimentally validated fatigue model for wood subjected to tension perpendicular to the grain. Wood Science and Technology, 43 (3): 343-357. https://doi.org/10.1007/s00226-009-0244-7

De Paz, L. V. G.; Ortega, N. F.; Rosales, M. B., 2019: Assessment of wood utility poles' deterioration through natural frequency measurements. Journal of Civil Structural Health Monitoring, 9 (1): 53-61. https://doi.org/10.1007/s13349-018-0314-3

Dubey, A.; Denis, V.; Serra, R., 2020: A damage identification strategy in beams based on natural frequencies shift. International Conference on Noise and Vibration Engineering (ISMA 2020), Leuven, Belgium.

Gaberščček Tuta, G.; Fajdiga, G.; Straže, A., 2025: Initial Insights into Spruce Wood Fatigue Behaviour Using Dynamic Mechanical Properties in Low-Cycle Fatigue. Forests, 16 (8): 1324. https://doi.org/10.3390/f16081324

Gillich, N.; Tufisi, C.; Sacarea, C.; Rusu, C. V.; Gillich, G.-R.; Praisach, Z.-I.; Ardeljan, M., 2022: Beam Damage Assessment Using Natural Frequency Shift and Machine Learning. Sensors, 22 (3): 3. https://doi.org/10.3390/s22031118

Horta-Rangel, J.; Carmona, S.; Castaño, V. M., 2008: Shift of natural frequencies in earthquake-damaged structures: An optimization approach. Structural Survey, 26 (5): 400-410. https://doi.org/10.1108/02630800810922748

Ibrahim, S. R., 1977: Random Decrement Technique for Modal Identification of Structures. Journal of Spacecraft and Rockets, 14 (11): 696-700. https://doi.org/10.2514/3.57251

Kessler, S. S.; Spearing, S. M.; Atalla, M. J.; Cesnik, C. E. S.; Soutis, C., 2002: Damage detection in composite materials using frequency response methods. Composites Part B: Engineering, 33 (1): 87-95. https://doi.org/10.1016/S1359-8368(01)00050-6

Khoshmanesh, S.; Watson, S. J.; Zarouchas, D., 2020: Characterisation of fatigue damage in a thick adhesive joint based on changes in material damping. Journal of Physics: Conference Series, 1618 (2): 022058. https://doi.org/10.1088/1742-6596/1618/2/022058

Klemenc, J.; Fajdiga, G., 2022: Statistical Modelling of the Fatigue Bending Strength of Norway Spruce Wood. Materials, 15 (2): 2. https://doi.org/10.3390/ma15020536

Klemenc, J.; Humar, M.; Fajdiga, G., 2023: Influence of insect damage to the fatigue life of an old larch wood. Construction and Building Materials, 375: 130976. https://doi.org/10.1016/j.conbuildmat.2023.130976

Kolesnikov, G. N.; Nazarev, D. P., 2023: Monotonic and cyclic load of pine wood under uniaxial compression: Experiments and modeling. E3S Web of Conferences, 458: 07021. https://doi.org/10.1051/e3sconf/202345807021

Kouroussis, G.; Ben Fekih, L.; Descamps, T., 2017: Assessment of timber element mechanical properties using experimental modal analysis. Construction and Building Materials, 134: 254-261. https://doi.org/10.1016/j.conbuildmat.2016.12.081

Liang, Z.; Ramakrishnan, K. R.; Ng, C.-T.; Zhang, Z.; Fu, J., 2024: Vibration-based prediction of residual fatigue life for composite laminates through frequency measurements. Composite Structures, 329: 117771. https://doi.org/10.1016/j.compstruct.2023.117771

Negru, I.; Gillich, G. R.; Praisach, Z. I.; Tufoi, M.; Gillich, N., 2015: Natural frequency changes due to damage in composite beams. Journal of Physics: Conference Series, 628: 012091. https://doi.org/10.1088/1742-6596/628/1/012091

Ogawa, K.; Shimizu, K.; Yamasaki, M.; Sasaki, Y., 2017: Fatigue behavior of Japanese cypress (*Chamaecyparis obtusa*) under repeated compression loading tests perpendicular to the grain. Holzforschung, 71 (6): 499-504. https://doi.org/10.1515/hf-2016-0227

Omar, I.; Khan, M.; Starr, A., 2023: Suitability Analysis of Machine Learning Algorithms for Crack Growth Prediction Based on Dynamic Response Data. Sensors, 23 (3): 1074. https://doi.org/10.3390/s23031074

Shah, A. J.; Pandya, T. S.; Street, J., 2020: Study of variation in natural frequencies of bio-composites due to structural damage. International Wood Products Journal, 11 (4): 166-172. https://doi.org/10.1080/20426445.2020.1780383

Shang, D., 2003: Effect of fatigue damage on the dynamic response frequency of spot-welded joints. International Journal of Fatigue, 25 (4): 311-316. https://doi.org/10.1016/S0142-1123(02)00140-8

Shang, D.-G., 2009: Measurement of fatigue damage based on the natural frequency for spot-welded joints. Materials & Design, 30 (4): 1008-1013. https://doi.org/10.1016/j.matdes.2008.06.048

Šraml, M.; Glodež, S.; Fajdiga, G., 2019: Fatigue life models of wood: A review. International conference MATRIB *20*, Vela Luka, Croatia.

Wang, G. Y.; Liaw, P. K.; Morrison, M. L., 2009: Progress in studying the fatigue behavior of Zr-based bulk-metallic glasses and their composites. Intermetallics, 17 (8): 579-590. https://doi.org/10.1016/j.intermet.2009.01.017

Wang, Z.; Li, L.; Gong, M., 2012: Measurement of dynamic modulus of elasticity and damping ratio of wood-based composites using the cantilever beam vibration technique. Construction and Building Materials, 28 (1): 831-834. https://doi.org/10.1016/j.conbuildmat.2011.09.001

Weibull, W., 1939: A Statistical Theory of The Strength of Materials. Stockholm: Generalstabens Litografiska Anstalts Förlag, 151: 1-45.

Wu, T.; Yao, W.; Xu, C.; Li, P., 2020: A natural frequency degradation model for very high cycle fatigue of woven fiber reinforced composite. International Journal of Fatigue, 134: 105398. https://doi.org/10.1016/j.ijfatigue.2019.105398

***ISO 3129, 2019: Wood—Sampling methods and general requirements for physical and mechanical testing of small clear wood specimens. International Organization for Standardization.

Development and Application of Laser Technology in Woodworking and Furniture Industry of Bulgaria

Halim, Engindzhan

Department of Woodworking Machines, Faculty of Forest Industry, University of Forestry, Sofia, Bulgaria
Corresponding author: e_halim@ltu.bg

ABSTRACT

The article discusses the history, development and application of laser technologies in the woodworking and furniture industry in Bulgaria. The manufacturers of lasers and laser equipment in Bulgaria are presented. An overview of the past and present of the Laboratory of Laser Technologies at the University of Forestry, which is a pioneer in Bulgaria in the application of CO_2 lasers for wood processing and wood-based materials (WBM) is presented. A part of the scientific research and practical work of the laboratory is presented, outlining the directions for its future development.

Key words: lasers, laser beam, laser technology in Bulgaria, woodworking, furniture industry, applications, University of Forestry

1. INTRODUCTION

Different technological equipment is used for processing solid wood and wood-based materials (WBM), depending on the technological operation. Globally, the most common machines for furniture production are numerically controlled (CNC), but when it comes to chipless cutting or engraving, they are giving way to laser machines. Although the laser beam is considered to be a relatively new cutting tool, in the woodworking and furniture industry (WWFI), some of its first applications were made in the early 1970s.

The beginning of the implementation of laser technologies in Bulgaria was set in 1974, when Acad. Nikola Sabotinov realized his idea for the creation of a low-temperature copper laser, and under his leadership a copper bromide vapor laser was put into operation at the Institute of Solid State Physics (ISSP) of the Bulgarian Academy of Sciences (BAS). This was later recognized as the invention of the year. Thus was created the most powerful, at that time, all-Bulgarian gas laser, which was patented in Bulgaria, France, USA, UK, Germany, Japan and Australia. (Bulgarian Academy of Sciences, 2024).

One year after the invention was recognized, in 1980, the first laser equipment factory was established in the city of Plovdiv, where industrial CO_2 lasers were manufactured. The popularization of lasers during these years has led to the beginning of different types of research and studies in the field of wood and WBM. The developed and defended dissertations (Barnekov, 1983; Gochev, 1996), scientific articles (Barnekov *et al*., 1986; Barnekov *et al*., 1986; Tayal *et al*., 1994; Gochev *et al*., 1994; Gochev, 1995; Dinkov *et al*., 1996, and others) and books (Filipov *et al*., 1988) show the then interest and development in the field of lasers, as well as contributing to new scientific literature.

Currently, the laser successfully performs a number of technological operations such as cutting, engraving, marking, hole cutting, etc., possessing a number of advantages compared to

traditional technologies. Thanks to the high concentrated thermal energy in the form of a laser beam in continuous or pulsed mode of operation, it is possible to cut or engrave the material to be processed, depending on the generated power density values and the scanning or feeding speed of the laser beam. The knowledge and correct application of the laser beam, enables it to be used for different needs and in the WFMI.

Today, laser cutting is preferred by both furniture manufacturers and hobbyists for creating "garage" projects. The high productivity, accuracy, lack of contact with the material during processing and other advantages of lasers are some of the main factors for their continued existence and development to this day. Currently, there are a a series of companies importing in Bulgaria that import CO_2 lasers or offer services in the field of laser cutting and engraving of wood and WBM.

Various universities around the world and in Bulgaria (including the University of Forestry in Sofia) are creating new laboratories in laser technology for the study, research and proper application of the laser beam by students, including PhD students. In this way, in the future, connections with similar structures from related universities in the country and abroad will be deepened, up-to-date information will be exchanged and new scientific research will be conducted.

2. HISTORICAL BACKGROUND. LASER MANUFACTURERS IN BULGARIA

From a historical point of view, the invention and introduction of the term "Laser" has several key names in the 1960s. The American physicist R. Gordon Gould expanded A. Einstein's theory of stimulated emission of radiation and in 1959 introduced the term "LASER", which means Light Amplification by Stimulated Emission of Radiation. (Wikipedia - Gould, 2025). The credit for this invention is disputed as Gould was not granted a patent and the first to publish the theory were Charles Townes and Arthur Schawlow. It is for this reason that Gould has waged a thirty-year struggle with the United States Patent and Trademark Office.

The first laser with practical applications (Figure 1A) was developed in 1960 by Theodore Maiman, who used a synthetic ruby known as the ruby laser (Wikipedia – Maiman, 2025). This success of the American engineer and physicist is defined as the beginning of laser technology and is the reason to consider him the "father" of this technology.

Theodore Maiman's pioneering achievement laid the foundation for future developments in laser cutting, yet the first laser was not applied to the cutting process.

Lasers found industrial application when Kumar Patel in 1963 developed a carbon dioxide CO_2 laser (Wikipedia – Kumar and Patel, 2025).

His invention is described as key for industrial applications due to its higher efficiency and ability to work on a wide range of materials compared to the ruby laser. Thanks to Patel's discovery, today CO_2 lasers find great application in laser cutting and engraving of a wide range of materials, including in WWFI.

The potential of lasers, in manufacturing, has been noticed through the experiments done for laser cutting of steels in different years. An experiment to cut a 1 mm thick sheet of steel was carried out at the instigation of Peter Holdcroft, Director at The Welding Institute (TWI) in Cambridge, just two years after Patel developed carbon dioxide lasers, and the results were published in 1967. For the first experiment in the history of laser cutting, a CO_2 laser with a

maximum output power of 300 W at 100 Hz was developed at the Scientific Electronics Research Laboratory (SERL), and in the same year a laser cutting nozzle (Figure 1B) with a circular aperture at the tip, 2.5 mm in diameter and 1.5 mm distance from the material was designed (Hilton, 2002).

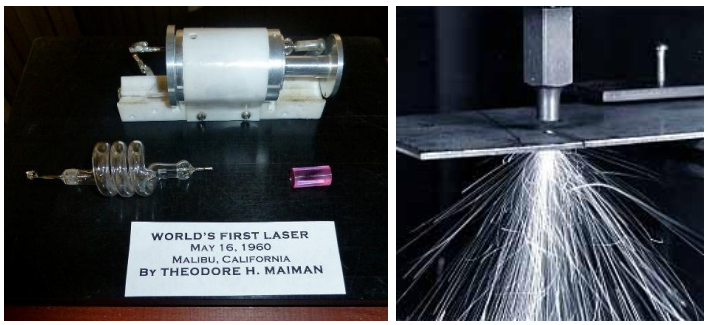

A ***B***

Figure 1. A – The world's first laser, developed by T. Maiman; B – The first laser cutting and the first designed nozzle

The conclusions that have been drawn, thanks to the experiment, prove the effectiveness of the laser beam and also suggest the importance of the distance between the laser nozzle and the material to be processed (focal length), mirrors, lenses and other essential factors that are the subject of research currently.

In 1969, the world-famous aerospace manufacturing company Boeing was the first company to use CO_2 lasers for industrial use to cut materials, such as titanium, in its production lines.

Significant discoveries and experimental studies in the 1960s, which were fundamental for the development of laser technology, had their echo in Bulgaria. It was around 1962 that a group of Bulgarian scientists was formed to study the new discovery. Weekly seminars were held at BAS, discussing various literature sources (The world of physics, 2011). The strong interest in the full understanding and functioning of the laser led to the construction and commissioning of the first ruby laser in Bulgaria in 1964 by Assoc. Prof. Vasil Stefanov from the Institute of Electronics (IE) at the Bulgarian Academy of Sciences (Figure 2).

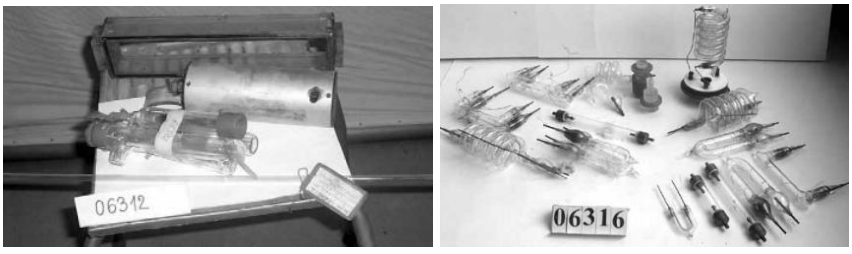

Figure 2. The first made Bulgarian ruby laser and pulsed excitation lamps

The research work of Acad. Sabotinov of the Institute of Physics at the Bulgarian Academy of Sciences, in the field of lasers, led to the creation of the first powerful metal vapor laser, also called copper laser in Bulgaria in 1974. Despite the problem of copper evaporation, which was achieved at a temperature of about 1500°, the scientist solved it by using the compound copper bromide. The academic applied for a copyright certificate and five years later the copper laser

was recognized as the invention of the year. The Bulgarian scientist has 30 patents in the field of lasers and thanks to him the laser technologies in Bulgaria are gaining significant importance, as well as the Bulgarian lasers are helping various areas around the world.

The low-temperature copper laser was introduced into regular production in the Plovdiv-based company Optical Technologies, founded in 1980, and then presented at the world exhibition in Hanover. This has helped attract the attention of foreign companies. Interest from other countries has led to an offer of a production licence. An Australian company continues to manufacture the Bulgarian laser to this day.

At the beginning of the 80's the first Bulgarian laser production plants were built in Bulgaria.

2.1. Laser equipment factory in town Plovdiv from 1980 to 1997

The plant for laser equipment in the town Plovdiv was established in 1980 and later developed into a complex called “Optoelectronics, Laser Equipment and Radiation Technologies”. A year later, the first industrial CO_2 laser, named "Hebar 1", with a power of 1000 W (Figure 3A) with longitudinal gas circulation and convective cooling, was produced in the beam technology complex. In 1982, it was demonstrated at the Technical Fair in Plovdiv. (Plovdiv Tech Park, n.d.).

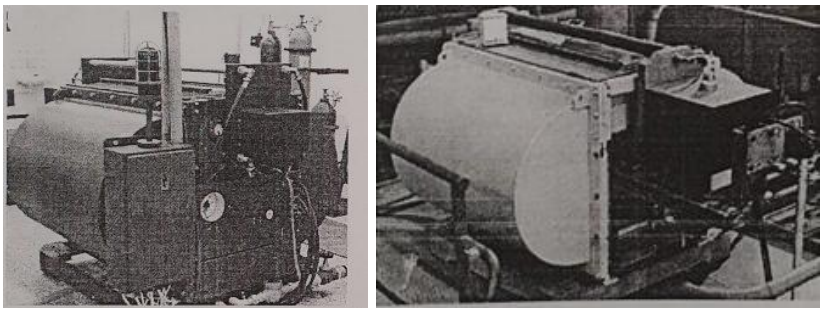

A ***B***

Figure 3. A – The first industrial CO_2 laser "Heber 1"; B – Serially produced laser model Heber 1A with power 1300 W

After the exhibition in Plovdiv, the Hebar 1 laser participated in the "Bulgaria-40" exhibition in Moscow, where the first export contract to the former Soviet Union (USSR) was signed. During the period 1982 to 1985 they have created 4 new models, one of which was presented at the world exhibition mentioned above. In the production programme of the complex, each subsequent model was produced with higher power - 500 W, 1000 W, 1300 W and 2500 W. The most successful model is considered to be the 1300 W Heber 1A (Figure 3B), and the 100th laser of this type was produced in 1988.

In addition to the production, demonstrations in Bulgaria and exhibitions around the world of the Heber 1, in the same year the first technological laser complex “TLC-1” (Figure 4) was produced, which is a program-controlled machine for laser cutting, welding and hardening. The complex of this type has been implemented in the technological process for cutting steel at the Beta plant in the town of Cherven Bryag.

In 1986 the complex “Optoelectronics, Laser Engineering and Radiation Technologies” was restructured as the Economic Association “Optical Technologies” and the Institute of Laser Engineering and Optics “Quantum” was established. It constructed various laser sources and

systems for complex technological processes, laser processing, infrared optics production, etc. (Plovdiv Tech Park, n.d.).

Figure 4. The first technological laser complex "TLC-1"

For the period from 1982 to 1990 were produced, approximately:

- 380 technological laser complexes, of which 200 units were exported to England, Italy, France, Turkey, Israel, Greece, Iraq, Iran, Egypt, India, Lebanon and about 150 units to the USSR;
- 120 installations for growing ZnSe crystals – RUMO, for the USSR;
- 20 copper bromide lasers – COBROL;
- 50 Prometheus laser medical systems;
- large quantities of laser optical elements.

By 1989, the volume of production had increased 7 times, and the staff in all units reached 1200 people. In that year, the state-owned company "Optical Technologies" was established, which included:

- The former business association "Optical Technologies" - Plovdiv;
- Scientific Research Institute of Laser Technology and Optics "Kvant";
- Laser equipment factory;
- Plant for special equipment of crystals;
- The Engineering Enterprise.

As a result of the political and socio-economic changes that took place after 1989, the company began to lose its positions and markets, and in 1997 a procedure was opened for its privatisation. The company created the Joint-stock company "Optela", and in the period 1998 - 2009 it regained part of the lost markets with new products: laser systems for cutting and engraving with solid-state and gas lasers, operating in the medium power range.

2.2. Laser equipment factory in Sofia from 1980 to 1994

In addition to the laser equipment factory in Plovdiv, in the same year the laser technological equipment factory “Iglika” at the Optical and New Technologies Center was also operating in Sofia. The most successful model produced by the factory is the CO_2 laser technological system (LTC) Iskar 500 with a maximum power of 500 W, with longitudinal flow circulation and convective cooling (Figure 5).

The Bulgarian laser cutting system Iskar 500 was available with an additional CAD/CAM computer system ("Prometheus") for automated preparation of laser cutting programs.

Figure 5. LTS Iskar 500, manufactured in 1980.

3. LABORATORIES AND RESEARCH WORK

The opening of new laser technology plants in the 1980s in Bulgaria also led to the establishment of laboratories for scientific research. An example of such a laboratory is the Laboratory of Laser Technologies at the UF - University of Forestry in the town of Sofia is still actively used by undergraduate and postgraduate students for research activities.

3.1. Laser Technology Laboratory at the Higher Institute of Forestry – HIF (now the University of Forestry) – from 1982 to 2014

The laboratory was started with the support of the institute management, at the Department of Mechanization and Automation of Woodworking (Faculty of Forest Industry) - successor is now the Department of Woodworking Machinery (WWM). This was done in the summer of 1982 by Assoc. Prof. Vladimir Barnekov, with the aim of conducting various scientific research activities, as well as carrying out limited production activities in the processing of wood and WBM.

The laboratory equipment included:

- Slow-flow tubular CO_2 laser source with diffusion cooling, model FEHA/LGL 200 (maximum power 200 W - Figure 6A) by Karl Zeiss Jena (former GDR - German Democratic Republic) - 1982;

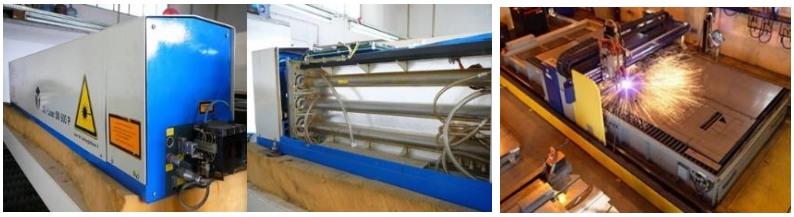

A ***B***

Figure 6. Laser technological equipment

- Electromechanical manipulator RB 256 (Figure 6B), a joint development with the Robot Plant SPCR (Scientific and Production Complex of Robotics) “Beroe”, town Stara Zagora - 1984 to CO_2 laser model FEHA LGL 200;
- FANUC CNC system, ZIT 500M (DSO “Izot” - Computing Plant, Sofia, Bulgaria) - 1984 to CO_2 laser model FEHA LGL 200;
- Fast-flow CO_2 laser source, with transverse flow circulation and convective cooling, model Heber 1 (Figure 7) with maximum power 1000 W, manufactured by the Laser Equipment Factory, Plovdiv (Bulgaria) – 1988;

Figure 7. CO_2 laser source Heber 1

- FANUC CNC system, ZIT 300M (DSO "Izot" - Computer Equipment Plant, Sofia, Bulgaria) - 1988 for CO_2 laser model Hebar 1;
- Electromechanical manipulator (Figure 8A), a joint development with ZDM - Koynare Ltd (ZDM - Koynare OOD), town of. Koynare (Bulgaria) - 1988 to CO2 laser model, Heber 1;

A ***B***

Figure 8. A – Electromechanical manipulator to Heber laser source; *B - Automated programming system IZOT 1027C*

- System for automated programming (punched tapes as programming media), model IZOT 1027C - Figure 8B (DSO "Izot" - Plant for computing equipment, Sofia, Bulgaria) - 1988 to ZIT 500M and ZIT 300M;
- Automated system for automatic preparation of NC control programs for the production of complex ornamental images and parts for CNC laser machines based on IBM-compatible personal computers, including: software package for NC control programs by inputting images with a scanner or by drawing based on a CAD system - LASER SCAN and LASER CAD (product of AUTOSKETCH of Autodesk Inc, USA); IBM PC compatible hardware optimized in accordance with the software requirements; hardware (dedicated board to the CNC) and software

means for direct, without using punch tape, sending of NC programs to the CNC of the laser machine (in 1995).

In the process of establishment and functioning of the laboratory, considerable scientific and practical potential has been accumulated. Two doctoral dissertations in the field of laser technology have been defended, a significant number of scientific articles have been published in Bulgarian and international journals and proceedings of international scientific conferences, a number of scientific research projects have been developed, and theses have been defended by students.

In implementation of the plan for the Scientific and Research Sector (SRS) of HIF, in 1988 a laser installation was installed in the Kitchen Furniture Factory – town Velingrad. Joint production with MAP (Mechanical Assembly Plant) - Koynare (later WWMP - Woodworking Machinery Plant - Koynare Ltd.) of the LWPS 003 laser system (LWPS - Laser Wood Processing System) was realized. One such system with a Heber 1A laser source was installed (with the participation of HIF and WWMP - Koynare) in 1993 in Lebanon (Figure 8A).

In 1984, the Laser Laboratory, on behalf of HIF and in cooperation with SPCR Beroe town in Bulgaria. n cooperation with Beroe, and in cooperation with Beroe in Stara Zagora, took part in the Technical Fair in Stara Zagora. The company participated in the Laser Technology Fair in Plovdiv and received a diploma for the laser technology system based on FEHA LGL 200 laser, electromechanical manipulator RB 256 and CNC ZIT 500M.

At the spring sample fairs in the city of Plovdiv in 1986, 1987 and 1988, the Laser Laboratory, on behalf of the HIF and jointly with the Furniture factory (FF) “Nikola Terziev” - the city of Haskovo, presented a set of children's and youth furniture, the front design of which was made with a laser beam. As a result of contracts concluded with the (FF) “Nikola Terziev”- Haskovo, over 1 200 sets of children's and youth furniture were manufactured in the Laser Laboratory, intended for export to the USSR. The laboratory has also worked on a number of other production tasks with FF “23 December” - Sofia, “Mebel” - Troyan (e.g. the production of over 500 ornamental tables for Great Britain) and other companies from the country. The contribution of the laboratory as the first manufacturer of souvenir products as well as advertisements made with the help of laser technologies is significant (Figure 9).

Figure 9. Samples of products produced by the laboratory in the 1980s and 1990s

3.2. Laboratory of Laser Technologies at LTU (WWM Department) – from 2024

Utilizing the accumulated experience and preserving the traditions of a pioneer in the application of laser technologies in the field of wood and WBM, a new Laboratory of Laser Technologies (Figure 10) has been built and equipped at UF, which:

- Slow-flow tubular CO_2 laser source with convective cooling, maximum power 40 W and dedicated software, model K40 - Figure 10A (China);

- Slow-flow tubular CO_2 laser source with convective cooling, maximum power 100 W and dedicated software, model AEON MIRA 9 - Figure 10B (China);
- Portable multifunction colorimeter, model LS173 (China), with specialized software (Figure 11A);
- Portable roughness profiler, model Surftest SJ-210, Mitutoyo (Japan) , with specialized software (Figure 11B);
- Infrared (IR) thermometer, model KIRAY 200 (China) (Figure 11C);
- ZnSe focusing lenses with focal lengths of 38.1 mm, 50.8 mm. 63.5 mm, and 76.2 mm (Figure 11D);
- Mira laser camera - CCD camera for automatic vectorization and laser contour cutting of raster images (Figure 11E);
- Rotation for cylindrical workpieces with Mira laser chuck (Figure 11F);
- LightBurn - software for laser cutting and engraving.

Figure 10. CO_2 laser sources of the Laser Technology Laboratory

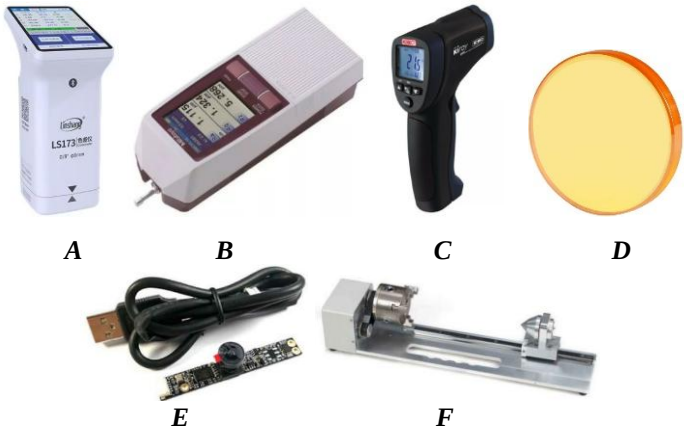

Figure 11. Equipment to the Laboratory of Laser Technologies

4. GUIDELINES FOR LASER TECHNOLOGY DEVELOPMENT IN BULGARIA

Currently in Bulgaria there are a number of companies offering services in the field of laser cutting and engraving of wood and MDF, working mainly with Chinese systems, as well as importers of laser equipment, also mainly from China. The advantages of the laser beam in cutting and engraving are a major factor for the increase in the application of this type of technology in the WWFI of Bulgaria. Their widespread application and constant improvement are the reason for new research in this field. The Laboratory of Laser Technologies at UF will continue to function and develop as a scientific research unit, where scientific research will be conducted, including by PhD students; students will be trained; methodical and scientific guidance of graduate students will be carried out; links with similar structures of similar universities in the country and abroad will be deepened.

Acknowledgments: This research is supported by the Bulgarian Ministry of Education and Science under the National Program "Young Scientists and Postdoctoral Students – 2" (2022 – 2025).

5. REFERENCES

Barnekov, V., 1983: Research on the cutting of wood fiber boards with a laser beam, dissertation for the award of the scientific degree of Candidate of Technical Sciences, Printed base VLTI, Sofia, pp. 147. (in Bulgarian)

Barnekov, V.; McMillin, Ch.; Huber, H., 1986: Factors influencing laser cutting of wood. Forest Product Journal, 36 (1): 55-58.

Barnekov, V.; Huber, H.; McMillin, Ch., 1986: Laser machining wood composites. Forest Product Journal, 39 (10): 76-78.

Dinkov, B.; Gochev, Zh.; Barnekov, V., 1996: Optimization of the Influence of the main factors of the slit formation in the interaction of a laser beam with wood and wood based materials. In: Proceedings of the International Scientific Conference "Mechanical Technology of Wood", 21-23 November 1996, Sofia, pp. 305-311. (in Bulgarian)

Filipov, G.; Barnekov, V., 1988: Chipless and laser cutting of wood, Zemizdat, Sofia, p. 131. (in Bulgarian)

Gotchev, J.; Barnekov, V.; Dinkov, B., 1994: Modeling the Laser Cutting of Particleboard. In: Proceedings of 2nd International Conference on Automated Lumber Processing Systems and Laser Machining of Wood and Composites, Michigan State University, East Lansing, Michigan, USA, pp. 71-81.

Gochev, Zh., 1996: Investigation of the process of laser cutting of furniture parts from wood particle board, Ph. D. thesis, LTU, Sofia, p. 200. (in Bulgarian)

Gochev, Zh., 1995: Chemical Destruction of Wood Particle Boards by Laser Beam Cutting. In: Proceedings of Jubilee Scientific Session with International Participation, Vol. II-MTD, VLTI, Sofia pp. 144-152. (in Bulgarian)

Tayal, M.; Barnekov, V.; Mukherjee, K., 1994: Focal point location in laser machining of thick hard wood. Journal of Materials Science Letters, 13 (9): 644-646. https://doi.org/10.1007/BF00271221

Hilton, P., 2002: In the beginning… (the history of laser cutting). https://www.twi-global.com/technical-knowledge/published-papers/in-the-beginning-the-history-of-laser-cutting-october-2002

***The world of physics, 2011: The ten most important achievements in physics in 2010. https://wop.phys.uni-sofia.bg/digital_pdf/wop/1_2011.pdf

***Bulgarian Academy of Sciences, 2024: 50 years since the invention of the copper bromide vapour laser in Bulgaria. https://www.bas.bg/?p=49497

***Wikipedia, 2025: Gordon Gould. https://en.wikipedia.org/wiki/Gordon_Gould

***Wikipedia, 2025: Theodore Maiman. https://en.wikipedia.org/wiki/Theodore_Maiman

***Wikipedia, 2025: C. Kumar, N. Patel. https://en.wikipedia.org/wiki/C._Kumar_N._Patel
***Plovdiv Tech Park (n.d.): History of Plovdiv Tech Park. https://optela.com/istoria/

Research on the Specific Cutting Energy of CO_2 Laser Beam Interaction with Solid Wood and Plywood

Halim, Engindzhan; Gochev, Zhivko*; Vitchev, Pavlin[1]

[1] Department of Woodworking Machines, Faculty of Forest Industry, University of Forestry, Sofia, Bulgaria
*Corresponding author: zhivkog@ltu.bg

ABSTRACT

This paper presents the results of experimental and theoretical studies on the specific energy for laser cutting of solid wood and plywood samples using a ZnSe lens with focal length F = 50.8 mm and focal position on the material surface. The studies were conducted on a CO2 laser machine, model AEON MIRA 9, at three levels of laser beam power and feed rate variation. The linear relationship between the weight of material vaporized by the laser beam, the total amount of energy and their relationship with the specific cutting energy represented as a linear equation was investigated using MS Excel and the Data Analysis module, which included a linear regression procedure. Based on this, a comparison is made between the experimentally obtained results and the theoretically determined ones, and relevant conclusions and recommendations are formulated.

Key words: CO_2 laser, solid wood, plywood, laser cutting, specific energy

1. INTRODUCTION

One field in the science of cutting wood and wood-based materials (WBM) is based on the physico-technological method of research, in which the methods of mathematics are used to summarize the experimental results of cutting processes into empirical formulas that are suitable for practical calculations (Gochev, 2018).

Some of the first researchers of wood cutting processes with chip formation found that the cutting work (*A*) is directly proportional to the volume of wood that is converted into chips, i.e. (Bershadsky *et al.,* 1975):

$$A = K.Q \tag{1}$$

The quantity K is called the *specific cutting work*, i.e. the work that is spent on converting 1 m^3 of wood into chips and has the dimension J/m^3.

$$K = \frac{A}{Q} \tag{2}$$

Where *Q* is the volume of wood that is converted to chips, m^3.

In the woodworking and furniture industry (WWFI), as well as in the souvenir industry in Bulgaria and worldwide, the CO_2 laser beam is increasingly used as a cutting and engraving tool.

Laser cutting, respectively engraving of wood and WBM is a process in which the electromagnetic energy of the laser beam is transformed into heat, resulting in new surfaces without chip formation.

A number of studies have been and are being conducted on the characteristics and effects of the laser beam in its interaction with different types of wood and WBM (Orech *et al*., 1987; Gochev *et al*., 1994; Gochev, 1996; Gochev *et al*., 1996; Dinkov *et al*., 1996; Batov *et al*., 1997; Pagano *et al*., 2009; Kubovský *et al*., 2012; Hernández-Castañeda *et al*., 2011; Eltawahni *et al*., 2013; Petutschnigg *et al*., 2013; Gurau *et al*., 2017; Martinez-Conde *et al*., 2017; Vidholdová *et al*., 2017; Jurek *et al*., 2021; Gochev *et al*., 2022; Gochev, 2023, and others).

When cutting wood and WBM with a CO2 laser beam, similar to the specific cutting work, the concept of specific laser cutting energy can be defined, i.e. the amount of laser beam energy that is required to remove a unit mass of wood material – E_s, J/kg (Orech *et al*., 1987; Gochev, 1996; Gochev *et al*., 1996; Kubovský *et al*., 2012; Gochev, 2016; Gochev *et al*., 2024).

Specific energy is widely used to estimate the energy consumption of a machining process, and is defined at the process level as net specific cutting energy. The net specific energy takes into account only the energy consumed for the actual removal of material and is influenced by the process conditions and the properties of the material being processed (Zhao *et al.*, 2017).

The weight of material removed (vaporized) by the laser beam can be represented by the relation:

$$\Delta m = \frac{1}{E_s}.E_t \tag{3}$$

Where $\Delta m = m_1 - m_2$ is the weight of the material vaporized by the laser beam, kg;

m_1 – the weight of the material before its laser beam treatment, kg;

m_2 – the weight of the material after its laser beam treatment, kg.

E_s – the specific energy of laser cutting, J/kg;

E_t – the total amount of energy that is transmitted by the laser beam in a unit neighborhood from the surface of the material, in time *t*, J.

The specific laser cutting energy (E_s) is defined by the equation:

$$E_s = \frac{P}{\rho.v_f.h.s} \tag{4}$$

Where *P* is the laser beam power, W;

ρ – material density, kg/m^3;

v_f – laser beam feed (scanning) speed, m/s;

h – kerf depth, m;

s – kerf width, m.

An equivalent form of equality (4) is:

$$\Delta m = \frac{E_t}{E_s} \tag{5}$$

Furthermore, equality (5) can be written as:

$$E_s = \frac{E_t}{\Delta m} = const \tag{6}$$

In fact, equation (6) is a way of mathematically expressing a hypothesis of a constant value of the specific laser cutting energy for a given wood species or WBM.

Based on equation (6), a formula can be presented to practically calculate the specific energy of laser cutting, such as:

$$E_s = \frac{P.l}{v_f.\Delta m} \quad (7)$$

Where l is the kerf length, m.

Based on the specific energy, the laser cutting process can be well described and it is possible to propose a theoretical model for the interaction of the laser beam with the wood or WBM, i.e. to investigate the kinetics of kerf formation.

Equations (3) and (6) express the linear relationship between Δm and E_t, and their relationship with E_s can be represented as a linear equation of the form:

$$y(x) = b_0 + b_1.x \quad (8)$$

Using this equation, it is possible to determine the values of Δm and E_t and to calculate those of E_s for the material under study. In this way, experimentally obtained and theoretically calculated specific energy results can be compared and the hypothesis of a constant value of laser cutting specific energy for a given wood species or WBM can be proved.

2. METHODS

2.1. Laser machine used

The studies were conducted using a CO_2 laser cutting and engraving machine, model AEON MIRA 9 (China) with a maximum power of 100 W (Figure 1).

Figure 1. CO_2 laser cutting and engraving machine, model AEON MIRA 9

2.2. Material for study

Solid wood and plywood specimens were used for the experiment. The density (ρ, kg/m^3) of the specimens was determined by the weight method, and its moisture content (W, %) by a

digital hygrometer, model MD (China) with a measurement range for wood and WBM from 5 % to 50 % (Figure 2A).

The starting material (Figure 2B) was cut into specimens with the dimensions: L – length, mm; b – width, mm and h – height (thickness), mm.

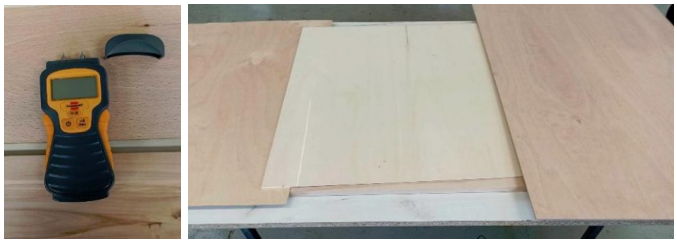

A **B**

Figure 2. A: digital hygrometer, model MD; B: tested material – solid wood and plywood

I. <u>Solid wood from the following species:</u>

i. Common beech (*Fagus sylvatica* L.) – *L* = 200 mm; *b* = 20 mm; *h* = 15 mm; *W* = 6%, ρ = 590 kg/m^3.
ii. Poplar - aspen (*Populus tremula* L.) – *L* = 200 mm; *b* = 20 mm; *h* = 14.5 mm; *W* = 6%, ρ = 340 kg/m^3.
iii. Common birch (Betula pendula Roth.) – *L* = 200 mm; *b* = 20 mm; *h* = 16.9 mm; *W* = 6%, ρ = 710 kg/m^3.

II. <u>Plywood of the following types:</u>

i. Common beech (*Fagus sylvatica* L.) – *L* = 200 mm; *b* = 20 mm; *h* = 4 mm; *W* = 5%, ρ = 707 kg/m^3.
ii. Poplar - aspen (*Populus tremula* L.) – *L* = 200 mm; *b* = 20 mm; *h* = 4 mm; *W* = 5%, ρ = 360 kg/m^3.
iii. Common birch (Betula pendula Roth.) – *L* = 200 mm; *b* = 20 mm; *h* = 3 mm; *W* = 5%, ρ = 630 kg/m^3.

2.3. Measuring equipment and measured values

To determine the specific energy of laser cutting, six series of 12 (twelve) specimens of parallelepiped shape and dimensions: *L* x *b* x *h* were made from the solid wood and plywood (Figure 3). Their weights before and after laser beam exposure were measured with an electronic balance, model RADWAG WLC 1/A2 (Poland), with an accuracy of 0.001 g (Figure 4 A). The values of the laser beam parameters were chosen in such a way that the condition of incomplete kerfing of the examined material was fulfilled (Figure 3; 4B).

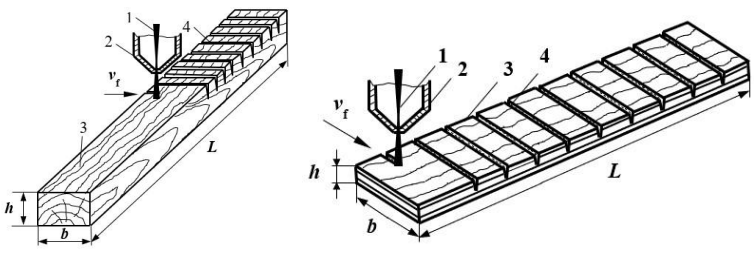

A **B**

Figure 3. Experiment scheme: 1 – laser beam, 2 – laser head, 3 – material, 4 – kerf; L – length; b – width; h – thickness; A – solid wood, B – plywood

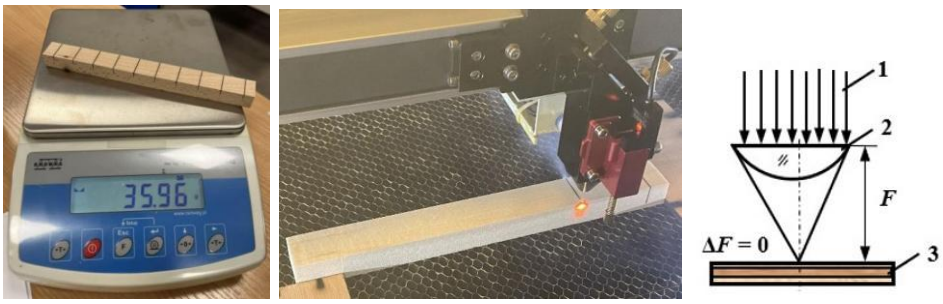

A **B** **C**

Figure 4. A – RADWAG WLC 1/A2 electronic balance; B – general view of the experiment; C – position of the focus on the material surface (ΔF = 0 mm): 1 – unfocused laser beam; 2 – focusing lens; 3 – material

2.4. Planning the experimental studies

The values of the variable factors – laser beam power (P, W) and laser beam scan (feed) speed (v_f, mm/s) in open and coded form are given in Table 1. The studies were conducted at the position of the laser beam focus, on the material surface (ΔF = 0 mm), ZnSe focusing lens with a focal length (F) of 50.8 mm (Figure 4C).

Table 1. Values of variable factors

Variable factors	Minimum value		Average value		Maximum value	
	open form	coded form	open form	coded form	open form	coded form
Solid wood						
$x_1 = P$, W	20	-1	25	0	30	+1
$x_2 = v_f$, mm/s	6	-1	8	0	10	+1
Plywood						
$x_1 = P$, W	12	-1	14	0	16	+1
$x_2 = v_f$, mm/s	25	-1	35	0	45	+1

The matrix of the planned two-factor experiment is shown in Table 2 for solid wood and in Table 3 for plywood.

On each test body of the six series of experimental specimens, in accordance with Table 2 and Table 3, ten (10) kerfs were made (Figure 3; 4B).

After the experiment, each of the test bodies was weighed and the value of its lost weight was recorded (Figure 4A).

Table 2. Matrix of the planned two-factor experiment for solid wood

Experiment №	Variable factors			
	$x_1 = P$, W		$x_2 = v_f$, mm/s	
1.	-1	20	-1	6
2.	+1	30	-1	10
3.	-1	20	+1	6
4.	+1	30	+1	10
5.	-1	20	0	8
6.	+1	30	0	10
7.	0	25	-1	6
8.	0	25	+1	10
9.	0	25	0	8
Experiments in the middle of the factor space				
10.	0	25	0	8
11.	0	25	0	8
12.	0	25	0	8

Table 3. Matrix of the planned two-factor experiment for plywood

Experiment №	Variable factors			
	$x_1 = P$, W		$x_2 = v_f$, mm/s	
1.	-1	12	-1	25
2.	+1	16	-1	25
3.	-1	12	+1	45
4.	+1	16	+1	45
5.	-1	12	0	35
6.	+1	16	0	35
7.	0	14	-1	25
8.	0	14	+1	45
9.	0	14	0	35
Experiments in the middle of the factor space				
10.	0	14	0	35
11.	0	14	0	35
12.	0	14	0	35

To evaluate the results of the two-factor experiment, the variance analysis methodology was used (*Vuchkov et al. 1986*). The regression equation under two factors of variation is of the form:

$$y_{pr.v.} = b_o + b_1x_1 + b_2x_2 + b_{11}x_1^2 + b_{22}x_2^2 + b_{12}x_1x_2 \quad (9)$$

Where $y_{pr.v.}$ is the predicted value of the output quantity;

b_o – coefficient in front of the free term;

b_1 and b_2 – coefficients in front of the linear terms;

b_{11} and b_{22} – coefficients in front of the nonlinear terms of the equation.

3. RESULTS AND DISCUSSION

Tables 4 to 9 present the values for the weight of material vaporized by the laser beam (Δm), according to the matrix of the two-factor experiment (Tables 2 and 3), and the values for E_s calculated by equation (7), where l is the length of all ten slits for a given specimen.

Table 4. Specific cutting energy E_s for solid wood (common beech: Fagus sylvatica L.)

№	Variable factors		Initial and output values		
	$x_1 = P$, W	$x_2 = v_f$, mm/s	Δm, kg	l, mm	E_s, J/kg
1.	20	6	0.00014	200	4.76×10^6
2.	30	10	0.00014	200	4.29×10^6
3.	20	6	0.00013	200	5.13×10^6
4.	30	10	0.00014	200	4.29×10^6
5.	20	8	0.00012	200	4.17×10^6
6.	30	10	0.00014	200	4.29×10^6
7.	25	6	0.00018	200	4.63×10^6
8.	25	10	0.00011	200	4.55×10^6
9.	25	8	0.00013	200	4.81×10^6
Experiments in the middle of the factor space					
10.	25	8	0.00013	200	4.81×10^6
11.	25	8	0.00013	200	4.81×10^6
12.	25	8	0.00013	200	4.81×10^6

Table 5. Specific cutting energy E_s for solid wood (poplar: Populus tremula L.)

№	Variable factors		Initial and output values		
	$x_1 = P$, W	$x_2 = v_f$, mm/s	Δm, kg	l, mm	E_s, J/kg
1.	20	6	0.00019	200	3.51×10^6
2.	30	10	0.00017	200	3.53×10^6
3.	20	6	0.00019	200	3.51×10^6
4.	30	10	0.00018	200	3.33×10^6
5.	20	8	0.00014	200	3.57×10^6
6.	30	10	0.00017	200	3.53×10^6
7.	25	6	0.00025	200	3.33×10^6
8.	25	10	0.00016	200	3.13×10^6
9.	25	8	0.00018	200	3.47×10^6
Experiments in the middle of the factor space					
10.	25	8	0.00016	200	3.91×10^6
11.	25	8	0.00017	200	3.68×10^6
12.	25	8	0.00019	200	3.29×10^6

Table 6. Specific cutting energy E_s for solid wood (common birch: Betula pendula Roth.)

№	Variable factors		Initial and output values		
	$x_1 = P$, W	$x_2 = v_f$, mm/s	Δm, kg	l, mm	E_s, J/kg
1.	20	6	0.000112	200	5.95×10^6
2.	30	10	0.000102	200	5.88×10^6
3.	20	6	0.00011	200	6.06×10^6
4.	30	10	0.00011	200	5.45×10^6
5.	20	8	0.000087	200	5.75×10^6
6.	30	10	0.00011	200	5.45×10^6
7.	25	6	0.00014	200	5.95×10^6
8.	25	10	0.00008	200	6.25×10^6
9.	25	8	0.000109	200	5.73×10^6
Experiments in the middle of the factor space					
10.	25	8	0.000108	200	5.79×10^6
11.	25	8	0.000107	200	5.84×10^6
12.	25	8	0.0001	200	6.25×10^6

Table 7. Specific cutting energy E_s for plywood (from common beech: Fagus sylvatica L.)

№	Variable factors		Initial and output values		
	$x_1 = P$, W	$x_2 = v_f$, mm/s	Δm, kg	l, mm	E_s, J/kg
1.	12	25	0.00002	200	4.80×10^6
2.	16	25	0.00003	200	4.27×10^6
3.	12	45	0.000012	200	4.44×10^6
4.	16	45	0.000015	200	4.74×10^6
5.	12	35	0.000017	200	4.03×10^6
6.	16	35	0.00002	200	4.57×10^6
7.	14	25	0.000024	200	4.67×10^6
8.	14	45	0.000015	200	4.15×10^6
9.	14	35	0.00002	200	4.00×10^6
Experiments in the middle of the factor space					
10.	14	35	0.000018	200	4.44×10^6
11.	14	35	0.000021	200	3.81×10^6
12.	14	35	0.0000198	200	4.04×10^6

Table 8. Specific cutting energy E_s for plywood (from poplar: Populus tremula L.)

№	Variable factors		Initial and output values		
	$x_1 = P$, W	$x_2 = v_f$, mm/s	Δm, kg	l, mm	E_s, J/kg
1.	12	25	0.00004	200	2.40×10^6
2.	16	25	0.00005	200	2.56×10^6
3.	12	45	0.00002	200	2.67×10^6
4.	16	45	0.00003	200	2.37×10^6
5.	12	35	0.00003	200	2.29×10^6
6.	16	35	0.00003	200	3.05×10^6
7.	14	25	0.00004	200	2.80×10^6
8.	14	45	0.00003	200	2.07×10^6
9.	14	35	0.00003	200	2.67×10^6
Experiments in the middle of the factor space					
10.	14	35	0.00003	200	2.67×10^6
11.	14	35	0.000031	200	2.58×10^6
12.	14	35	0.00003	200	2.67×10^6

Table 9. Specific cutting energy E_s for plywood (from common birch: Betula pendula Roth.)

№	Variable factors		Initial and output values		
	$x_1 = P$, W	$x_2 = v_f$, mm/s	Δm, kg	l, mm	E_s, J/kg
1.	12	25	0.00003	200	3.20×10^6
2.	16	25	0.00003	200	4.27×10^6
3.	12	45	0.000013	200	4.10×10^6
4.	16	45	0.000017	200	4.18×10^6
5.	12	35	0.00002	200	3.43×10^6
6.	16	35	0.000028	200	3.27×10^6
7.	14	25	0.00003	200	3.73×10^6
8.	14	45	0.000018	200	3.46×10^6
9.	14	35	0.000018	200	4.44×10^6
Experiments in the middle of the factor space					
10.	14	35	0.000017	200	4.71×10^6
11.	14	35	0.000024	200	3.33×10^6
12.	14	35	0.000023	200	3.48×10^6

The linear relationship between Δm and E_t and their relationship with E_s represented as linear equation (8) was investigated using MS Excel and the Data Analysis module, which included a linear regression procedure.

Tables 10 to 21 give the summary data, ANOVA analysis of variance and other quantities for solid wood and plywood at $\Delta F = 0$ mm.

Table 10. Summary results for common beech wood

Regression Statistics	
Multiple R	0.889516
R Square	0.791238
Adjusted R Square	0.770362
Standard Error	8.04E-06
Observations	12

Table 11. Dispersion analysis for common beech wood

ANOVA					
	df	***SS***	***MS***	***F***	***Significance F***
Regression	1	2.45E-09	2.45E-09	37.90152	0.000107413
Residual	10	6.47E-10	6.47E-11		
Total	11	3.1E-09			

Table 12. Summary results for poplar wood

Regression Statistics	
Multiple R	0.93139
R Square	0.867488
Adjusted R Square	0.854237
Standard Error	1.02E-05
Observations	12

Table 13. Dispersion analysis for poplar wood

ANOVA						
	df		***SS***	***MS***	***F***	***Significance F***
Regression	1		6.85E-09	6.85E-09	65.46479	1.07E-05
Residual	10		1.05E-09	1.05E-10		
Total	11		7.89E-09			

Table 14. Summary results for common birch wood

Regression Statistics	
Multiple R	0.952676
R Square	0.907592
Adjusted R Square	0.898351
Standard Error	4.65E-06
Observations	12

Table 15. Dispersion analysis for common birch wood

ANOVA					
	df	***SS***	***MS***	***F***	***Significance F***
Regression	1	2.13E-09	2.13E-09	98.21588	1.73E-06
Residual	10	2.16E-10	2.16E-11		
Total	11	2.34E-09			

Table 16. Summary results for plywood from common beech

Regression Statistics	
Multiple R	0.951701
R Square	0.905735
Adjusted R Square	0.896308
Standard Error	1.5E-06
Observations	12

Table 17. Dispersion analysis for plywood from common beech

ANOVA					
	df	***SS***	***MS***	***F***	***Significance F***
Regression	1	2.16E-10	2.16E-10	96.08377	1.91E-06
Residual	10	2.25E-11	2.25E-12		
Total	11	2.38E-10			

Table 18. Summary results for plywood from poplar

Regression Statistics	
Multiple R	0.924763
R Square	0.855186
Adjusted R Square	0.840705
Standard Error	3E-06
Observations	12

Table 19. Dispersion analysis for popl plywood from poplar

ANOVA					
	df	***SS***	***MS***	***F***	***Significance F***
Regression	1	5.31E-10	5.31E-10	59.05429	1.67E-05
Residual	10	8.99E-11	8.99E-12		
Total	11	6.21E-10			

Table 20. Summary results for plywood from common birch

Regression Statistics	
Multiple R	0.868051
R Square	0.753512
Adjusted R Square	0.728864
Standard Error	3.13E-06
Observations	12

Table 21. Dispersion analysis for plywood from common birch

ANOVA					
	df	***SS***	***MS***	***F***	***Significance F***
Regression	1	3E-10	3E-10	30.56998	0.000251
Residual	10	9.83E-11	9.83E-12		
Total	11	3.99E-10			

The coefficient of multiple correlation (*Multiple R*), which in this case is the coefficient of linear correlation between the dependent factor (Δm) and the independent factor (Et) is: for solid wood – common beech 0.89, poplar 0.93 and common birch 0.95; for plywood of – beech 0.95, poplar 0.92 and birch 0.87.

The coefficient of determination (*R Square*) has the following values: for solid wood – common beech 0.79, poplar 0.88 and common birch 0.91; for plywood of – beech 0.91, poplar

0.86 and birch 0.75. This means that for the materials studied, 79 %, 88 %, 91 %, 91 %, 86 % and 75 % of the variation in the dependent factor (Δm) is "explained" by the regression, respectively.

In the examples considered, the *F*-ratio has the following values: for solid wood – common beech 37.9, poplar 65.4 and common birch 98.2; for plywood of – beech 96.1, poplar 59.1 and birch 3.6, which are significantly greater than the corresponding critical values in the F-distribution tables (*Significance F*). This gives reason to conclude that the part of the variance of the dependent factor (Δm) that is "explained" by the regression is significantly larger than the residual variance (*Residual*), which is due to unobserved factors.

The results of the experimental and theoretical determination of the specific laser cutting energy at the interaction of the laser beam with solid wood and plywood are presented in Table 22.

Table 22. The specific energy of the laser beam when interacting with ordinary birch plywood

Material	**Specific laser cutting energy (E_s)**			
	Experimental results	**Theoretically calculated results**		
		ΔF = 0 mm		
	E_s, J/kg (x 10^6)	**E_s, J/kg (x 10^6)**	**Equation (3; 8)**	***R***
Solid wood				
Common beech	4.61	4.59	$\Delta m = 2.65.10^{-5} + 1.75.10^{-7}E_t$	0.89
Poplar (Aspen)	3.48	3.47	$\Delta m = -3.00.10^{-6} + 2.93.10^{-7}E_t$	0.93
Common birch	5.86	5.85	$\Delta m = 4.76.10^{-6} + 1.63.10^{-7}E_t$	0.95
Plywood				
Beech	4.33	4.32	$\Delta m = 1.59.10^{-6} + 2.12.10^{-7}E_t$	0.95
Poplar	2.57	2.56	$\Delta m = 4.79.10^{-6} + 3.33.10^{-7}E_t$	0.92
Birch	3.80	3.74	$\Delta m = 1.43.10^{-6} + 2.50.10^{-7}E_t$	0.87

Since the moisture content of the wood is in the room dry range - it does not affect the variation of the specific energy of laser cutting. The strong influence exerted by the type of material and its density is confirmed (Kubovský *et al*., 2012; Gochev, 2016; Gochev *et al*., 2024).

The specific energy was the highest for laser cutting of birch, which is explained by the fact that the studied samples had the highest density. Dried birch wood is characterized by high strength and is similar in strength to ash, one of the strongest hardwoods. Possibly the higher values for specific energy are also influenced by the wavy structure of the wood.

In the case of plywood, the specific laser cutting energy of beech plywood is the highest, which is about 12% higher than that of birch plywood. This is most likely due to the dense and uniform structure of the fibers and the saturation with adhesive, which together prevent effective ablation.

Comparative studies by Kubovský *et al*., (2012) also show that the specific energy required for laser cutting depends strongly on the type and density of the material. However, density alone is not enough to fully explain the difference in laser cutting specific energy, especially when comparing solid wood and WBM. As a result, more energy is absorbed or lost within the layered structure, reducing the material removal efficiency.

It can be seen from Table 22 that the difference between the experimental and theoretically calculated results is in the range of 0.2 % to 1.6 %, which confirms the hypothesis that the

specific laser cutting energy for a given wood species or WBM, can be considered as a constant quantity.

Based on the conducted experimental studies and after mathematical processing of the data using specialized software *Q-StatLab* and checking for adequacy, the following were derived:

- **Regression equations for solid wood at ΔF = 0 mm:**

  - common beech (*Fagus sylvatica* L.);

$$Y_1 = 4.71 + 0.198X_1 - 0.048X_2 + 0.276X_1^2 + 0.084X_2^2 - 0.093X_1X_2 \quad (10)$$

  - poplar - aspen (*Populus tremula* L.);

$$Y_1 = 3{,}54 + 0{,}133X_1 - 0{,}067X_2 + 0{,}101X_1^2 + 0{,}219X_2^2 - 0{,}05X_1X_2 \quad (11)$$

  - common birch (Betula pendula Roth.);

$$Y_1 = 5{,}90 + 0{,}1633X_1 - 0{,}003X_2 + 0{,}284X_1^2 + 0{,}216X_2^2 - 0{,}135X_1X_2 \quad (12)$$

- **Regression equations for plywood at ΔF = 0 mm:**

  - common beech (*Fagus sylvatica* L.);

$$Y_1 = 4{,}09 + 0{,}093X_1 - 0{,}068X_2 + 0{,}19X_1^2 + 0{,}30X_2^2 - 0{,}208X_1X_2 \quad (13)$$

  - poplar - aspen (*Populus tremula* L.);

$$Y_1 = 2{,}64 + 0{,}133X_1 - 0{,}108X_2 + 0{,}044X_1^2 + 0{,}191X_2^2 - 0{,}115X_1X_2 \quad (14)$$

  - common birch (Betula pendula Roth.);

$$Y_1 = 3{,}83 + 0{,}165X_1 - 0{,}09X_2 + 0{,}149X_1^2 + 0{,}096X_2^2 - 0{,}248X_1X_2 \quad (15)$$

Where Y_1 is the expected variation of the specific cutting energy E_s in coded form at the corresponding focal length;

X_1 – the laser beam power (P) in coded form;

X_2 – the feed rate (v_f) in coded form.

From equations (10) - (15), it can be seen that it is the coefficient in front of X_1 corresponding to the cutting power that will have the greatest influence, and to a greater extent than the feed rate, on the specific cutting energy (E_s). The sign in front of the coefficient is "plus", i.e. as P increases, E_s will also increase. The coefficient in front of X_2 has a negative sign, i.e. as the feed (scan) speed increases, the specific cutting energy will decrease. The sign in front of the coefficient X_1X_2 is negative, indicating the divergent influence of laser beam power (P) and feed rate (v_f) on the specific cutting energy (E_s).

Figures 5 to 10 present the graphical relationships showing the variation of specific cutting energy E_s versus laser beam feed rates (v_f) at different beam powers (P).

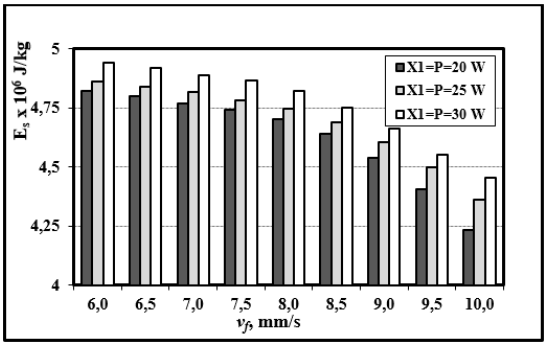

Figure 5. Variation of the specific cutting energy E_s for solid wood from common beech as a function of the laser beam feed rates (v_f) at different beam powers (P)

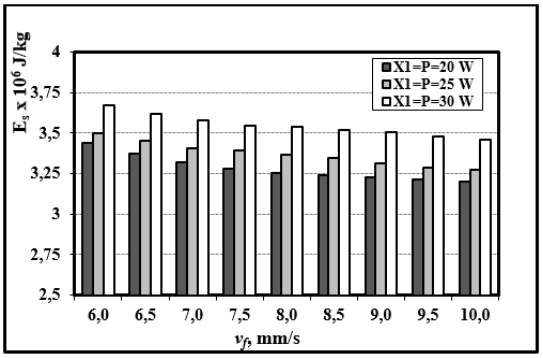

Figure 6. Variation of the specific cutting energy E_s for solid wood from poplar as a function of laser beam feed rates (v_f) at different beam powers (P)

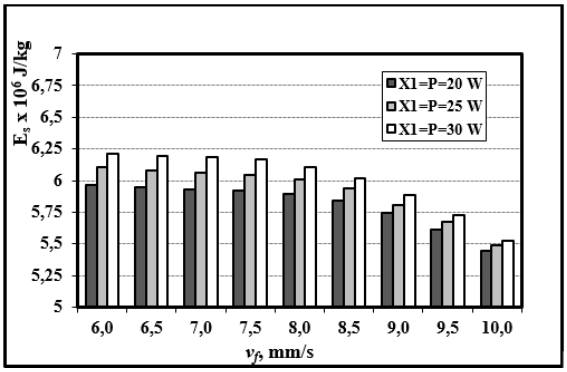

Figure 7. Variation of specific cutting energy E_s for solid wood from common birch as a function of laser beam feed rates (v_f) at different beam powers (P)

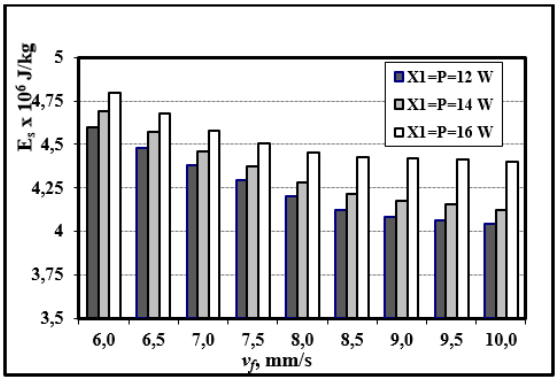

Figure 8. Variation of specific cutting energy E_s for plywood from common beech as a function of laser beam feed rates (v_f) at different beam powers (P)

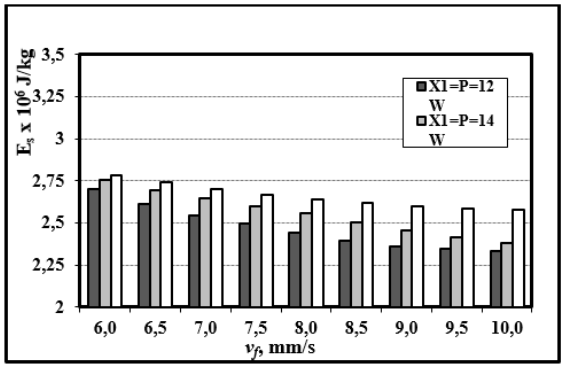

Figure 9. Variation of specific cutting energy E_s for plywood from poplar as a function of laser beam feed rates (v_f) at different beam powers (P)

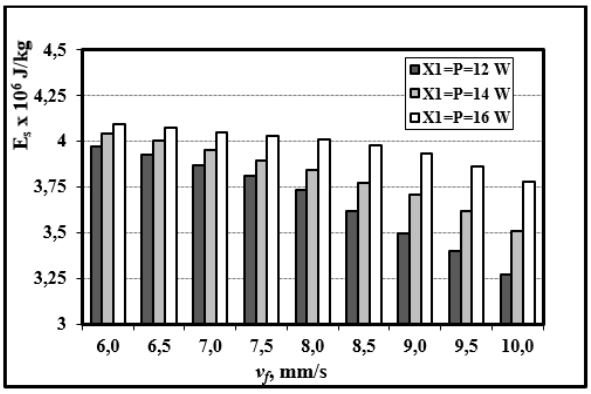

Figure 10. Variation of specific cutting energy E_s for plywood from common birch as a function of laser beam feed rates (v_f) at different beam powers (P)

4. CONCLUSIONS

The following more important conclusions and recommendations can be drawn from the research conducted:

1. The largest specific energy values for the solid wood samples are obtained when laser cutting birch, which has the highest density, and these larger values are probably influenced by the wavy structure of the wood. In addition, dried birch wood is characterized by high strength and is similar in strength to ash.

2. The specific energy of laser cutting of beech plywood is the highest, and it is about 12% higher than that of birch plywood. The explanation for this is the dense and uniform fibre structure and adhesive saturation, which together prevent effective ablation. However, density alone is not sufficient to fully explain the difference in specific laser cutting energy, especially when comparing solid wood and WBM. As a result, more energy is absorbed or lost within the layered structure.

3. From the summarized results presented in Table 22, it can be seen that the experimentally obtained and statistically calculated values of Es for the studied solid wood and plywood materials are very close in value. The difference is in the range of 0.2% to 1.6%, which confirms the hypothesis that the specific laser cutting energy for a given wood species or WBM, in this case plywood, can be considered as a constant value that can be used in a model describing the kinetics of notch formation.

4. As the feed (scanning) speed of the laser beam increases, the specific energy of laser cutting decreases, which is logical, taking into account formula (7), but this is also confirmed by the smaller amount of material removed (table 4-9).

Acknowledgements: We would like to thank the Research Sector of the University of Forestry, Sofia, Bulgaria, with whose support, through Contract No. NIS-B-1284/19.10.2023, this research was carried out.

5. REFERENCES

Batov, I.; Gotchev, Zh.; Dinkov, B.; Janic, Z., 1997: Study on the head field and the structural changes during the interactions between CO_2 laser beam and wood material, In: Proceedings of The 3rd International Conference on the Development of Forestry and Wood Science/Technology, Volume II, Belgrade, pp. 560-568. ISBN 86-7299-048-x

Bershadsky, A.; Tsvetkova, N., 1975: Cutting of wood, Vysheyshaya Shkola Publishing House, Minsk, p. 303. (in Russian)

Dinkov, B.; Gochev, Zh.; Barnekov, V., 1996: Optimizing the influence of main factors for the formation of cutting kerf in the interaction of a laser beam with wood and wood based materials. In: Proceedings of Scientific Reports, International Scientific Conference, University of Forestry, section Mechanical technology of wood, November 21-23, 1996, Sofia, Publishing house at UF, pp. 305-311. (in Bulgarian)

Eltawahni, H., Rossini, N.; Dassisti, M.; Alrashed, K.; Aldaham, T.; Benyounis, K.; Olabi, A., 2013: Evaluation and optimization of laser cutting parameters for plywood materials. Optics and Lasers in Engineering, 51 (9): 1029-1043.

Gochev, Zh., 1996: Investigation of the laser cutting process of furniture details from wood particle boards, Ph.D thesis, LTU Printing Base, Sofia, p. 200. (in Bulgarian)

Gochev, Zh.; Dinkov, B., 1996: Specific cutting energy in interaction of a laser beam with wood and wood based materials. In: Proceedings of Scientific Reports, International Scientific Conference, University of Forestry, section Mechanical technology of wood, November 21-23, 1996, Sofia, Publishing house at UF, pp. 298-304.

Gochev, Zh., 2018: Wood cutting and cutting tools, PH Avangard Prima, Sofia, p. 523, ISBN 978-619-239-047-1. (in Bulgarian)

Gotchev, J.; Barnekov, V.; Dinkov, B., 1994: Modeling the Laser Cutting of Particleboard. In: Proceedings of 2nd International Conference on Automated Lumber Processing Systems and Laser Machining of Wood and Composites, Michigan State University, East Lansing, Michigan, USA, pp. 71-81.

Gochev, Zh., 2016: Laser wood cutting and modification in its structure. In: Proceedings of 2nd International Furniture Congress: proceedings of papers, 13-15 October, Muğla Sitki Koçman University Faculty of Technology Department of Wood Product Industrial Engineering, Turkey, pp. 210-215.

Gochev, Zh.; Vichev, P., 2022: Color modifications in plywood by different mode of CO_2 laser engraving. Acta Facultatis Xylologiae, Zvolen, 64 (2): 77-86. https://doi.org/10.17423/afx.2022.64.2.08

Gochev, Zh., 2023: Real Parametefrs of a Focused CO_2 Laser Beam and its Determination when Using Lenses with Different Focal Lengths. In: Proceedings of 32nd International Conference on Wood Science and Technology – ICWST 2023, Unleashing the Potential of Wood-Based Materials, proceeding of papers, 7-8 December, Zagreb, pp. 67-74. ISBN 978-953-292-083-3

Gochev, Zh.; Vitchev, P., 2024: Specific cutting energy of CO_2 laser beam interaction with plywood. In: Proceedings of 12th International Scientific Conference „Innovation in Woodworking industry and Engineering Design“, Bulgaria, October 7-9, pp. 33-42. ISSN: 3031-1005

Gurau, L., Petru, A.; Varodi, A.; Timar, M., 2017: The Influence of CO_2 Laser Beam Power Output and Scanning Speed on Surface Roughness and Colour Changes of Beech (Fagus sylvatica). BioResources, 12 (4):7395-7412.

Hernández-Castañeda, J.; Kursad, H.; Li, L., 2011: The effect of moisture content in fibre laser cutting of pine wood. Optics and Lasers in Engineering, 49 (9-10): 1139-1152.

Jurek, M.; Wagnerová, R., 2021: Laser beam calibration for wood surface colour treatment. European Journal of Wood and Wood Products, 79 (5): 1097-1107.

Kubovský, I.; Babiak. M.; Cipka, Š., 2012: A determination of specific wood mass removal energy in machining by CO_2 laser. Acta Facultatis Xylologiae Zvolen, 54 (2): 31-37.

Martinez-Conde, A.; Krenke, T.; Frybort, S.; Müller, U., 2017: Review: Comparative analysis of CO_2 laser and conventional sawing for cutting of lumber and wood-based materials. Wood Science and Technology, 51: 943-966.

Orech, J.; Jůza F., 1987: Měrná energie úběru a její určení při interakci laserového záření se dřevem. Drevársky výskum, 114: 29-40.

Pagano, N.; Genna, S.; Leone, C.; Lopresto, V., 2009: Wood Laser machining using CO_2 30W laser in CW and pulse regime. In: Innovative production machines and systems. LAPT, Napoli, pp. 145-150.

Petutschnigg, A.; Stöckler, M.; Steinwendner, F.; Schnepps, J.; Gütler, H.; Blinzer, J.; Holzer, H.; Schnabel1, Th., 2013: Laser Treatment of Wood Surfaces for Ski Cores: An Experimental Parameter Study. Advances in Materials Science and Engineering, 2013 (11): 123085.

Vidholdová, Z.; Reinprecht, L.; Igaz, R., 2017: The Impact of Laser Surface Modification of Beech Wood on its Color and Occurrence of Molds. BioResources, 12 (2): 1930-2126.

Vuchkov I.; Stoyanov, S., 1986: Mathematical modelling and optimization of technological objects, SPH Tehnika, Sofia, p. 341. (in Bulgarian)

Zhao, G.; Liu, Z.; He, Y.; Cao, H.; Guo, Y., 2017: Energy consumption in machining: Classification, prediction, and reduction strategy. Energy, 133: 142-157.

Health Assessment of Wooden Constructions of Old Buildings Damaged in the Earthquake

Hasan, Marin[1]; Hasan, Adriana[2]; Tomić, Zvonimir[3]; Župčić, Ivica[1*]

[1] Department of Wood Technology, University of Zagreb Faculty of Forestry and Wood Technology, Zagreb, Croatia
[2]Adria Wood Solutions j.d.o.o., Dugo Selo, Croatia
[3]Franakustik d.o.o., Zagreb, Croatia
*Corresponding author: izupcic@sumfak.unizg.hr

ABSTRACT

On May 22, 2020, Zagreb experienced a 5.5 magnitude earthquake, causing significant damage to many buildings, particularly in the city's historic districts. In the aftermath, it was crucial to assess the condition and quality of wooden load-bearing beams in the affected structures and to provide recommendations for their reconstruction and, where necessary, chemical protection. Biological degradation is one of the most significant threats to historic wooden structures, alongside fire, earthquakes, and collapse. This type of damage can occur after decades of use and is especially common in buildings that are centuries old. Xylophagous insects and lignicolous fungi are the primary agents of damage, typically affecting unused spaces such as roofs and underfloor areas. The extent of damage is influenced by factors such as the biological resistance of the wood species and microclimatic conditions (e.g., temperature, moisture presence, roof leaks, condensation in thermal bridges, and moisture uptake in cold, damp climates). Assessing wood health involves not only identifying the type and extent of infestation but also selecting appropriate remediation methods, requiring expertise in wood technology and pathology. This paper presents two case studies of historic buildings in Zagreb: Object A (Lower Town – Donji Grad) and Object B (Upper Town – Gornji Grad), illustrating the most common forms of biological damage and the preservation measures needed to ensure the longevity of these structures.

Key words: biological degradation, high-risk areas, wooden beams, wood health assessment methods

1. INTRODUCTION

Zagreb's historic center, which includes the Lower Town (Donji Grad) and Upper Town (Gornji Grad), is home to many 19th-century buildings featuring timber floor and roof structures. The 2020 earthquake caused widespread structural damage, particularly to heritage buildings, emphasizing the need for a systematic assessment of existing timber elements. The most severe damage occurred in wooden constructions, particularly in elements that had been affected by xylophagous and lignicolous organisms.

Certain insect species specialize in attacking sapwood or entire wood tissue, without distinguishing between heartwood and sapwood. Some species are specific to hardwoods or softwoods, while others, including wood-rotting fungi, are non-selective and can degrade both types. Some xylophagous insects that infest wood in service prefer fungal mycelium in the wood, which can exacerbate degradation (Binker *et al*, 2014; Eaton and Hale, 1993; Grosser, 1985; Langendorf, 1988; Reinprecht, 2007; Reinprecht, 2016; Reinprecht *et al*., 2009; Scheiding *et al*., 2016; Turkulin and Hasan, 2025; Unger, *et al*., 2001).

The most dominant insect species in Croatian structures are common woodborers (Anobiidae): Anobium punctatum, Anobium pertinax, and Xestobium rufovillosum, as well as the house longhorn beetle (*Hylotrupes bajulus*). Even minor insect infestations can allow moisture ingress into the larvae tunnels and exit holes, fostering a synergistic attack by insects and wood-rotting fungi (Binker *et al*, 2014; Cruz and Machado, 2013; Eaton and Hale, 1993; Grosser, 1985; Langendorf, 1988; Reinprecht, 2007; Reinprecht, 2016; Reinprecht *et al*., Rohanova, 2020; 2009; Scheiding *et al*., 2016; Turkulin and Hasan, 2025; Unger, *et al*., 2001; Zabel and Morrell, 1992).

Fungal infestations are common in historic buildings, as they often contain damp zones. The most frequent locations for fungal attack are building corners with restricted ventilation and areas where wood is embedded in walls, such as the ends of tie beams and floor beams. Moisture uptake in these zones, combined with hygroscopic moisture and capillary action, can result in wood moisture content (MC) exceeding the critical threshold of around 20 % (EN 17121, 2019; Binker *et al*, 2014; Eaton and Hale, 1993; Reinprecht, 2007; Reinprecht, 2016; Reinprecht *et al*., 2009; Turkulin and Hasan, 2025; Unger, *et al*., 2001).

This paper illustrates the most common forms of biological damage in historic buildings and discusses methods for assessing wood degradation and residual cross-sectional strength in wooden beams.

2. MATERIALS AND METHODS

A detailed in-situ visual inspection was conducted across all affected structures to identify critical inspection and measurement points.

2.1. Visual Inspection and Documentation

A comprehensive visual inspection and photographic documentation were carried out to identify decay, deformation, and insect damage at each measurement point (Figure 1).

Figure 7. Visual inspection of building A – Example of a building corner with beams inserted into the wall, completely rotted.

2.2. Nail-Hammer Test

The Pilodyn method for determining wood health is based on the depth of penetration of a steel needle into the wood surface (Clarke and Squirrell, 1985; Imai *et al*., 2023; Rohanova, 2020). Inspired by this method, the authors introduced the Nail-hammer test. A TÜV-certified Picard hammer (600 g) with two sharp "DBGM" edges was used for this test. The Nail-hammer method was applied as a fast and effective way to evaluate the mechanical integrity of the beams. The penetration depth of the hammer nail under equal impact energy was measured (Figure 2, 3).

Figure 8. Example of the Nail-hammer test at a measurement point – beam inserted into the wall

Each point was classified from 1 (sound wood) to 8 (severely decayed wood), based on the penetration depth of the hammer nail (Table 1).

Table 1. The nail-hammer penetration depth and corresponding soundness grade

The grade	Nail penetration depth
1	< 5 mm
2	5 to 10 mm
3	11 to 15 mm
4	16 to 20 mm
5	21 to 30 mm
6	31 to 40 mm
7	41 to 50 mm
8	> 50 mm

The reduction of the effective load-bearing cross-section (R) was calculated using the equation (1):

$$R = \frac{(A_0 - A_1)}{A_0} \times 100\% \quad (1)$$

where A_0 is the original cross-section area and A_1 is the remaining effective cross section of the wooden beam (Figure 3).

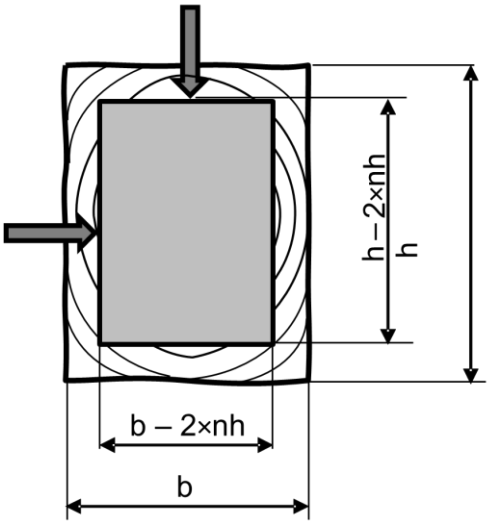

Figure 9. Determination of remaining effective cross-section by the Nail-hammer test (nh – Nail-hammer penetration depth)

2.3. Moisture Content (MC) and Density Measurement

Wood moisture content was measured using an electrical resistance moisture meter (GANN HT 85T) in-situ and by the gravimetric method in the laboratory (HRN EN 13183-1, HRN EN 13183-2). Core specimens were drilled out from the beams at each measurement point (Figure 4 right). Density was determined gravimetrically, and strength class was assessed according to HRN EN 338.

Figure 10. Electrical resistance moisture content measurement, core drilling for samples, and core drill specimen

2.4. Microbiological Analysis

Small pieces from the core drill specimens were incubated on Potato Dextrose Agar (PDA) nutrient medium in Petri dishes at (24 ± 1) °C and (75 ± 5) % relative humidity for 14 days. Specimens were taken from the surface (top and bottom) and from the central part of the

wooden beam (left and right) (Figure 5 left). Molds, bacterial colonies, and decay fungi were identified (Figure 5 right).

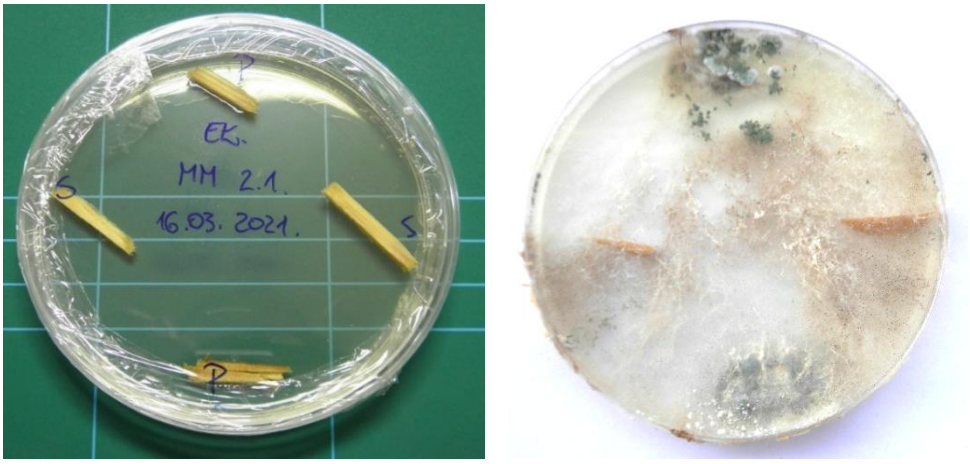

Figure 11. Placement of wood pieces in nutrient agar in Petri dishes and developed microbiological cultures

3. RESULTS AND DISCUSSION

3.1. Object A – Lower Town (Donji Grad)

The beam ends inserted into masonry external walls on the northern side showed the highest degree of decay. Condensation, due to temperature gradients, increased moisture levels above 28 %, resulting in severe degradation, particularly in attic floors (Figure 6). The average density of the beams ranged from 374 to 676 kg/m³, corresponding to strength classes C16 – C50 (Table 2).

Table 2. Summary of the density values of wooden beams from all measurement locations (28 data points from core samples) and corresponding strength class designations (according to HRN EN 338)

Property	Average	Value 15 % of the lower limit	Median	Min	Max	Standard Deviation
Density, kg/m^3	477	401	462	374	676	76.49
Strength class (HRN EN 338)	C30	C20	C27	C16	C50	

According to Nail-hammer test results, the beams on the ground and first floor of the building were rated as follows: 8 beams had the reduction of the load bearing cross section for 18 %, 26 beams had the reduction for 35 %, 5 beams had the reduction for 65 % and 5 beams had the reduction of load bearing cross section for more than 75 %.

Figure 12. Beam insert in the wall: a) entire cross section decayed and degraded by insects; b) surface brown rot 12 mm in depth with sound inner part of the beam

3.2. Object B – Upper Town (Gornji Grad)

Object B exhibited moderate degradation, with attic beams most affected by condensation. Northern facades showed more significant biological activity, correlating with moisture condensation and moisture uptake. The density of the beams ranged from 398 to 556 kg/m³, with strength classes C20 – C50.

Table 3. Summary of the density values of wooden beams from all measurement locations (25 data points from core samples) and corresponding strength class designations (according to HRN EN 338)

Property	Average	Value 15 % of the lower limit	Median	Min	Max	Standard Deviation
Density, kg/m^3	464	417	467	398	556	47.38
Strength class (HRN EN 338)	C30	C22	C30	C20	C50	

Figure 13. Severely rotten and attacked by insect beam ends inserted in north faced outer wall

According to Nail-hammer test results, the beams on the ground and first floor of the building were rated as follows: 2 beams had the reduction of the load bearing cross section for 35 %, 5 beams had the reduction for 50 %, 4 beams had the reduction of load bearing cross

section for more than 65 %. All the beams of the attic floor were almost entirely rotten, two adjacent beams have a complete transverse crack at their midpoint (Figure 7).

Figure 14. Attic floor beams: Left - two adjacent transversely cracked attic floor beams; Right - completely rotten beams of the northwestern part of the building

3.3. Comparative Analysis

Both objects lack thermally insulated attics, and during the winter months, significant temperature differences between the upper floors and attics caused condensation, leading to moisture accumulation in the attic floor beams. As a result, these beams suffered extensive rotting and insect infestation.

Northern facades were more degraded than southern ones, and insect infestations were particularly pronounced in poorly ventilated, humid zones. Although EN 17121 and other sources do not specifically address insect infestation, focusing only on reducing the load-bearing cross-section of structural elements, an analysis of these buildings revealed that even minimal fungal mycelium can lead to significant damage by xylophagous insects, which prefer feeding on the mycelium.

3.4. Repair Recommendations

Mechanical repairs should include partial beam replacement with scarf joints or laminated inserts, and reinforcement with side planks or steel elements. The authors recommend chemical protection using Adolit BQ1, Adolit BQ20, Impralit KDS, or Tanalith E, applied through surface brushing and injection. Injection holes (Ø3 mm, ½ – ⅔ beam height) should be drilled alternately on opposite sides to ensure maximal penetration and even distribution of the preservative (Figure 8). After drying, surfaces should be sealed, and attics should be thermally insulated to prevent further condensation.

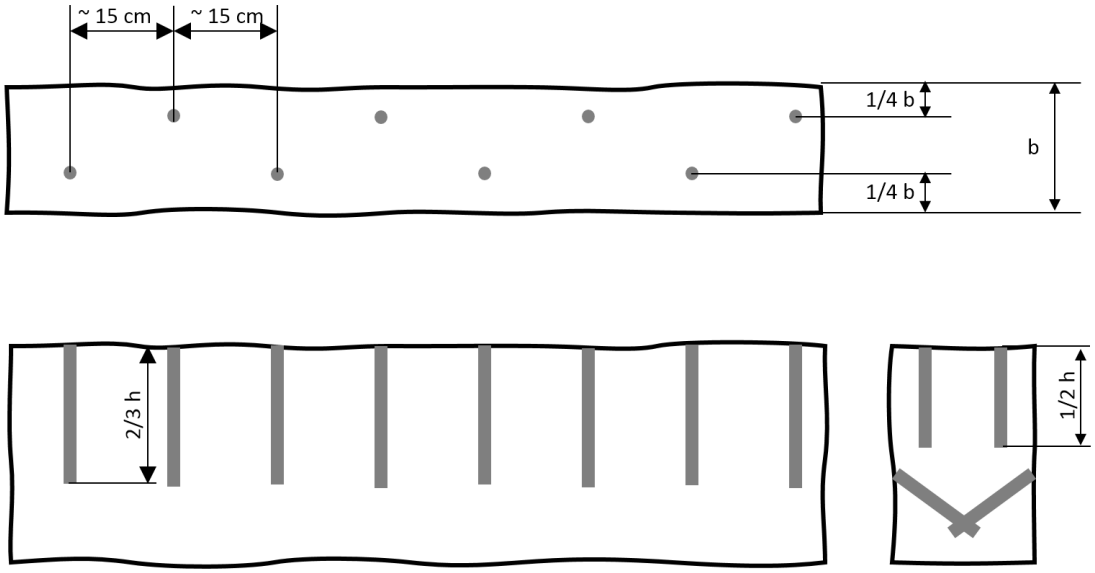

Figure 15. The arrangement, depth, and diameter of injection holes must ensure maximum penetration and distribution of the biocidal solution without compromising the load-bearing cross-section

4. CONCLUSIONS

The Nail-hammer test proved to be an efficient method for assessing wood degradation and calculating the reduction in load-bearing cross-section. Attic beams and northern facades were most affected by condensation, which facilitated insect infestation and fungal decay. Combining non-destructive and laboratory analyses is essential for the long-term preservation of Zagreb's timber heritage. Recommendations include mechanical strengthening, chemical protection, and improved ventilation of beam pockets.

5. REFERENCES

Binker, G.; Brückner, G.; Flohr, E.; Huckfeldt, T.; Noldt, U.; Parisek, L.; Rehbein, M.; Wegner, R., 2014: Praxis-Handbuch Holzschutz. Köln: Rudlof Müller Verlag.

Clarke, R. W.; Squirrell, J. P., 1985: The Pilodyn—an instrument for assessing the condition of waterlogged wooden objects. Studies in Conservation, 30 (4): 177-183. https://doi.org/10.1179/sic.1985.30.4.177

Cruz, H.; Machado, J. S., 2013: Effects of beetle attack on the bending and compression strength properties of pine wood. Advanced Materials Research, 778: 145-151.

Eaton, R. A.; Hale, M. D. C., 1993: Wood – Decay, pests and protection. Chapman & Hall, London, UK.

Grosser, D., 1985: Pflancliche und tierische Bau und Werkholz-Schädlinge. Leinfelden-Echterdingen: DRW -Verlag.

Imai, M.; Kobayashi, H.; Hara, T., 2023: Proposal of a method for estimating the residual Strength from the depth of pilodyn penetrating for a Cylindrical member. In: Proceeding of the World Conference on Timber Engineering, Oslo, pp. 882-887. https://doi.org/10.52202/069179-0120

Langendorf, G., 1988: Holzschutz – (Wood Protection). Fachbuchverlag Leipzig, Germany. (in German language)

Reinprecht, L., 2007: Ochrana dreva – (Wood Protection). Technical University in Zvolen, Slovakia. (in Slovak)

Reinprecht, L., 2016: Wood deterioration, protection and maintenance. Chichester: WILEY Blackwell.

Reinprecht, L.; Štefko, J.; Kuklík, P., 2009: Wooden Structures: Construction, Protection and Maintenance. Prague.

Rohanova, A., 2020: Non-destructive penetration method for determining the quality of structural spruce wood (*Picea Abies* Karst. L.) in situ. Acta Facultatis Xylologiae, 62 (1): 113-123. https://doi.org/10.17423/afx.2020.62.1.10

Scheiding, W.; Grabes, P.; Haustein, T.; Haustein, V.; Nieke, N.; Urban, H.; Weiß, B., 2016: Holzschutz. München: Carl Hanser Verlag.

Turkulin, H.; Hasan, M., 2025: Biological Degradation in Historic Timber Structures: Appearance, Extent, Relevance and Sanation. In: Proceedings of the SHATIS 2025 – 7th International Conference on Structural Health Assessment of Timber Structures, Zagreb, Croatia, pp. 278-290.

Unger, A.; Schniewind, A. P.; Unger, W., 2001: Conservation of Wooden Artifacts – A Handbook. Springer-Verlag, Berlin Heidelberg, Germany.

Zabel, R. A.; Morrell, J. J., 1992. Wood Microbiology: Decay and Its Prevention. Academic Press, INC. London, UK.

***EN 17121, 2019: Conservation of cultural heritage – Historic timber structures – Guidelines for the on-line assessment of load-bearing structures.

***HRN EN 13183-1, 2008: Moisture content of a piece of sawn timber -- Part 1: Determination by oven dry method.

***HRN EN 13183-2, 2008: Moisture content of a piece of sawn timber -- Part 2: Estimation by electrical resistance method.

***HRN EN 338, 2016: Structural timber -- Strength classes.

Design and Construction of a Wood–Metal Dining Furniture Set Using Partially Recycled Materials

Ištvanić, Josip; Pervan, Dario*; Vondra, Mislav; Jurišić, Mario; Antonović, Alan; Klarić, Miljenko[1]

[1] Department of Material technology, Faculty of Forestry and Wood technology, University of Zagreb, Zagreb, Croatia

* Corresponding author: dpervan@sumfak.unizg.hr

ABSTRACT

In modern times, most furniture is discarded after a period of use due to wear, dysfunction, or outdated aesthetic-design features. Another contributing factor is the availability of low-cost, mass-produced furniture, which leads consumers to overlook the potential for restoring or reusing parts of their existing furniture. The aim of this study is to demonstrate how combining old, used furniture with new components made from attractive wood species can produce products that are reused rather than discarded. This approach contributes to environmental protection by reducing waste, turning it into material for everyday use. For the construction of a tabletop, rowan wood (*Sorbus aucuparia* L.) was used, while the seat and backrest of the chair were made from common walnut wood (*Juglans regia* L.). The study also includes technical drawings of the table and chair to illustrate the construction assembly and provide clear insight into the materials used and their dimensions.

Key words: dining set, European walnut, recycled materials, rowan wood, wood-metal combination

1. INTRODUCTION

The rapid advancement of technology has significantly altered consumer behaviour concerning furniture replacement, leading to increased frequency in discarding used furniture items. This trend has resulted in substantial accumulation of waste materials, with wooden furniture constituting a considerable portion. Data indicate that China alone generates approximately 60 million tons of discarded wooden furniture annually (Zhang *et al*. 2023). The rapid expansion of the furniture industry, as with any other industry, has also contributed to environmental degradation through increased pollution, highlighting the urgent need for more sustainable practices.

In response, a growing body of research emphasizes the importance of adopting recyclable design principles and enhancing wood waste recycling (Figure 1) in the context of a circular economy (Pihno *et al*., 2023). Various evaluation index system and evaluation models where developed to verify feasibility of recycling specific cases of wooden furniture and Taiwan serves as a leading example, where advanced cradle-to-cradle production systems have been developed to optimize the reuse and recycling of waste furniture, delivering both environmental and economic benefits (Lin *et al*., 2022) (Zhang *et al*., 2023). Furthermore, China initiated the "Specification for Recycling and Utilization of Waste Wood Materials" in 2009, aiming to institutionalize the recycling and reprocessing of solid wood furniture waste and improve national sustainability outcomes (Xiong *et al*., 2023).

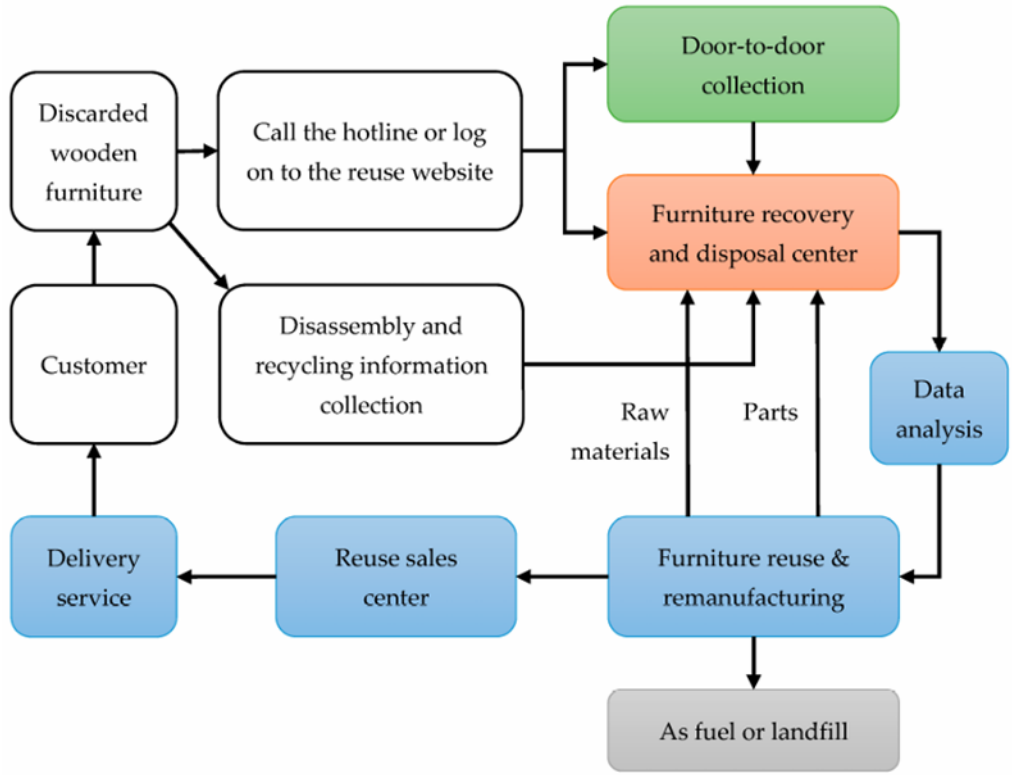

Figure 1. Waste wooden furniture recycling process (Zhang et al. 2023)

The integration of recycled wood and metal in furniture design represents a sustainable strategy consistent with circular economy principles. Recycled wood, in particular, offers notable advantages in terms of structural durability and resistance to deformation, such as warping and cracking, thereby serving as a credible substitute for newly harvested timber. The synergy between wood and metal enables a wide range of versatile design applications, facilitating the creation of eclectic yet cohesive pieces that cater to various aesthetic preferences. The educational potential of recycled furniture design has also been recognized. Studies involving interior design students indicate that engagement with recycled materials fosters both creativity and environmental awareness. By incorporating wood and metal waste into their design projects, students are encouraged to develop innovative, sustainability-focused solutions, thereby contributing to broader environmental conservation goals (Al-Saud *et al*., 2024). Furthermore, the aesthetic and functional merits of combining wood and metal have been validated in various design contexts, reinforcing the capability of recycled materials to satisfy both technical and artistic demands. In line with this, the application of eco-design principles in furniture manufacturing promotes the use of environmentally responsible materials and processes, further advancing the transition toward sustainable production systems (Munteanu, 2021).

This study aims to design and construct a sustainable dining set comprising a table and four chairs by combining recycled and new materials in a wood–metal configuration. Metal components will be repurposed from decommissioned office furniture, while new elements will include European walnut (*Juglans regia* L.) and plywood for the chair seats and backrests, and a combination of plywood and solid rowan wood (*Sorbus Aucuparia* L.) for the tabletop. The objective is to demonstrate that high-quality, aesthetically appealing furniture can be produced through the integration of reused and newly fabricated parts. This approach not only reduces

material waste and supports environmental sustainability but also illustrates the potential of circular design in contemporary furniture manufacturing.

2. MATERIALS AND METHODS

2.1. Construction and technical drawing of the dining furniture set

During the design process of the dining furniture set (comprising of four chairs and a table), several alternatives were considered regarding the shape of the chair backrests and the tabletop. After evaluating the options in terms of aesthetics and functionality, the variants deemed most practical and visually appealing were selected. In terms of material selection, both new and recycled materials were used. The new materials included rowan wood, walnut wood, plywood, screws, adhesive, loose tongue joints, and an oil-based surface finish. The recycled materials consisted of metal frames from discarded furniture components obtained through inventory clearance. Following the selection of an aesthetically and functionally optimal design and the definition of the required materials, it was essential to ensure that the final product would meet the necessary strength and durability standards. These qualities are critical for furniture intended for everyday use in a household setting.

Following the completion of the structural design, the next step involved creating a technical drawing of the product using AutoCAD software. In the program, the three fundamental projections of the product (front view, top view, and side view) were drawn to a reduced scale (Figures 3 and 4). These drawings include marked cross-sections and elements, all of which are dimensioned accordingly.

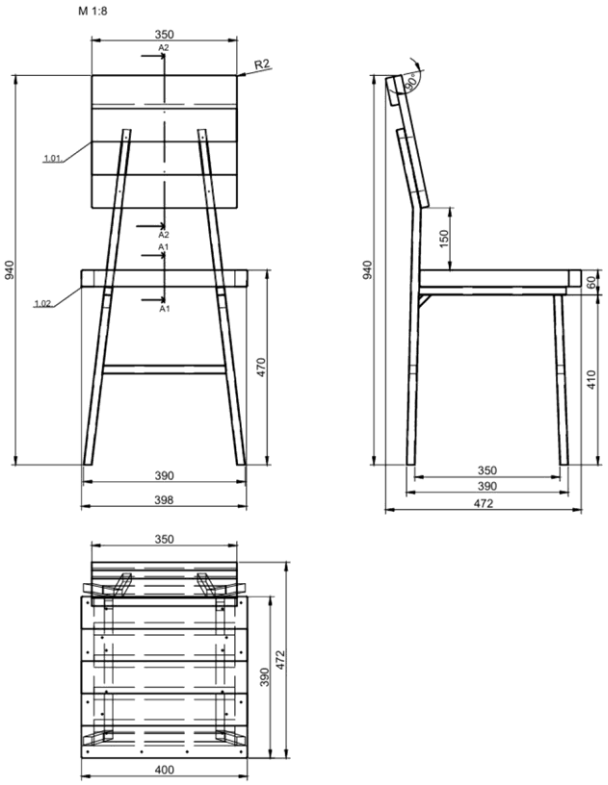

Figure 2. Technical drawing of the chair

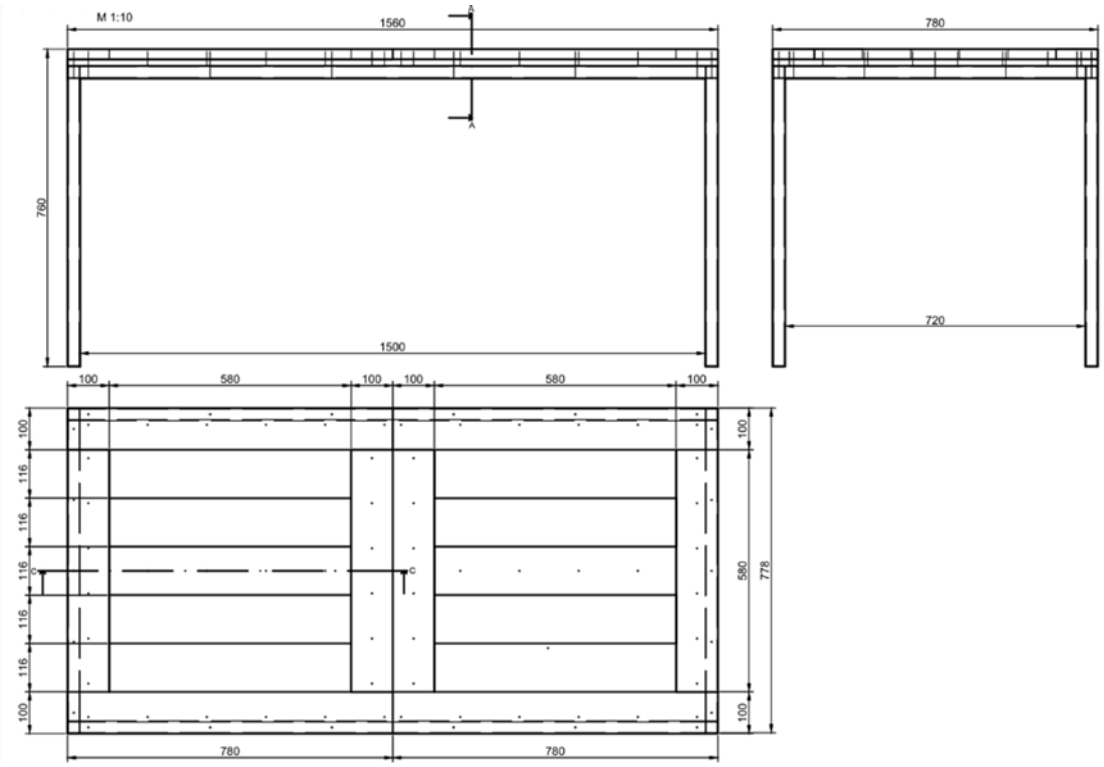

Figure 3. Technical drawing of the table

2.2. Manufacturing of the dining furniture set

The wooden components of the dining set were constructed using rowan wood (*Sorbus aucuparia* L.), European walnut (*Juglans regia* L.) (Figure 4), and plywood. The metal bases were repurposed from office desk and chair frames (Figure 5), obtained through the decommissioning of obsolete institutional furniture. Wood processing was carried out in the faculty's carpentry workshop, while the final assembly took place in a designated facility at the University of Zagreb Faculty of Forestry and Wood technology.

Figure 4. Unedged rowan wood boards

Figure 5. Recycled metal frames of chairs and table prior to surface treatment and assembly

The metal frame of the table and chairs was first manually sanded using P60 grit sandpaper to remove rust and any rough areas, as the structure had been previously used and had not been maintained for an extended period. Following this initial coarse sanding, the surface was further treated with P150 grit sandpaper to achieve a smooth finish suitable for subsequent processing, specifically lacquering. Once the surface was rust free and adequately smooth, the lacquering process began. The coating was applied using an anthracite metallic effect lacquer and a brush, in two layers, to ensure thorough coverage of the old surface and to enhance the final appearance of the metal.

The first step in this production phase of wooden parts was the edging of unedged boards (Figure 4). All boards were initially trimmed to appropriate dimensions using a cross-longitudinal cutting method with a table circular saw. This edging process resulted in straight and mutually parallel edges and removed the bark as well as any irregular sections from each board. The resulting boards were thus prepared for the next phase. The subsequent phase in the production of the dining set involved planing each board. Using a jointer, all boards were processed on two lateral and one flat surface to achieve optimal flatness and prepare them for precise downstream operations. After jointing, the boards were thicknessed to final dimensions of 25 mm for the table's outer frame elements and 20 mm for internal components using a thickness planer, with approximately 3 mm removed per pass until the required thickness was reached. The boards were then cut to a width of 105 mm using a table saw. To eliminate saw marks and ensure clean, smooth edges suitable for effective gluing, an additional 5 mm was trimmed from each side. The chair seats and backrests, as well as sections of the tabletop, were edge-glued using tongue-and-groove joints with loose tenons. Loose tenons, cut to 5 mm in thickness and 30 mm in width, ensured strong and durable joints capable of supporting safe seating. Both the tenons and grooves were made using a table saw, with the blade adjusted to the appropriate height to ensure precise alignment during assembly. Care was taken not to extend the grooves to the edges of the boards, thereby preventing the tenon from being visible after assembly. A D3 water-resistant adhesive was used for bonding, known for its excellent curing properties and ability to form strong joints. The assembled components were then clamped tightly using specialized clamps to ensure proper adhesion. Once the glue had cured, all four chair seats and backrests (Figure 6) were trimmed to final dimensions on a table saw.

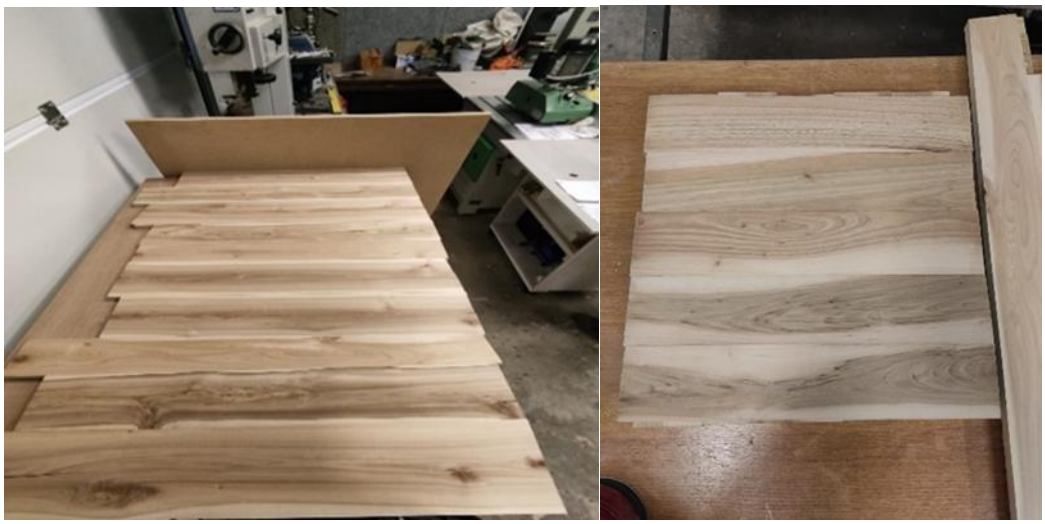

Figure 6. Chair backrest (left) and one section of the tabletop (right) after gluing and before final trimming

All wooden components, including the chair seats, backrests, and tabletop, were mounted onto a 16 mm thick plywood board. Assembly was achieved using adhesive and screws, with 4 mm diameter pilot holes and countersinks drilled beforehand to ensure a clean visual finish. After assembly, the surfaces were sanded using a handheld random orbital sander with P120 grit sandpaper. Due to the small sanding surface and the need for uniformity, this process was time-consuming. Additionally, all edges were manually rounded using progressively finer sandpaper to eliminate sharp corners, enhancing both safety and aesthetic appeal. Before oiling, the final surface treatment, all elements were hand-sanded with fine-grit paper (P120 or higher) to ensure a smooth finish. Surface finishing involved oiling, a process where oil is applied to enhance the natural texture and colour of the wood without producing the yellowish film typical of many varnishes. Oil was chosen because it penetrates deeply into the wood, offering water resistance and dimensional stability. However, unlike lacquer, oil finishes require regular maintenance to preserve their appearance. For this project, a blend of oil and wax was applied in two coats over two days. This combination significantly enhanced the wood's natural texture and visual vibrancy (Figure 7), contributing to an attractive and durable final product, an intended outcome of the design process.

Figure 7. Tabletop, backrests, and seats after surface treatment with oiling

The tabletop was constructed from edge-glued elements of rowan wood, forming the central section, onto which a frame made from the same wood species was later attached. This design choice was made to enhance the visual appeal and distinctiveness of the table. A 16 mm thick plywood board was affixed beneath the solid wood tabletop using 4 × 35 mm screws. This addition not only increased the structural stability of the table but also contributed to a more substantial and visually heavier appearance. For this reason, the plywood board was intentionally left visible on the table's lateral sides. The assembled tabletop was then secured to the metal frame using 4 × 65 mm screws.

3. RESULTS

The chair seat consists of a top layer made of edge-glued walnut wood elements joined with loose tongue-and-groove joints, a thickened edge on three sides, and a bottom layer of plywood board. All components were connected using both adhesive and screws to ensure a stable and durable structure. Similarly, the backrest was constructed using edge-glued walnut elements joined by loose tongue-and-groove, with an additional solid wood strip glued to the top to create a more robust and visually balanced form. The tabletop, chair backrests, and seats were all mounted onto the metal base using 4 × 65 mm screws. Once fully assembled, the dining table set was arranged in the faculty building lobby (Figure 8) to display the final product.

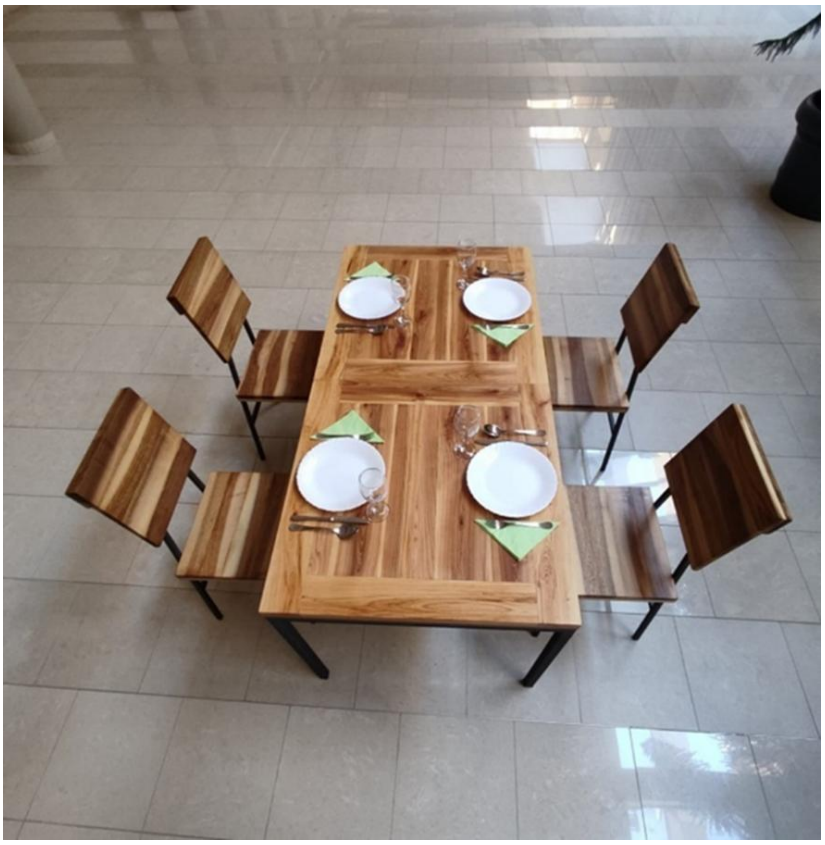

Figure 8. Final appearance of the assembled dining set

4. CONCLUSION

This study demonstrates the feasibility and advantages of producing a dining furniture set using a combination of virgin and recycled materials. The table and four chairs were constructed from solid rowan wood (*Sorbus aucuparia* L.), used for the tabletop, and European walnut (*Juglans regia* L.), used for the backrests and seats of the chairs. A plywood board was incorporated to enhance structural integrity and aesthetic quality, while recycled metal frames from decommissioned furniture served as the base structures for both the table and chairs. The use of D3 adhesive, connecting screws, and a surface finish of oil mixed with wax ensured mechanical stability and a visually appealing, durable finish.

Through careful design and material selection, approximately 0.03 m^3 of rowan wood, 0.026 m^3 of walnut wood, and 0.03 m^3 of plywood were efficiently utilized for the production of the entire set. This approach not only achieved the desired functionality and modern aesthetics but also emphasized sustainability by significantly reducing the environmental footprint through the reuse of discarded components. The successful integration of recycled and natural materials confirms that high-quality, functional, and visually attractive furniture can be produced in a resource-efficient manner. This method contributes to the reduction of raw material consumption, minimization of waste, and promotion of circular design principles in furniture manufacturing. The final product, characterized by its natural wood tones and modern form, serves as a compelling example of how ecological and economic benefits can be harmonized through thoughtful design and material innovation. This dining set design can serve

as a template for future sustainable furniture collections, encouraging wider adoption of recycled components and promoting responsible consumption in the furniture industry.

5. REFERENCES

Al-Saud, K.; Al Ali, R.; Al Saud, A. M.; Abouelela, A. S.; Shehab, R. T.; Moneim, D. A. A.; Hamid, A. E. M., 2024: Exploring the aesthetic and functional aspects of recycled furniture in promoting sustainable development: An applied approach for interior design students. Sustainability, 16 (10): 4003.

Lin, C. W. R.; Chen, M. T.; Tseng, M. L.; Chiu, A. S.; Ali, M. H., 2020: Profit maximization for waste furniture recycled in Taiwan using cradle-to-cradle production programming. Mathematical Problems in Engineering, 2020 (1): 2948049.

Munteanu, A., 2021: Eco-design. Furniture made of recycling materials—a new concept for the contemporan design. Journal of Social Sciences, 4 (3): 60-70.

Pinho, G. C. D. S.; Calmon, J. L.; Medeiros, D. L.; Pinho, C., 2025: Furniture wood waste management towards the circular economy. Applied Sciences, 15 (3): 1360.

Xiong, X.; Yue, X.; Dong, W.; Xu, Z., 2022: Current status and system construction of used-furniture recycling in China. Environmental Science and Pollution Research, 29 (55): 82729-82739.

Zhang, Z.; Zhu, J.; Qi, Q., 2023: Research on the recyclable design of wooden furniture based on the recyclability evaluation. Sustainability, 15 (24): 16758.

Shear Strength of Reinforced Plywood

Jakimovska Popovska, Violeta*; Iliev, Borche[1]

[1] Faculty of design and technologies of furniture and interior-Skopje, SS. Cyril and Methodius University in Skopje, Republic of N. Macedonia
*Corresponding author: jakimovska@fdtme.ukim.edu.mk

ABSTRACT

The aim of this research is to study the shear strength of beech plywood reinforced with non-wood materials in its structure, such as fiberglass and cotton fabrics pre-impregnated with alcohol-soluble phenol-formaldehyde resin (fiberglass prepreg and cotton prepreg). The same resin was used for veneer bonding. The thickness of the veneers used in plywood structure was 1.5 and 1.85 mm. Eight experimental reinforced plywood models were made, four of them reinforced with fiberglass prepreg and the other four with cotton prepreg. The reinforcement was made by inserting certain numbers of sheets of fiberglass/cotton prepreg into the different adhesive layers of the plywood structure. One comparing model of plywood without reinforcement was made. Plywood shear strength was tested in dry-conditioned state at 20 ℃/65% relative humidity and after immersion of the test specimens for 6 hours in boiling water, followed by cooling in water at a temperature of 20±3 ℃ for 2 hours. In all plywood models, the shear strength was tested in the central veneer layer. The results obtained from the shear strength tests are an indicator of increasing the shear strength values by reinforcing the plywood with pre-impregnated cotton and fiberglass fabrics.

Key words: Plywood, reinforcement, pre-impregnated, fiberglass fabric, cotton fabric, phenol-formaldehyde resin

1. INTRODUCTION

Many studies explore the possibilities of improvement of plywood properties through application of non-wood materials in its structure (Davalos *et al*., 2000; Jakimovska Popovska and Iliev, 2019; 2021; 2025). Enhancement of plywood properties can be achieved by fiber-reinforced polymers that give the plywood better durability and water resistance (Hardeo and Karunasena, 2002; Choi *et al*., 2011; Zīke and Kalniņš, 2011). Different fibers and resins were used for plywood reinforcement (Xu *et al*., 1996; Xu *et al*., 1998; Brezović *et al*., 2002; Brezović *et al*., 2003; Brezović *et al*., 2010; Biblis and Carino, 2000; Hrázský and Král, 2007; Maniņš and Zīke, 2011).

The possibilities to reinforce wood with pre-impregnated materials were first explored by Rowland *et al.* (1986). Reinforcement of plywood with fiberglass prepreg significantly decreases the water absorption and thickness swelling of plywood (Jakimovska and Iliev, 2023), as well as increases the bending strength and modulus of elasticity in bending (Jakimovska Popovska and Iliev, 2019). The application of pre-impregnated cotton fabric in the structure of plywood significantly increases its hardness (Jakimovska Popovska and Iliev, 2021) and in-plane compressive strength of plywood (Jakimovska Popovska and Iliev, 2023).

The bonding quality of plywood is determined by the shear strength tests of plywood. The aim the research is to study the shear strength of plywood reinforced with fiberglass and cotton fabrics pre-impregnated with methyl alcohol-soluble phenol-formaldehyde resin.

2. MATERIALS AND METHODS

For the realization of the research, eight experimental models of reinforced plywood were made from beech veneers with thickness of 1.5 and 1.85 mm, with cross-laminated layup of veneers. Four of the reinforced models were made through inserting sheets of fiberglass prepreg (fiberglass fabric pre-impregnated with resin) into different adhesive layers in plywood structure, while the other four models were made by inserting sheets of cotton prepreg (cotton fabric pre-impregnated with resin). In both experimental types of plywood (with fiberglass prepreg and cotton prepreg) the reinforcement sheets have the same layout in plywood structure.

In six models (three models reinforced with fiberglass prepreg and three models reinforced with cotton prepreg), each reinforcement layer is consisted of four sheets of fiberglass/cotton prepreg placed one above the other and inserted symmetrically on both sides with respect to its axis of symmetry. In the first model (FP-1/CP-1), the reinforcements are inserted in the fifth and sixth adhesive layer, while in the second model (FP-2/CP-2) they are inserted into the third and eighth adhesive layer. In the third model (FP-3/CP-3), the reinforcements are positioned as surface layers of plywood. The fourth model of plywood (FP-4/CP-4) has single sheets of fiberglass/cotton prepreg inserted in each adhesive layer of the panel. In all of reinforced plywood models, the orientation of the wrap of the fabric is parallel to grain direction of the surface veneers. One control model (C) of plywood without reinforcement was made for comparison of the results.

The fiberglass prepreg was made form fiberglass fabric made of E-glass fibers, while the cotton prepreg was made from cotton fabric. Both fabrics were pre-impregnated with methyl alcohol soluble phenol-formaldehyde resin with 51 % dry matters content, in quantity of 140 g/m2 for fiberglass fabric and 300 g/m^2 for cotton fabric. The same resin was used for veneer bonding, applied on the veneers in quantity of 180 g/m^2. The thickness of the fiberglass and cotton fabric before impregnation was 0.173 mm and 0.3 mm, respectively, while the thickness of the fiberglass and cotton prepreg was 0,22 mm and 0.6 mm respectively.

The pattern and cross-section of reinforced plywood models, technical characteristics of the fiberglass fabric and cotton fabric, the resin characteristics, as well as the impregnation process are given in previous research papers (Jakimovska and Iliev, 2019 and 2021).

Assembled plywood compositions were pressed in a hot press under specific pressure of 18 kg/cm^2 at temperature of 155 ºC for 30 min.

The shear strength of plywood was tested according to the standard МКС EN 314-1 and МКС EN 314-2. Given the limited number of test specimens, the shear strength of all models was tested only in the central veneer sheet of the plywood panel. Pre-treatment of the test specimens was done which depends on its application according to humidity conditions. The pre-treatment includes immersion of test specimens in boiling water for 6 hours and subsequent cooling in water at a temperature of (20±2) ºC for 2 hours. After the treatment in water, the shear strength test was conducted. In this way, five test specimens from each panel model were tested. At the same time, five air-conditioned test specimens from each model were also tested.

SPSS Statistic was used for statistical analysis of the obtained data. One way ANOVA was used for determination of the significance of the effect of reinforcements on plywood shear strength. Tukey's test was applied to evaluate the statistical significance between the mean

values of this property of different plywood models. The tests were conducted at 0.05 probability level.

3. RESULTS AND DISCUSSION

The results obtained from the shear strength test in an air-conditioned state (Figure 1) and after treatment in boiling water for 6 hours (Figure 2) show that all experimental models have a much higher value of this property than the minimal value of 1N/mm^2 defined by the EN 314 standard.

The analysis of the obtained data from the shear strength test of the experimental plywood panels shows that during the test in air-conditioned state and after treatment in boiling water, the values of this property in models CP-1 and FP-1 are higher compared to the values obtained in the other experimental models. The mean values of these two models in air-conditioned state are almost equal (8.11 and 8.04 N/mm^2), while those of the other models range from 5.30 N/mm^2 in model FP-3 to 6.43 N/mm^2 in model FP-2. During the test after immersion in boiling water for 6 hours, the mean values of models CP-1 and FP-1 are again similar i.e., 6.31 and 6.89 N/mm^2, respectively. The mean values of other reinforced models range from 3.40 N/mm^2 in model CP-2 to 5.12 N/mm^2 in model FP-4.

The analysis of variance of the obtained data for the shear strength in the air-conditioned state (ANOVA: $F(8,36)=19.96$; $p << 0.001$) and after treatment in boiling water (ANOVA: $F(8,36)=57.40$; $p << 0.001$) showed that the differences in the mean values of at least two models are statistically significant. The conducted post-hoc Tukey's test for multiple comparison between models showed that the mean values of the shear strength in the conditioned state and after treatment in boiling water of the models CP-1 and FP-1 are statistically significantly different from the mean values of all other models. The difference in the mean values of these two models is not statistically significant.

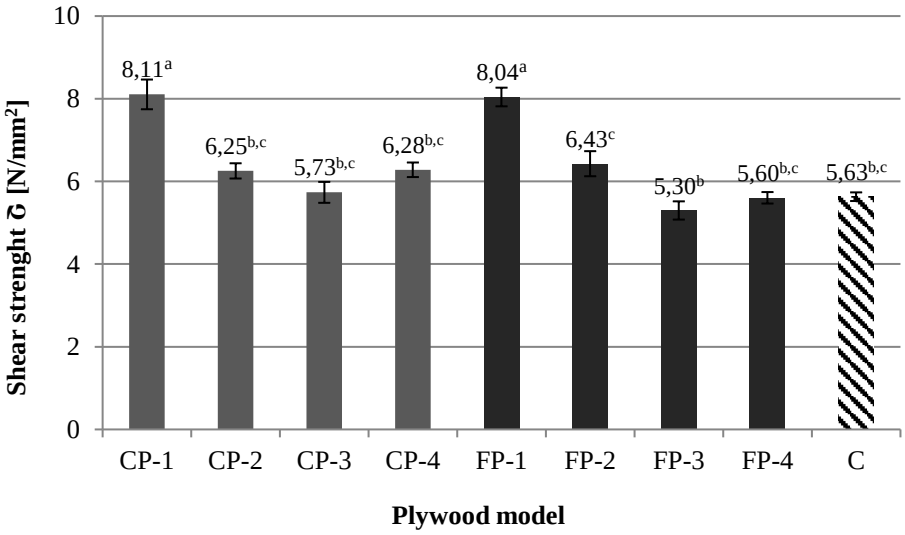

**The mean values with the same letters are not significantly different at 0.05 probability level*

Figure 1. Shear strength of experimental plywood in air-conditioned state

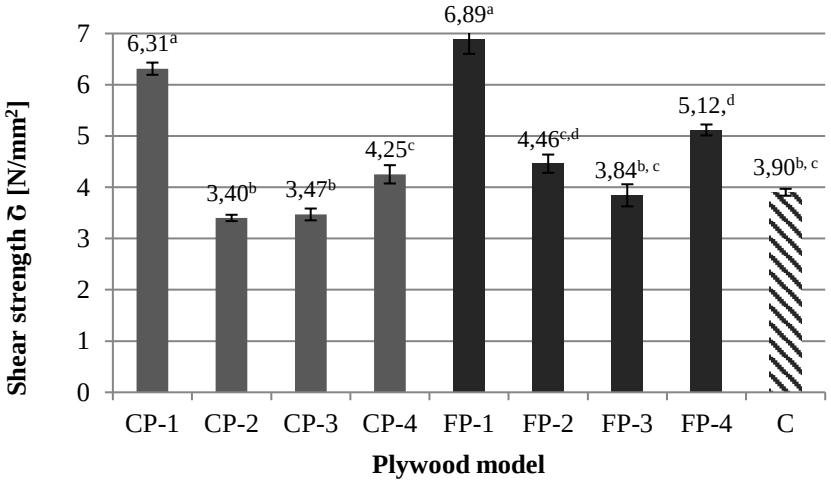

**The mean values with the same letters are not significantly different at 0.05 probability level*

Figure 2. Shear strength of experimental plywood after immersion in boiling water for 6 hours

The percentage of apparent cohesive wood failure in the shear strength test in the air-conditioned state ranges from 10 to 20 %, while in the test of this property after treatment in boiling water, the percentage of the wood failure ranges from 80 to 90 %. According to the standard, at shear strength above 1 N/mm^2, there are no limiting values for the percentage of wood failure on the shear surfaces. The wood fiber failure on the shear surfaces in the shear strength test of the experimental plywood panels are shown on Figures 3, 4, 5 and *6*.

Given the fact that the shear strength was tested only in the central veneer sheet of the experimental models, the obtained test values shown on *Figures 1* and *2* do not show the overall value of the shear strength of the plywood panels, but only the shear strength in the adhesive layers next to the central veneer sheet.

In models CP-1 and FP-1, the adhesive layers next to the central veneer sheet in which the shear occurs, represent adhesive layers between the veneer sheet and the reinforcement. In the remaining tested models, with the exception of models CP-4 and FP-4, these adhesive layers represent adhesive layers between two veneer sheets. The difference in the shear strength values of models CP-1 and FP-1 on the one hand and the other models on the other hand, indicates that the presence of multilayer reinforcements in the plywood structure will increase the shear strength of plywood.

If the shear strength is also tested in the other veneer sheets of plywood structure, it is to be expected that higher values of this property will be obtained in the other models, precisely in those veneer sheets that are located between two multilayer reinforcements.

Despite the fact that in models CP-4 and FP-4 single sheets of reinforcement are inserted in each adhesive layer of the plywood structure, the mean shear strength values in these two models are lower compared to the mean values of models CP-1 and FP-1. This ratio of values between models CP-1 and FP-1 on the one hand and models CP-4 and FP-4 on the other hand indicates that the presence of single sheets of reinforcement in the structure of the panels does not increase the value of the shear strength, as is the case when panels are reinforced with multilayer reinforcements. However, when testing the shear strength after treatment in boiling

water, higher values of the shear strength of models CP-4 and FP-4 can be observed in comparison with models CP-2, CP-3, FP-2, FP-3 and the control model C.

The values obtained from the shear strength test of the experimental plywood panels are an indicator of an increase of the values of the shear strength by reinforcing plywood with pre-impregnated cotton and fiberglass fabrics. It must be noted that confirmation of this statement can only be obtained by expanding the tests of the shear strength to all layers of the plywood panel.

Figure 3. Wood fibre failure of reinforced plywood in air-conditioned state

Figure 4. Wood failure of control model of plywood in air-conditioned state

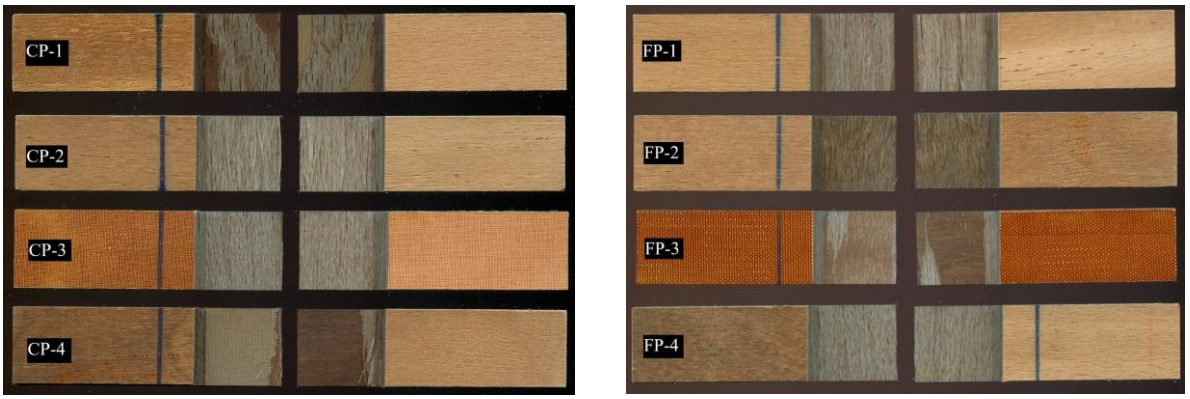

Figure 5. Wood fibre failure of reinforced plywood after immersion in boiling water for 6 hours

Figure 6. Wood fibre failure of plywood after immersion in boiling water for 6 hours

4. CONCLUSIONS

Based on the obtained values for the shear strength of the experimental plywood in an air-conditioned state and after immersion in boiling water for 6 hours, it can be concluded that a high bonding quality of plywood has been achieved. All experimental models have a much

higher value of this property than the minimum prescribed value of 1N/mm^2 by the EN 314 standard.

The obtained results from the shear strength test of the experimental plywood indicate the possibility of increasing the values of this property by applying multilayer reinforcements of pre-impregnated cotton and fiberglass fabrics in the structure of the plywood panel. Confirmation of this statement can only be obtained by expanding the tests of the shear strength to all layers of the plywood panel.

The research presented in the paper can help in the selection of materials and defining the technological parameters for production of high quality plywood durable for application in high humidity conditions.

5. REFERENCES

Biblis, E. J.; Carino, H. F.; 2000: Flexural properties of southern pine plywood overlaid with fiberglass-reinforced plastic. Forest Prod Journal, 50 (1): 34-36.

Brezović, M.; Jambreković V.; Kljak, J., 2002: Utecaj karbonskih vlakana na neka relevantna svojstva furnirskih ploča. Drvna industrija, 53 (1): 23-31.

Brezović, M.; Jambreković, V.; Pervan, S., 2003: Bending properties of carbon fiber reinforced plywood. Wood Research, 48 (4): 13-24.

Brezović, M.; Kljak, J.; Pervan, S.; Antonović, A., 2010: Utjecaj kuta orientacije sintetskih vlakana na savojna svojstva kompozitne furnirske ploče. Drvna industrija, 61 (4): 239-243.

Choi, S. W.; Rho, W. J.; Son, K. J.; Lee, W. I., 2011: Analysis of buckling load of fiber-reinforced plywood plates for NO 96 CCS. In: Proceedings of the Twenty-first International Offshore and Polar Engineering Conference, Maui, Hawaii, USA, pp. 79-83.

Davalos, J. F.; Qiao, P. Z.; Trimble, B. S., 2000: Fiber-reinforced composite and wood bonded interfaces: Part 1. Durability and shear strength. Journal of Composites Technology & Research, 22 (4): 224-231.

Hardeo, P.; Karunasena, W., 2003: Buckling of fiber-reinforced plywood plates. In: Proceedings of Second International Conference on Structural Stability and Dynamics, Singapore, pp. 442-447.

Hrázský, J.; Král, P., 2007: A Contribution to the properties of combined plywood materials. Journal of Forest Science, 53 (10): 483-490.

Jakimovska Popovska, V.; Iliev, B., 2019: Bending Properties of Reinforced Plywood with Fiberglass Pre-Impregnated Fabrics. In: Proceedings of 30th International Conference on Wood Science and Technology - ICWST and 70th anniversary of Drvna industrija Journal "Implementation of wood science in woodworking sector". Croatia, Zagreb, pp. 77-85.

Jakimovska Popovska, V.; Iliev, B., 2021: Janka hardness of plywood reinforced with pre-impregnated cotton fabrics. In: Proceedings of the 5th International Scientific Conference "Wood Technology & Product Design". Macedonia, Ohrid, pp. 7-14.

Jakimovska Popovska, V.; Iliev, B., 2025: Compressive strength of plywood reinforced with pre-impregnated fiberglass fabrics. In: Proceedings of the 7th International Scientific Conference "Wood Technology & Product Design". Macedonia, Ohrid, pp. 203-210.

Maniņš, M.; Zīke, S., 2011: Textile fabrics reinforced plywood with enhanced mechanical properties. In: Abstracts of the International Scientific Conference „Civil Engineering'11", Latvia, p. 35.

Rowlands, R. E.; Van Deweghe, R. P.; Launferbeg, T. L.; Krueger, G. P., 1986: Fiber-reinforced wood composites. Wood and Fiber Science, 18 (1): 39-57.

Xu, H.; Tanaka, C.; Nakao, T.; Nisano Y.; Katayama, H., 1996: Flexural and shear properties of fiber reinforced plywood. Mokuzai Gakkaishi, 42: 376-382.

Xu, H.; Nakao, T.; Tanaka, C.; Yoshinobu, M.; Katayama, H., 1998: Effects of fiber length orientation on elasticity of fiber-reinforced plywood. Journal of Wood Science, 44: 343-347.

Zīke S.; Kalniņš K., 2011: Enhanced impact properties of plywood. In: Proceedings of the 3rd International Conference Civil Engineering'11, Latvia, pp. 125-130.

***Macedonian standard MKC EN 314-1, 2011: Plywood – Bonding quality – Part 1: Test methods.
***Macedonian standard MKC EN 314-1, 2011: Plywood – Bonding quality – Part 2: Requirements.

Influence of the Corner Joints of the Window Frame and Sash on the Final Quality of the Window

Jevtoska, Elena*; Gruevski, Gjorgi; Mihajlovski, Nikola[1]

[1] Faculty of Design and Technologies of Furniture and Interior – Skopje, University of Saint Cyril and Methodius in Skopje, Skopje, Republic of North Macedonia
*Corresponding author: jevtoska@fdtme.ukim.edu.mk

ABSTRACT

The quality of a product is a characteristic that demonstrates how well it meets the needs for which it is intended. Given that, a window purpose is to provide light and desired ventilation to a room, while at the same time protecting the building from external influences such as air permeability, water permeability and wind resistance, we prove that it is of high quality the more it provides us with these conditions. A window as a product is a complex composition of different materials and parts. The different parts of a window include the basic structural elements, filling elements, fitting, and additional accessories. The basic structural elements of a window are the supporting frame and the window sash. The corner joints of these elements will be the target of research, in terms of how the strength of the joint of the corner segments of windows made of wooden frame, PVC frame or aluminium frame can affect the window's resistance to air permeability, water permeability and wind resistance.

Key words: window, construction carpentry, window profiles, air permeability, water permeability, wind resistance

1. INTRODUCTION

The purpose of the windows as a construction product is to provide the building with natural light and the opportunity to ventilate the interior and at the same time providing protection of the room against external influences such as wind and rain, as well as to prevent uncontrolled cooling or heating of the room or the whole building in which they are built in. Considering the purpose, a good quality window is one that protects against air permeability, water permeability, wind resistance as well as uncontrolled loss of energy.

The window as a product is a complex composition of different materials and parts. As different parts of the window, the basic structural elements, filling elements, fittings, additional accessories are distinguished. Basic structural elements of the window are the supporting frame, which is contained of a case and a window sash.

The supporting frame – case. The supporting frame is a fixed structural element, attached to the sides of the communication opening. This case bears the window sash (Kyuchukov, 2009)

The window sash is the mobil part of the basic structural elements. Depending on the need, it can rotate along a horizontal or vertical axis, slide laterally, but also a combination of several directions of rotation.

Quality is a process in which only our customers, not our products, keep coming back (Ristevska-Jovanoska, 2010). Businesses are not paid to change customers, but to satisfy them

(Drucker, 2005). Quality is the set of characteristics of a product or service that fulfil the satisfaction of consumer needs (Shuklev, 2011).

Windows are elements of construction carpentry that are composed of movable and immovable parts. Depending on the function that the windows of the building have to achieve, it is chosen from which materials they will be made and which attributes have to be achieved by the materials for constructing a window. If the windows have to only provide daylight in the space, they are constructed as fixed, in other words, they have only a stationary part, and if, in addition to light, they are to provide ventilation of the space, the windows are constructed with a fixed, specifically immovable case and a movable sash that, according to needs, has the possibility to open. In order to choose the most appropriate combination of materials for the construction of a good quality window which will satisfy all the required features, it is necessary to know the attributes of the built-in materials and how they affect the quality of the window.

Windows made of profiles of different materials were taken as samples for this research. The samples will be divided into two groups: group 1/12 of frame samples and group 2/12 of sash samples. In both groups, results will be given for three subgroups of windows. The window subgroups will be divided depending on the profile used, i.e. a subgroup of windows made of Aluplast Ideal 4000 – PVC profile, Alumil M9650 – aluminium profile and wooden profile (Figure 1). Each subgroup will have three windows with dimensions 800/800 mm. 12 samples of the frame and 12 samples of the sash will be taken from the subgroup.

The windows will be tested for air permeability, water permeability and wind resistance before sample preparation. The results for air permeability and wind resistance will be given as an average value, while for water permeability the lowest water penetration time of the sample from the subgroup will be taken into consideration.

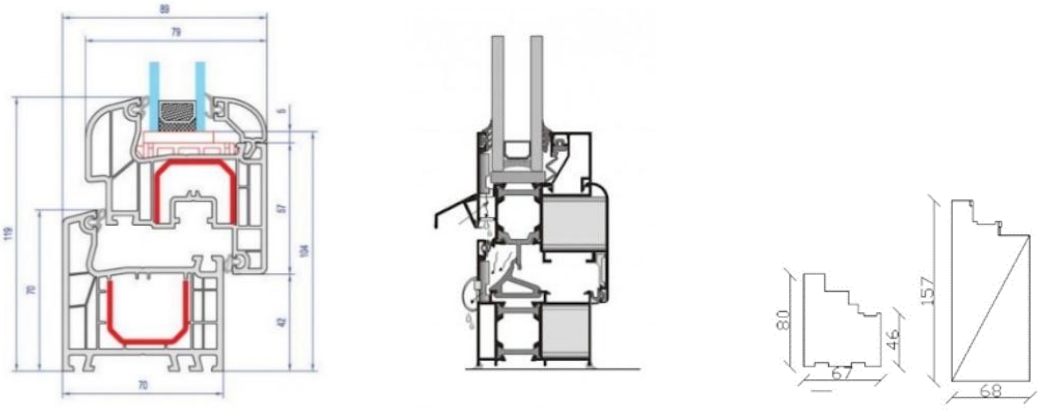

Aluplast Ideal 4000 ALUMIL M9650 Wooden profile

Figure 1. Cross-section of window profiles (according to the Aluplast and Alumil manufacturings)

First, windows made of profiles of different materials with similar dimensions and glazed with the same glass will be tested according to the standard/test-method EN 1026:2016 Windows and doors - Air permeability - Test method. According to the standard/test-method, how much air loss there is at a certain pressure will be measured and the average class of air permeability will be determined according to the classification of EN 12207:2016 Windows and doors - Air permeability - Classification. A water permeability test will also be done according to the standard method EN 1027:2016 Windows and doors - Water tightness - Test method. According to the method, the resistance of the windows to water under different

pressures will be determined and it will be determined in which class they are counted for water resistance according to EN 12208:2016 Windows and doors - Water tightness - Classification. Wind resistance deviation will be measured on the samples accordingly EN 12211:2016 Windows and doors - Resistance to wind load - Test method and it will be determined in which class they are counted for wind resistance accordingly EN 12210:2016 Windows and doors - Resistance to wind load - Classification.

Afterwards, the samples are prepared according to the standard EN 514:2018 Plastics - Poly (vinyl chloride) (PVC) based profiles - Determination of the strength of welded corners and T-joints. The results of the test will give us data on the strength of the welded corners made from the same profile and how much it differs between the sash and the case.

2. RESEARCH OBJECTIVES

The goal of this research is to show how and to what extent the material of the window frame profile can affect the final quality of the window.

The aim is to prove whether the strength of the corner joints of profiles made of different materials such as wood, aluminium or PVC can affect the air permeability, water tightness and resistance to wind load.

3. HYPOTESIS

It is assumed that the strength of the corner joint between the sash and the frame affects the overall quality of the window. However, the strength of the joint varies with the different materials of which the window profile is made. The assumption is that the difference in the strength of the corner joints provided by profiles made of different materials such as wood, aluminum and PVC has no impact on the quality of the window in terms of air permeability, water permeability and wind resistance.

4. RESULTS AND DISCUSSION

Air permeability measurements, water tightness measurements and wind resistance tests according to European and national standards will be carried out using a window testing machine from the manufacturer K.Schulten mbH&Co.KG model KS 3040/650 shown in Figure 2.

Figure 2. Measurement according to standards EN 1026:2016, EN 1027:2016, EN 12211:2016

4.1. Results of the air permeability

Tables 1, 2 and 3 give the average values of the group of windows tested from the same profile. Three windows were tested from each group and the average value of air permeability was calculated.

Table 1. Sample 1 – air permeability (PVC profiles)

Normal pressure, Pa		50	100	150	200	250	300	450	600	**General class**
Actual pressure, Pa		50	100	150	201	251	301	452	603	
Air permeability	m³/h	0.71	1.33	1.82	2.30	2.73	3.17	4.51	6.08	
Perimeter	m³/(h/m)	0.25	0.46	0.63	0.79	0.94	1.09	1.56	2.10	
Class		4	4	4	4	4	4	4	4	4
Window surface	m³/(h/m²)	0.83	1.90	2.65	3.28	3.84	4.35	5.61	6.66	
Class		4	4	4	4	4	4	4	4	4
										4

Table 2. Sample 2 – air permeability (aluminium profiles)

Normal pressure, Pa		50	100	150	200	250	300	450	600	**General class**
Actual pressure, Pa		50	99	150	199	250	300	452	598	
Air permeability	m³/h	6.06	9.98	14.55	19.82	25.19	30.26	54.28	80.50	
Perimeter	m³/(h/m)	1.19	1.96	2.86	3.89	4.95	5.95	10.66	15.81	
Class		3	3	3	2	2	2	0	0	2
Window surface	m³/(h/m²)	3.33	5.48	8.00	10.89	13.84	16.63	29.82	44.23	
Class		3	3	3	3	3	3	303	0	2
										2

Table 3. Sample 3 – air permeability (wooden profiles)

Normal pressure, Pa		50	100	150	200	250	300	450	600	**General class**
Actual pressure, Pa		51	100	150	201	251	301	463	602	
Air permeability	m^3/h	2.04	3.08	3.99	4.78	5.50	6.18	8.06	9.90	
Perimeter	$m^3/(h/m)$	0.70	1.06	1.37	1.65	1.90	2.13	2.78	3.41	
Class		3	3	3	3	3	3	3	3	3
Window surface	$m^3/(h/m^2)$	3.18	4.82	6.23	7.46	8.60	9.65	12.59	15.47	
Class		3	3	3	3	3	3	3	3	3
										3

4.2. Results of the water permeability

Tables 4, 5 and 6 show the lowest values of the group of windows tested from the same profile. Three windows from each group were tested and the lowest water permeability value was obtained.

Table 4. Sample 1 – water permeability (PVC profiles)

Class	**Pressure in Pa**		**Time**	**Water entrance**		**Observation**
	Normal	**Actual**		**Dripping**	**Flowing**	
A1	0	0	00:15:00	00:00:00	00:00:00	**OK**
A2	50	50	00:05:00	00:00:00	00:00:00	**OK**
A3	100	100	00:05:00	00:00:00	00:00:00	**OK**
A4	150	150	00:05:00	00:00:00	00:00:00	**OK**
A5	200	201	00:05:00	00:00:00	00:00:00	**OK**
A6	250	250	00:05:00	00:00:00	00:03:44	**NOT OK**

Table 5. Sample 2 – water permeability (aluminium profiles)

Class	**Pressure in Pa**		**Time**	**Water entrance**		**Observation**
	Normal	**Actual**		**Dripping**	**Flowing**	
A1	0	0	00:15:00	00:00:00	00:00:00	**OK**
A2	50	50	00:05:00	00:00:00	00:00:00	**OK**
A3	100	100	00:05:00	00:00:00	00:00:00	**OK**
A4	150	149	00:05:00	00:00:00	00:00:00	**OK**
A5	200	201	00:05:00	00:00:00	00:01:38	**NOT OK**

Table 6. Sample 3 – water permeability (wooden profiles)

Class	**Pressure in Pa**		**Time**	**Water entrance**		**Observation**
	Normal	**Actual**		**Dripping**	**Flowing**	
A1	0	0	00:15:00	00:00:00	00:00:00	**OK**
A2	50	50	00:05:00	00:00:00	00:00:00	**OK**
A3	100	100	00:05:00	00:00:00	00:00:00	**OK**
A4	150	148	00:05:00	00:00:00	00:00:00	**OK**
A5	200	201	00:05:00	00:00:00	00:00:00	**OK**
A6	250	251	00:05:00	00:00:00	00:00:09	**NOT OK**

4.3. Results of resistance to wind load

During wind resistance testing, the frontal deflections that appear on the profile under a wind load of 1600 Pa were measured. All windows were subjected to the same pressure. Table 7 provides the limit values of the classes according to the EN 12211:2016 standard.

Table 7. Maximum deflection to the classification at the base width

Class (a-c) 660 mm			Deflection f, mm
A	(a-c)/	150	4.40
B	(a-c)/	200	3.30
C	(a-c)/	300	2.20

Tables 8, 9 and 10 give the average values of the groups for frontal deflections observed at a wind pressure of 1600 Pa. The average values are taken for PVC profile windows, aluminium profile windows and wooden profile windows.

Table 8. Measuring results of the deflection in mm – PVC windows

Wind pressure, Pa	Point 1(a)	Point 2(b)	Point3(c)	Deflection f, mm
1603Pa	0.32	0.43	0.30	0.12
0Pa	0.00	0.00	0.00	0.00
-1600Pa	0.34	0.40	0.31	0.08
0Pa	0.00	0.00	0.00	0.00

Table 9. Measuring results of the deflection in mm – aluminium windows

Wind pressure, Pa	Point 1(a)	Point 2(b)	Point3(c)	Deflection f, mm
1603Pa	0.27	0.43	0.20	0.20
0Pa	0.00	0.00	0.00	0.00
-1600Pa	0.15	0.27	0.12	0.14
0Pa	0.00	0.00	0.00	0.00

Table 10. Measuring results of the deflection in mm – wooden windows

Wind pressure, Pa	Point 1(a)	Point 2(b)	Point3(c)	Deflection f, mm
1603Pa	0.68	1.03	0.73	0.33
0Pa	0.00	0.00	0.00	0.00
-1600Pa	0.41	0.92	0.94	0.25
0Pa	0.00	0.00	0.00	0.00

4.4. Results from windows made from PVC profile windows, aluminium profile windows and wooden profile windows, determining the strength of the corner joints of the frame (sash, frame)

The extracted corner samples were divided into a group of frame samples and a group of window sash samples. The measurement was recorded for all samples and an average value was extracted for frame and wing for each profile type.

4.4.1. Results from a group of frame tests

Figure 3 shows samples from the group of window frames that are subjected to force.

Figure 3. Force applied on samples from a group of frame

Table 11. Determining the strength of the corner joints of the frame – PVC windows

Measured force at the moment of breaking the sample											
F_{1-1} (N)	F_{2-1} (N)	F_{3-1} (N)	F_{4-1} (N)	F_{5-1} (N)	F_{6-1} (N)	F_{7-1} (N)	F_{8-1} (N)	F_{9-1} (N)	F_{10-1} (N)	F_{11-1} (N)	F_{12-1} (N)
5814	5612	5334	5612	5551	5125	5866	5328	5811	5817	5421	5577
Average value						F1 = 5572 N					

Table 12. Determining the strength of the corner joints of the frame – aluminium windows

Measured force at the moment of breaking the sample											
F_{1-2} (N)	F_{2-2} (N)	F_{3-2} (N)	F_{4-2} (N)	F_{5-2} (N)	F_{6-2} (N)	F_{7-2} (N)	F_{8-2} (N)	F_{9-2} (N)	F_{10-2} (N)	F_{11-2} (N)	F_{12-2} (N)
7625	7890	8001	8115	7930	8005	8120	7930	7844	7860	8001	7863
Average value						F2 = 7932 N					

Table 13. Determining the strength of the corner joints of the frame – wooden windows

Measured force at the moment of breaking the sample											
F_{1-3} (N)	F_{2-3} (N)	F_{3-3} (N)	F_{4-3} (N)	F_{5-3} (N)	F_{6-3} (N)	F_{7-3} (N)	F_{8-3} (N)	F_{9-3} (N)	F_{10-3} (N)	F_{11-3} (N)	F_{12-3} (N)
7301	7311	7483	7930	7280	7912	7866	7771	7890	7913	7821	7882
Average value						F3 = 7697 N					

4.4.2. Results from a group of sash tests

Figure 4 shows samples from the group of window sash that are subjected to force.

Figure 4. Force action on samples from a group of sash

Table 14. Determining the strength of the corner joints of the sash – PVC windows

Measured force at the moment of breaking the sample											
F_{1-4} (N)	F_{2-4} (N)	F_{3-4} (N)	F_{4-4} (N)	F_{5-4} (N)	F_{6-4} (N)	F_{7-4} (N)	F_{8-4} (N)	F_{9-4} (N)	F_{10-4} (N)	F_{11-4} (N)	F_{12-4} (N)
5620	5691	5705	5628	5708	5630	5699	5811	5600	5603	5809	5496
Average value							F1 = 5667 N				

Table 15. Determining the strength of the corner joints of the sash – aluminium windows

Measured force at the moment of breaking the sample											
F_{1-5} (N)	F_{2-5} (N)	F_{3-5} (N)	F_{4-5} (N)	F_{5-5} (N)	F_{6-5} (N)	F_{7-5} (N)	F_{8-5} (N)	F_{9-5} (N)	F_{10-5} (N)	F_{11-5} (N)	F_{12-5} (N)
8312	8401	8150	8492	8318	8701	8625	8312	8282	8120	8113	8319
Average value							$F_{2=}$ 8345 N				

Table 16. Determining the strength of the corner joints of the sash – wooden windows

Measured force at the moment of breaking the sample											
F_{1-6} (N)	F_{2-6} (N)	F_{3-6} (N)	F_{4-6} (N)	F_{5-6} (N)	F_{6-6} (N)	F_{7-6} (N)	F_{8-6} (N)	F_{9-6} (N)	F_{10-6} (N)	F_{11-6} (N)	F_{12-6} (N)
7286	7405	7211	7312	7632	7628	7005	7093	7113	7441	7321	7105
Average value							F3 = 7296 N				

4.5. Results of resistance to wind load

The results obtained from air permeability show that the PVC profile achieves best results, second best are windows with wooden profile and at the end are windows with the aluminum profile. The water permeability results show approximately identical results with minimal deviation in the results of the aluminum profile. The wind resistance results are in the same class in all three profiles. Research on the strength of corner joints shows that the greatest strength of the joint is in aluminum profile, followed by wooden profile, and the lowest strength of the joint is in PVC profiles.

5. CONCLUSION

A total of 36 samples of window frames and 36 samples of window sashes were used in the research.”. The samples were divided into three groups, i.e. groups of different profiles made of different materials. 12 samples of frames and 12 samples of sashes were used from the test. Before taking the samples, the windows were tested for air permeability, water permeability and wind resistance. The obtained breaking moment forces of the compression tests are compared with the results of air penetration, water penetration and wind resistance. Such a comparison provides information that in addition to the hardware used, the method of manufacture and connection also has an impact on air permeability, water permeability and wind resistance.

The profile used to make windows has a significantly large impact on frontal deflections during wind gusts.

Window construction has a significant impact on frontal deflections during wind gusts.

The material used to construct the window does not solely determine whether the window performs adequately.

The construction of the window and the hardware used are key factors in the quality of the window.

6. REFERENCES

Drucker, P., 2005: Najvaznije o menadzmentu, izbor iz radova o menadzmentu, M.E.PConsult, Zagreb.
Kyuchukov, G., 2009: Konstruiranje na mebeli, vrati I prozorci, Matkom, Sofia.
Ristevska-Jovanovska, S., 2010: Marketing teorija I praktika, Ekonomski fakultet, Skopje.
Suklev, B., 2013: Menadzment, Ekonomski fakultet, Skopje.
***EN 1026, 2016: Windows and doors - Air permeability - Test method
***EN 12207, 2016: Windows and doors - Air permeability – Classification
***EN 1027, 2016: Windows and doors - Water tightness - Test method
***EN 12208:2016 Windows and doors - Water tightness – Classification
***EN 12211, 2016: Windows and doors - Resistance to wind load - Test method
***EN 12210, 2016: Windows and doors - Resistance to wind load – Classification
***EN 514, 2018: Plastics - Polyvinyl chloride) (PVC) based profiles - Determination of the strength of welded corners and T-joints.
***Technical Catalog Aluplast manufacturing.
***Technical Catalog Alumil manufacturing.

The Impact of Global Crises on FSC-Certified Wood Industry: Insights from Croatia, Slovenia, and Slovakia

Klarić, Kristina[1*]; Jošt, Matej[2]; Paluš, Hubert[3]; Katarina Remic[2]; Klarić, Miljenko[1]; Grošelj, Petra[2]; Dzian, Michal[3]

[1] Faculty of Forestry and Wood Technology, University of Zagreb, Zagreb, Croatia
[2] Biotechnical Faculty, University of Ljubljana, Ljubljana, Slovenia
[3] Faculty of Wood Sciences and Technology, Technical University in Zvolen, Zvolen, Slovakia
*Corresponding author: kklaric@sumfak.unizg.hr

ABSTRACT

This research examines the impact of global crises, including the COVID-19 pandemic and the conflict in Ukraine, on FSC-certified wood-based companies in Croatia, Slovenia and Slovakia. The wood-based industry is crucial to these economies, and FSC certification plays a key role in promoting sustainability and competitiveness in the market. In recent years, these external shocks have disrupted supply chains, changed market demand and impacted production processes. Data were collected through an online survey of FSC certificate holders in Croatia, Slovenia and Slovakia. Statistical analyses using χ^2 tests and Spearman rank correlation were conducted to assess differences in responses across the surveyed markets. The results show that Slovenian companies experienced a smaller negative impact of the COVID-19 pandemic compared to Croatian and Slovak companies. Difficulties in sourcing materials and selling products varied, with challenges being more pronounced in Croatia and Slovakia. Similarly, the impact of the conflict in Ukraine was relatively evenly distributed across countries. The findings provide valuable insights to policy makers and industry stakeholders in developing strategies to enhance economic resilience and sustainability in the timber industry.

Key words: Croatia, FSC certification, global crises, Slovakia, Slovenia, wood industry

1. INTRODUCTION

Forest-based industries are a very important part of the European Union economy. They include woodworking, furniture, pulp and paper manufacturing and converting, and printing. This part of the industry accounts for 7 % of EU GDP from manufacturing. Another important aspect of this sector is that it employs 3.5 million people in 40,000 companies. The number of employees in this sector increased from 2012 to 2022 by 1.4 % (Eurostat, 2024). The sector is mostly composed of medium and micro companies. Forest-based industries are largely located in underdeveloped and rural areas, which provides employment and livelihoods in these areas (EU Commission, 2025).

The current state of Slovenia's wood industry is not the best, the latest data from the Statistical Office of the Republic of Slovenia (UNECE, 2025) mention a decline in sales revenue in wood processing (7.3 %) and furniture production (5.7 %). According to UNECE (2025), Slovakia also records a decline in the wood processing industry. In 2023, there was a significant decrease in the amount of processed wood, by more than 20 %, therefore there was also a significant decrease in income by 15.2 % in that sector. The wood industry in Croatia is very important for the economy, Croatia is the largest exporter of sawn hardwood in Europe (EOS, 2023), but this still represents a small share on a global scale. The export orientation

makes the wood sector extremely vulnerable and dependent on external, global economic trends.

Wood is a natural and renewable material that stores carbon. That is why it is very important in the development of low carbon and bio economy. Regardless of its positive properties in terms of bio-economy and renewability, it is very important that the forests from which the wood for the wood industry comes are managed responsibly (Klarić et al., 2016). Confirmation of responsible forest management is achieved through certification, and in Europe the most represented schemes for certification are FSC - Forest Stewardship Council and PEFC - Programme for the Endorsement of Forest Certification. Certified companies face many challenges on the market and some of the main problems connected to certified supply chain relate to the overpricing of certified material inputs followed by difficulties associated with the consistency and quantity of supply (Paluš *et al.*, 2018).

In this study, we investigated how global changes such as the COVID-19 pandemic and the conflict in Ukraine have affected the wood processing sector. According to numerous literature, these changes have affected supply chains (Klarić *et al*., 2023; Klarić *et al*., 2024; Vukman *et al*., 2024), and export-oriented markets have shown great vulnerability during this period. Given that the basic material for the wood processing industry comes from forests, sustainability and responsible forest management have become important for the competitiveness of the sector. Therefore, we wanted to investigate how FSC certified companies have responded to the current global changes. The aim of this study is to analyse the impact of recent global crises on wood processing companies in Slovenia, Slovakia and Croatia.

2. RESEARCH METHOD

The research method used in this paper is an online survey. In addition to general questions about the profile of the respondents, it consisted of 6 closed-ended questions about the impact of COVID-19 pandemic and the conflict in Ukraine on company business operations. The object of the research was all FSC certified companies in Croatia (CRO), Slovenia (SLO) and Slovakia (SVK). The list of certified companies is obtained from the FSC certificate holder database, and contact information was collected from available national databases. The invitation to complete the survey was sent via e-mail containing a link to the survey. The surveys in Slovenia and Croatia were created using the 1ka application tool, and in Slovakia using Google forms. The data collection in Croatia was conducted in mid-2023, and in Slovenia and Slovakia in early 2024. The response rate in Croatia was 34.4%; in Slovenia 23.7%; and in Slovakia 17.7%. The data were analysed using descriptive statistics.

3. RESULTS

The profile of respondents in all three countries surveyed includes the highest proportion of limited liability companies (more than 87 %). The most common core activity in Croatia and Slovakia is wood processing, while in Slovenia wood processing and trade companies are equally represented. Most companies in all surveyed countries are engaged in exports. Regarding the number of employees, in Slovenia and Slovakia the majority are companies with

fewer than 10 employees, while in Croatia the largest share consists of companies with 10-49 employees.

The results of the impact of the COVID-19 pandemic on business operations are shown in Figure 1. The largest share of companies that had impact from the pandemic was in Slovakia (79.55 %), while Croatia also recorded a significant negative impact (69.00 %). In Slovenia, less than half of the surveyed companies (45.45 %) stated that the pandemic had an impact on their business operations.

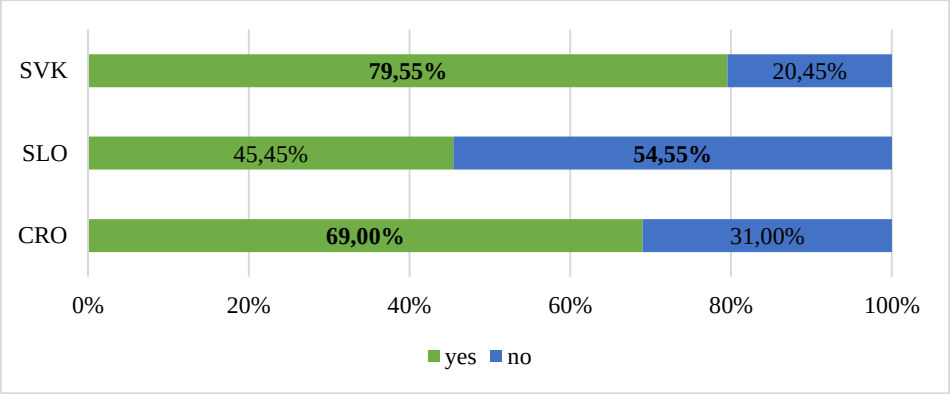

Figure 1. Impact of the COVID-19 crisis on business

The intensity of the impact of the COVID-19 pandemic on material sourcing for production is shown in Figure 2. The highest share of companies with a medium impact of the pandemic on procurement was recorded in Slovakia (38.64b%) and Croatia (32.29 %). In contrast, the highest share of companies in Slovenia reported a very low level of difficulties in procurement (26.97%). High and very high difficulties of the impact of the COVID-19 pandemic on material sourcing for production are similar in all three countries.

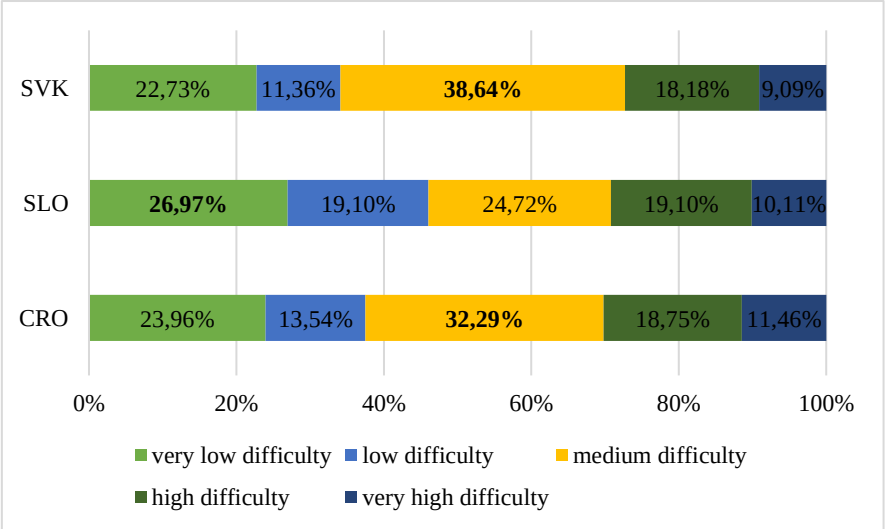

Figure 2. Impact of the COVID-19 crisis on material sourcing for production

According to Figure 3, it is evident that the levels of difficulties in sales associated with the COVID-19 crisis differed between countries. In Slovenia and Slovakia, the largest proportion of companies had very low difficulties in sales. In Croatia, the most common

response was a medium level of difficulties (29.90 %). The share of companies with high and very high difficulties was highest in Croatia and lowest in Slovenia.

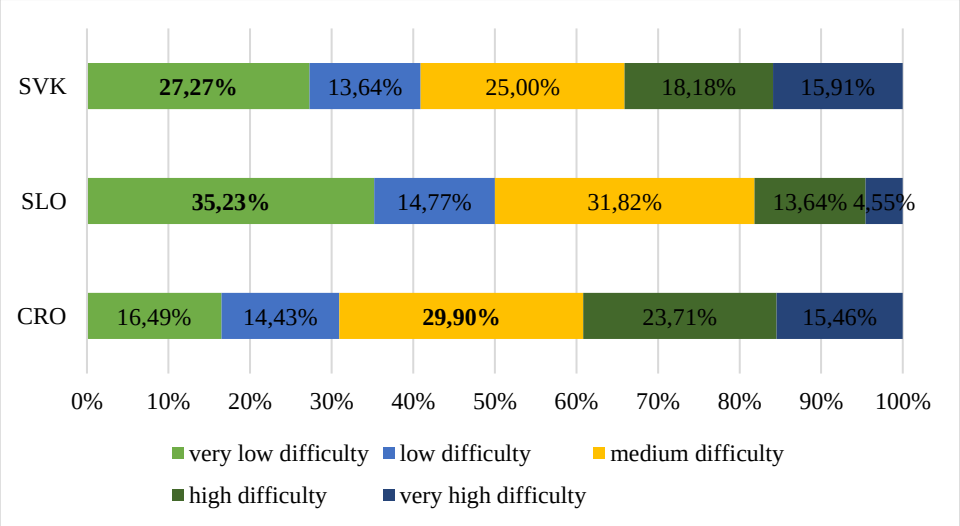

Figure 3. Impact of the COVID-19 crisis on product sales

Figure 4 presents the distribution of responses regarding changes in wood product prices during and after the COVID-19 crisis. Across all surveyed countries, the highest percentage of respondents stated that prices did not change due to the COVID-19 crisis. When comparing whether prices decreased or increased, all countries recorded a greater prices increases than their decrease. The largest price increase was recorded in Croatia.

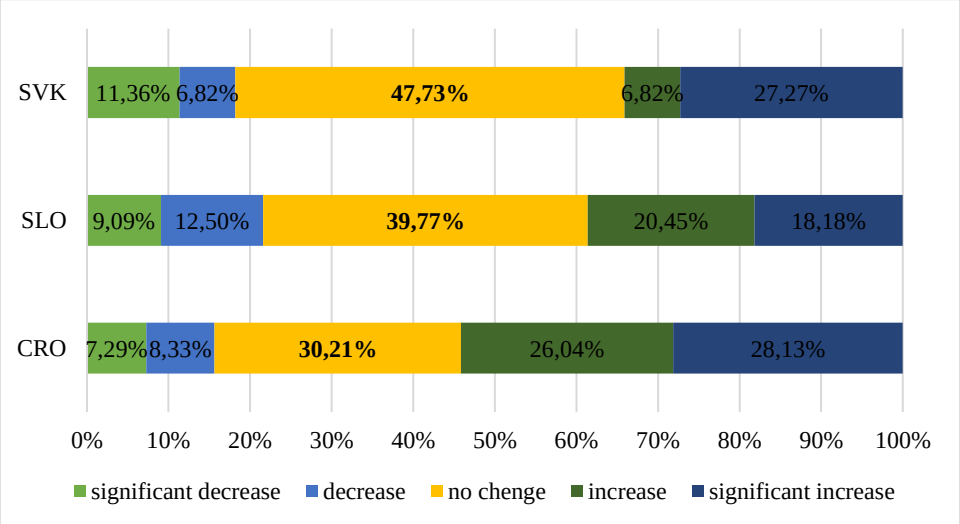

Figure 4. Change in wood product prices during and after the COVID-19 crisis

Figure 5 shows that companies in all three countries experienced negative consequences of the conflict in Ukraine on their business. The largest negative effect was recorded in Slovakia (68.18 %), and the share of companies with a negative effect was also in Croatia (53.54 %), and Slovenia (52.81 %).

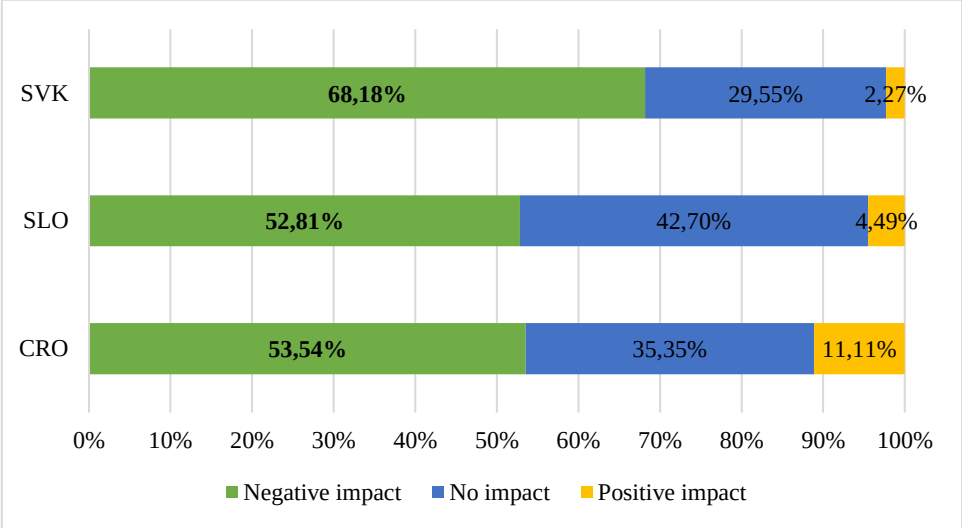

Figure 5. Impact of conflict in Ukraine on business

According to the data presented in *Figure 6*, in all three countries the largest share of companies stated that the demand for wood products had not changed significantly due to the conflict in Ukraine. The largest decline in demand was recorded in Slovakia (38.64 %), followed by Slovenia (33.71 %), and Croatia (30.93 %). The largest proportion of companies that recorded an increase in demand was in Croatia (17.53 %).

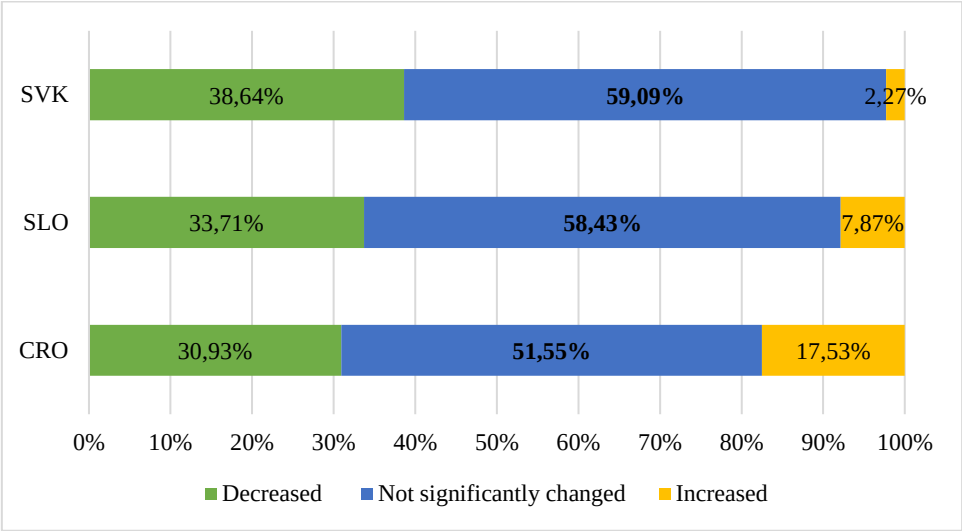

Figure 6. Impact of Ukraine war on wood product demand

4. CONCLUSION

This paper analyses the impact of the COVID-19 pandemic and the conflict in Ukraine on FSC-certified wood processing companies in Croatia, Slovenia and Slovakia.

The most significant conclusions are:

Slovenian companies experienced less negative effects from COVID-19 pandemic than Croatian and Slovak companies.

Difficulties in procurement were more evident in Croatia and Slovakia, while they were less evident in Slovenia. Regarding sales, Slovenia and Slovakia had very low difficulties in sales, while in Croatia medium and high intensity difficulties were more common. Most respondents in all three countries stated that prices did not change due to the pandemic. However, price increases were more common than price decreases, and the largest increase was recorded in Croatia.

The negative effects of the conflict in Ukraine were reported in all three countries, most strongly in Slovakia. In most cases, the conflict did not affect demand. The decline in demand is the largest in Slovakia, while Croatia had the largest share of demand growth.

Given that the sector is predominantly made up of micro and small enterprises with a high export orientation, the results are expected.

This confirms that wood processing companies are very sensitive to global shocks. Considering our results, the role of FSC is important because certification contributes to traceability and provides security to customers. Furthermore, this is in line with previous research (Klarić et al., 2016) given that companies have mostly certified themselves at the request of customers, FSC is a tool of trust.

5. REFERENCES

Klarić, K.; Greger, K.; Klarić, M.; Andrić, T.; Hitka, M.; Kropivšek, J., 2016: *An Exploratory Assessment of FSC Chain of Custody Certification Benefits in Croatian Wood Industry.* Drvna industrija, 67 (3): 241-248. https://doi.org/10.5552/drind.2016.1540

Klarić, K.; Pirc Barčić, A.; Basarac Sertić, M., 2023: *Assessing the Role of Forest Certification and Macroeconomic Indicators on Croatian Wood Exports to the EU: A Panel Data Approach.* Forests, 14 (9): 1908. https://doi.org/10.3390/f14091908

Klarić, K.; Klarić, M.; Josipović, S.; Tafro, A., 2024: *The Evolving Role of FSC Certification in Croatia: From Market Pressures to Sustainable Practices.* Forests, 15 (10):1717. https://doi.org/10.3390/f15101717

Paluš, H.; Parobek, J.; Vlosky, R.P.; Motik, D.; Oblak, L.; Jošt, M.; Glavonjić, B.; Dudík, R.; Wanat, L., 2018: *The status of chain-of-custody certification in the countries of Central and South Europe*. European Journal of Wood and Wood Products, 76: 699-710. https://doi.org/10.1007/s00107-017-1261-0

Vukman, K.; Klarić, K.; Greger, K.; Perić, I., 2024*: Driving Efficiency and Competitiveness: Trends and Innovations in ERP Systems for the Wood Industry*. Forests, 15 (2): 230. https://doi.org/10.3390/f15020230

***European Commission, 2025: *Forest-based industries.* https://single-market-economy.ec.europa.eu/sectors/raw-materials/related-industries/forest-based-industries_en.

***EUROSTAT, 2024: *Forestry and wood industry jobs up 1.4 % from 2012 to 2022.* https://ec.europa.eu/eurostat/web/products-eurostat-news/w/edn-20240321-1.

***UNECE, 2025: *Forest Tracks: Country-Level Market Insights 2024/2025.* United Nations Economic Commission for Europe, Geneva. https://unece.org/sites/default/files/2025-10/forest-tracks-2024-2025%20_0.pdf.

Design And Analysis of Corner Assemblies With 3D Printed Elements Intended for Cabinet Furniture

Konsa, Petar*; Prekrat, Silvana[1]

[1] Department for Furniture and Wood Products, Faculty of Forestry and Wood Technology, University of Zagreb, Zagreb, Croatia
*Corresponding author: petarkonsa@gmail.com

ABSTRACT

The objective of this work was to develop an innovative methodology for the optimization of 3D-printed connecting elements designed for carcass furniture made of 12 mm MDF panels, utilizing computer simulations via the Finite Element Method (FEM). The research encompassed six iterative optimization stages (Step 0 to Step 5) and compared the performance of PLA and ABS materials under a 750 N load. Multivariate Analysis of Variance (MANOVA) confirmed that the optimization stage factor has a highly significant effect on the combination of maximum stress and deformation ($p = 0.000019$). Detailed Tukey HSD analysis established that Optimization 4 (hollow element with a 2 mm wall thickness), due to excessive material removal, resulted in statistically the worst performance, showing the highest stress (PLA; 217.3 MPa, ABS; 211.8 MPa) and the largest deformation (ABS; 17.5 mm, PLA; 9.9 mm), thus differing significantly from all other steps. Simultaneously, Optimization 5 (reinforced partition in the panel groove) proved to be the most favorable in terms of stiffness, achieving the lowest deformation (PLA; 1.85 mm). In the material comparison, PLA demonstrated superiority, achieving a statistically significantly lower average deformation (≈ 3.66 mm) compared to ABS (≈ 6.45 mm) ($p = 0.034$), confirming it as the optimal material for maintaining the joint's geometric stability. These results validate that the methodology of iterative optimization based on FEM allows for informed decisions regarding the optimal design and material solution prior to physical production.

Key words: 3D printed joints, polymer materials, FEM analysis, case furniture joints, structural optimization

1. INTRODUCTION

Innovation often encounters implementation challenges within industrial frameworks even before being offered to the market. Therefore, a broader understanding and methodology of development are required to streamline the development and eventual production processes, making them as economical as possible while satisfying all safety requirements and normative regulations that the product must meet upon market entry. The objective of this paper is to present a contemporary innovation development methodology through new and modern procedures for an innovative approach to the design, construction, and general engineering of carcass furniture. The methodology should be highly applicable within industrial settings and potent for future implementation. Rationalization, specifically reducing material consumption, plays a crucial role herein. The thesis aims to provide a clear vision of the methodological approach's applicability to all design criteria that may arise as a potential market need. The working hypothesis is to prove the applicability of the innovative development approach through computer simulations in the product optimization process during the initial design and construction phases. These simulations address elements critical to normative requirements for

safety, durability, and other regulatory factors that the product must satisfy on the market. The paper by Jarž *et al*., (2022) provides a comprehensive overview of additive technologies, with a specific focus on 3D printing and its application in the furniture industry. It explores the positive and negative aspects of this technology, analyzes its impact on design, product development, and manufacturing processes, and forecasts its future importance. The authors cite a number of advantages to using additive technologies, from reducing the cost of product development itself to the potential recyclability of the structural forms printed by this method. According to the work of Nicolau *et al*. (2022), additive manufacturing is increasingly utilized in the furniture industry for producing parts and joints. Replacing traditional wooden joints with 3D-printed connecting elements facilitates the assembly process, reduces production time, and lowers costs.

2. MATERIAL AND METHODS

2.1. Material

2.1.1. Carcass material

Medium-density fiberboard (MDF) with a thickness of 12 mm was selected for the carcass construction. Although MDF panels exhibit a lower capacity for accommodating classic mechanical joints, their homogeneous structure is suitable for precise numerical simulations. Additional advantages include availability, favorable cost, and suitability for surface finishing. The mechanical properties of MDF used in the simulations are presented in Table 1 (according to Ganev *et al*., 2003).

Table 1. Mechanical properties of MDF panel (ρ = 650 kg/m³, 10% moisture content)

E_1=E_2, MPa	E_3, MPa	G_{12}, MPa	ν_{12}	ν_{13}
1109	18.9	73.1	0.27	0.24

2.1.2. Materials of the connecting elements

The connecting elements were designed for panels with a thickness of 12 mm. Although 18 mm thick panels are more commonly used in industrial practice, the choice of a thinner panel represents an attempt at material rationalization, reduction of mass and cost, and exploration of the feasibility of applying 3D-printed joints in less expensive constructions. The joint design was executed using intuitive methods, starting with an L-shape corresponding to the contact of two panel elements. Common filaments PLA (Polylactic Acid) and ABS () were selected for 3D printing. The mechanical properties are presented in Table 2 (Travieso-Rodriguez *et al*., 2019; Vidakis *et al*. 2020).

Table 2. Mechanical properties of filaments

	E_1, E_2, MPa	E_3, MPa	G_{12}, MPa	G_{13}, G_{23}, MPa	ν_{12}, ν_{13}, ν_{23}
PLA	3600	1800	1380	690	0.36
ABS	2000	2000	1600	620	0.35

2.1.3. Connecting Elements

The design structures of the connecting elements are presented as follows (Table 3).

Table 3. Design variations of the connecting elements

Optimization step	Geometric representation of the connecting element	Description of the connecting element
Step 0 (Figure 1)	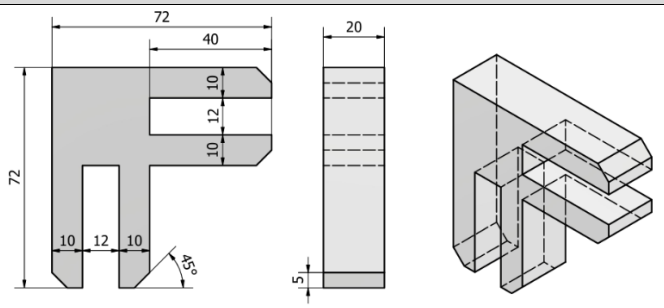 *Figure 1. Initial connecting element*	Complete connecting element produced with the defined geometry and stated dimensions
Step 1 (Figure 2)	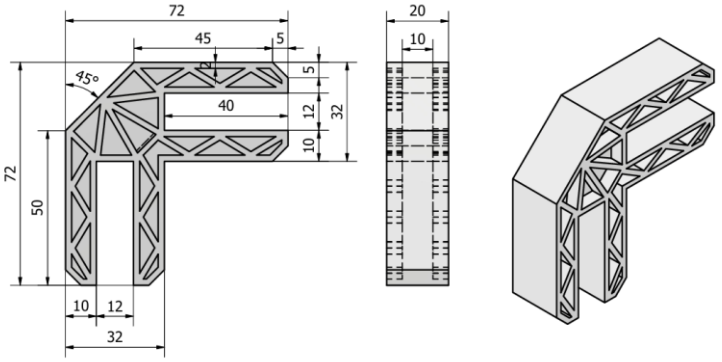 *Figure 2. Connecting element of the first optimization stage*	In relation to the initial geometry, the corner section was removed and a 2 mm thick mesh was created on each side of the connecting element. The center was filled to a thickness of 20 mm.
Step 2 (Figure 3)	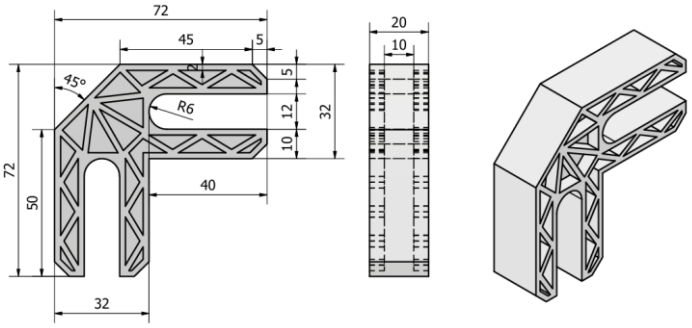 *Figure 3. Connecting element of the second optimization stage*	In relation to the previous iteration (optimization), a 6 mm radius fillet (rounding) was added to the contact area between the panel and the connecting element.
Step 3 (Figure 4)	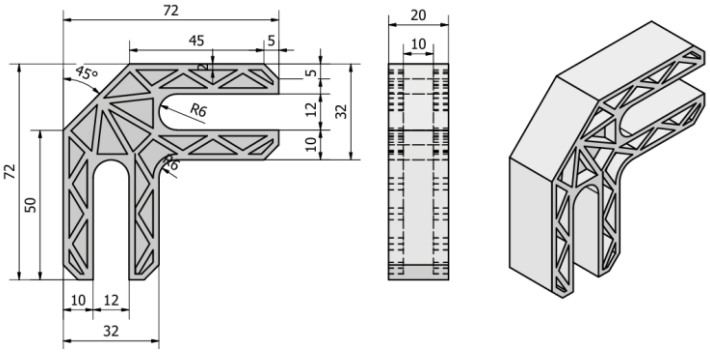 *Figure 4. Connecting element of the third optimization stage*	In relation to the previous iteration (optimization), a fillet was added to the corner of the connecting element with an internal radius of 6 mm and an external radius of 8 mm.

Step 4 (Figure 5)	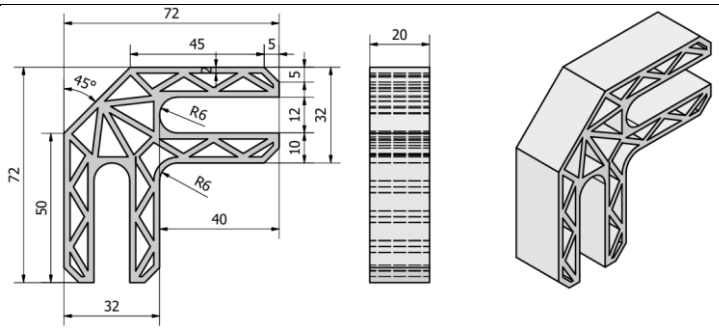 *Figure 5. Connecting element of the fourth optimization stage*	In relation to the previous iteration (optimization), the internal structure was completely removed; the connecting element is hollow with a 2 mm thick wall in the specified geometry.
Step 5 (Figure 6)	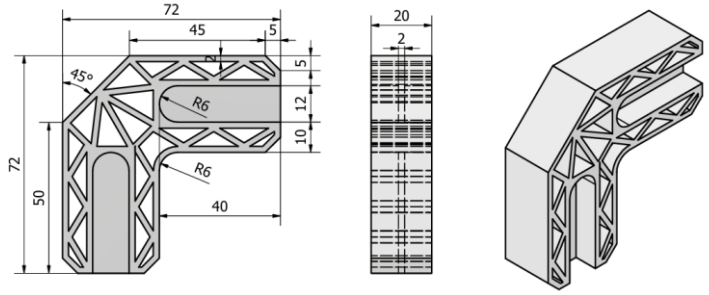 *Figure 6.. Connecting element of the fifth optimization stage*	In relation to the previous optimization, a 2 mm thick partition was added to the panel groove. This optimization requires notching the panel

2.2. Methods

The optimization focuses on an individual connecting element within the furniture assembly, which is analyzed using computer simulations via the Finite Element Method (FEM) within the framework of Autodesk Inventor 2023 software and the Nastran 2023 add-on. The research encompasses a 3D model of the element designed according to the desired properties of the final product. Material properties of the selected material (PLA) are defined, including its orthotropic 3D character, tangent modulus, and yield strength. The model is subjected to the application of fixed supports on surfaces that replicate real contacts within the assembly, neglecting the effect of moment, while a force of 750 N is applied along the Y-axis of the coordinate system, corresponding to a 150 kg load on the upper edge of the horizontal panel. The geometry is discretized into a mesh with a uniform element size of 1.2 mm, utilizing parabolic tetrahedrons with ten nodes. This approach enables precise tracking of curved surfaces and the model's design structure while maintaining an optimal balance between simulation accuracy and computational resources. This optimization is iterative, meaning the results of each simulation are used to adjust the dimensions, shape, and material properties of the connecting element. All obtained data are analyzed using statistical methods, while a qualitative inspection identifies any potential abnormalities, such as excessive deformation or loss of basic shape, thereby leading to a conclusion about the optimal dimensional and design solution before future actions (Figure 7).

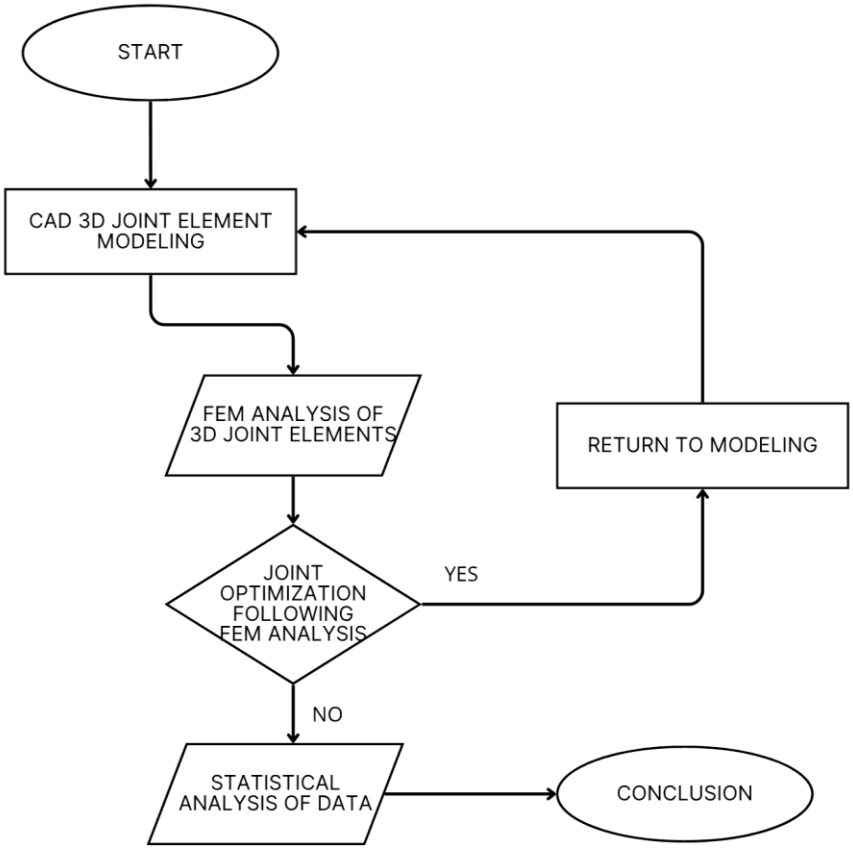

Figure 7. Scheme of the methodology

2.3. Methodology for designing the connecting elements

The connecting elements are designed to meet specific mechanical requirements that the elements must fulfil. Based on the areas of increased stress from the previous optimization and tested in accordance with the general testing methodology within the work, a specific design modification is introduced on each subsequent connecting element (Figure 8).

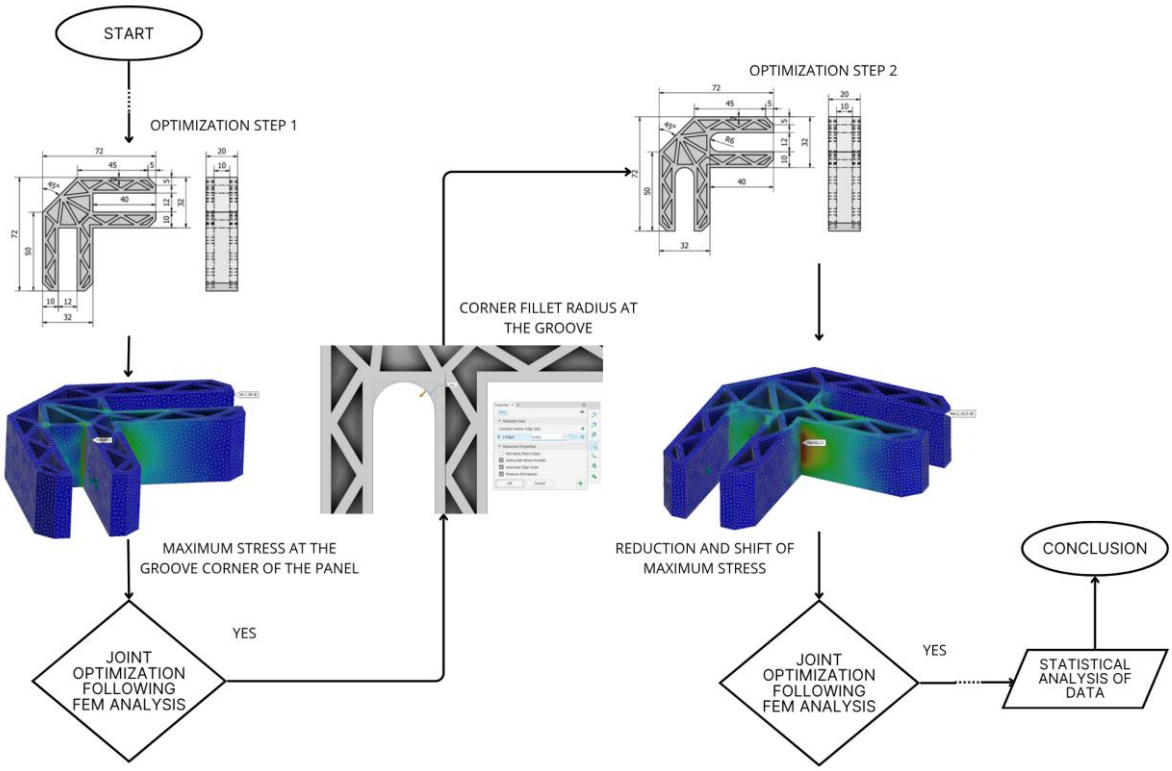

Figure 8. Fetail od the methodology scheme presentation

3. RESULTS AND DISCUSSION

In the subsequent (lower-level) optimization of the connecting element, key parameters are monitored to enable the assessment of mechanical behavior and material efficiency. Firstly, the maximum deformation is tracked, which indicates how much the element bends or displaces under the specified load, serving as an indicator of joint stiffness and the preservation of geometric stability. Alongside deformation, the maximum stress according to the von Mises model is monitored. This value expresses the level of internal forces in the material relative to its ultimate strength and allows for the identification of stress concentration zones. Special attention is dedicated to local stresses in critical parts of the joint, such as groove corners or connections, to detect zones that require modification or reinforcement. It is also important to monitor the behavior of these parameters throughout all optimization stages, which enables the observation of trends and the identification of the optimal shape and dimensions of the element. Finally, statistical analysis, including ANOVA and Tukey HSD tests, confirms the significance of changes between different materials and optimization stages. This approach allows for informed decisions regarding the dimensional, design, and material solution of the connecting element, resulting in an optimal combination of strength and stiffness.

Table 4. Results of the testing

Material	Optimization step	Maximum stress, MPa	Maximum deformation, mm
PLA	Step 0	99.34	2.26173
PLA	Step 1	144.00	3.27963
PLA	Step 2	93.54	2.4329
PLA	Step 3	100.4	2.1727
PLA	Step 4	217.296	9.9306
PLA	Step 5	99.788	1.85224
ABS	Step 0	100.6	4.02305
ABS	Step 1	137.5	5.76988
ABS	Step 2	87.03	4.3033
ABS	Step 3	93.31	3.84121
ABS	Step 4	211.799	17.5144
ABS	Step 5	96.873	3.26419

The results (Table 4) of the lower-level optimization simulations for the PLA material showed clear changes in stress and deformation across all optimization stages. The zero-optimization recorded local stresses of 99.34 MPa and a maximum deformation of 2.26 mm, while the first optimization increased the stress to 144.00 MPa with a deformation of 3.28 mm due to the removal of material and the creation of a mesh structure. The second optimization, which involved filleting the critical corners, reduced the stress to 93.54 MPa and the deformation to 2.43 mm, thereby improving load distribution. The third optimization, focused on the L-corner of the connecting element, resulted in a stress of 100.4 MPa and a deformation of 2.17 mm, whereas the fourth optimization, due to excessive material removal in the center of the element, caused an abrupt increase in stress to 217.30 MPa and a deformation of 9.93 mm, indicating a risk of stress concentration. The fifth optimization, which reinforced critical sections by adding material, reduced the stress to 99.79 MPa and the deformation to 1.85 mm, achieving an optimal combination of joint strength and stiffness. Statistical analysis confirmed that PLA material achieves the lowest deformations and most stable results in most cases compared to PETG and ABS, while the high stresses in the fourth optimization showed the potential limits of material removal. Accordingly, PLA was identified as the optimal material for further research, and the selected optimization stages for continued analysis are zero, first, third, and fifth.

Table 5. Multivariate Analysis of Variance (MANOVA)

Effect	Test	Value	F	Effect df	Error df	p
Intecept	Wilks	0.000132	15178.56	2	4	0.000000
Material	Wilks	0.226427	6.83	2	4	0.051269
Optimization step	Wilks	0.000544	33.49	10	8	0.000019

The Multivariate Analysis of Variance (Table 5) was performed to assess the cumulative effect of independent factors on the combination of dependent variables (Maximum stress and Maximum deformation). The results of the Wilks' Lambda test indicate that the Material factor has a marginally significant multivariate effect, with a p-value of $p = 0.051269$, which is only slightly above the conventional significance threshold of $\alpha = 0.05$. This result suggests that the multivariate difference between PLA and ABS materials on the combination of observed properties is on the boundary of statistical significance. Conversely, the Optimization Stage factor exhibits a highly significant multivariate effect, as evidenced by the extremely low p-value of $p = 0.000019$. The rejection of the null hypothesis in this case strongly confirms that changes in the optimization stages cause a statistically very significant change in the combination of maximum stress and maximum deformation. As shown by the ANOVA analysis for the material effect on maximum stress (Figure 9) and maximum deformation (Figure 10), the subsequent Tukey HSD tests (Table 6 and Table 7) confirm the statistical differences between materials.

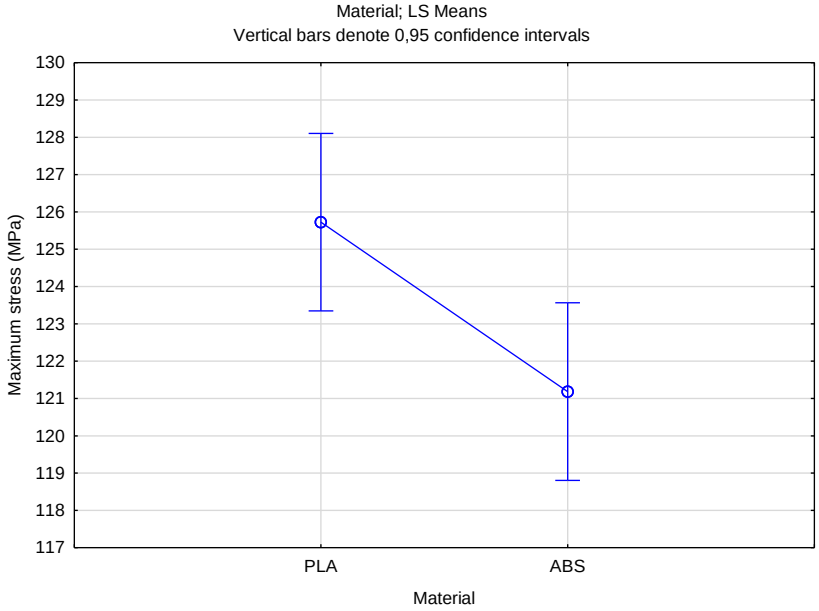

Figure 9. ANOVA Results for Material Effect on Maximum Stress

Table 6. Tukey HSD test; variable Maximum stress (MPa)

Cell No.	Material	{1} 125.73	{2} 121.19
1	PLA		0.018048
2	ABS	0.018048	

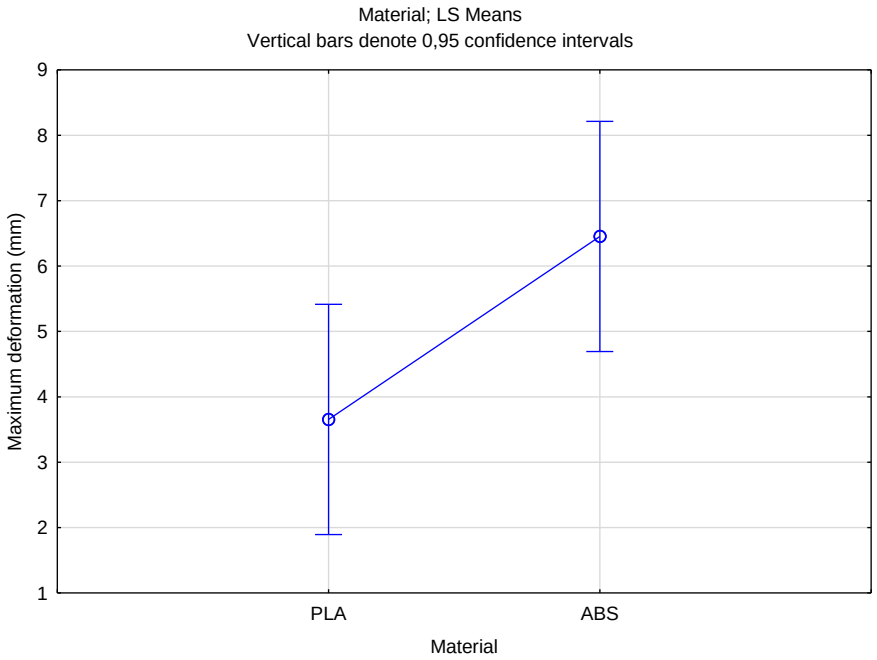

Figure 160. ANOVA Results for Material Effect on Maximum Deformation

Table 7. Tukey HSD test; variable Maximum deformation (mm)

Cell No.	Material	{1} 3.6550	{2} 6.4527
1	PLA		0.034414
2	ABS	0.034414	

The analysis of the Tukey HSD test for material comparison (PLA and ABS) demonstrated statistically significant differences in both key mechanical parameters. For Maximum stress, a significant difference was established (p=0.018048), with PLA material achieving a higher average maximum stress (~125.73 MPa) compared to ABS (~121.19 MPa). More importantly, regarding Maximum deformation, the difference was also significant (p=0.034414); joints made from PLA material showed a significantly lower average deformation (~3.66 mm) compared to ABS (~6.45 mm). This finding suggests a greater stiffness of the joint made from PLA, which is a key indicator of its superiority in the context of maintaining geometric stability under load. The results of the ANOVA analysis for the Optimization Stage factor for maximum stress (Figure 11) and maximum deformation (Figure 12) are detailed in the corresponding Tukey HSD test tables (Table 8 and Table 9).

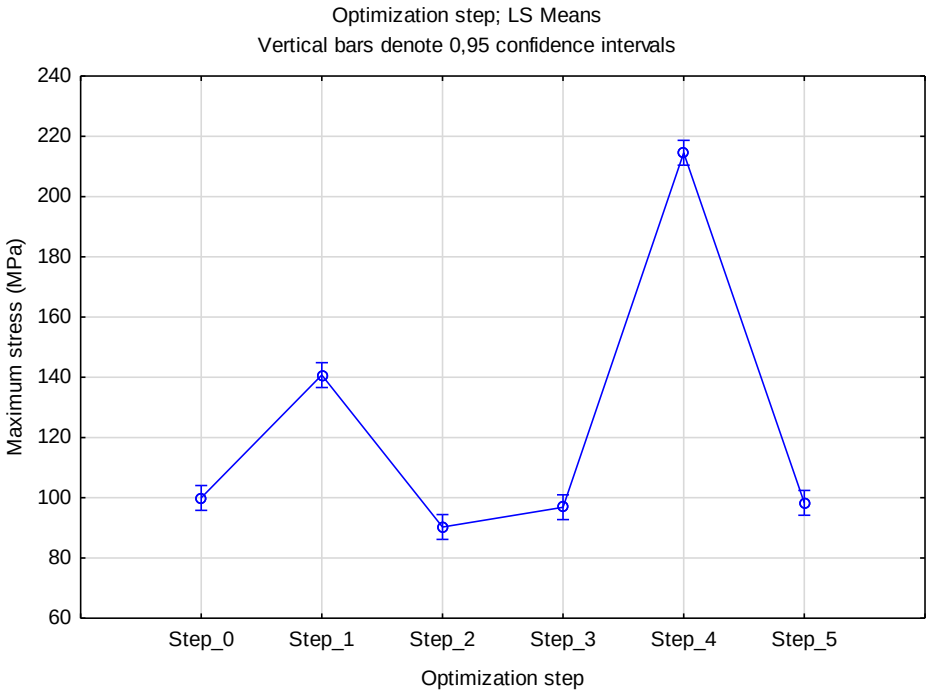

Figure 11. ANOVA Results for Optimization Stage Effect on Maximum Stress

Table 8. Tukey HSD test; variable Maximum stress (MPa)

Cell No.	Optimization step	{1} 99.970	{2} 140.75	{3} 90.285	{4} 96.855	{5} 214.55	{6} 98.331
1	Step 0		0.000281	0.049844	0.741733	0.000262	0.970260
2	Step 1	0.000281		0.000264	0.000271	0.000262	0.000275
3	Step 2	0.049844	0.000264		0.185111	0.000262	0.097478
4	Step 3	0.741733	0.000271	0.185111		0.000262	0.980733
5	Step 4	0.000262	0.000262	0.000262	0.000262		0.000262
6	Step 5	0.970260	0.000275	0.097478	0.980733	0.000262	

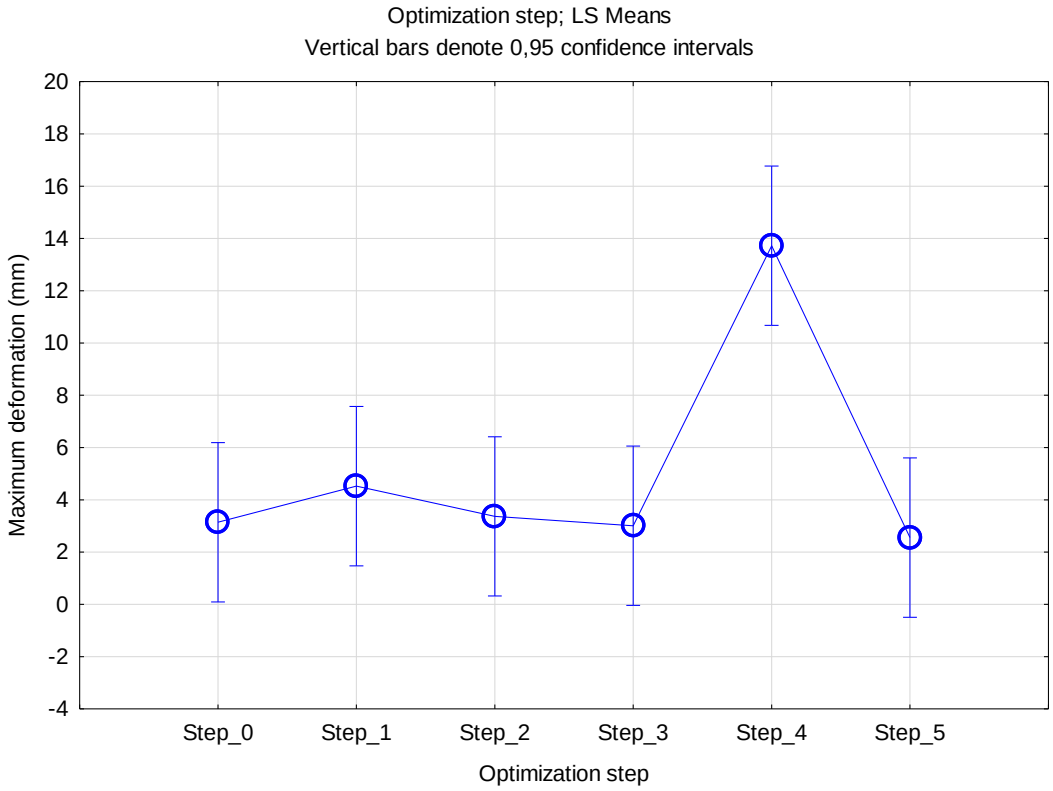

Figure 12. ANOVA Results for Optimization Stage Effect on Maximum Deformation

Table 9. Tukey HSD test; variable Maximum deformation (mm)

Cell No.	Optimization step	{1} 3.1424	{2} 4.5248	{3} 3.3681	{4} 3.0070	{5} 13.723	{6} 2.5582
1	Step 0		0.950261	0.999989	0.999999	0.010061	0.998866
2	Step 1	0.950261		0.975464	0.929631	0.018288	0.833771
3	Step 2	0.999989	0.975464		0.999889	0.011043	0.994790
4	Step 3	0.999999	0.929631	0.999889		0.009523	0.999680
5	Step 4	0.010061	0.018288	0.011043	0.009523		0.007952
6	Step 5	0.998866	0.833771	0.994790	0.999680	0.007952	

4. CONCLUSIONS

The Optimization Stage factor has a highly significant multivariate effect on maximum stress and deformation.There are significant differences in both maximum stress and deformation between the tested materials (PLA and ABS). Specifically, optimization stage 4 differs significantly from all other stages, resulting in the significantly highest maximum stress and maximum deformation. PLA material exhibits a significantly lower maximum deformation compared to ABS (PLA 3.66 mm vs. ABS 6.45 mm).

5. REFERENCES

Ganev, S.; Gendron, G.; Cloutier, A.; Beauregard, R., 2003: Mechanical properties of MDF as a function of density and moisture content. Wood and Fiber Science, 36 (4): 543-555.

Jarža, L.; Čavlović, A. O.; Pervan, S.; Španić, N.; Klarić, M.; Prekrat, S., 2023: Additive Technologies and Their Applications in Furniture Design and Manufacturing. Drvna industrija, 74 (1): 115-128. https://doi.org/10.5552/drvind.2023.0012

Nicolau, A.; Pop, M. A.; Coșereanu, C., 2022: 3D Printing Application in Wood Furniture Components Assembling. Materials, 15 (8): 2907. https://doi.org/10.3390/ma15082907

Travieso-Rodriguez, J. A.; Jerez-Mesa, R.; Llumà, J.; Traver-Ramos, O.; Gomez-Gras, G.; Roa Rovira, J. J., 2019: Mechanical Properties of 3D-Printing Polylactic Acid Parts subjected to Bending Stress and Fatigue Testing. Materials, 12 (23): 3859. https://doi.org/10.3390/ma12233859

Vidakis, N.; Petousis, M.; Maniadi, A.; Koudoumas, E.; Liebscher, M.; Tzounis, L., 2020: Mechanical Properties of 3D-Printed Acrylonitrile–Butadiene–Styrene TiO_2 and ATO Nanocomposites. Polymers, 12 (7): 1589. https://doi.org/10.3390/polym12071589

Determination of Bearing Loading During Longitudinal Milling of Specimens from Scots Pine and Oak

Kovachev, Georgi*; Atanasov, Valentin[1]

[1] Department of Woodworking Machines, Faculty of Forest Industry, University of Forestry, Sofia, Bulgaria
*Corresponding author: g_kovachev@ltu.bg

ABSTRACT

Technological factors have a significant influence over bearing loading of the cutting mechanism in a woodworking spindle moulder machine. The rotation frequency used for the experiments was 6000 min^{-1} as it is one of the most commonly used in practice for milling machines. Measurements were made at four points in the radial direction. Two of them are located in the upper bearing units and the other two are in the lower bearing units. A universal woodworking spindle moulder machine with a lower position of the working shaft is used for the experiment. This type of machine continues to be very widespread. During the research, the focus was on some technological factors such as feed speed of the processed material which is from 2m/min to 10m/min, milling width 12 mm and thickness of removed layer 12 mm. Within the experiment scots pine (*Pinus sylvestris*) and oak (*Quercus robur*) test samples were milled.

Key words: woodworking spindle moulder machine, vibration speed, bearings

1. INTRODUCTION

Milling is an extremely important process, directly related to the quality of the processed materials and the resulting surfaces. This, in turn, has a great impact for the quality of the entire product. Finely processed details can be performed on various milling machines like planers, thicknessers, spindle moulder machines and others. They allow different types of detail processing: straight, oblique or profiled milling. We can also mount various attachments to the machine. This opens up possibilities for many other types of processing. The different types of details processing also require the machines to be able to work in different operating modes suitable for the respective technological operations. The different cutting speeds are also bound by the possibility that the machine can work with different rotation frequencies. Most often, speed ranges are between 30 m/s – 60 m/s (Obreshkov, 1997). This is a clear prerequisite for the occurrence of different cutting forces. They load the cutting mechanism and cause forced oscillations with different magnitudes. Bearings are the machine elements that take the loads from the cutting process and allocate them over the machine body. This creates conditions for bearing wear and the occurrence of various damages, which is extremely undesirable. Common failures are the breakage of the cage (Figure 1) and the appearance of deformations on the various elements of the bearing (Figure 2) (https://motion-drives.com; www.picard.de/en/; Sokolovski, 2007).

Bearings are most important both for the machine itself and for the entire material processing process. Poor bearings state directly affects the quality of the processed materials. Each processed detail of the milling machines must have a certain shape, dimensions and class of roughness to meet the tolerances laid down in the technical documentation (Adamcik *et al.*,

2024; Adamcik *et al.*, 2023; Atanasov, 2023; Kminiak *et al.*, 2018; Korcok *et al.*, 2018; Sydor *et al.*, 2021). In order to comply with these requirements, it is necessary to choose the right technological cutting modes, correct selection and preparation of the cutting tools, as well as to check the serviceability of the machine on which the processing process will take place (Doichinov, 2023; Halim *et al.*, 2024; Vitchev *et al.*, 2019).

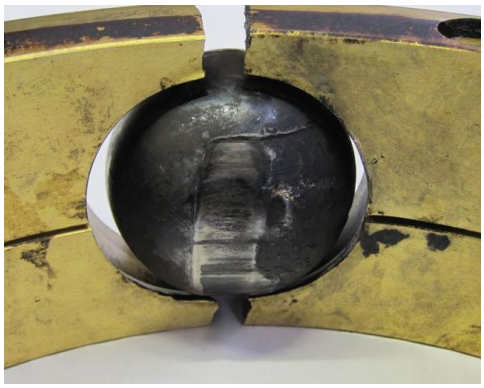

Figure 1. Ball bearing damaged cage

Figure 2. Ball bearing damaged inner ring

The aim of the present work is to measure and analyse the vibration speed in the milling process of scots pine (*Pinus sylvestris*) and oak (*Quercus robur*) test samples on a universal woodworking spindle moulder machine with the bottom location of the working shaft. The object of research is the bearings load at different feed speeds. The study is aimed at improving the reliability and efficiency of a woodworking spindle moulder machine to ensure the accuracy and quality of products.

2. MATERIALS AND METHODS

The whole experiment in the present work was conducted on a woodworking spindle moulder machine with the bottom location of the working shaft. These machines are widespread in practice. The general view of the machine is shown in (Figure 3) (www.felder-group.com).

Figure 3. Spindle moulder machine general view

The cutting mechanism of the selected machine consists of a working shaft with bottom position, belt drive and electric motor. The cutting mechanism is driven by an asynchronous electric motor at 3 kW of power and rotation frequency of 2880 min^{-1}. The rotation frequency used for the experiments was 6000 min^{-1}. This allows serious technological possibilities for

achieving different cutting speeds by using cutting tools of different diameters. The bearing of the working shaft is carried out in a bearing body, which is a cast iron monolithic moulding (Figure 4). This allows the use of single-row ball bearings, which are most suitable since machines of this type have the ability to operate at high rotational speeds. Also the shaft can be mounted by using two separate bearing units (Figure 5). In this case, it is more appropriate to use double-row self-aligning ball bearings, as this compensates for mounting inaccuracies (www.ntn-snr.com).

Figure 4. Cast iron bearing body

Figure 5. Bearing units

For this study was used a cutter with diameter D = 140 mm. The technical data of the cutting tool are shown in Table 1.

Table 1: Technical data of the cutting tool

Type of instrument	D mm	d mm	B mm	α °	β °	γ °	z бр	Material of the teeth
Groove cutter	140	30	12	16	55	19	6	HM

The inscriptions in the table are: *D* - diameter of the milling cutter, *d* – diameter of the bore, *B* – milling width, α – back angle of cutting, β – angle of sharpening, γ – front angle of cutting, *z* – number of teeth.

The cutting speed was calculated by the formula 1 (Gochev, 2005). At a rotation frequency of 6000 min^{-1} the calculated cutting speed was v = 44 m/s.

$$V = \pi.D.n, \text{ m/s} \quad (1)$$

D – diameter of the cutting tool, *m*;

n –rotation frequency of the cutting tool, s^{-1}.

During the experiment scots pine (*Pinus sylvestris*) and oak (*Quercus robur*) test samples with cross-sectional dimensions of 50 mm × 50 mm and length of 1000 mm were milled. The milling width is 12 mm and the thickness of the removed layer is 12 mm. A universal roller feeding mechanism is mounted on the machine. Through it, we regulate the feeding speed of the test samples. The feed speeds of the treated material with which the experiments were made are respectively U_1=2,0 m/min, U_2=6,0m/min, U_3=10,0 m/min.

The measurements were performed at four measuring points located in the bearing units. Two of them are located near the upper bearing, next to the cutting tool. The other two are located near the lower bearing, next to the belt pulley. The measurement points are located

mutually perpendicular, radial to the main shaft of the machine (Figure 6) (BDS ISO 10816: 2002).

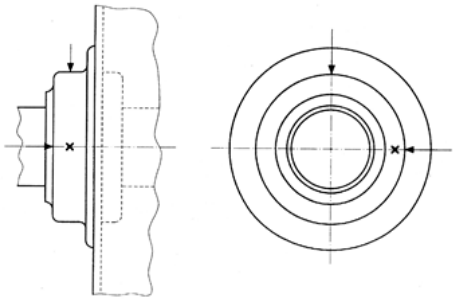

Figure 6. Measurement points

Vibration speed V mm/s (r.m.s.) is measured using a specialised device model Bruel & Kjaer Vibrotest 60 (Figure 7). The sensor, which measured the intensity of vibration, is attached to the bearing house with a magnet (Figure 8).

Figure 7. Bruel & Kjaer Vibrotest 60

Figure 8. Measuring sensor

3. RESULTS AND DISCUSSION

The experimental part includes work trials in milling scots pine (*Pinus sylvestris*) and oak (*Quercus robur*) test samples at different feed speed. During processing of the test specimens the root mean square value of the vibration speed (V mm/s (r.m.s.) is measured. The measurement points near the upper bearing are respectively: A_x – radial direction parallel to the feed direction, A_y – radial direction perpendicular to the feed direction. The measurement points near the lower bearing are respectively the Bx – radial direction parallel to the feed direction and the B_y – radial direction perpendicular to the feed direction.

Figure 9 shows the vibration speed (V mm/s (r.m.s.)) measured at idle in the four directions.

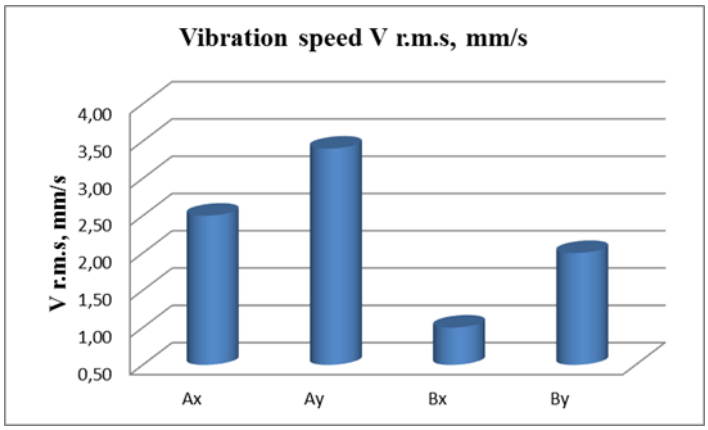

Figure 9. Vibration speed measured at idle

From (Figure 9) it can be seen that the vibration speed levels are higher at points Ax and Ay. This is completely normal, since they are located close to the cutting tool, and more weight is concentrated there. The measured vibration speed values at points Bx and By located next to the pulley are lower. They are lower more than double as those measured in the upper bearing. Figure 10 and (Figure 11) show the variation of the vibration speed measured near the upper bearing when the rotation frequency of the working shaft is 6000 min^{-1} and when milling scots pine (*Pinus sylvestris*) and oak (*Quercus robur*) test samples.

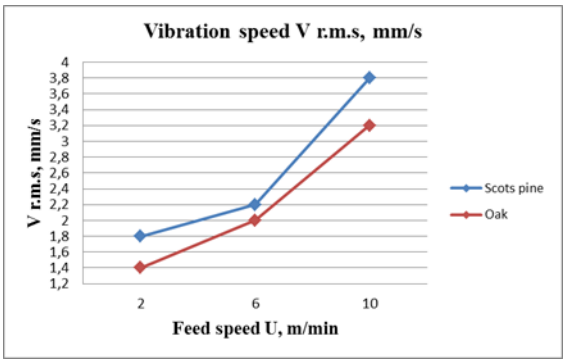

Figure 10. Vibration speed measured at point A_x when milling scots pine (Pinus sylvestris) and oak (Quercus robur) test samples

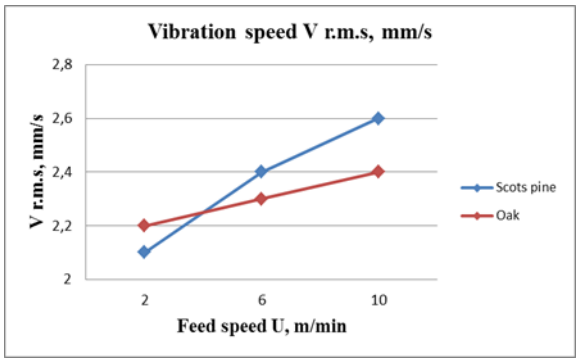

Figure 11. Vibration speed measured at point A_y when milling scots pine (Pinus sylvestris) and oak (Quercus robur) test samples

Figure 10 shows how the vibration speed changes at point A_x. When the feed speed (*U*, m/min) of the processed material increases, the vibration speed (V mm/s (r.m.s.)) also increases. This tendency was observed for both tree species. The lowest measured values are when feed speed (*U*, m/min) is U_1=2 m/min, and the highest at U_3=10 m/min. The maximum measured vibration varies from 3.2 mm/s to 3.8 mm/s. When milling oak (*Quercus robur*) the measured vibration values are slightly lower. This can be explained by the fact that this wood species reduces vibrations and serves as a damper. Figure 11 shows the variation of the vibration speed measured at point A_y. Here too when the feed speed (*U*, m/min) of the processed material increases, the vibration speed (V mm/s (r.m.s.)) also increases. The maximum values range from 2.4 mm/s to 2.6 mm/s at feed rate U_3=10 m/min. At point A_y the measured vibration speed levels are close to each other no matter what type of material is processed. Figure 12 and (Figure 13) show the variation of the vibration speed measured near the bottom bearing when the rotation frequency of the working shaft is 6000 min^{-1} and when milling scots pine (*Pinus sylvestris*) and oak (*Quercus robur*) test samples.

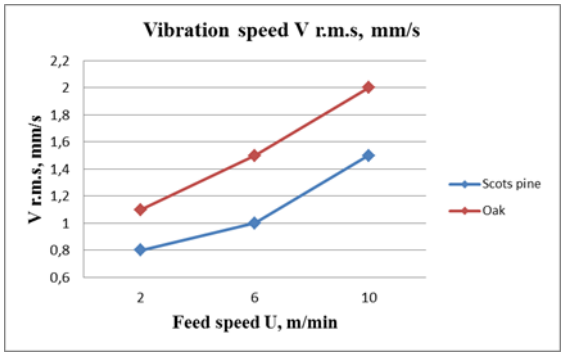

Figure 12. Vibration speed measured at point B_x when milling scots pine (Pinus sylvestris) and oak (Quercus robur) test samples

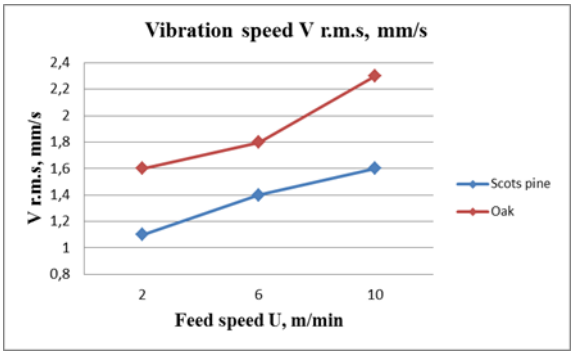

Figure 13. Vibration speed measured at point B_y when milling scots pine (Pinus sylvestris) and oak (Quercus robur) test samples

The variation of the vibration speed at point B_x is shown in (Figure 12). When the feed speed (*U*, m/min) of the processed material increases, the vibration speed (V mm/s (r.m.s.)) also increases for both tree species. The measured values are significantly lower than in the same direction for point A_x. This is completely normal, as the lower bearing is significantly further from the cutting area. The highest values were measured at feed speed U_3=10 m/min and ranged from 1.5 mm/s to 2 mm/s. The same trend is also observed at point B_y shown in (Figure13). When the feed speed (*U*, m/min) of the processed material increases, the vibration speed (V mm/s (r.m.s.)) also increases for both tree species. In comparison with point A_y the measured values are again lower. The highest values were measured at feed speed U_3=10 m/min and ranged from 1.6 mm/s to 2.3 mm/s. When milling oak (*Quercus robur*) test samples, the vibration speed is higher at both measurement points. The vibration values are slightly lower when cutting scots pine (*Pinus sylvestris*) test samples.

4. CONCLUSION

On the basis of the conducted experimental studies, the following more important conclusions and recommendations can be drawn:

When the feed speed (*U*, m/min) of the processed material increase the vibration speed (V mm/s (r.m.s.)) also increase at all four measurement points for both tree species. It is recommended to feed the processed material at lower feed speeds (*U*, m/min). This puts less strain on the bearings and protects the machine from costly repairs (Kminiak *et al.*, 2016; Kminiak *et al.*, 2017; Kovatchev *et al.*, 2021).

The vibration speed measured near the upper bearing is higher. This indicates that the bearing is more loaded during operation, because it is located in next to the cutting tool. Furthermore, this is the bearing exposed to a higher risk of damage.

The vibration speed measured near the bottom bearing is lower. The bearing, located next to the belt pulley, is less loaded. It is quite far from the cut area. The vibrations caused by cutting forces do not load it as much as upper bearing. Future research may focus on the different designs of bearing units and their behavior in operating mode.

5. REFERENCES

Adamcik, L.; Kminiak, R.; Banski, A., 2024: Comparison of the roughness of the CNC milled surface of selected wood species. Acta Facultatis Xylologiae Zvolen, 66 (2): 61-74. https://doi.org/10.17423/afx.2024.66.2.06

Adamcik, L.; Kminiak, R.; Schmidtova, J., 2023: Measurement of the roughness of the sanded surface of beech wood with the profile measurement software of the Keyence VHX-7000 microscope. Acta Facultatis Xylologiae Zvolen, 65 (1): 73-85. https://doi.org/10.17423/afx.2023.65.1.07

Atanasov, V., 2023: Power-kinematic parameters in wood milling and their influence on the design of the main mechanisms of the machines, Sofia, p. 160. ISBN 978-619-239-901-6 (in Bulgarian)

Doichinov, A., 2023: Optimization of the CNC milling process via modifying some parameters of the cutting mode when processing MDF workpieces. Acta Facultatis Xylologiae Zvolen, 65 (2): 99-107. https://doi.org/10.17423/afx.2023.65.2.09

Gochev, Z., 2005: Manual for Wood Cutting and Woodworking Tools, Sofia, p. 232.

Halim, E.; Vitchev, P., 2024: Changes in the level of noise emissions, generated by cnc woodworking center, depending on the cutting mode and the geometry of the cutting tool. In: Proceedings of 12th international Scientific and Technical Conference Innovations 2024, in forest industry and engineering design, Sofia, 7-9 October, pp. 49-60, ISSN: 3033-1005.

Kminiak, R.; Siklienka, M.; Sustek, J., 2016: Impact of tool wear on the quality on the quality of the surface in routing of MDF boards by milling with reversible blades. Acta Facultatis Xylologiae Zvolen, 58 (2): 89-100. https://doi.org/10.17423/afx.2016.58.2.10

Kminiak, R.; Banski, A.; Chakhov, D., 2017: Influence of the thickness of removed layer on the quality of created surface during milling the MDF on CNC machining centers. Acta Facultatis Xylologiae Zvolen, 59 (2): 137-146. https://doi.org/10.17423/afx.2017.59.2.13

Kminiak, R.; Siklienka, M.; Sustek, J., 2018: Influence of the thickness of removed layer on the quality of created surface when milling oak blanks on the CNC machining center. Chip and Chipless Woodworking Processes 11 (1): 79-86.

Korcok, M.; Vanco, M.; Barcik, S.; Goglia, V., 2018: Influence of tool angular geometry on surface quality after milling of thermally modified oak wood. Chip and Chipless Woodworking Processes 11 (1): 87-96.

Kovatchev, G.; Atanasov, V., 2021: Determination of vibration during longitudinal milling of wood-based materials. Acta Facultatis Xylologiae Zvolen, 63 (1): 85-92. https://doi.org/10.17423/afx.2021.63.1.08

Obreshkov, P., 1997: Woodworking Machines, Sofia, p. 182. (in Bulgarian)

Sokolovski, S., 2007: Machine elements, Sofia, p. 318. ISBN 978-954-332-044-38 (in Bulgarian)

Sydor, M.; Mirski, R.; Stuper-Szablewska, K.; Rogozinski, T., 2021: Efficiency of Machine Sanding of Wood. Applied Sciences, 11 (6): 2860. https://doi.org/10.3390/app11062860

Vitchev, P.; Angelski, D.; Mihailov, V., 2019: Influence of the processed material on the sound pressure level generated by sliding table circular saw. Acta Facultatis Xylologiae Zvolen, 61 (2): 73-80. https://doi.org/10.17423/afx.2019.6

***BDS ISO 10816-1, 2002: Evaluation of machine vibration by measurement on non – rotating parts – Part 1: General guidelines, p. 25.

***Felder Group: Woodworking macines, 2025: https://www.felder-group.com.

***Motion Drives, 2025: https://motion-drives.com.

***NTN Europe: Manufacturer of bearings, 2025: https://www.ntn-snr.com.

***PICARD, 2025: https://www.picard.de/en/.

Analysis of the Efficiency of Furniture Modeling Using Parametric 3D CAD Program

Kristić, Denis*; Prekrat, Silvana[1]

[1] Department for Furniture and Wood Products, Faculty of Forestry and Wood Technology, University of Zagreb, Zagreb, Croatia
*Corresponding author: kristic962@gmail.com

ABSTRACT

This paper examines the limitations of the exact approach to 3D furniture modeling, which, due to repeated manual modifications, increases the risk of errors and extends the modeling process. The study aimed to determine whether a parametric approach can improve efficiency, ensure consistency, and reduce manual interventions during modifications. The analysis included three cabinet variants: V1 (single-door with four shelves), V2 (double-door with four shelves and a drawer), and V3 (double-door with five shelves, a partition, and two drawers). Modeling was carried out in Autodesk Inventor 2023.1 with the Woodwork for Inventor add-in. Both approaches were assessed by measuring the time required for initial modeling, the duration of modifications, and the number of sketches altered. Results showed that the parametric approach reduced initial modeling time by 33.9–46.6% (V1 from 9:58 to 5:19, V2 from 18:32 to 10:53, V3 from 26:41 to 17:39). Savings during modifications were even greater, reaching 83.5–97%. Unlike the exact method, which requires changes to each sketch individually, the parametric approach implements adjustments through parameter values. In conclusion, while it requires careful planning and parameter definition, the parametric approach enables faster modifications and more reliable technical documentation. The exact method remains applicable for simple or unique projects but shows limitations with increasing complexity.

Key words: Autodesk Inventor, exact modeling, furniture, multibody method, parametric modeling, Woodwork for Inventor

1. INTRODUCTION

Modern furniture production is increasingly oriented toward rapid adaptation of products to diverse customer requirements and spatial constraints. With the growing demand for personalized and modular solutions, manufacturers face the challenge of shortening product development cycles, accelerating design modifications, and minimizing errors during data transfer between the design and manufacturing stages. According to Zhang (2017), an effective response to these challenges lies in the integration of CAD/CAM technologies into the design process, where digital tools enable simultaneous technical modeling, visualization, and production preparation.

Parametric modeling has emerged as a key method in this context. Unlike the conventional exact approach, in which all components are defined manually and fixedly, parametric models are based on variable parameters and relational dependencies between components. This modeling strategy enables rapid generation of product variants, efficient implementation of design changes, and improved control over geometric consistency (Felek, 2022). In the furniture industry, where products are frequently produced in multiple dimensional and functional variants, this represents a significant technological advantage.

Hamad and Husein (2020) emphasize that parametric tools enhance designer creativity and flexibility, as modifications can be executed quickly without the need to remodel individual elements. Furthermore, the introduction of scriptable and algorithmic design systems has expanded the potential for process automation and reduced manual intervention, a trend increasingly reflected in contemporary CAD/CAM solutions (Li and Li, 2025).

In current industrial practice, integrated tools that combine engineering precision with the technological requirements of furniture production and other wood-based products are becoming standard. Autodesk Inventor, an established CAD platform widely used in mechanical engineering, when combined with the Woodwork for Inventor add-in, provides complete digital integration from parametric modeling of components and furniture assemblies to automatic generation of technical documentation, bills of materials, and data preparation for CNC machining.

2. MATERIALS AND METODS

Furniture modeling was performed using two distinct approaches, exact and parametric, to analyze their constructive principles and applicability in the design of wooden products. The comparison between the exact and parametric approaches was carried out on three variants of the same cabinet-type furniture (Figure 1), which differ in their level of structural complexity (Table 1).

V1: single-door cabinet consisting of 10 parts, of which 3 are unique; includes side panels, top, bottom, and four shelves, without drawers.

V2: double-door cabinet with a total of 17 parts, 8 of which are unique; includes sides, top, bottom, four shelves, and one drawer.

V3: double-door cabinet with 26 parts, 16 of which are unique; includes bottom, top, intermediate bottom, five shelves, a middle partition, and two drawers.

The construction complexity coefficient (Ks) represents a ratio that defines the structural complexity of an assembly or product. It is calculated as the ratio between the total number of unique parts and assemblies and the overall number of parts and assemblies. According to this parameter, three categories of structural complexity are defined:

Low structural complexity ($Ks \leq 0.33$): simple construction composed of a smaller number of unique components and a higher share of repeating elements.

Medium structural complexity ($0.34 \leq Ks \leq 0.60$): moderately complex construction with a balanced ratio of unique and repeating components.

High structural complexity ($0.61 \leq Ks \leq 1.00$): highly complex construction characterized by a large number of unique parts and high structural diversity.

Table 4. Coefficients of complexity for the three cabinet variants

Cabinet variant	Description	Ks coefficient
V1	Single-door cabinet with four shelves	0.30
V2	Double-door cabinet with four shelves and one drawer	0.47
V3	Double-door cabinet with five shelves, midere partition, and two drawers	0.62

As shown in Table 1, the single-door cabinet (V1) is categorized as low in structural complexity, the double-door cabinet with one drawer (V2) as medium, and the most complex variant (V3), containing more unique parts and drawers, as high in complexity.

Each cabinet variant was modeled using both the exact and parametric approaches. Modeling efficiency was evaluated based on the total time required to create a valid 3D model and assembly, as well as the time needed to perform controlled design modifications. Measured modeling time covered the period from opening a new project file to the completion of a fully constrained 3D assembly. The preparation or updating of documentation, bill of materials, CAM, and nesting outputs was not included.

To assess the flexibility of both methods, four standardized modification scenarios were applied: S1 change of height, S2 change of width, S3 change of panel thickness, and S4 simultaneous change of all dimensions. For each scenario, the number of edited sketches, updated features, and reapplied assembly constraints was recorded.

Structural complexity was further analyzed through the number of components, subassemblies, constraints, and modeling features per element. Results of total modeling time and dimensional modifications were compared to evaluate performance differences between the two modeling approaches.

All models were created in Autodesk Inventor Professional 2023 with the Woodwork for Inventor add-in version 11 and tested on an HP Pavilion Gaming 15 workstation with an AMD Ryzen 5 3350H processor, 16 GB RAM, NVIDIA GeForce GTX 1650 graphics card, and Windows 10 Pro operating system.

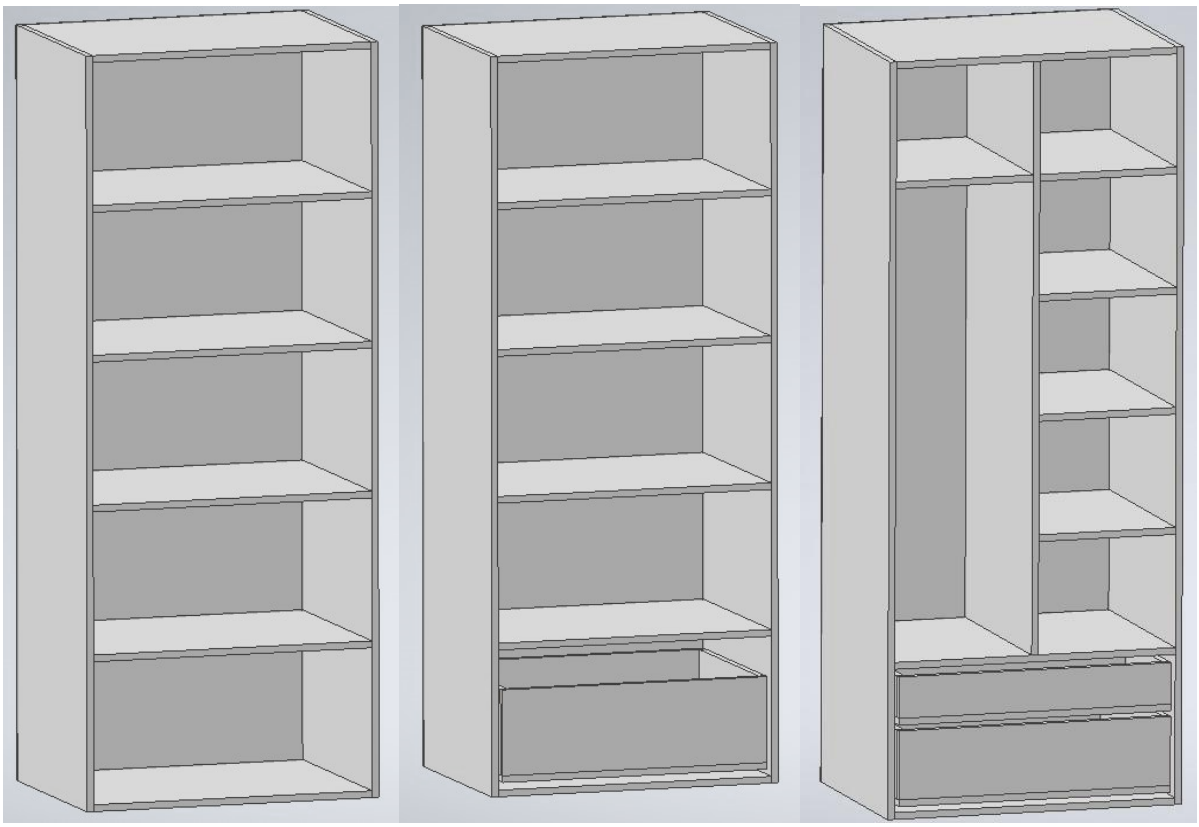

Figure 1. Sample representation of cabinet variants V1, V2, and V3 modeled in Autodesk Inventor

3. RESULTS

3.1. Time required for initial model creation

The results presented in Table 1 show the total modeling times for all three cabinet variants using both approaches and the corresponding time savings.

Table 5.Modeling time results for both methods

Cabinet variant	Ks	Unique parts	Exact, min	Parametric, min	Saving
V1 – single-door cabinet with 4 shelves	0.30	3	09:58.0	05:19.4	46.60%
V2 – double-door cabinet with 4 shelves and one drawer	0.47	8	18:32.3	10:52.8	41.30%
V3 – double-door cabinet with 5 shelves, partition, and two drawers	0.62	16	26:41.1	17:39.1	33.17%

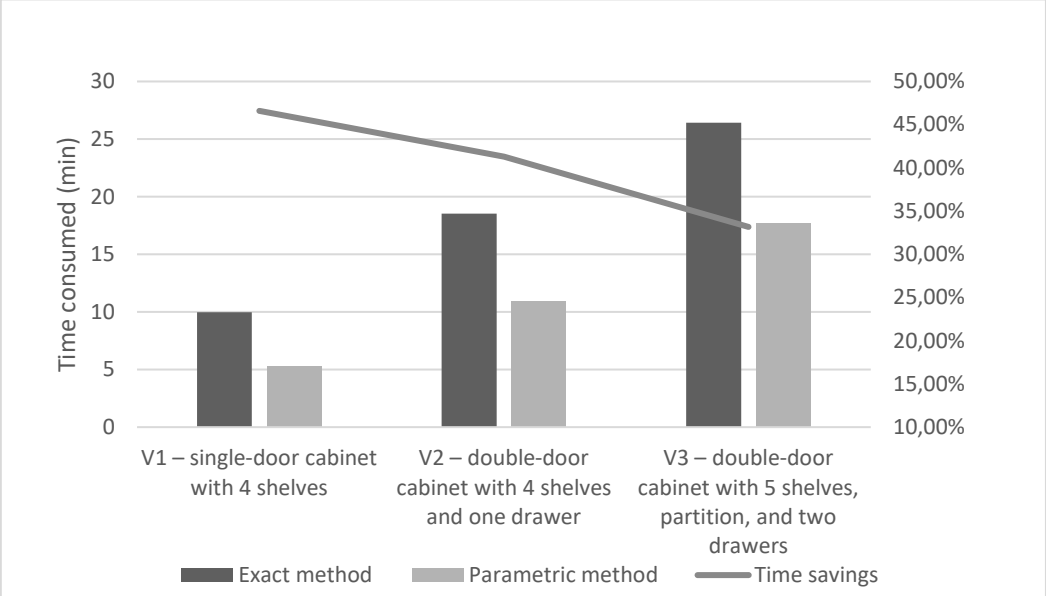

Figure 17. Modeling time comparison between exact and parametric approaches

The parametric approach achieved significantly shorter modeling times for all cabinet variants. The highest relative saving (46.6 %) was recorded for V1, while V2 and V3 achieved savings of 41.3 % and 33.2 %. Although the percentage saving decreases with increasing complexity, the absolute time difference becomes more pronounced. Overall, parametric modeling proved more efficient and consistent, reducing repetitive operations and the likelihood of design errors.

3.2. Modeling with hardware fittings

Table 6. Modeling time with added dowel fittings

Variant	Unique parts	Dowels	Exact, min	Parametric, min	Saving
V1	3	24	27:16.1	06:12.4	77.24 %
V2	8	34	44:18.6	12:06.3	72.68 %
V3	16	62	72:38.4	19:14.6	73.51 %

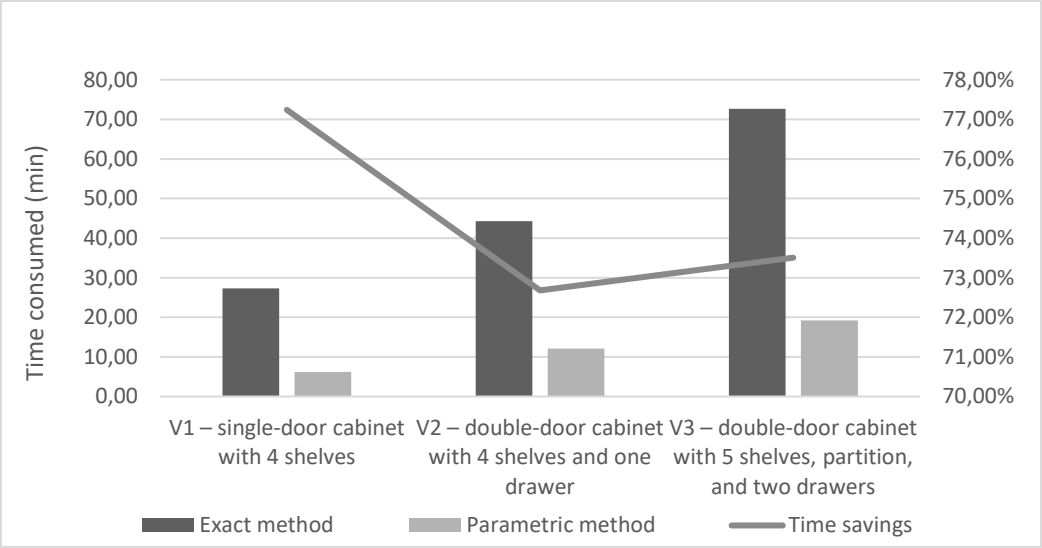

Figure 18. Modeling time with fittings for both methods

The parametric method demonstrated a consistent advantage in modeling time when hardware fittings were added. Time savings ranged between 72 and 77 percent across all cabinet variants. The process of inserting dowels was significantly faster in the parametric environment, where predefined connection libraries in Woodwork for Inventor automatically recognized panel surfaces and applied the correct positioning and orientation of fittings. In contrast, the exact approach required each dowel to be placed manually, demanding repeated alignment and constraint operations. This not only extended the total modeling time but also increased the potential for dimensional inconsistencies within the assembly. The results clearly confirm that parametric modeling provides a more efficient and reliable workflow when adding fittings, ensuring precision and reducing repetitive manual operations.

3.3. Dimensional modification results

3.3.1. Modification of height, width, panel tickness

Table 4 presents the times required for changing cabinet height, width, and panel thickness in both modeling approaches. In the exact method, each modification required manual editing of multiple sketches, and the duration increased with model complexity. In contrast, the parametric method used global parameters (*skeleton_height*, *skeleton_width*, *panel_thickness*), which automatically updated all related parts.

Table 7. Time required for changes in different scenarios

Scenario	Description	Variant	Exact, min	Parametric, min	Time saving, %
S1	Change of height	V1	01:53.1	00:10.5	91.20
		V2	02:42.3	00:10.3	93.80
		V3	05:13.1	00:11.0	96.70
S2	Change of width	V1	01:02.0	00:10.2	83.50
		V2	02:48.3	00:10.3	94.00
		V3	07:32.5	00:10.0	97.00
S3	Change of panel thickness	V1	01:05.5	00:10.2	84.50
		V2	01:32.5	00:10.5	89.00
		V3	03:05.2	00:10.1	96.90

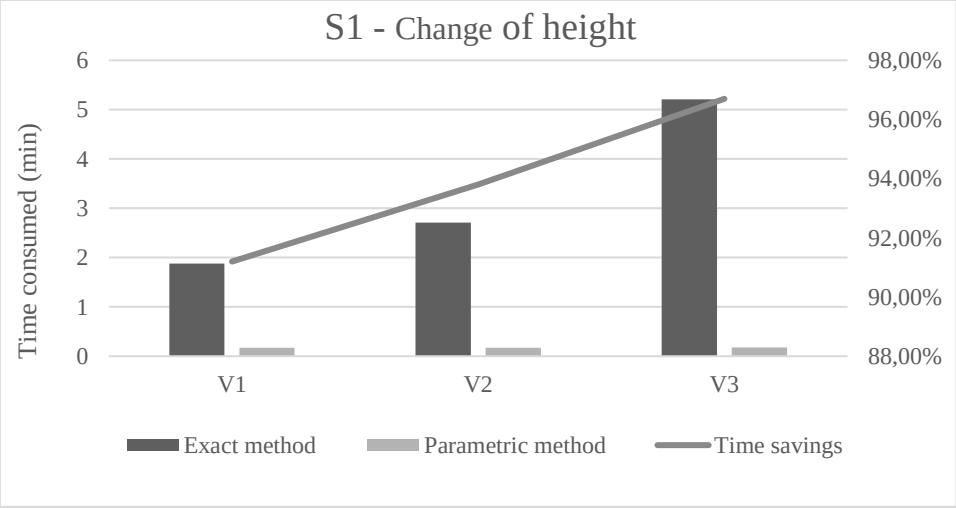

Figure 19. Results of changing cabinets height in both methods

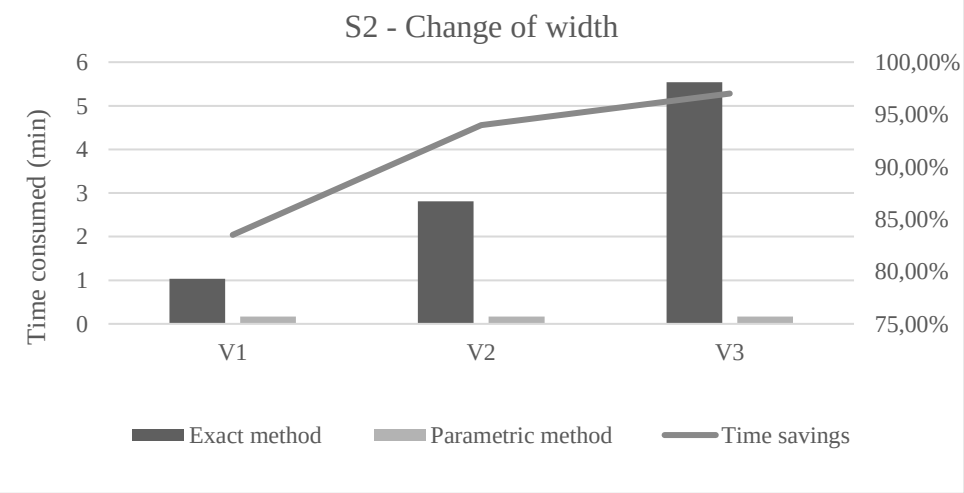

Figure 20. Results of changing cabinets width in both methods

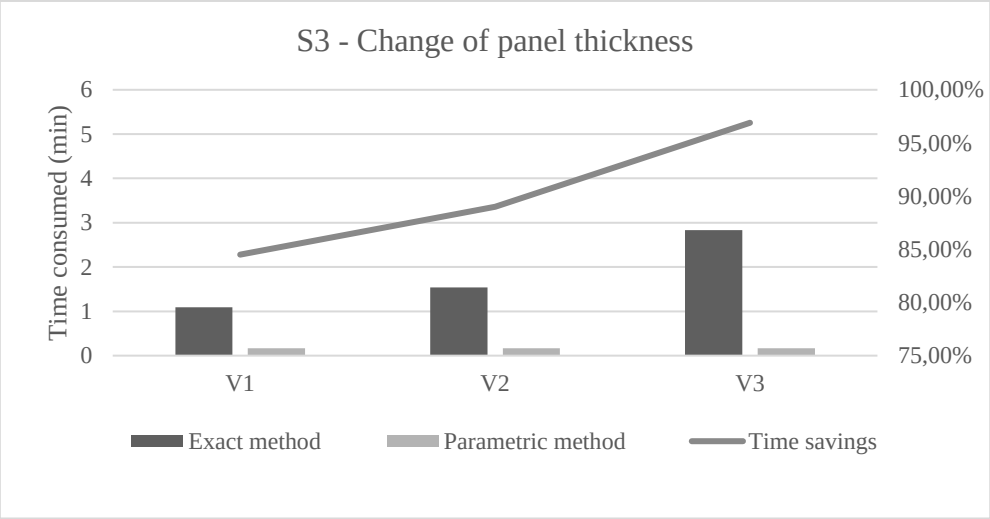

Figure 21. Results of changing cabinets panel thickness in both methods

The results presented in Table 4 and Figures 3, 4, and 5 demonstrate a clear and consistent advantage of the parametric modeling approach across all modification scenarios. Regardless of the type of dimensional change such as height, width, or panel thickness, the parametric method maintained almost constant update times of about ten seconds for all cabinet variants. In contrast, the exact approach required significantly more time, with modification duration increasing proportionally to model complexity and the number of edited sketches. The greatest efficiency was achieved in complex assemblies, where parametric models automatically updated all dependent components without manual intervention. Overall time savings ranged between 83 and 97 percent, confirming that the parametric approach provides a faster, more accurate, and more stable workflow for dimensional adjustments in furniture modeling.

3.3.2. Simultaneous change of all dimensions

Table 8. Time required for simultaneous dimensional changes

Variant	Edited sketches	Exact, min	Parametric, min	Saving
V1	3	01:52.9	00:24.3	78.52 %
V2	8	03:48.8	00:24.2	89.42 %
V3	16	07:35.7	00:24.1	96.70 %

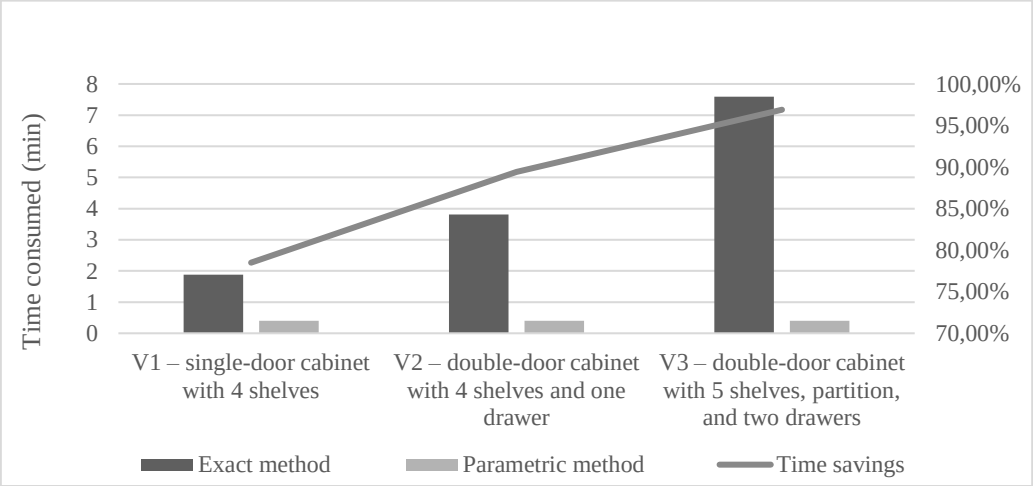

Figure 22. Results of simultaneous dimensional changes

Simultaneous dimensional adjustments confirmed the high efficiency of the parametric modeling approach. When height, width, and panel thickness were changed at the same time, all related components automatically updated while maintaining full geometric consistency. The exact method required multiple manual edits for each part, which greatly extended the process and increased the chance of errors. Even with higher model complexity, the parametric method maintained an average update time of about 24 seconds, ensuring accuracy and time savings of up to 96.7 percent.

4. CONCLUSIONS

The study confirms that parametric modeling in Autodesk Inventor, enhanced with the Woodwork for Inventor add-in, significantly improves the efficiency of digital design in furniture engineering. Compared to the exact method, it allows faster model creation, automated dimensional updates, and more reliable documentation. While the exact method remains relevant for simple, fixed-dimension designs, the parametric approach is essential for modern production environments focused on customization and digital integration.

5. REFERENCES

Felek, M., 2022: Parametric modeling strategies for adaptive furniture design. Wood Design and Technology, 8 (2): 55-64. https://doi.org/10.56038/ejrnd.v2i2.29

Hamad, R.; Husein, A., 2020: Advances in parametric design tools for woodworking industries. International Journal of Furniture Engineering, 12 (1): 23-31. https://doi.org/10.23918/eajse.v6i1p199

Li, J.; Li, W., 2025: Algorithmic and scriptable modeling in modern CAD/CAM environments. Computer-Aided Design and Applications, 22 (3): 211-220. https://dl.acm.org/doi/10.1145/3703619.3706030

Zhang, Y., 2017: Integration of CAD/CAM systems in digital product development. Journal of Manufacturing Systems, 36 (4): 112-119. https://doi.org/10.1109/ICSGEA.2017.121

Comparison of Measurements from a Coordinate Measuring Machine and Manual Instruments in Quality Control of Mortise and Tenon Joints

Mihajlovski, Nikola*; Gruevski, Gjorgi; Jevtoska, Elena[1]

[1] Faculty of Design and Technologies of Furniture and Interior-Skopje, Ss. Cyril and Methodius University in Skopje, North Macedonia
*Coresponding author: mihajlovski@fdtme.ukim.edu.mk

ABSTRACT

The development of final wood processing is closely associated with the introduction and application of appropriate measurement methods. The use of measurements is a critical factor for the advancement of technology. Measurement accuracy is an essential aspect of production metrology, significantly influencing the monitoring of tolerances and fits as well as quality control in manufacturing. The precision of measuring dimensions is a vital component of production, and measurements are conducted throughout all technological phases. As science and technology evolve, measuring devices also advance. Currently, due to their high accuracy and rapid measurement capabilities, coordinate measuring systems are increasingly employed, with coordinate measuring machines (CMM) being the most prevalent. These machines are widely used to assess the dimensional and geometric characteristics of various products. This paper presents measurements of joint dimensions using a coordinate measuring machine and compares them with measurements obtained from manual instruments commonly utilized in manufacturing. The difference in measurements is statistically significant, indicating that the values obtained with a coordinate measuring machine are 0.49% lower than those from manual instruments.

Key words: mortise and tenon, coordinate measuring machine, measuring instruments

1. INTRODUCTION

The development of secundary wood processing is closely associated with the introduction and application of appropriate measurement methods. The use of measurements is a critical factor for the advancement of technology.

Metrology is a crucial component of the product quality management chain and offers dimensional and geometric quality control in manufacturing. Maintaining tolerances and fits as well as quality control in production depend on measurement accuracy as part of production metrology (Pfeifer, 2015). Accurate dimensional measurements are crucial to production. Every stage of the technological process involves measurements.

The quality of certain products relies heavily on precise tolerance ranges in the joints. In furniture manufacturing, this is evident in the mortise and tenon joints used in chair construction. The strength and durability of the chair are influenced by the fit and tolerances of these joints. In the final stage of production, this joint type includes an overlap. According to various researchers, an overlap of 0.1mm to 0.2mm achieves optimal joint strength (Potrebic, 1970; Tkalec, 1990).

With advancements in science and technology, measuring devices are also evolving. Currently, coordinate measuring systems are being used more frequently due to their high

accuracy and measurement speed, with coordinate measuring machines (CMM) being the most prevalent. These machines have a broad range of applications in measuring the dimensional and geometric characteristics of various products (Dhoska *et al*., 2015).

The aim of this paper is to compare measurements of joint dimensions obtained from a coordinate measuring machine with those from manual instruments typically used in manufacturing.

2. MATERIALS AND METHODS

The measurement was performed on chair parts that had a mortise and tenon joints. The parts were made of beech wood (*Fagus Silvatica*). The joints were made on conventional machines, a tenon machine and an oscillating drill, from a chair production plant. The measurement was performed on 15 randomly selected parts. The dimensions of the joint are shown in Figure 1.

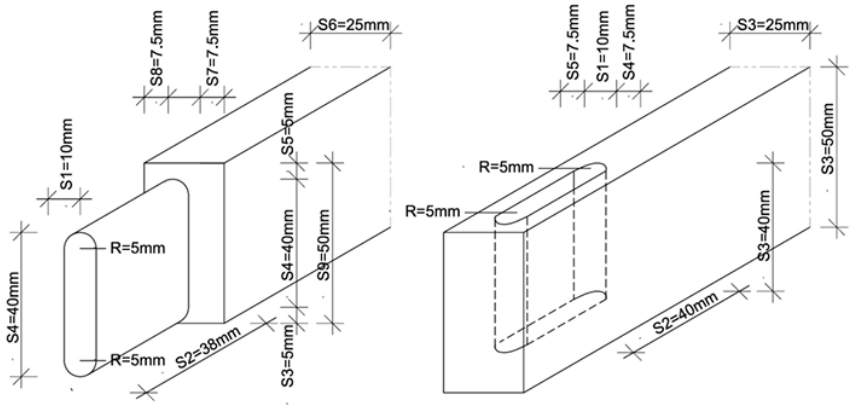

Figure 1: Dimensions of mortise and tenon joint

The type of fit and tolerances for the presented joint were determined based on the standards DIN 68100:2010 and DIN 68101:2012. The accuracy class of the processing machines, NT15, was considered for the calculation of the tolerances and fit. The tolerance limits for the tenon are provided in Table 1.

Table 1: Tolerance limits of tenon

Nominal size	d = 10 mm
Upper limit deviation	ag = 0.36 mm
Lower limit deviation	ad = 0.15 mm
Uper limit size	dg = 10.36 mm
Lower limit size	dd = 10.15 mm

According to the standard, the common hole system is used with a nominal hole dimension of 10mm. Only the thickness of the tenon is measured, with tolerances and the type of fit in the mortise specified. The fit was established with a 0.2mm overlap, so the processed tenon thickness should be 10.2mm. The tenon thickness was measured at three points, and an average

value was calculated along with an indicator for each tenon individually. The measurement point positions are determined according to the guidelines in the ISO17450-3:2016 standard.

The details were measured using a coordinate measuring machine produced by Hexagon Metrology, model Global 123010, which has an accuracy range of 0.002 to 0.005mm according to the manufacturer's specifications. After measurements were taken on the machine, additional measurements were conducted using a manual instrument. The thickness of the tenon was measured with a digital vernier caliper from the manufacturer "MIB," which has a stated accuracy of ± 0.03mm. The measuring equipment is illustrated in Figure 2.

Figure 2: Measuring equipment: digital varnier caliper – MIB (left), coordinate measuring machine Hexagon Metrology Global 123010 (right)

The accuracy of the measurements was analyzed through the parameters of absolute and relative error. The absolute error of the measurements was calculated according to the formula:

$$E_{abs} = M_m - M_m \quad (1)$$

E_{aps} – Absolute error of measurement (mm)
Mm – Measured value (mm)
Mn – Nominal value (mm)

The absolute error of the measurements was calculated according to the formula:

$$E_{rel} = \left(\frac{E_{abs}}{M_n}\right) \times 100 \quad (2)$$

E_{rel} – Relative error of measurement (%)

Statistical processing of measurements and determination of the significance of mean values was performed according to the ISO 2854:1976 standard.

3. RESULTS AND DISCUSSION

The values from the tenon thickness measurements are presented in Table 2. The average measurement taken with a caliper was 10.261 mm, while the average measurement from the coordinate measuring machine was 10.210 mm. Both measurement methods display consistency, as indicated by the coefficients of variation and the standard deviation. The measured values fall within the upper and lower limit intervals specified in Table 1. The absolute difference between the caliper and machine measurements is 0.051 mm. This difference is statistically significant with a T-value of 3.33. The average measurement from the coordinate measuring machine is 0.49% lower than that from the caliper.

Table 2: Tenon thickness measurements

No.	Digital varnier caliper			Coordinate measuring machine		
	Mm, mm	Eaps, mm	Erel, %	Mm, mm	Eaps, mm	Erel, %
1	10.250	0.250	2.5	10.175	0.175	1.75
2	10.290	0.290	2.9	10.184	0.184	1.84
3	10.280	0.280	2.8	10.251	0.251	2.51
4	10.310	0.310	3.1	10.218	0.218	2.18
5	10.220	0.220	2.2	10.206	0.206	2.06
6	10.350	0.350	3.5	10.281	0.281	2.81
7	10.250	0.250	2.5	10.223	0.223	2.23
8	10.220	0.220	2.2	10.188	0.188	1.88
9	10.170	0.170	1.7	10.183	0.183	1.83
10	10.260	0.260	2.6	10.196	0.196	1.96
11	10.230	0.230	2.3	10.211	0.211	2.11
12	10.190	0.190	1.9	10.181	0.181	1.81
13	10.280	0.280	2.8	10.177	0.177	1.77
14	10.330	0.330	3.3	10.248	0.248	2.48
15	10.280	0.280	2.8	10.231	0.231	2.31
n	15	15	15	15	15	15
$\bar{x}$	10.261	0.261	2.6	10.210	0.210	2.1
σ	0.050	0.050	0.499	0.032	0.032	0.317
v(%)	0.49	19.15	19.15	0.31	15.10	15.10

Mm – measured value, E_{aps} – absolute error, E_{rel} – relative error, n – number of measurements, $\bar{x}$ – average value of measurement, σ – standard deviation of measurement, v – coefficient of variation

When examining the deviations of the measurements from the nominal size, the absolute error for the thickness of the tenon measured with a caliper is 0.261 mm, while the absolute error for the coordinate measuring machine is 0.210 mm. The measured values fall within the range of the lower and upper limit sizes presented in Table 1. The absolute error for the coordinate measuring machine is 0.05 mm less than that of the caliper. The standard deviations from the nominal size are 0.050 mm and 0.032 mm, indicating significant deviations from the tenon's nominal size in both measurement methods, which is further highlighted by the high coefficients of variation. This outcome aligns with the expected processing accuracy of the machines, classified as HT15, indicating a medium processing class. However, the deviations observed with the coordinate measuring machine are smaller, indicating that the measurement is more closely aligned with the nominal size of the tenon. This is also evidenced by the 0.5 % difference when analyzing the relative error in the measurements.

Mortise and tenon joints are critical components that contribute to the structural integrity and require precise tolerances and fitting. If a tenon exceeds the upper or lower tolerance limits, it may not be considered a processing error despite a measurement variation of 0.05 mm when

using a caliper. This could potentially lead to issues such as a cracked joint during the assembly phase of the product. Thus, a difference of 0.05 mm when measured with a caliper compared to measurements taken with a coordinate measuring machine is significant.

The method of positioning the instrument during measurement significantly impacts the accuracy of the results. For instance, when using a caliper, its jaws should be positioned perpendicular to the surface being measured to ensure optimal contact between the instrument and the object. Whenever feasible, it is advisable to apply Abbe's principle (Abbe, 1890), which indicates that the most precise measurements occur when the quantity being measured is aligned in the same straight line as the measuring scale, or when it is collinear with the instrument's measuring scale. Failing to adhere to this guideline can introduce additional measurement errors. This principle is relevant to length measurement instruments.

4. CONCLUSIONS

When comparing measurements from a coordinate measuring machine and a manual caliper during quality control of mortise and tenon joints, the following conclusions were drawn:

The mean value of measurements obtained with a coordinate measuring machine is 0.051 mm or 0.49 % lower than the mean value of measurements obtained with a caliper. This difference in measurements is statistically significant.

The absolute error in measurements with a coordinate measuring machine is 0.05mm lower than that for the caliper.

The relative error in measurements with a coordinate measuring machine is 0.5 % lower than the relative error for the caliper.

The deviations in measurements with a coordinate measuring machine are smaller, indicating that these measurements are closer to the nominal size of the tenon.

In terms of quality control, the manual caliper is essential for quick measurements with larger tolerances, while the coordinate measuring machine is more suitable for precise measurements in functional parts requiring small tolerances.

5. REFERENCES

Abbe, E., 1890: Messapparate für Physiker [Measuring Instruments for Physicists]. Zeitschrift fur Instrumentenkunde [Journal of Scientific Instruments] 10:446-448 (in German)

Dhoska, K.; Kübarsepp, T.; Dorri, A.; Pramono, A., 2015: Metrological Overview for Coordinate Measuring Machines. Applied Mechanics and Materials, 771: 195-199.

Potrebić, M., 1970: Joint tolerance as effecting factor on strength of mortise joint. Master thesis, Belgrade University, Faculty of Forestry, pp. 105-107.

Pfeifer, T., 2015: Production metrology. Walter de Gruyter GmbH & Co KG.

Tkalec, S., 1990: Ispitivanje čvrstoće spojeva zaoblenim čepom. Drvna industrija, 41 (1-2): 3-8.

***DIN 68100, 2010: Tolerance system for wood working and wood processing - Concepts, series of tolerances, shrinkage and swelling.

***DIN 68101, 2012-02: Fundamental deviations and tolerance zones for wood working and wood processing.

***ISO 17450-3, 2016: Geometrical product specifications (GPS) — General concepts — Part 3: Toleranced features.

***ISO 2854, 1976: Statistical interpretation of data — Techniques of estimation and tests relating to means and variances.

Bonding Properties of Differently Modified Beech *(Fagus sylvatica L.)* Wood

Obucina, Murco[1]; Ibrisevic, Alen[1*]; Mahmutspahic Eldina[2]; Mihulja, Goran[3]

[1] Department of Wood Technology, Faculty of Mechanical Engineering, University of Sarajevo, Sarajevo, Bosnia and Herzegovina
[2] Student of the Department of Wood Technology, Faculty of Mechanical Engineering, University of Sarajevo, Sarajevo, Bosnia and Herzegovina
[3] Department of Wood Technology, Faculty of Forestry and Wood Technology, University of Zagreb, Zagreb, Croatia
*Corresponding author: ibrisevic@mef.unsa.ba

ABSTRACT

Various technological processes for wood modification were developed to improve durability, mechanical properties, and bonding quality. This study aimed to determine the effects of different wood modifications and adhesive type on the bonding characteristics of joints. In accordance with the purpose of the study, samples made from differently modified beech wood (un-treated, steam-treated, and heat-treated beech) were bonded with polyvinyl acetate (PVAc) and polyurethane (PUR) adhesives. The shear strength of joints was measured. An analysis of variance (ANOVA) was performed to evaluate the effects of wood modification type and adhesive on joint bonding characteristics. According to the results of this study, bonding wood with PVAc adhesive results in a higher shear strength of joints by 30% compared to samples bonded with PUR adhesive and made from un-treated and steam-treated beech. For heat-treated beech wood, a higher bonding strength (40 %) was obtained with PUR adhesive. Heat-treated beech had lower bonding strength than untreated or steam-treated beech, regardless of the adhesive type. The highest shear strength (13.2 N/mm^2) was obtained for steam-treated beech bonded with PVAc adhesive.

Keywords: wood modification, steam-treated beech, heat-treated beech, polyvinyl acetate adhesive (PVAc), polyurethane adhesive (PUR), shear strength

1. INTRODUCTION

Wood is one of the most popular materials, mainly used for construction and furniture production. As interest in solid wood products grows, with prices rising and timber quality declining, bonding wood processes are becoming essential in the manufacturing of wood products (Mihulja *et al.*, 2023). Today, many wood products are created by bonding pieces together. Bonded wood elements are often exposed to various environmental conditions, which can cause damage to the glue line and the wood. Plywood, cross-laminated timber, laminated veneer lumber, and other bonded wood elements are mainly used as construction elements, due to their high strength/weight ratio (Lia *et al*., 2022), so the bonding strength of the glue line is crucial for the stability of the construction. The wood type, adhesive type, wood treatment, and pressing parameters are closely related to glue line strength (Fang *et al*., 2019).

Beech (*Fagus sylvatica L.)* wood is one of the most widespread wood species in Europe and an important resource, often used for interior furniture and other interior design elements (Timar *et al*., 2016). These products are mostly made from solid wood panels produced by bonded finger joints or solid wood strips. The properties of beech wood enable the production

of high-quality products at a lower cost. One of the most important criteria customers consider when buying wood products is wood colour, price, and quality (Sedliacikova and Moresova, 2022). Colour differences caused by the red heartwood of beech are the main problem when using beech wood. These problems lead to beech wood being in a less favourable position and used with caution in the furniture industry. Beech wood used for these products is mostly modified before drying (Timar *et al*., 2016). So many techniques for wood modification have been developed to prevent disruption of stability when wood is destroyed. The most commonly used modification processes are steam treatment and heat treatment.

The aim of steam treatment is to improve the stability and permeability of the beech wood to obtain a desirable colour, reduce wood deformations, and soften the wood (Timar *et al*., 2016). Depending on the steaming conditions, beech wood acquires a pale pink to red-brown colour shade (Milic *et al*., 2015). Heat treatment of wood affects weight loss, and higher treatment temperatures result in greater weight loss (Xue *et al*., 2022). Thermal modification is performed at temperatures between 180 and 260 °C, without the use of any chemicals, in the absence of oxygen (Can, 2020). It increases its durability, reducing hygroscopicity, and improves the dimensional stability of wood.

Most commonly used adhesives are polyvinyl acetate (PVAc) and polyurethane (PUR). Polyvinyl acetate (PVAc) is a thermoplastic adhesive, and it is not generally recommended for joints under continuous load or for joints subjected to high humidity and temperature. PVAc adhesives are produced in different classes (D1-D4) according to EN 204. Polyurethane (PUR) adhesives are frequently used in mass timber production. PUR adhesives have good mechanical performance, especially under dry and wet conditions. It has good elasticity performances and the ability to form strong bonds with wood fibres (Yau *et al*., 2024).

This study investigated the effects of beech wood treatments and different adhesives on the bonding properties of bonded elements. The aim was to determine the shear strength of untreated and treated (heat and steam treatments) beech wood bonded with the two types of adhesive.

2. MATERIALS AND METHODS

Three types of beech wood samples *(Fagus sylvatica L.)* were used to test the bonding strength. Un-treated beech wood, steam-treated beech wood, and heat-treated beech wood elements were used to make samples in the experimental investigation.

Un-treated beech wood was obtained from commercial logs processing in the company Secom (Visoko, Bosnia and Herzegovina) from the standardly dried elements. Steamed elements were obtained by steam treatment in an industrial direct steamer with the usual industrial procedure at a constant steam temperature of nearly 100 °C for 24 hours. At atmospheric pressure, the temperature of freshly cut water-saturated wood was gradually raised in 3 steps: 40 °C for 4 hours, 60 °C for 5 hours, and 80 °C for 4 hours, followed by 12 hours at 100 °C. Steamed wood was dried to a standard moisture content of 8-10 %. Heat treatment was performed in a vacuum heat-treatment chamber, starting with preheating at 100 °C for 3 hours, then heating from 100 °C to 150 °C for an additional 5 hours, remaining at 150 °C for 4 hours, and finally cooling from 150 °C to 30 °C for 12 hours.

The testing elements were manufactured at the Secom doo factory (Visoko, Bosnia and Herzegovina). A four-sided planer machine, SCM Compact 22 (Rimini, Italy), with a feed speed of 15 m/min, was used for planning elements. The obtained elements, measuring 34 mm × 34 mm × 350 mm, had no visible defects and were produced using a combination of tangential and radial sections.

The bonding process was carried out using polyvinyl acetate (PVAc) adhesive (Kleiberit 303.2) and polyurethane (PUR) adhesives (Cosmo PU-180.150) under production conditions. The adhesives were applied to the contacting surfaces of both wood pieces at 180-200 g/m^2.

Joining was done in a hydraulic press (Figure 1) to join two pairs of elements. Bonding was performed following the parallel to the grain direction. Pressing time was 30 min, and the bonded samples were conditioned for 24 hours in production conditions (temperature 22±2 °C, humidity 50±5 %) and, after that, for 7 days in conditions with a relative air humidity of 50±5 % and a temperature of 23±2 °C. Samples were cut according to the standard BAS EN 13354. The dimensions of testing samples were 50 mm × 40 mm × 35mm. Each test sample was labelled with a letter to identify the type of materials (UB - un-treated beech, SB - steam-treated beech, HB - heat-treated beech), and the number indicates the types of adhesive used (1 - PVAc, 2 – PUR).

Figure 1. Bonding process

The samples were tested in the laboratory at the Faculty of Mechanical Engineering in Sarajevo. The shear strength of the prepared test samples was determined in accordance with EN 13354 using a Zwick machine (Ulm, Germany). The method of fixing the samples on the machine is shown in Figure 3. A constant loading speed of 1 mm/min was set, and the failure appeared between 30 and 40 s. The maximum loading force was recorded on the force indicator placed on the machine.

The shear strength was calculated using equation 1.

$$f_v = \frac{F}{b \cdot l}(MPa) \tag{1}$$

where f_v is the shear strength (N/mm^2), F is the maximum loading force (N), b is the shear width (mm) and l is the shear length (mm)

Figure 2. ZWICK testing machine, and testing procedure

The wood failure percentage analysis was performed using a visual method. After bonding strength testing, the fractured test samples are divided along the fracture line and the percent of adhesive on both sides of the fracture surface was analysed as a percent of total area. Statistical analysis and data visualisation were performed using Statistica (Statsoft Inc., Oklahoma, USA). Analysis of variance (ANOVA) was used to evaluate variation in bonding strength across samples grouped by wood type and adhesive. A Tukey pairwise comparison (post hoc) test was performed if the one-way ANOVA proved statistical significance. The effect sizes of the pairwise test were estimated using Holm-adjusted p-values. Graphic displays were made using whiskers and bar plots, and Excel software was used. Descriptive statistics were also used to display the results on graphs. All results are at the 95 % family-wise confidence level

3. RESULTS AND DISCUSSION

The results of the measurements of shear strength on elements bonded with PUR and PVAc adhesives are shown in Figure 3. Shear strength depends on the type of adhesive used. One-way ANOVA was performed on the results of each type of adhesive to compare the influence of the adhesive on the shear strength of joints made from differently modified beech wood. Results obtained by ANOVA show a statistically significant difference between samples bonded with PUR and PVAc adhesive and made from un-treated and heat-treated beech wood ($p<0.001$). Samples made from steam-terated beech show no statistically significant difference between samples bonded with PUR and PVAc adhesive ($p=0.113$).

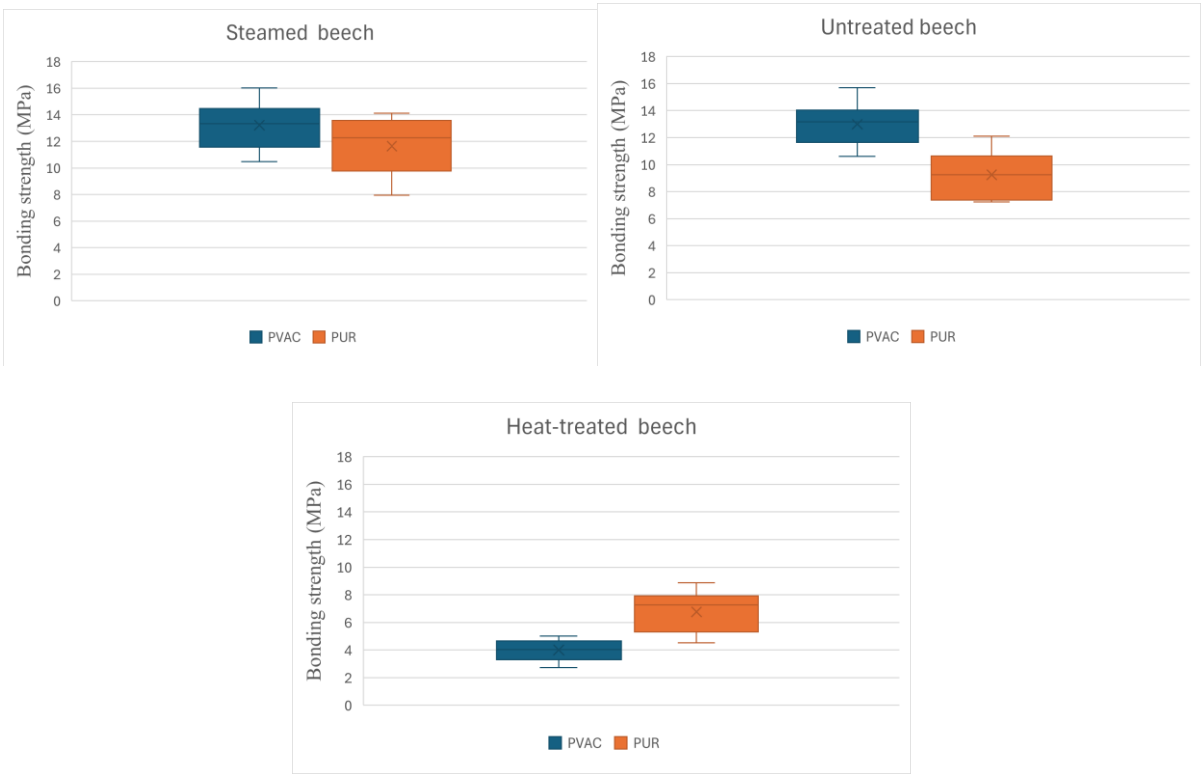

Figure 3. The effect of used adhesives on the mechanical characteristics of joints made with differently modified beech wood (whiskers show 5th–95th percentile)

Generally, it is assumed that PUR adhesives achieve higher bonding strength than PVAc adhesives. Our results show that bonding wood with PVAc adhesive yields joints with 30% higher shear strength than those bonded with PUR adhesive. These results were present in un-modified and steamed-treated beech wood. The same results were obtained by the study of Gasparik et al., 2017. They found that the beech bonded with the PVAc adhesive had slightly higher shear strength than with the PUR adhesive. (about 1.7 %). These results are the opposite of those of a 2023 study by Fodor and Bak which found that the PUR adhesive exhibited significantly higher bonding strength than PVAc. When bonding heat-treated beech wood, opposite results were obtained. PUR adhesives show higher results of bonding strength of joints by 40% compared to samples bonded with PVAC adhesive. This result is corroborated by a 2021 study of Fodor and Bak, 2023 who found that joints bonded with PUR adhesive had higher shear strength than those bonded with PVAc adhesive.

Several factors are identified that may cause samples bonded with PVAc adhesive to yield higher results than those bonded with PUR adhesive. The first factor is that bonding was performed under production conditions, without adequate control for PUR adhesives. The same bonding parameters were used for both types of adhesives, based on their experience with PVAc adhesives. The second factor which could cause a problem was the amount of adhesive and pressure. If the amount of PUR adhesive was too low, too high pressure in the hydraulic press could have forced the glue out of the joint, resulting in a weak joint. The third crucial factor was pressing time. The same pressing time was used for both adhesives, although the technical data state that the pressing time for the PUR adhesive must be longer than that for the PVAc adhesive. The study by Kujawinska *et al*. (2025), shows that increasing pressing time for PVAc adhesive has a positive effect on bonding strength. The behaviour of PUR adhesive proved

more complex. Short pressing time (20 min) and long pressing time (40 min) have been shown to improve bonding strength, whereas an intermediate pressing time (30 min) reduces it. Short pressing may allow adequate adhesive flow and initial polymerisation, while long pressing ensures good flow with complete chemical curing. Intermediate pressing time appears insufficient for complete curing, with the gel state of adhesive in a critical position to receive any movement that can happen during pressure release, leading to weaker joints due to initial cracks appearing in the glue layer, resulting in cohesive weakness in the adhesive layer (Kujawinska *et al*., 2025).

The obtained results were statistically analysed to determine trends in the modification effect of the wood elements on the bonding properties of the joints bonded with PUR and PVAC adhesives. The results of the bonding-strength measurements for elements bonded with PUR and PVAc adhesives are shown in Figure 5.

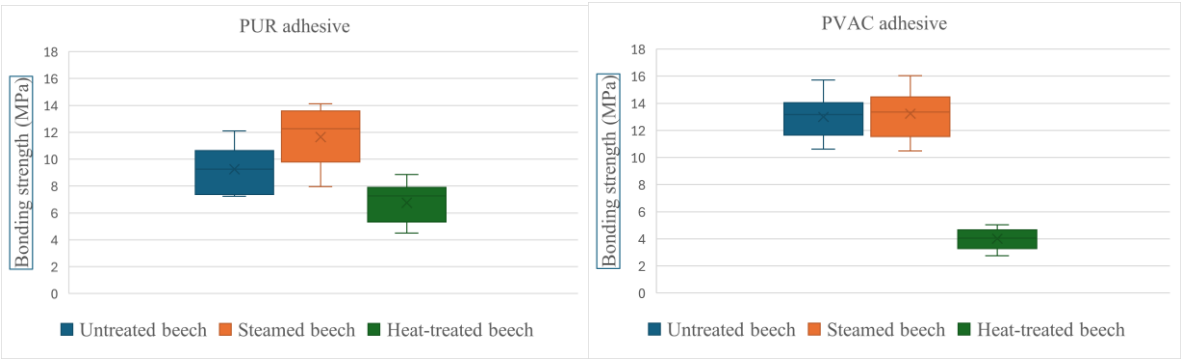

Figure 4. The effect of wood modification on the mechanical characteristics of joints bonded with different adhesives (whiskers show 5th–95th percentile)

According to Figure 5, the highest results of shear strength were obtained for the steamed beech regardless of which adhesives were used. Steam-treated samples bonded with PUR adhesive had 27% higher shear strength than un-treated samples. When using PVAc adhesive, steam-treated samples had slightly higher shear strength than untreated beech samples (1,5 %), but the difference was not statistically significant (Table 5). Steam-treated beech has better bonding performance than un-treated beech due to lower extractive content (Vassiliou *et al*., 2007). Heat-treated wood had lower bonding strength than untreated or steam-treated beech with both adhesives. Heat-treated samples bonded with PUR adhesive had 45% lower shear strength than steam-treated wood, and 25 % lower than un-treated beech wood. Heat-treated samples bonded with PVAc adhesive had 70 % lower shear strength than steam-treated, and un-treated beech wood. These results are according to the research conducted by Uzun *et al*. (2016), which shows that un-treated wood had a better bonding strength than the heat-treated wood. Bonding strength of higher-density wood is higher than that of lower-density wood (Uzun *et al*., 2016; Sogutlu and Dongel, 2007). The shear strength reduction of bonds created from thermally modified timber can be attributed to: (a) a reduction of polar groups in the cell walls of wood due to the degradation of amorphous polysaccharides by the heat treatment, resulting in less sites available for bonding, (b) an increased stiffness of the cell walls after heat treatment, which results in a reduction of internal surfaces for chemical bonding or mechanical interlocking of adhesives, and (c) a reduction in wettability that may retard the proper

penetration and curing of water-based adhesives such as PVAc adhesive. (Taghiyari *et al*., 2020)

One-way ANOVA was performed for each type of wood to compare the influence of the modification of beech wood on the shear strength of bonded elements. There was a statistically significant difference in mean shear strength between samples from differently treated beech wood ($p<0.001$). A Tukey pairwise comparison (post hoc) test was performed, and the test results are shown in Table 1.

In the case of samples bonded with PVAc adhesive, there are no statistically significant differences in mean shear strength between samples made from un-treated and steam-treated beech wood.

Table 1*: The correlations between un-treated beech (UB), steam-treated beech (SB) and heat-treated beech (HB), for different adhesives used. The green colour indicates no significant differences between samples*

PVAC			**PUR**		
SB	HB		SB	HB	
0.934	0.001	UB	0.019	0.015	UB
	0.001	SB		0.001	SB

significant at $p < 0.05$ (Tukey)

The quality of wood bonding depends primarily on wood properties, and the basic parameter that affects the bonding process is density (Fodor and Bak, 2023). Heat-treatment of wood reduces wood density (Candelier *et al*., 2016), and accordingly, heat-treated samples had lower shear strength than untreated and steam-treated beech wood. The second factor influencing the decrease in bonding strength of heat-treated wood is its reduced strength (Kariz and Sernek, 2010).

Analysing failure patterns is essential for gaining deeper insights into joint quality. Wood failure is desirable and indicates that the strength of the joint is greater than the cohesive strength of the wood (Mihulja and Bogner, 2025). Adhesive failure is undesirable and often shows high shear strength due to the cohesive strength of the adhesive (Gržan *et al*., 2023).

From Table 2, it can be seen that in the case of un-treated, and steam-treated beech wood, adhesion failure is dominant, regardless of which adhesives were used. Samples made from heat-treated beech wood had dominant cohesion (wood) failure. A high percentage of wood failure indicates greater adhesive penetration and interfacial bonding between the wood and the adhesive, as observed in the conditioned samples (Fodor and Bak, 2023). The second key, which indicates high wood failure at heat-treated wood, is the mechanical properties of wood. Heat-treatment of wood influences the reduction in mechanical properties of wood (Ibrisevic *et al*., 2025).

Table 2. Fracture analysis and estimation of the main wood failure pattern

Wood	**Adhesive**	**Wood failure, %**	**Stdev**
Un-treated beech	PVAC	10	6.12
	PUR	10	6.85
Steamed-treated beech	PVAC	10	6.12
	PUR	10	5.50
Heat-treated beech	PVAC	75	15.81
	PUR	40	8.33

4. CONCLUSION

In this work, the effect modification process of beech wood and the type of adhesives used on the shear strength of joints were investigated. The test results for the achieved bonding characteristic indicate that wood modification influences joint changes.

Based on this study's results, joint bonding strength depends on several factors. Both wood modification and adhesive type affect bonding quality. Results showed that heat-treatment of beech wood reduced joint bonding quality by 40-70 %, depending on the adhesive used. Generally, lower shear strength values for the samples made from un-treated and steam-treated beech wood were obtained for the polyurethane (PUR) adhesives. For samples made from thermal-treated beech wood, lower shear strength were obtained for polyvinyl acetate (PVAc)

The test results for the achieved bonding characteristic indicate that the steaming process affects joint strength only when using PUR adhesive.

5. REFERENCE

Candelier, K.; Thevenon, M.; Petrissans, A.; Dumarcay, S.; Gerardin, P.; Petrissans, M., 2016): Control of wood thermal treatment and its effects on decay resistance: a review. Annals of Forest Science, 73: 571-583. https://doi.org/10.1007/s13595-016-0541-x

Can, A., 2020: Effects of heat treatment systems on the physical properties of coated Scots pine (*Pinus sylvestris* L.) and poplar (*Populus euramericana*). BioResources, 15 (2): 2708-2720. https://doi.org/10.15376/biores.15.2.2708-2720

Fang, L.; Xiong, X.; Wang, X.; Chen, H.; Mo, X., 2017: Effects of surface modification methods on mechanical and interfacial properties of high-density polyethylene-bonded wood veneer composites. Journal of Wood Science, 63: 65-73. Journal of Wood Science10.1007/s10086-016-1589-9

Fodor, F.; Bak, M., 2023: Studying the Wettability and Bonding Properties of Acetylated Hornbeam Wood Using PVAc and PUR Adhesives. Materials, 16 (5): 2046. https://doi.org/10.3390/ma16052046

Gasparik, M.; Gaff, M.; Ruman, D.; Zaborsky, V.; Kasickova, V.; Sikora, A.; Sticha, V., 2017: Shear Bond Strength of Two-Layered Hardwood Strips Bonded with Polyvinyl Acetate and Polyurethane Adhesives. BioResources, 12 (1): 495-513. https://doi.org/10.15376/biores.12.1.495-513

Gržan, T.; Grieco, L.; Živkovic, V.; Mihulja, G., 2023: UV Irradiation of Wood Surface: Bonding Properties. Polymers, 15: 3318. https://doi.org/ 10.3390/polym15153318

Ibrisević, A.; Obucina, M.; Hajdarević, S.; Mihulja, G., 2025: Bending Properties of Finger-Jointed Elements of Differently Modified Beech (Fagus sylvatica L.) Wood. Forests, 16 (9): 1400. https://doi.org/10.3390/f16091400

Kariz, M.; Sernek, M., 2010: Bonding of heat-treated spruce with phenolformaldehyde adhesive, Journal of Adhesion Science and Technology, 24: 1703- 1716. https://doi.org/10.1163/016942410X507768

Kujawinska, A.; Rogalewicz, M.; Hryb, M.; Zywicki, K., 2025: Effect of Adhesive Bonding Process Parameters on the Joint Quality of the Middle Layer in Floorboards. Materials, 18 (20): 4674. https://doi.org/10.3390/ma18204674

Mihulja, G.; Poljak, D.; Sedlar, T., 2023: Joint Durability of Steam-Treated Beech Wood. Polymers, 15: 3318. https://doi.org/10.3390/polym15153318

Mihulja, G.; Bogner, A. 2005: Strength and Durability of Glued Wood Part One: Factors of Glued Joint Strength. Drvna industrija, 56: 69.

Milić, G.; Todorović, N.; Popadić, R., 2015: Influence of steaming on drying quality and colour of beech timber. Glasnik Šumarskog fakulteta, 112: 83-96. https://doi.org/10.2298/GSF1512083M

Neese, J. L.; Reeb, J. E.; Funck, J. W., 2004: Relating Traditional Surface Roughness Measures to Gluebond Quality in Plywood. Forest Products Journal, 54: 67-7.

Sedliacikova, M.; Moresova, M., 2022: Are Consumers Interested in Colored Beech Wood and Furniture Products? Forests, 13 (9): 1470. https://doi.org/10.3390/f13091470

Sogutlu, C.; Dongel, N., 2007: Tensile shear strengths of some local woods bonded with polyvinyl acetate and polyurethane adhesives, Journal of Polytechnic, 10 (3): 287-293. https://doi.org/10.2339/2007.10.3.287-293

Taghiyari, H. R.; Esmalpour, A.; Adamopoulos, S.; Zereshki, K.; Hosseinpourpia, R., 2020: Shear strength of heat-treated solid wood bonded with polyvinyl-acetate reinforced by nanowollastonite. Wood Research, 65 (2): 183-194.

Timar, M. C.; Varodi, A.; Hacibektasoglu, M.; Campean, M., 2016: Color and FTIR analysis of chemical changes in beech wood (*Fagus sylvatica* L.) after light streaming and heat treatment in two different environments. BioResources, 11 (4): 8325-8343.

Wanzhao Lia, W.; Liub, C.; Wangb, X.; Shib, J.; Meia, C.; Jan Van den Bulcke, J.; Van Ackerb, J., 2022: Understanding the impact of wood type and moisture on the bonding strength of glued wood. Wood Material Science and Engineering, 18 (1): 1-11. https://doi.org/10.1080/17480272.2021.2021448

Xue, J.; Xu, W.; Zhou, J.; Mao, W.; Wu, S., 2022: Effects of High-Temperature Heat Treatment Modification by Impregnation on Physical And Mechanical Properties of Poplar. Materials, 15: 7334. https://doi.org/10.3390/ ma15207334

Yau, Y.; Ocholi, A.; Kaura, J. M.; Lawan; A., 2024: Evaluation of the Bonding Performance of Polyurethane (PUR) and Epoxy Resin (ER) Adhesives with Gmelina Arborea Timber Using Different Testing Methods. UNIZIK Journal of Engineering and Applied Sciences, 3 (4): 1245-1256.

Moisture Content Estimation Using Halogen Analyzer on Several Wood Species

Pervan, Dario; Klarić, Miljenko*; Jambreković, Vladimir; Ivanda, Anamaria; Klarić, Kristina; Ištvanić, Josip[1]

[1] Wood Technology Department, Faculty of Forestry and Wood Technology, University of Zagreb, Zagreb, Croatia
*Corresponding author: mklaric@sumfak.unizg.hr

ABSTRACT

The moisture content in wood significantly influences its mechanical properties, usability, and suitability for various manufacturing processes. Accurate determination of moisture content is crucial for optimizing product quality in the wood industry. This paper investigates the applicability of halogen moisture analyzer for measuring moisture content in different wood species (beech, ash, cherry, larch, and oak), comparing its performance with the conventional gravimetric method according to the standard HRN EN 13183-1:2008. The study aims to evaluate the usability of halogen moisture analyzer in comparison with the traditional gravimetric method identifying potential advantages for use in industrial wood processing. Additionally, the research seeks to confirm if the sampling method used, is suitable and provides reliable results comparable with the gravimetric method.

Key words: halogen moisture analyzer, wood, moisture content, gravimetric method, wood drying

1. INTRODUCTION

Drying of sawn timber represents a critical stage in wood processing, as it adds substantial commercial value, facilitates access to moisture content controlled markets, and supports subsequent manufacturing operations such as furniture production. Inadequate drying practices can substantially increase production costs through material degradation, reduced yield, and complications in downstream processing, while excessive energy consumption further diminishes overall profitability (Denig, 2020). Consequently, the development and implementation of reliable and efficient methods for determining wood moisture content (MC) are fundamental for ensuring product quality and maintaining cost-effective production in both industrial and research contexts (Dietsch *et al.*, 2015). Moisture content is among the most influential parameters governing the physical, mechanical, and dimensional behavior of wood, as timber continuously exchanges moisture with the surrounding microclimate until equilibrium moisture content (EMC) is achieved (Skaar, 2012; Teodorescu, 2021). The target EMC depends primarily on the intended end use as well as the environmental temperature and relative humidity.

Inaccurate determination of MC can lead to dimensional instability, surface checking, or other defects that compromise the performance and longevity of wood products (Pervan *et al.*, 2013). The oven dry (gravimetric) method, as specified in standard EN 13183-1, remains the reference technique for MC determination because it directly quantifies the mass loss associated with moisture removal after drying to a constant weight. However, this method is labor-

intensive and time-consuming, making it less suitable for rapid or routine assessments. Halogen moisture analyzers offer an alternative approach based on thermogravimetric principles, wherein the sample is continuously weighed while subjected to halogen or infrared radiation, and the MC is computed from the corresponding mass loss. Although this technique enables rapid measurements and real-time data acquisition, the results may be influenced by factors such as sample geometry, surface heating dynamics, and material thermal conductivity, potentially leading to deviations from reference values (KERN & Sohn manual). Furthermore, halogen-based methods are not yet incorporated into European standards for timber moisture determination, which continue to designate the oven-dry procedure as the normative reference.

The present study investigates the applicability and accuracy of halogen moisture analysis for determining the moisture content of several hardwood and softwood species. Using the oven dry method as a reference method.

2. MATERIALS AND METHODS

The study was conducted on five wood species commonly used in industrial applications. The examined species include beech (*Fagus* spp.), ash (*Fraxinus* spp.), cherry (*Prunus* spp.), larch (*Larix* spp.), and oak (*Quercus* spp.). Representative samples were prepared from kiln-dried boards and machined to uniform dimensions of 300 (L) × 30 (T) mm (Figure 1). From each board, two types of specimens were produced: shavings (Figure 2) for halogen moisture analysis and small stick samples for gravimetric determination.

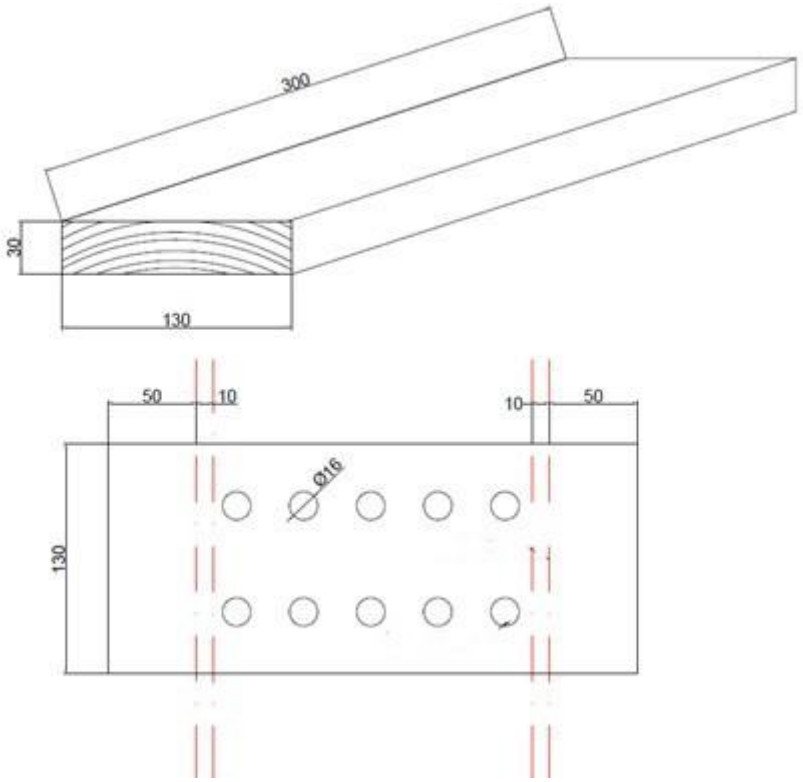

Figure 1. Sampling sketch of the boards used for making shavings and stick samples

Figure 2. Representative shavings prepared for moisture content determination prior to testing

Shavings were obtained by drilling at ten positions along each element using a 16 mm Auger drill bit (Figure 3) to ensure representative sampling. Immediately after drilling, the shavings were sealed in labeled glass vials to prevent moisture loss prior to testing. Stick samples were cut 50 mm from the edge of each board, with a cross-sectional thickness of 10 mm. To minimize moisture loss from frictional heating, all machining was performed at low feed rates, and the samples were immediately sealed in airtight plastic bags after preparation.

Figure 3. Sampling of shavings with a 16 mm spiral drill bit

Two stick samples were taken from each species to determine the average moisture content using the oven dry (gravimetric) method, following HRN EN 13183-1:2008. The initial mass of each sample was measured with an analytical balance (±0.001 g), after which samples were dried at (103 ± 2) °C for 24 hours until constant mass was reached. Dried samples were cooled in a desiccator to room temperature before final weighing to prevent reabsorption of atmospheric moisture. Halogen moisture analysis was conducted immediately after shavings collection at an ambient temperature of approximately 35 °C. Prior to testing, the instrument was calibrated according to the manufacturer's specifications. The drying program was set to a constant temperature of 103 °C, which the analyzer gradually reached and maintained throughout the measurement. For accurate results, samples were evenly distributed in the weighing pan, as irregular sample geometry can cause uneven heat distribution and affect drying time. Halogen moisture analyzer with sample can be seen in Figure 4.

Figure 4. Halogen moisture analyzer with weighted sample

In the conducted experiment, the smallest recorded sample mass of shavings was 1.212 g, and the largest was 2.153 g. Sample mass significantly influenced both drying time and measurement precision: smaller samples reduced drying duration, while larger masses improved accuracy but extended total testing time. The halogen results were compared with gravimetric reference.

3. RESULTS AND DISCUSSION

Results of moisture content analysis using halogen analyzer and gravimetric method are showed in Figures 5., 6., 7., 8. and 9.

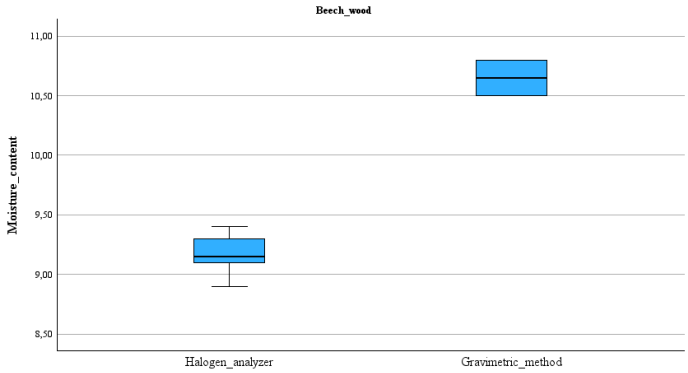

Figure 5. Results of moisture content for beech wood

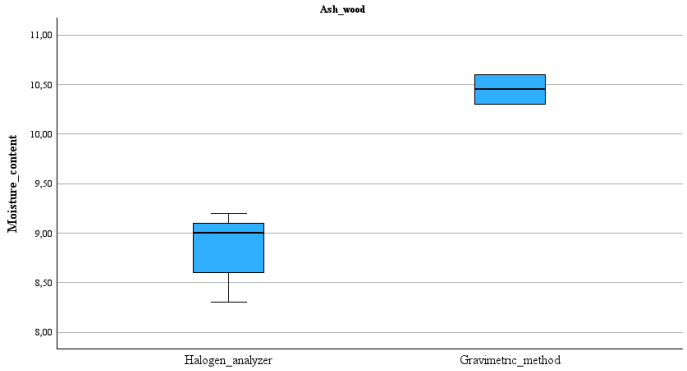

Figure 6. Results of moisture content for ash wood

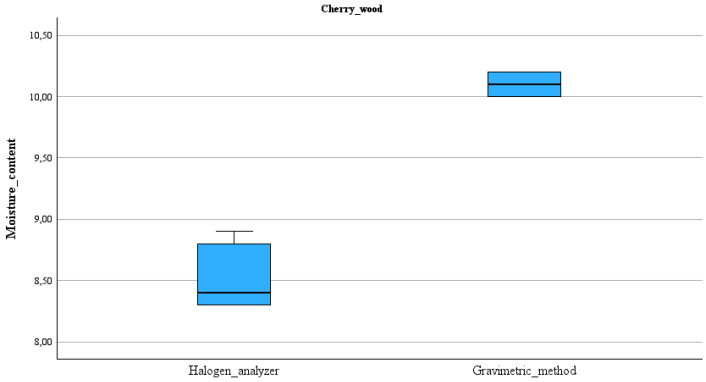

Figure 7. Results of moisture content for cherry wood

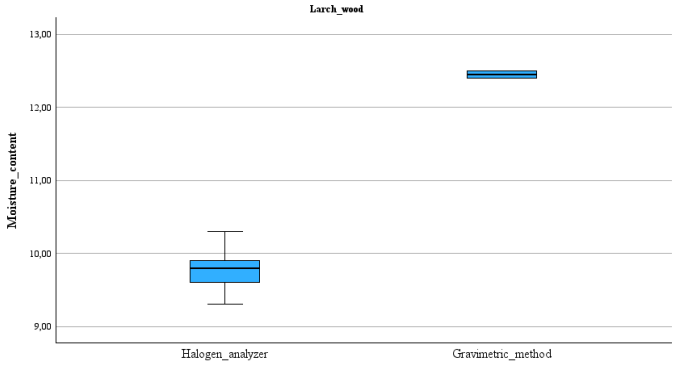

Figure 8. Results of moisture content for larch wood

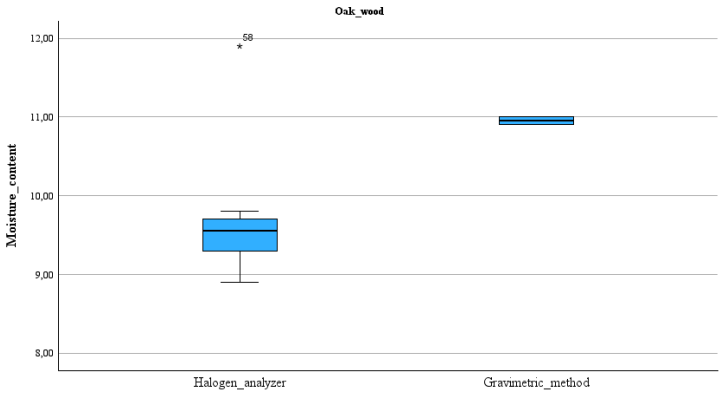

Figure 9. Results of moisture content for oak wood

For all five examined wood species, the halogen analyzer consistently yielded lower mean moisture content values compared to the gravimetric (oven dry) method. In halogen measurements, mean moisture content ranged from 8.52 % (cherry) to 9.80 % (larch), whereas the gravimetric method produced higher corresponding means, from 10.10 % (cherry) to 12.45 % (larch). The smallest variation in halogen results was observed for beech (SD = 0.17 %), while oak exhibited the greatest variability (SD = 0.82 %). In contrast, gravimetric measurements showed very low standard deviations across all species (0.07–0.21 %), confirming the high precision of the oven-dry method. The largest discrepancy between the two methods was recorded for larch, where the halogen analyzer underestimated the moisture content by approximately 2.65 %, whereas the smallest deviation occurred for cherry wood (≈ 1.58 %). These results indicate a systematic underestimation trend in halogen-based measurements, likely resulting from uneven heat distribution and differing drying kinetics between the two methods. The standard deviation of moisture content obtained in this study falls within the range reported by previous research conducted on wood chips (Mendel et al. 2016) and is consistent with observed deviations from reference values determined by the gravimetric method (Rimar and Kuna, 2013). Although the halogen analyzer produced slightly lower values, it offers a substantial time advantage over the conventional 24 hour oven-dry procedure (Figure 10.). The duration of halogen-based testing varied among the examined wood species. Mean drying times ranged from 6 min 41 s for cherry to 9 min 16 s for larch, reflecting interspecies differences in thermal behavior and moisture release dynamics. The shortest average testing time was recorded for cherry wood, which also exhibited the lowest standard deviation (0 min 47 s), indicating uniform heating and relatively low initial moisture content. Beech wood showed a similar average duration of 7 min 09 s, while ash wood and oak wood required slightly longer testing times of approximately 8 minutes. The longest drying duration was observed for larch wood, averaging 9 min 16 s, corresponding to its higher measured moisture content and greater resinous content, both of which can retard moisture diffusion and prolong drying.

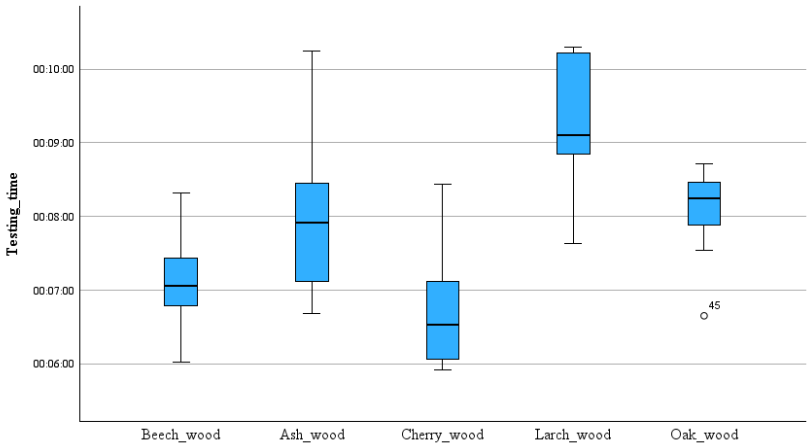

Figure 10. Results of time needed for halogen measurement testing

Overall, halogen analyzer based moisture determination provides rapid results, typically within 6–10 minutes, depending on wood species. Variations in testing time can be attributed primarily to differences in wood density, anatomical structure, and extractive composition, which influence both heat transfer and evaporation rate during the thermogravimetric process (Zanuncio *et al*. 2016; Zhou *et al*. 2016; Myronycheva *et al*. 2018; Niemz *et al*. 2022). In conclusion, while the halogen analyzer offers fast and repeatable measurements, it tends to slightly underestimate moisture content compared with the gravimetric reference method, particularly for species with higher resin or extractive content such as larch and oak.

4. CONCLUSION

This study compared a halogen moisture analyzer with the oven dry (gravimetric) reference method across several commercially important wood species. The halogen analyzer consistently produced lower moisture content estimates than the gravimetric method, and halogen-derived values displayed greater between-sample variability. However, the halogen analyzer delivered results in a fraction of the time required by the oven dry procedure, demonstrating clear advantages for rapid screening and process control. Observed differences between methods are plausibly explained by factors that affect thermogravimetric drying, (sample mass and geometry, heat-transfer dynamics, wood density, anatomy and extractive content) all of which can alter evaporation kinetics during halogen analysis. Species with higher extractive or resin content tended to show larger method deviations and longer halogen drying times. Based on these findings, the halogen analyzer is recommended as an effective tool for rapid moisture monitoring, provided its limitations are acknowledged. For applications requiring high absolute accuracy, the gravimetric method should remain the reference. To improve the practical utility of halogen measurements, we recommend: (1) developing species specific calibration or correction factors against gravimetric values; (2) standardizing sample preparation (mass, geometry and handling) and instrument settings; (3) routinely validating a subset of halogen results by oven-drying; and (4) conducting further studies with larger sample

sizes to quantify the effects of sample mass, anatomy and extractive content and to derive robust calibration models.

5. REFERENCES

Denig, J., 2000: Drying Hardwood Lumber. Vol. 118. US Department of Agriculture, Forest Service, Forest Products Laboratory.

Dietsch, P.; Franke, S.; Franke, B.; Gamper, A.; Winter, S., 2015: Methods to Determine Wood Moisture Content and Their Applicability in Monitoring Concepts. Journal of Civil Structural Health Monitoring, 5 (2): 115-127.

Mendel, T.; Überreiter, A.; Kuptz, D.; Hartmann, H., 2016: Comparison of Rapid Moisture Content Determination Methods for Wood Chips. In: Proceedings of the 49th International Symposium on Forestry Mechanization (FORMEC 2016). September 7th, 2016. pp. 1-8.

Myronycheva, O.; Karlsson, O.; Sehlstedt-Persson, M.; Öhman, M.; Sandberg, D., 2018): Distribution of low-molecular lipophilic extractives beneath the surface of air- and kiln-dried Scots pine sapwood boards. PLOS ONE, 13 (10): e0204212.

Niemz, P.; Njankouo, J. M.; Torres, M.; Bachtiar, E. V., 2022): Investigations on the sorption behaviour of selected wood species from Cameroon. Maderas. Ciencia y tecnología, 24: 1-10.

Pervan, S.; Klarić, M.; Slivar, M., 2013: Normirane metode određivanja i procjenjivanja sadržaja vode u drvu u Republici Hrvatskoj. Drvna industrija, 64 (2): 149-157.

Rimár, M.; Kuna, Š., 2013: Design of Methodology for Wood Chips Moisture Evaluation. Applied Mechanics and Materials, 308: 141-146.

Skaar, C., 2012: Wood-water relations. Springer Science & Business Media.

Teodorescu, I.; Erbaşu, R.; Branco, J. M.; Tăpuşi, D., 2021: Study in the Changes of the Moisture Content in Wood. In: IOP Conference Series: Earth and Environmental Science, 664 (1): 012017.

Zanuncio, A. J. V.; Carvalho, A. G.; Damásio, R. A. P.; Oliveira, B. D. S. D.; Carneiro, A. D. C. O.; Colodette, J. L., 2016: Relationship between the Anatomy and Drying in Eucalyptus grandis × Eucalyptus urophylla Wood. Revista Árvore, 40 (4): 723-729.

Zhou, H.; Xu, R.; Ma, E., 2016: Effects of Removal of Chemical Components on Moisture Adsorption by Wood. BioResources, 11 (2): 3110-3122.

***HRN EN 13183-1, 2008: Moisture Content of a Piece of Sawn Timber – Part 1: Determination by Oven Dry Method.

***KERN & Sohn GmbH, n.d.: Application Note – Moisture Analyzer ZB. https://dok.kernsohn.com/manuals/files/English/Application%20Note_Moisture%20analyzer-ZB-e-1210.pdf (Accessed 22 August 2024).

Optimization of Wood Sampling for Moisture Content Determination Using a Halogen Moisture Analyzer in Multilayer Parquet Production

Pervan, Dario; Klarić, Miljenko*; Jambreković, Vladimir; Sabljak, Marin; Klarić, Kristina; Ištvanić, Josip[1]

[1] Wood Technology Department, Faculty of Forestry and Wood Technology, University of Zagreb, Zagreb, Croatia
*Corresponding author: mklaric@sumfak.unizg.hr

ABSTRACT

Accurate determination of wood moisture content is a critical factor in the production of multilayer parquet, where dimensional stability and product quality depend on controlled moisture levels. This research aimed to optimize the sampling procedure of spruce wood for reliable determination of moisture content using a halogen moisture meter. Experimental sampling was carried out on sawn spruce intended for the middle layer of three-layer parquet. Three different sample types were prepared – plugs, shavings, and small sticks – and analyzed by the halogen moisture method, while reference samples were tested gravimetrically according to HRN EN 13183-1:2008.

Key words: halogen moisture meter, spruce wood, moisture content, gravimetric method, multilayer parquet

1. INTRODUCTION

Multilayer (engineered) parquet has become widely used in modern construction because its stable construction offers clear advantages over traditional solid wood flooring, including faster installation and better compatibility with underfloor heating (Guo *et al.*, 2017). Compared with solid parquet, multilayer elements, consisting of a broadly based layer glued together as a wood-based panel or coniferous core and a high quality wear layer, have better cross-layer stability, which minimizes the risk of cupping while maintaining the same quality in terms of tactile and visual aspects (Barbuta *et al.*, 2012; Blanchet *et al.*, 2003). These attributes make multilayer reconstituted parquet particularly useful where ease of fitting and consistent performance in service are important. The norms and standards that define the minimal thickness of the wear layer in multilayer parquet (e.g. HRN EN 13489), as well as minimal material properties, are specified by the same terms; moisture content is an important parameter influencing dimensional behavior and installation success. While the gravimetric oven drying method for measuring moisture content (HRN EN 13183-1) is still regarded as the reference standard due to its precision, it is quite slow. This makes it less suitable for real-time checks on production lines. Thermogravimetric analyzers, such as halogen moisture analyzers, provide quicker moisture estimates and are therefore often used instead (Rasti and Razavi, 2020). However, to achieve consistent results with these instruments in factory quality control, a robust sampling process is essential. This process should preserve the moisture content of the samples and yield results comparable to those obtained with the gravimetric method. This is particularly

important for coniferous sawn timber used in three layer parquet, as it originates from various sources and is exposed to a range of conditions.

This study aims to determine whether a halogen moisture analyzer provided rapid and reliable moisture content readings in kiln dried spruce intended for parquet core layering, and to develop an improved sampling method for routine production monitoring. To this end, various sample shapes and preparation methods, reflecting typical factory workflows, were tested alongside traditional drying oven methods. The resulting data were then analyzed to identify sampling routines that minimize moisture loss and produce comparable results suitable for monitoring the entire manufacturing process.

2. MATERIALS AND METHODS

The study focused on optimizing sampling procedures for determining the moisture content of spruce (*Picea abies* L.) used in the core layer of three layer parquet. Kiln dried spruce timber, previously conditioned to (7.5±0.7) % moisture content, was sampled at a parquet manufacturing facility in Croatia, which served as the experimental site. The raw material arrived in packages of elements approximately 4000 mm in length, 120 mm in width and 28 mm in thickness. Two defect free boards were selected and cut into specimens measuring 470 mm × 120 mm × 28 mm. Sixteen specimens (Figure 1) were prepared in total, sealed in stretch film immediately after cutting to prevent moisture loss, and transported to the laboratory for analysis.

Figure 1. Spruce boards used for testing

From each element, three types of samples were prepared: shavings, plugs and sticks. Each type was stored in airtight plastic containers or bags with zip closures to avoid moisture exchange with the environment. The plugs were further subdivided into thin splinters to ensure uniform drying during measurement (Figure 2).

Figure 2. Spruce plugs and splinters made from them

For moisture content determination using a halogen analyzer, sample masses of 0.5 g and 2 g were used, while two stick samples from each element were used for gravimetric oven-drying according to HRN EN 13183-1:2008, serving as reference values. Sample preparation was carried out using a bench drill (Farrox DP 51032F) with a ϕ 20 mm plug cutter and a ϕ 12 mm spiral drill, and a table saw (Makita MLS100N) for cutting sticks. To minimize heating and moisture loss caused by heat released during drilling and cutting, these actions were performed at low spindle speeds using sharp tools. Each sample was labelled, sealed, and transported to the laboratory immediately after preparation.

Moisture content was measured using a Kern DBS 60-3 halogen moisture analyzer, which operates on the thermogravimetric principle by comparing the initial and final sample masses during controlled heating at 103 °C. The device automatically records the moisture content once the change in mass (Δm) remains constant over a 30 second interval. Measurements were performed on RADWAG PS 750.X7 analytical balances with a precision of 0.1 mg for mass determination before and after drying.

a) 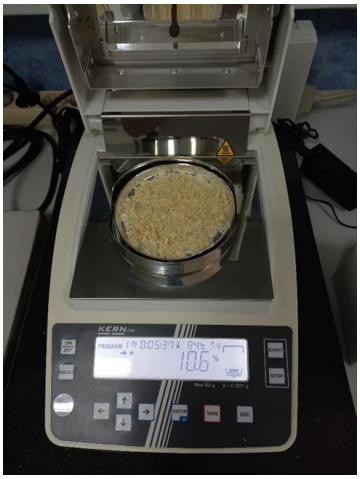 b) 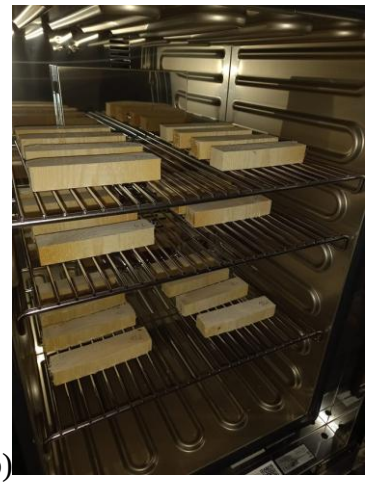

Figure 3. a) Shavings sample placed inside the halogen moisture analyzer and b) Drying of reference samples in the laboratory oven

For the gravimetric reference method, stick samples were weighed and dried in Memmert UN75 oven dryer at (103±2) °C for approximately 24 hours to reach an absolutely dry state, cooled in a desiccator, and reweighed. Moisture content was then calculated according to the

HRN EN 13183-1:2008 standard. Preliminary tests indicated that a 2 g sample mass provided greater measurement precision (2.3 % variation) compared to 0.5 g samples (5.4 % variation), with only a minor increase in measurement time (2.3 minutes). For these reasons, the final testing protocol adopted a 2 g sample mass as optimal for reliable, repeatable, and comparable halogen moisture analysis under conditions similar to those present in a factory.

3. RESULTS

The moisture content results for different sample types are presented in Figure 4.

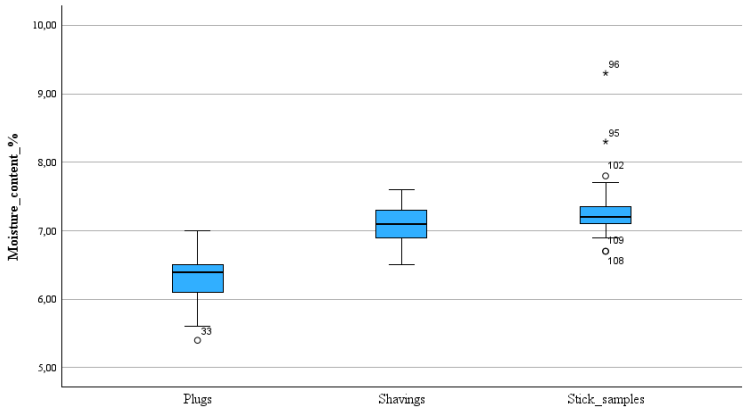

Figure 4. Moisture content results as by sample type

Results of moisture content reveal a consistent pattern: halogen measured plugs and shavings had mean moisture contents of 6.33 % and 7.09 % , whereas the reference samples (measured using gravimetric method) averaged 7.31 %. In case of other samples, plugs measured with the halogen analyzer are on average ~0.98 percentage points lower than the gravimetric reference samples, while shavings are closer (≈0.22 percentage points lower). The halogen derived measurements (especially shavings) also show smaller dispersion than the gravimetric sticks, whereas the sticks exhibit the largest range and standard deviation, suggesting greater heterogeneity or sensitivity to local moisture gradients.

A two way ANOVA (Table 1.) was conducted to examine whether sample type and measuring method exert a statistically significant effect on the measured moisture content.

Table 1. Two way ANOVA results for moisture content by sample type and measuring method

Source	Type III Sum of Squares	df	Mean Square	F	Sig.
Corrected Model	21.669	2	10.834	69.485	<0.001
Intercept	5152.753	1	5152.753	33046.138	<0.001
Sample type	21.669	2	10.834	69.485	<0.001
Error	16.996	109	0.156		
Total	5254.330	112			
Corrected Total	38.665	111			
$R^2 = 0.560$, Adjusted $R^2 = 0.552$					

ANOVA showed that the influence of sample type on moisture content is statistically significant ($F(2,109) = 69.49$, $p < 0.001$). The presented model explains 56 % of the total

variance in moisture content. A relatively low error variance is also observed, indicating consistent measurements within sample groups and good model precision. According to the findings presented so far, there is a statistically significant difference between the measured moisture contents of samples of different shapes, which also indicates a difference between the moisture contents measured by the halogen moisture meter and the gravimetric method.

4. CONCLUSION

This study examined the optimization of wood sampling for determining moisture content using a halogen moisture analyzer in the production of multilayer parquet made from spruce samples. The findings confirmed that the halogen method meets the required accuracy and reliability criteria while offering a fast and practical solution for process control during the manufacturing of the parquet's middle layer. Among the tested sampling techniques, shavings obtained using a spiral drill proved to be the most suitable form for measurements using the halogen analyzer, showing moisture content values nearly identical to those determined by the reference gravimetric method, with an average deviation of only 0.1 %. This demonstrates that, when appropriate sampling procedures and equipment are used, the halogen moisture analyzer can provide precise and reproducible results comparable to standard oven drying. Implementing this method in routine quality control can significantly reduce testing time and improve production efficiency. However, if exact moisture content is needed it is recommended to use gravimetric method to determine moisture content because of its relatively higher precision. Therefore, investing in adequate measuring equipment, along with operator training, is recommended to ensure consistent product quality and long term production stability.

5. REFERENCES

Barbuta, C.; Blanchet, P.; Cloutier, A.; Deteix, J.; Fortin, A., 2012: Moisture-induced stresses in engineered wood flooring with OSB substrate. Journal of Wood Science, 58 (4): 327-335.

Blanchet, P.; Beauregard, R.; Cloutier, A.; Gendron, G.; Lefebvre, M., 2002: Evaluation of various engineered wood flooring constructions. Forest Products Journal, 53 (5): 30-37.

Guo, X.; Wang, H.; Chen, Q.; Na, B.; Huang, L.; Xing, F., 2017: The dimensional stability of engineered wood flooring in heating systems. Wood Research, 62 (1): 103-112.

Rasti, A.; Pineda, M.; Razavi, M., 2020: Assessment of soil moisture content measurement methods: Conventional laboratory oven versus halogen moisture analyzer. Journal of Soil and Water Science, 4 (1): 151-160

***HRN EN 13183-1, 2008: Moisture content of a piece of sawn timber – Part 1: Determination by oven dry method.

***HRN EN 13489:2017: Wood flooring – Multi-layer parquet elements.

MycoWall: Organic Insulation for Future Timber Constructions

Petržela, Benjamín[1*]; Jozífek, Miroslav[2], Hýsek, Štěpán[1]

[1] Department of Wood Processing and Biomaterials, Faculty of Forestry and Wood Sciences, Czech University of Life Sciences Prague, Prague, Czech Republic
[2] Department of Horticulture, Faculty of Agrobiology, Food and Natural Resources, Czech University of Life Sciences Prague, Prague, Czech Republic
*Corresponding author: petrzela@fld.czu.cz

ABSTRACT

The construction sector requires new insulation materials that reduce environmental impact and contribute to carbon storage. Conventional synthetic insulations are energy-intensive and difficult to recycle, whereas mycelium-based biocomposites (MBB) offer a sustainable bio-based alternative. Cultivated from lignocellulosic substrates bonded by fungal mycelium, they utilise low-value biomass and need no additional adhesive. This study investigates the application of MBB as an insulation material in timber buildings. Tests confirmed promising thermal performance, with a conductivity of 0.076 W/(m·K) achieved using recycled wood and mycelium of *Ganoderma* sp. fungi. A prototype wall panel was subsequently developed with heat transfer coefficient (U-value) 0.295 W/(m^2·K). The construction concept combines MBB as the core insulation layer with cross-laminated timber (CLT) as the primary load-bearing system. Deciduous wood species (*Quercus* sp., *Fagus* sp.) were employed for complementary elements, treated with an innovative protective method. The external layer is designed as a ventilated façade made of oak profiles coated with a transparent finish containing metal oxide nanoparticles and UV stabilisation. The results demonstrate the potential of MBB to serve as an efficient, carbon-storing insulation material and to enhance the sustainability of building envelopes in modern timber architecture.

Key words: composite material, fungi, insulation, mycelium, recycled wood

1. INTRODUCTION

The global push for climate-resilient practices places the construction industry at the forefront, given that buildings are major contributors to global energy consumption and carbon emissions. Consequently, the development of renewable, bio-based, and circular materials is a critical priority.

A highly promising sustainable solution are Mycelium-Based Biocomposites (MBBs) (Hýsek *et al*., 2025). MBBs utilize fungal mycelium to bind lignocellulosic substrates, creating lightweight, biodegradable, and low-carbon alternatives to conventional materials (Parhizi *et al*., 2025). The production process is notably energy-efficient and relies on waste feedstocks (Elsacker *et al*., 2020). Scientific interest in MBBs is escalating, evidenced by over 70 studies issued in 2022, with China being the leading contributor (Alaneme *et al*., 2023). The focus of this research is highly applicable to the built environment, with 18.4 % of studies addressing engineering and 14.4 % focusing on materials, underscoring their potential as competitive building components (Aiduang *et al*., 2024). Beyond construction, MBBs are researched for thermal insulation (Schritt and Pleissner, 2022; Elsacker *et al*. 2021; Javadian *et al*. 2020), acoustic insulation (Javadian *et al*., 2020), and packaging (Yang *et al*., 2017; Holt *et al*., 2012),

among other applications including interior design and biomedicine (Alaneme *et al*., 2023; Attias *et al*., 2017).

Several companies (e.g., Ecovative Design, MYCO Works, Myco, Mykilio) have successfully commercialized mycelium-derived products, demonstrating the technology's readiness to transition from research to real-world deployment.

This study addresses circular economy principles by proposing a novel application for end-of-life recycled wood, utilizing it as the substrate for MBBs. Unlike approaches that rely on agro-waste, which often has competitive alternative uses, this research demonstrates the viability of upcycling genuine waste material. We present a complete methodology for MBB production, characterize its critical thermal properties, and detail its successful integration as insulation within a novel timber construction wall panel. This research thus provides a practical pathway for incorporating high-performance, truly circular bio-based materials into modern building envelope design.

2. MATERIALS AND METHODS

A wall panel was designed with implementation of Mycelium-Based Biocomposite (MBB). Following methodology desribes production of MBB, design of the wall panel and it´s composition.

Figure 1. MycoWall

2.1. Mycelium incubation

Wheat grains (De Heus a.s., Choceň, Czech Republic) were rinsed with water to remove coarse impurities. Gypsum (2,5 % d.w.; KittfortPraha s.r.o., Neratovice, Czech Republic) was added into the wheat grain to provide minerals, adjust pH and prevent grain agglomeration. Mixture was hydrated (47±2 % moisture content), sterilized in autoclave (3 hours, 121 °C; MLS-3781L, Sanyo Electric Co., Ltd., Moriguchi City, Japan) and inoculated by *Ganoderma sessile* (Boston edison, Terrestrial fungi USA) from Petri dish in flow box (FAST H, Faster s.r.l., Cornaredo, Italy). The inoculum was incubated (10 days, 24 °C, RH 70 %) in glass bottles. The inoculum from glass bottles was afterwards used to inoculate more wheat inoculum, which

was incubated in polypropylene (PP) bags. Colonized inoculum was transferred in cooling box (4 °C) for storage until the day of use.

2.2. MBB production

The composite production follows methodology introduced by Hýsek et al. 2023. Composite was produced by mycelia growth on substrate from recycled wood obtained from Kronospan CR company with particles fraction used for particle board (PB) middle layer (Hýsek et al. 2023). The substrate was hydrated to reach the absolute moisture of 60 % (Hýsek *et al*., 2023). Substrate was put in polypropylene (PP) bags (model PP50/SEU4/V40-51, SAC O2 nv, Deinze, Belgium) and sterilized in autoclave MLS-3781L (Sanyo Electric Co., Ltd., Moriguchi City, Japan) for 3 hours at 121 °C. The inoculation rate was 10 % (wet weight/wet weight). Inoculated substrate was conditioned (24±1 °C, RH 70 %). After 14 days the substrate was fully colonized by fungi. Colonized substrate was semi-automatically shredded in shredding machine and filled into molds (500 mm × 500 mm × 200 mm). Molds was manufactured from Polymethyl methacrylate (PMMA) for touching surface and wooden completely detachable construction. Composite grew in mold for 7 days (24±1°C, RH 70%). Afterwards, composite was removed form molds and placed into "sarcophagus" etc. polystyrene (XPS) box for 70±2 hours (30.8±1.8 °C, RH ≈99 %) with frequent moisturizing. After removing from sarcophagus, composite was let to dry out in lab conditions (20±3 °C, RH 60 %) with indirect regular ventilation by fan for 10 days. Finally, composite was completely dried drying chamber for 24 hours (103±3 °C, RH 0 %) with ventilation. Real scale MBB with dimensions of 485 mm × 482 mm × 184 mm was produced.

Figure 2. MBB production

2.3. Thermal characteristics

The thermal insulation characteristics were determined using the ISOMET 2114 measuring device (Applied Precision Ltd., Slovakia) and the IPS 1105 surface probe, which is designed for measuring hard and rigid materials. The principle of the measurement is based on monitoring the material's response to a temperature change over time, caused by a dynamic thermal impulse from the probe. This method allows for the measurement of thermal conductivity (λ) [W/(m·K)], volumetric heat capacity (cρ) [J/(m³·K)], and thermal diffusivity

(a) [m²/s]. The device was calibrated according to the manufacturer's instructions before measurement.

2.4. Wall composition

The wall composition concept was fundamentally driven by the idea of designing a structure that anticipates the future composition of Central European forests. While coniferous species currently dominate the region, climate change projections indicate a future shift favoring deciduous species. This concept, therefore, explores utilizing deciduous timber in applications traditionally dominated by softwoods.

Using the Teplo EDU 2017 software , a prototype wall panel was designed based on the determined thermal characteristics of the materials, with the primary requirement being the incorporation of MBB as the core insulation. The final design integrates the MBB layer with a Cross-Laminated Timber (CLT) system serving as the primary load-bearing structure. Secondary structural elements employ oak (*Fagus sp*.), which was treated with a lavender oil-based method following the methodology introduced by Šimůnková *et al*. (2022). The MBB insulation is externally protected by an Egger DHF board. The exterior finish is provided by a ventilated façade consisting of oak (*Quercus sp*.) profiles. These profiles are coated with a transparent finish (DColor FK 47 UV Protect), developed and patented by the Czech University of Life Sciences Prague, containing metal oxide nanoparticles for UV stabilization.

2.5. Thermal transmittance

For the comprehensive assesment of the building structure composition Teplo EDU 2017 software was used. Composition was evaluated from the perspective of heat and water vapor transfer accordnig to EN ISO 13788 and EN ISO 6946 standards. Thermal transmittance was calculated for designed wall composition.

Table 1. Teplo: input values

No.	Item	D, mm	λ, W/(m*K)	C, J/(kg*K)	ρ, kg/m^3	Mi [-]
1	CLT Novatop	84	0.130	1600	490	200
2	MBB	184	0.076	1000	150	2
3	Egger DHF	15	0.100	1700	650	11

Boundry condition of calculation were set:

- Internal surface thermal resistence Rsi: 0.13 m^{2}K/W
  - dtto for internal surface temperature calculation Rsi: 0.25 m^{2}K/W
- External surface thermal resistence Rse: 0.04 m^{2}K/W
  - dtto for internal surface temperature calculation Rse: 0.04 m^{2}K/W
- Design outdoor temperature Te: -13.0°C
- Design internal air temperature Tai: 20.6°C
- Design outdoor relative humidity RHe: 84%
- Design internal relative humidity RHi: 60%

3. RESULTS AND DISCUSSION

Table 2 summarizes results of thermal characteristics of produced MBB expressed by thermal conductivity (λ) [W/(m·K)], volumetric heat capacity (cρ) [J/(m³·K)], and thermal diffusivity (a) [m²/s].

Table 2. Thermal characteristics of MBB

No.	Thermal conductivity, W/(m*K)	Volumetric heat capacity, J/m³*K	Thermal diffusivity, m²/s
1	0.078	0.208	0.375
2	0.078	0.206	0.379
3	0.075	0.155	0.487
4	0.076	0.154	0.493
5	0.075	0.193	0.391
6	0.076	0.192	0.395
Avr.	0.076 ± 0.001	0.184 ± 0.024	0.420 ± 0.055

Density of Mycelium-Based Biocomposite produced was measured resulting in ρ = 158.42 kg/m^3 after conditioning at w = (65 ± 5) %, t = (20 ± 3) °C.

Thermal transmittance was calcutaled via Teplo EDU 2017 software modelation which resulted in heat transfer coefficient (U-value) 0.295 W/(m^2·K). It was confirmed, that no water vapor condensation occurs in the structure at the design outdoor temperature.

4. CONCLUSION

This study successfully demonstrated the viability of Mycelium-Based Biocomposites (MBBs) as a highly circular and sustainable insulation material by utilizing end-of-life recycled wood as the substrate, offering an alternative to mycelium composites relying on agro-waste. The real scale MBB was produced with thermal conductivity λ = 0.076 ± 0.001 W/(m·K) affirming its suitability for thermal applications.

Furthermore, this research presented an innovative wall panel concept designed to reflect future Central European forest compositions by incorporating deciduous species alongside the MBB core. Thermal transmittance modeling of this novel wall composition confirmed satisfactory hygrothermal performance, achieving (U-value) of 0.295 W/(m^2·K) and demonstrating no water vapor condensation under design outdoor temperatures.

This research provides a clear, practical pathway for integrating low-carbon, bio-based materials into modern timber construction, supporting the construction industry's transition toward climate-resilient and circular practices.

Acknowledgements: This project was supported by Internal Grant Agency from Faculty of Forestry and Wood Sciences, Czech University of Life Sciences Prague with project no. A_04_25. I would like to sincerely thank to my supervisor Štěpán Hýsek for his great mentoring.

5. REFERENCES

Aiduang, W.; Jatuwong, K.; Jinanukul, P.; Suwannarach, N.; Kumla, J.; Thamjaree, W.; Teeraphantuvat, T.; Waroonkun, T.; Oranratmanee, R.; Lumyong, S., 2024: Sustainable Innovation: Fabrication and

Characterization of Mycelium-Based Green Composites for Modern Interior Materials Using Agro-Industrial Wastes and Different Species of Fungi. Polymers, 16 (4): 550.

Alaneme, K. K.; Anaele, J. U.; Oke, T. M.; Kareem, S. A.; Adediran, M.; Ajibuwa, O. A.; Anabaranze, Y. O., 2023: Mycelium Based Composites: A Review of Their Bio-Fabrication Procedures, Material Properties and Potential for Green Building and Construction Applications. Alexandria Engineering Journal, 83: 234-50.

Attias, N.; Danai, O.; Ezov, N.; Tarazi, E.; Grobman, Y. J., 2017: Developing Novel Applications of Mycelium Based Bio- Composite Materials for Design and Architecture. In: Building with Bio-Based Materials: Best Practice and Performance Specification, Final COST FP1303 International scientific conference, Zagreb.

Elsacker, E.; Søndergaard, A.; Van Wylick, A.; Peeters, E.; De Laet, L., 2021: Growing Living and Multifunctional Mycelium Composites for Large-Scale Formwork Applications Using Robotic Abrasive Wire-Cutting. Construction and Building Materials, 283: 122732.

Elsacker, E.; Vandelook, S.; Van Wylick, A.; Ruytinx, J.; De Laet, L.; Peeters, E., 2020: A Comprehensive Framework for the Production of Mycelium-Based Lignocellulosic Composites. Science of The Total Environment, 725: 138431.

Holt, G. A.; Mcintyre, G.; Flagg, D.; Bayer, E.; Wanjura, J. D.; Pelletier, M. G., 2012: Fungal Mycelium and Cotton Plant Materials in the Manufacture of Biodegradable Molded Packaging Material: Evaluation Study of Select Blends of Cotton Byproducts. Journal of Biobased Materials and Bioenergy, 6 (4): 431-39.

Hýsek, Š.; Daňková, M.; Jozífek, M.; Němec, M.; Wimmer, R., 2023: Mycelium-based biocomposites from recycled wood: influence of fungal species on properties of biocomposites. In: 32th International Conference on Wood Science and Technology - ICWST 2023 "Unleashing The Potential of Wood-based Materials". Croatia, Zagreb.

Hýsek, Š.; Jozífek, M.; Petržela, B.; Němec, M., 2025: Artificial Neural Network Prediction of Mechanical Properties in Mycelium-Based Biocomposites. Polymers, 17 (18): 2506.

Javadian, A.; Le Ferrand, H.; Hebel, D. E.; Saeidi, N., 2020: Application of Mycelium-Bound Composite Materials in Construction Industry: A Short Review. SOJ Materials Science & Engineering, 7 (2): 1-9.

Parhizi, Z.; Dearnaley, J.; Kauter, K.; Mikkelsen, D.; Pal, P.; Shelley, T.; Burey, P., 2025: The Fungus Among Us: Innovations and Applications of Mycelium-Based Composites. Journal of Fungi, 11 (8): 549.

Schritt, H.; Pleissner, D., 2022: Recycling of Organic Residues to Produce Insulation Composites: A Review. Cleaner Waste Systems, 3: 100023.

Šimůnková, K.; Hýsek, Š.; Reinprecht, L.; Šimůnková, K.; Šobotník, J., 2022: Lavender oil as eco-friendly alternative to protect wood against termites without negative effect on wood properties. Scientific Reports, 12: 1909.

Yang, Z.; Zhang, F.; Still, B.; White, M.; Amstislavski, P., 2017: Physical and Mechanical Properties of Fungal Mycelium-Based Biofoam. Journal of Materials in Civil Engineering, 29 (7): 04017030.

***EN ISO 6946 (year not specified): Building components and building elements – Thermal resistance and thermal transmittance – Calculation method.

***EN ISO 13788 (year not specified): Hygrothermal performance of building components and building elements – Internal surface temperature to avoid critical surface humidity and interstitial condensation – Calculation methods.

Evaluation of Processing Time in Primary Sawmilling of Scots Pine (*Pinus sylvestris*) Logs on a Vertical Band Saw

Stamenkoska, Ana Marija[1*]; Temelkova, Anastasija[2]; Zlateski, Goran[1]; Trposki, Zoran[2]; Rabadjiski, Branko[1]; Koljozov, Vladimir[2]

[1] Department of Primary Wood Processing, Faculty of Design and Technologies of Furniture and Interior - Skopje, Ss. Cyril and Methodius University in Skopje, North Macedonia
[2] Department of Machines, Energy and Transport Faculty of Design and Technologies of Furniture and Interior - Skopje, Ss. Cyril and Methodius University in Skopje, North Macedonia
*Corresponding author: stamenkoska@fdtme.ukim.edu.mk

ABSTRACT

The efficiency of primary wood processing largely depends on the optimal utilization of macines and tools. Beyond the rational use of sawlogs in sawmilling, the profitability and effective operation of sawmill capacities critically rely on the efficient application of primary processing machines. These machines are primarily tasked with transforming logs into semi-finished products, through which logs are converted into sawn timber through the sawing process. Among the most implemented machines for primary processing are band saws. These types of primary machines allow individual log sawing, where each log is processed separately according to its dimensions and quality class. In such operations, determining the technological capacity is essential, defined as the volume of logs a machine can process within a given timeframe. A key factor affecting technological capacity is the processing time per log, which represents the cumulative duration of all sawing operations and factors involved in sawing , such as log rotation, number of cuts, log length and other related activities. The processing time can be divided into components dependent on the machine's technological parameters and those influenced by the organization of production within the sawmill. This study presents a detailed analysis of processing times for Scots pine (*Pinus sylvestris*) sawlogs using a vertical band saw.

Keywords: band saw, primary processing, processing time, sawlogs, Scots pine, technological capacity.

1. INTRODUCTION

The rentability of the primary wood processing industry depends directly on the rational and efficient use of both machines and sawlogs. Within sawmills, the technological equipment is generally divided into two functional groups: machines for primary processing and machines for secondary processing. Traditional sawmilling plants typically utilize several types of primary processing machines. Frame saws and band saws are the most common. These machines are responsible for the transformation of roundwood into sawn lumber. The machines used for secondary processing are responsible for determining the final width and length of the produced elements. These are most often circular saws designed for transversal or longitudinal cutting.

The coordinated operation of primary and secondary machines defines the overall sawmilling process, since they perform the essential technological steps that convert the roundwood into a marketable wood product. Although sawmilling is often perceived as a simple transformation process, it is in reality a complex technological workflow defined by numerous heterogeneous processing elements, variable raw material conditions, and multi-stage machine

interactions (Borz *et al*., 2010). Primary processing in particular remains a crucial stage in the conversion of roundwood into marketable lumber assortments.

As noted by Rabadjiski (2019), Nikolić (2010) and Brežnjak (2000) among all machines used for primary processing, band saws appear to be the most widely implemented. Band saws can be constructed in either a horizontal or a vertical configuration. Their advantages include the ability to process sawlogs with a wide spectrum of diameters, lengths, shapes, and sawing patterns. Compared to frame saws, they provide greater flexibility and allow the operator to employ individual sawing methods. This is especially important when logs of different dimensions or quality classes must be processed (Rabadjiski, 2019).

As stated by Ištvanić *et al*. (2007), when planing the capacity of a band saw is it important to take into account the quantity of logs intended for processing, in other words the quantity of roundwood that can be processed within a defined time frame measured in m^3/shift. These capacities depend on many factors such as: the wood species being processed, the quality class of the sawlogs, the moisture content of the material, the condition and maintenance of the saw blades, the level of mechanization in the sawmill, and the organization of the workflow. Since machine capacity is mainly determined by time it is important to understand the dynamics of the sawing process. Processing time has a direct influence on the economic efficiency of sawmilling operations.

In contemporary industrial practice, optimization efforts increasingly rely on accurate time management. For this reason, the relationship between theoretical and real processing time has become an important subject of investigation. Classical formulas used to estimate sawing time usually consider only the motion of the carriage during cutting and the return movement after each pass. However, practical experience in manufacturing conditions indicates that these formulas frequently underestimate the real duration of the process. This difference arises because several auxiliary activities are not included in the theoretical time calculation. Such activities include log alignment, hydraulic clamping, operator decision time, micro adjustments of the carriage or blade, removal of sawdust, examination of internal defects, reactions to irregular taper, and the handling of crooked or knotty logs. Previous studies have mostly examined yield optimization, surface quality, and sawing accuracy (Smajić *et al.*, 2021; Šoškić and Milić, 2025; Ivanovskiy, 2021; Gholamiyan, 2022). Limited attention has been given to the evaluation of processing time for band saws under authentic manufacturing conditions (Borz *et al*, 2010; Câmpu and Derczeni, 2023).

This paper addresses the difference between the theoretical processing time obtained through a widely applied formula from sawmilling literature and real measured processing time recorded during production activities in a sawmill. The aim is to quantify this difference and to identify the factors that contribute to the additional time that is not accounted for in the classical formula. The research seeks to provide a more realistic understanding of primary processing efficiency and to contribute toward more accurate machine capacity planning in sawmills.

2. MATERIALS AND METHODS

For the purpose of this research, a total of 20 Scots pine (*Pinus sylvestris*) sawlogs were selected and processed under working conditions. The experimental work was conducted in a

medium-sized sawmill located in the Republic of North Macedonia. The study was carried out during regular production. There weren't any interference in the technological flow, in order to record realistic operating conditions. All observations and measurements were performed directly on the production line.

The sawlogs were processed on a vertical band saw Primultini 1300 SCA (Figure 1). This type of machine is widely used in primary sawmilling due to its flexibility in handling logs of different diameters, lengths, and quality classes, as well as its ability to perform individual sawing patterns for each sawlog. The main technical characteristics of the band saw are presented in Table 1. The sawing speed corresponds with the optimum feed speed according to Bariska and Pásztory (2015), which is 34.0 m/min.

All twenty logs were selected with a consistent length of 5.0 m, in order to eliminate the influence of length variability on time. The diameters of the small end and butt end of the logs were measured prior to processing. The volume and diameter taper of each log was calculated accordingly. The mean diameter of the sawlogs varied from 34.0 cm to 68.0 cm. The mean diameter has a wide dimensional range typical of medium-capacity sawmills. The taper values varied from 0.25 cm/m to 2.50 cm/m, indicating noticeable variation in log geometry. The diameter taper can influence both processing stability and time. Log grading was performed visually according to European standards EN 1927-2:2008 and EN 1315:2010. Accordingly, the logs were classified into I, II and III class. This grading took into account observable characteristics such as straightness of the stem, presence of knots, sweep, taper, surface defects, etc. The distribution of the logs among quality classes reflects typical manufacturing material input. The majority of the logs were grades as I and II class. The moisture content of the analyzed sawlogs varied from 45 % to 55 %. All sawing operations were carried out in October, therefore the logs were not frozen.

Table 1. Technical characteristics of the band saw

Machine type	**Horizontal band saw**
Manufacturer	Primultini
Model	1300 SCA
Year of production	1996
Power unit force	75 Kw
Wheel diameter	1300 mm
Crown width	180 mm
Type of carriage	Hydraulic
Length of carriage	6,5 m
Sawing carriage speed	34 m/min
Return motion carriage speed	50 m/min

Figure 1. Band saw used in the research

The selected sawlogs were processed into sawn lumber and beams intended for construction use. The sawn boards were sawn with thicknesses of 25 mm and 30 mm. The beams were sawn in dimensions of 120 mm × 150 mm, 100 mm × 120 mm and 50 mm × 80 mm. All logs were processed using the cant sawing method. In this method, the log is sawn into a central squared or rectangular section called a cant. This cant is then further sawn into boards or beams of predetermined dimensions. Cant sawing is commonly applied in industrial sawmilling because it allows the possibility of sawing different dimensions. The cant sawing method also yields a higher percentage of sawn lumber. Although it may generate a slightly higher amount of side slabs in comparison to live sawing, cant sawing provides more flexibility in dimensions when sawing logs of greater diameters.

Two independent stopwatches were used in order to separately measure the different time components and the total sawing time. The first device was used to record the duration of log positioning and log rotation. Both times represent the auxiliary operations included in the theoretical time calculations. The second device was used to measure the total processing time for each log. The total processing time was defined as the interval starting at the moment the log was fed onto the carriage and ending when the final sawn lumber was fully detached from the carriage and transferred onto the conveyor.

Time measurements were conducted in four separate batches. Two batches were processed by one machine operator and two by another, in order to reflect normal variation in operational execution. All time measurements and calculations were primarily recorded in seconds (s), in accordance with SI units.

2.1. Theoretical evaluation of the sawing time

In this research, the theoretical sawing time was calculated using a standard formula commonly applied in sawmilling literature, proposed by Nikolić (2010), The formula is based on the summation of basic operational components involved in the sawing of a single log on a band saw:

$$t_{sawlog} = t_{adj} + t_{rot} \cdot m_{rot} + \frac{l_{sawlog} \cdot z_{cut}}{v_{sawing}} + (z_{cut} - m_{rot}) \cdot \frac{l_{sawlog}}{v_{return}} (s) \qquad (1)$$

t_{sawlog} – processing time for a single sawlog (s)
t_{adj} – adjusting time of the sawlog onto the carriage (s)
t_{rot} – rotation time of the sawlog (s)
m_{rot} – number of rotations
l_{sawlog} – sawlog length (m)
z_{cut} – number of cuts on the cross section of the sawlog
v_{sawing} - carriage speed while cutting (m/s)
v_{return} – return speed of the carriage (m/s)

According to Nikolić (2010), the production capacity of a band saw is directly determined by time-dependent parameters: t_{sawlog}, t_{adj}, m_{rot} and z_{cut}. These parameters are significantly influenced by the degree of mechanisation of the band saw and the efficiency of the operational workflow. This formula considers only the main operational movements of the band saw: the forward cutting motion of the carriage, the return motion, the initial positioning, and the rotations of the log between successive cuts. In that sense, it represents an idealized or theoretical model of the sawing process, under the assumption of continuous, uninterrupted operation. Although the formula provides a structured and standardized approach for estimating sawing time, it does not include several unavoidable activities. These activities occur in real production conditions and include positioning adjustments, hydraulic clamping actions, operator decision time, clearing of sawdust, small operational interruptions, and adaptations. As a result, the theoretically calculated time often differs from the real processing time observed under industrial conditions. The comparison between the theoretical time from the above equation and the experimentally measured total time represents the central methodological framework of this study.

3. RESULTS AND DISCUSSION

Table 2 presents the descriptive statistics of the main characteristics of the Scots pine sawlogs. The mean diameter of the logs was 47.4 cm. The minimum and maximum diameters ranged from 34.0 cm to 68.0 cm, confirming a relatively wide dimensional distribution. The standard deviation of diameter suggests a noticeable variation among the logs, which is a relevant factor when analyzing the processing time. The average volume was 0.931 m³, with values varying from 0.453 m³ to 1.814 m³. Larger volumes are usually associated with increased inertia during carriage movement, more demanding rotations, and a greater number of cuts. All of these factors increase the processing time. The sawlog taper, which expresses the gradual decrease of the diameter from butt end to small end of the log, varied between 0.25 cm/m and 2.50 cm/m. The taper has an average value of 1.12 cm/m. The taper values indicate that some logs exhibited pronounced variability along the length. The logs with higher taper cause difficulties while positioning on the carriage and require precise planning of the cuts.

Table 2. Descriptive statistics of the processed sawlogs parameters

Parameter	Mean	Std. deviation	Min	Max
d_m (cm)	47.4	11.2	34.0	48.0
V_{sawlog} (m^3)	0.931	0.996	0.453	1.814
S_{taper} (cm/m)	1.12	0.171	0.25	2.50

d_m – mean diameter, V_{sawlog} – sawlog volume, S_{taper} – diameter taper

The comparison between theoretical and measured processing time is shown in *Table 3*. It is clearly evident that the measured processing time of each log substantially exceeded the theoretically calculated time. On average, the theoretical processing time was 686 s per log, while the actual measured value was 1443 s per log. This results in an average time difference of 690 s, which corresponds to a mean deviation of 210.3 %. This means that the real processing time was more than twice as long as the theoretical estimation in most cases.

Table 3. Comparison between the theoretical and measured processing time

Sawlog	$t_{theoretical}$, s	$t_{measured}$, s	Difference, s	Difference, %
1	662	1165	503	176.0
2	872	2225	1353	255.2
3	920	1155	235	125.5
4	781	1375	594	176.1
5	361	699	338	193.6
6	912	1615	703	177.1
7	903	2125	1222	235.3
8	1029	1759	730	170.9
9	584	1628	1044	278.8
10	739	1331	592	180.1
11	812	1326	514	163.3
12	982	2995	2013	305.0
13	615	1713	1098	278.5
14	395	2042	1647	517.0
15	541	1539	998	284.5
16	705	1395	690	197.9
17	639	989	350	154.8
18	491	1211	720	246.6
19	393	788	395	200.5
20	1068	1446	378	135.4
Mean	686	1443	690	210.3

$t_{measured}$ equivalent to t_{sawlog}

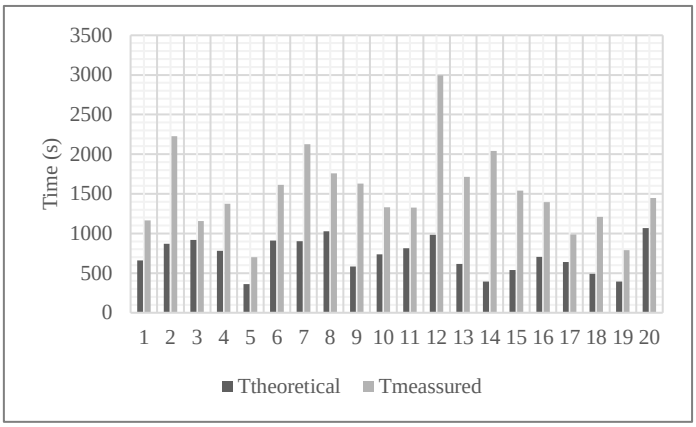

Figure 2. Visual representation of the theoretical and measured processing time

The difference between the theoretical and measured time confirms the main hypothesis of this research. The traditional formula proposed by Nikolić (2010) does not incorporate several time components that are unavoidable under real manufacturing conditions. The existing formula considers only adjusting time, rotation time, cutting time and return time of the carriage, and assumes a continuous, uninterrupted flow. In practice, many other factors are present. Other operations present in the total time include micro-adjustments of the log position, clearing of sawdust, inspection of knots or internal defects, correction of log orientation due to taper or curvature, etc . All of these activities contribute to the additional and unaccounted time.

The difference between the theoretical and measured time is particularly evident in some individual logs, such as sawlog 14, where the theoretical time was 395 s, but the measured time reached 2042 s, resulting in a difference of 1647 s or more than 500 %. Similar significant differences were observed in sawlogs 12, 13, 15 and 9. These logs were characterized either by greater taper, lower quality class, or more complex sawing patters. These factors which required a higher number of corrections during processing. This further supports the assumption that log geometry plays a key role in time inefficiency, even when the cutting speed and machine parameters remain constant.

Figure 2 provides a visual comparison between the theoretical processing time and the measured total processing time for each sawlog. The graphical representation clearly demonstrates a consistent gap between the two values.

Figure 3 presents the relationship between the mean diameter of the sawlogs and the measured processing time. A moderate positive correlation of 0.245 can be observed, indicating that larger diameters generally require longer processing time. This is expected, as logs with greater cross-sectional area require a higher number of cuts. In addition, larger logs tend to be heavier, more difficult to stabilize on the carriage, and more sensitive to vibrations which further complicates handling and increases processing time. A strong correlation between the log mean diameter and the total processing time could not be identified suggesting that the total time was influenced by non-machine dependent factors, such as precise positioning and additional checking of cutting accuracy.

Figure 4 illustrates the relationship between diameter taper and measured processing time. While the correlation is in the strong range (with value of 0.655). There is an evident trend indicating that sawlogs with higher taper values tend to require longer processing time. Increased taper causes instability during sawing, uneven pressure distribution on the blade, and

greater risk of geometric deviation. As a result, the operator is forced to reduce feed speed, re-adjust the log's position, and sometimes interrupt the cutting cycle in order to ensure stability and dimensional accuracy. These results show that taper is an important geometric parameter influencing time consumption in sawmilling. There is no explicit reflection on the taper in the theoretical calculation time.

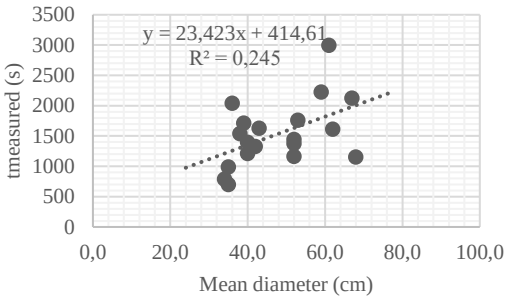

Figure 3. Relationship between mean diameter and total processing time

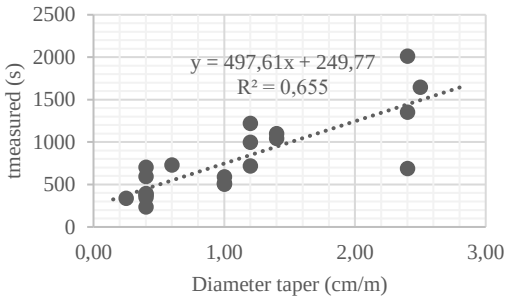

Figure 4. Relationship between diameter taper and total processing time

Another important element influencing the measured time is the role of the human operator. The human decision-making, reaction time and caution strongly affect the duration of each operation. Operator hesitation occurs when internal defects are suspected, when the stability of the log is uncertain, or when the cutting path must be visually verified. These real-time decisions are part of manufacturing process. According to the presented results, the total processing time consists of the calculated time ($t_{theoretical}$) and auxiliary/additional time ($t_{auxilay}$). The auxiliary time includes time required for cleaning, visual checks and operator hesitation time. These tasks are influencing mainly by the sawlogs properties and human factors.

Based on the reviewed literature and the results of the present analysis, it can be concluded that the classical approach often underestimates the real duration of the sawing process. The following model proposed by Brežnjak (2000) provides a more realistic representation of the total processing time. This formula incorporates both the actual cutting time and the additional time that inevitably occurs under manufacturing conditions.

$$t_{total} = t_{sawing} + t_{additional}\ (s) \tag{2}$$

t_{total} – total time (s)
t_{sawing} – actual sawing time (s)
$t_{additional}$ – time required for additional operations in sawing (s)

$$t_{additional} = t_1 + t_2 + n_r \cdot (t_3 + t_4) + t_5(s) \tag{3}$$

t_1 – time required for log loading on the carriage (s)
t_2 – time for positioning (turning) on the carriage (s)
n_r – number of cuts per log (s)
t_3 – time for setting the board thickness (s)
t_4 – time for return of the carriage (s)

t_5 – other time required in the whole log processing cycle (s)

4. CONCLUSION

This study confirmed that the classical theoretical formula for estimating sawing time on underestimates the real processing time under manufacturing conditions. The theoretical formula, based on the main technological movements of the machine, remains highly valuable for planning and comparative analysis. However, it does not reflect the complexity of real production environments. In this research, the average theoretical processing time was 686 s per log, whereas the average measured time reached 1443 s per log. The mean difference of 690 s, corresponding to 210.3 %, clearly indicates that additional activities represent an unavoidable part of the total processing time.

Based on the obtained results, it can be concluded that processing time is not determined only by machine feed rates and the number of cuts. The processing time is influenced by log geometry, especially diameter taper, as well as log diameter. Logs with higher taper values required significantly longer processing time due to increased instability, more frequent repositioning, and greater operator intervention. Although a weaker correlation was observed between mean diameter and total time, larger logs still tended, in general, to require a longer processing time. The formula according to Brežnjak (2000) best fits the results presented in this paper. The real processing time is a summation of time required of actual sawing and time required for additional operations. These additional operations often have greater shares in the total time (Ištvanić, 2009), which is confirmed by the difference between the theoretical and measured time. When planing a sawmill and calculating the band saw capacity, accurate processing time must be considered. The accuracy of this consideration defines the efficiency of the sawing processes.

5. REFERENCES

Bariska, M.; Pásztory, Z., 2015: The Optimum Log Feed Speed with Bandsaw. European Journal of Wood and Wood Products, 73 (2): 245-250.

Borz, S.; Oghnoum, M.; Marcu, M.; Lorincz, A.; Proto, A., 2021: Performance of Small-Scale Sawmilling Operations: A Case Study on Time Consumption, Productivity and Main Ergonomics for a Manually Driven Bandsaw. Forests, 12 (6): 810-829.

Brežnjak, M., 2000: Sawmilling technology – Part II. Faculty of Forestry, Zagreb, Croatia.

Câmpu, R.; Derczeni, R., 2023: European Beech Log Sawing Using the Small-Capacity Band Saw: A Case Study on Time Consumption, Productivity and Recovery Rate. Forests, 14 (26): 1137-1145.

Gholamiyan, H.; Gholampoor, B.; and Hassanpoor Tichi, A., 2022: Effects of cutting parameters on the sound level and surface quality of sawn wood. BioResources, 17 (1): 1397-1410.

Ištvanić, J; Beljo Lučić, R.; Jug, M.; Karan, R., 2009: Analysis of Factors Affecting Log Band Saw Capacity. Croatian Journal of Forest Engineering: Journal for Theory and Application of Forestry Engineering, 30 (1): 27-35.

Ivanovskiy, V., 2021: Improving the quality of the band saw cut. In: IOP Conference Series: Earth and Environmental Sciences, 875 (1): 1-6.

Nikolić, M., 2010: Sawmilling Technology. Faculty of Forestry, Belgrade, Serbia.

Rabadjiski, B., 2019: Sawmilling Technology. Faculty of Design and Technologies of Furniture and Interior, Skopje, Republic of North Macedonia.

Smajić, S.; Ištvanić, J; Obućina, M.; Jovanović, J., 2021: Determination of Success Sawmill Processing of Pedunculate Oak (Quercus robur L.) Logs by Live Sawing Method. In: Proceedings of the 14-th

International Scientific Conference WoodEMA 2021 "THE RESPONSE OF THE FOREST-BASED SECTOR TO CHANGES IN THE GLOBAL ECONOMY", pp. 363-368.

Šoškić, B.; Milić, G., 2005: Influence of quality of beech logs on yield in sawmill conversion. Prerada drveta, 12 (1): 15-22.

*** EN 1927-2, 2008: Qualitative classification of softwood round timber – Part 2: Pines.

*** EN 1315, 2010: Dimensional classification of round timber.

Innovation as a Fundamental Instrument of Entrepreneurship

Stankevikj Shumanska, Mira[1*]; Nikolovska, Angela[2]; Antovska, Ivana[1]

[1] Faculty of Design and Technologies of Furniture and Interior, Ss Cyril and Methodius University in Skopje, North Macedonia
[2] Kara5 Entertainment – Skopje, North Macedonia
*Corresponding author: stankevik@fdtme.ukim.edu.mk

ABSTRACT

Innovation plays a fundamental role in entrepreneurship and significantly contributes to economic growth, as well as to providing a competitive advantage in the rapidly changing global market. This scientific paper analyses the theoretical aspects of innovation and provides a deeper understanding of its various dimensions, classifications and impact on enterprises. The research focuses on the complex relationship between innovation and business development and explores how different forms and levels of innovation contribute to improving organisational capabilities and achieving sustainable growth. The research results show that innovation is the foundation for businesses that want to maintain their competitive advantage, adapt to market dynamics and ensure long-term success in the digitalised economy.

Keywords: innovation, entrepreneurship, competitiveness, business, economy

1. INTRODUCTION

Innovation is a central driver of entrepreneurship and a key factor in supporting economic growth and competitiveness in a changing global market. As organisations face rapid technological progress and shifting market conditions, the ability to innovate has become essential for maintaining relevance and ensuring long-term development. Through innovation, firms can anticipate market needs, respond to consumer expectations and generate value by introducing new or improved products and services.

This paper examines innovation as a core element of entrepreneurship and provides a theoretical basis for understanding how it influences business processes and organisational performance. Innovation extends beyond new products and services. It includes improvements in processes, marketing and management practices that enhance operational capacity and strengthen market presence. These developments enable enterprises to adapt effectively, increase efficiency and sustain growth within competitive economic environments.

2. AIM AND OBJECTIVES OF THE RESEARCH

The paper examines innovation as a central element of entrepreneurship and analyses how it influences competitiveness, organisational performance and the long-term development of enterprises. It aims to explain the contribution of innovation to entrepreneurial activity and to clarify how innovative practices support adaptation, efficiency and sustainable business growth. The objectives are to present the main forms of innovation and to assess how these forms affect

organisational processes, particularly in sectors where production, materials and technology play a key role.

3. CONCEPT AND DEFINITION OF INNOVATION

Understanding the concept of innovation is essential for analysing its role in entrepreneurship and economic development. Innovation is the introduction of a new or substantially improved product, process, marketing method or organisational practice within business operations, workplace structures or external relations (OECD, 2024).

Innovation holds significant importance in entrepreneurship. As global markets become increasingly competitive, businesses that fail to innovate risk falling behind their competitors. More than 84% of executives and general managers believe that the future growth of their companies depends on innovation (McKinsey and Company, 2023). It enables companies to respond to market developments, adapt to changing conditions and maintain readiness for new opportunities. In practice, innovation supports the establishment and expansion of ventures, strengthens organisational capacity and contributes to business sustainability.

Innovation may take several forms. It can be technological, involving the introduction of new software. It can be process-related, such as the improvement of production techniques. It can also be organisational, for example, through changes in management structures. A common characteristic of any innovation is that it must be implemented. A new or improved product becomes an innovation only when it is introduced to the market. In the same way, new processes, marketing methods or organisational approaches qualify as innovation once they become an integral part of a company's operations.

Innovation is not limited to large corporations with extensive resources. Small businesses also have opportunities to innovate. Historically, many transformative products and services have originated from small enterprises and this trend continues today with radical innovations emerging from this sector. For small businesses, innovation is essential because it drives growth and success. It enables them to remain competitive and to adapt to changing market conditions (Filiposki and Kostovska Bogoevska, 2024).

4. THEORETICAL FRAMEWORK OF INNOVATION

The study of innovation covers multiple disciplines, including economics, sociology and business management. Over time, key theoretical frameworks have been developed to explain how innovations arise, spread and influence industries and economies. These frameworks provide important insights into why some businesses and sectors innovate more effectively than others and suggest approaches for encouraging innovation within various organisational contexts.

4.1. The Theory of "Creative Destruction" — Joseph Schumpeter

One of the most prominent theories of innovation is Joseph Schumpeter's Theory of "Creative Destruction" (Schumpeter, 1942). Schumpeter argues that innovation is the primary

driving force behind economic growth and industrial transformation. He describes innovation as a disruptive force that leads to the destruction of old industries and the creation of new ones, a process known as "creative destruction." This concept refers to the cyclical process in which outdated technologies, products or business models are replaced by newer and more efficient alternatives.

The introduction of innovation often leads to the decline of traditional industries and the rise of new sectors. The shift from film to digital photography illustrates this process, where the introduction of digital cameras reduced demand for conventional film cameras and created a new market segment.

The role of entrepreneurs: Schumpeter emphasises the essential role of entrepreneurs as the driving force behind creative destruction. Entrepreneurs introduce radical innovations that challenge and disrupt existing market structures. They identify opportunities for new combinations of resources, technologies and products that reshape entire industries.

4.2. The Theory of "Diffusion of Innovations" — Everett Rogers

The Diffusion of Innovations theory, developed by Everett Rogers, explains how, why and at what rate new ideas, products or technologies spread within societies or industries. According to Rogers, the adoption of innovation follows a bell-shaped curve that includes five distinct categories of adopters (Rogers, 1983).

Innovators: The first individuals or businesses to adopt a particular innovation. Typically risk-takers and visionaries, motivated by the desire to create new markets.

Early adopters: They play an influential role in promoting innovations to a wider audience and are crucial to their broader acceptance.

Early majority: They adopt an innovation after demonstrated benefits. More cautious about risk, accept innovations only once their value has been proven in the market.

Late majority: More sceptical and resistant to change. They embrace innovation only after it has become mainstream and widely accepted.

Laggards: The most resistant to change and driven more by necessity than by desire.

Several factors influence the diffusion of innovations, including:

Relative advantage: The extent to which an innovation is perceived as superior to the existing solution.

Compatibility: The degree to which the innovation aligns with the existing values, experiences and needs of potential consumers.

Complexity: The perceived difficulty of using or understanding the innovation.

Trialability: The extent to which an innovation can be tested or experimented with before full adoption.

Observability: The visibility of the innovation's benefits to others, which can accelerate its adoption.

Understanding how innovation diffuses helps businesses identify the right time to enter new markets and adopt new technologies.

4.3. "Open Innovation" — Henry Chesbrough

The concept of "Open Innovation", developed by Henry Chesbrough (Chesbrough, 2003), challenges the traditional closed model of innovation in which businesses rely solely on their internal R&D activities. Chesbrough proposed an approach based on collaboration, where companies work with external partners to develop new ideas, technologies and solutions.

Internal research and development (R&D) versus external collaboration: In the open innovation model, companies no longer restrict innovation to their internal R&D departments. Instead, they actively seek ideas and technologies from external sources such as universities, research institutions, startups and even competitors. This collaborative approach enables companies to access a broader pool of knowledge and accelerate the implementation of innovations.

Benefits of open innovation: Open innovation allows businesses to reduce development costs, share risks and bring products to market more quickly. By utilising external expertise, companies can enhance their innovation capacity without bearing the full costs of internal R&D. According to IBM research, organisations that have implemented the concept of open innovation achieved a 59% higher revenue growth rate (IBM, 2023).

4.4. "Disruptive Innovation" — Clayton Christensen

The theory of "Disruptive Innovation", developed by Clayton Christensen (Christensen, 1997), explains how smaller companies with limited resources can successfully compete with and even surpass larger and well-established firms. Disruptive innovations typically begin by targeting small, niche markets that are underserved by major companies, with the idea of gradually improving until they eventually overtake the mainstream markets.

Sustaining versus disruptive innovation: Sustaining innovation improves existing products or services and typically adopted by industry leaders. In contrast, disruptive innovations introduce simpler and more accessible alternatives aimed at small, specialised markets.

Example of disruptive innovation: Initially limited to prototyping and small-scale production, 3D printing has advanced to the point where it has a significant impact on traditional manufacturing, particularly in the automotive parts industry and in custom-made furniture production.

Disruptive innovation reshapes industries and changes market dynamics. The decline of firms such as Blockbuster following the entry of Netflix illustrates the effect of failing to respond to disruptive change.

4.5. 4.5 The Theory of "Innovation-Driven Growth" — The 2025 Nobel Prize in Economic Sciences

The 2025 Nobel Prize in Economic Sciences was awarded to Joel Mokyr, Philippe Aghion and Peter Howitt for their contributions to explaining innovation-driven economic growth (The Royal Swedish Academy of Sciences, 2025). Their research provides valuable insight into how technological progress became a continuous process and how it continues to drive modern economies. Mokyr shows that continuous innovation emerges when scientific knowledge and practical know-how reinforce each other, creating a sustained process of technological advancement. Aghion and Howitt emphasise that growth is supported by the replacement of

older technologies with more productive ones, a process driven by research, development and entrepreneurship. They also highlight that innovation progress depends on institutions that encourage openness, competition, education and investment in research. Their combined work demonstrates that innovation is a central mechanism linking technological progress, enterprise development and economic growth.

5. TYPES AND LEVELS OF INNOVATION

Innovation can take many forms that differ in scope, timeframe and impact on enterprises and society. The classification of innovations is complex, as different types may overlap and the same innovation can fall into several categories depending on how it is applied by different companies. According to the subject of innovation, four main types can be distinguished:

Product innovation: Introduction of new or significantly improved products or services. For instance, a furniture manufacturer may develop products made from sustainable materials to meet growing demand for environmentally friendly products.

Process innovation: Improving internal processes to increase efficiency or reduce costs. This may include adopting automation in production, streamlining supply chains or using digital platforms to enhance customer services. Process innovation helps businesses of all sizes to improve productivity and remain competitive.

Marketing innovation: Adoption of new marketing strategies to influence and communicate with customers more effectively. This may include the use of social media to expand audience reach, the application of detailed analytics for targeted advertising or the development of a new brand identity.

Organisational innovation: Changes in business practices, workplace organisation or external relations. This may include restructuring management hierarchies, adopting flexible working arrangements or encouraging collaboration with external partners. Organisational innovation can lead to improved productivity, greater employee satisfaction and enhanced business performance.

Each of these groups of innovations can be implemented at different levels:

Incremental innovation: Small and continuous improvements to existing products, processes or business practices. Incremental innovations are generally easier to implement for most enterprises because they require fewer resources and involve lower risk. Over time, these improvements can significantly enhance a company’s competitiveness and operational efficiency.

Radical innovation: Major transformations that create entirely new industries or market segments. Such innovations often lead to disruption, as they challenge existing technologies, products or business models. Although radical innovation carries greater uncertainty and risk, it also offers substantial potential rewards for companies that are willing to pursue bold and transformative ideas.

6. GLOBAL INNOVATION INDEX

The Global Innovation Index ranks countries based on their innovation capabilities and performance. It evaluates factors such as infrastructure, human capital, R&D expenditure,

patent applications and the exchange of knowledge and information. It provides a comprehensive overview of global innovation trends and highlights the countries that lead in innovation performance (WIPO, 2025).

According to the Global Innovation Index Report 2025, the countries with the best performance are:

- Switzerland,
- Sweden,
- United States,
- Republic of Korea,
- Singapore.

Switzerland remains the global leader for the 15th consecutive year, excelling across nearly all pillars of innovation performance, particularly creative outputs.

In the Balkan region innovation progress remains uneven. Countries such as Slovenia and Croatia perform relatively well, whereas others, including North Macedonia, continue to face structural limitations in financing, digitalisation and the adoption of new technologies. These differences reflect broader challenges for innovation-driven development in smaller and less diversified economies.

7. INNOVATION TRENDS IN EUROPE

The innovation landscape in Europe in 2025 is shaped by efforts to improve market integration, simplify regulation and strengthen the conditions for investment. Europe performs well in research and sustainability, yet converting scientific progress into commercial outcomes remains a key challenge (EIB, 2025). For manufacturing industries, including the woodworking and furniture sector, competitiveness increasingly depends on digitalisation, efficient use of materials and the ability to respond to environmental requirements. Studies from the Croatian furniture industry show that many Balkan wood-manufacturing firms face typical barriers such as low R&D investment, limited export activity, modest innovation culture and digital lack of competencies among workers (Barčić *et al*., 2016). These characteristics correspond with broader regional challenges in adopting advanced technologies and sustaining innovation capacity.

Market integration and simplification: Fragmented markets and differing national rules still restrict the expansion of enterprises across Europe. The EIB highlights that greater financial integration and more consistent regulation would support investment and strengthen the environment for innovation (EIB, 2025).

Investment and policy coordination: Public investment continues to support innovation, especially in sectors adapting to digital and environmental change. Enterprises receiving targeted support are more likely to invest in new technologies and climate-related projects.

Digital transformation and Industry 4.0: Digitalisation remains a central driver of innovation in European manufacturing. Woodworking and furniture industry research shows that adopting Industry 4.0 technologies such as automation, CNC systems and integrated production software can increase efficiency by 30 % to 50 % (Červený *et al*., 2022). Adoption,

however, is uneven. Large enterprises integrate these solutions more easily, while many SMEs face financial barriers and limited technical capacity.

Green and sustainable innovation: Europe maintains a strong position in environmental innovation. In the wood sector, companies increasingly focus on material efficiency, reduced waste and circular production practices in response to environmental expectations and raw material pressures. Wood products generally have significantly lower greenhouse-gas emissions across their life cycle than steel, concrete or plastics, reinforcing the role of the wood sector in the circular bioeconomy (FAO, 2022).

Human capital and skills: Skill shortages remain one of the main constraints on innovation. Many European enterprises report difficulties recruiting workers with technical and digital skills (EIB, 2025). In the woodworking industry, companies note that graduates often require significant retraining to work with automated and digitalised production systems, highlighting the importance of improved vocational training and continuous skill development (Červený *et al*., 2022).

8. THE IMPORTANCE OF INNOVATION IN BUSINESS

8.1. Economic growth and competitiveness

Innovation is a critical factor for business success, supporting economic growth and strengthening competitiveness in domestic and global markets. In 2023 the EU invested €389 billion in research and development, representing 2.26% of GDP, with businesses providing most of the funding (1.51 % of GDP). Despite this, the EU still lags behind leading innovation economies such as South Korea, highlighting the need to strengthen private-sector research capacity and cooperation between public and private institutions (Eurostat, 2025). Countries such as Sweden, Belgium, Austria and Germany achieve the highest R&D intensity, illustrating how sustained investment supports productivity and long-term competitiveness.

In contrast, manufacturing sectors in the Balkans, including the woodworking and furniture industry, generally record lower R&D investment and slower technology adoption. Limited financial resources, outdated equipment and small enterprise size continue to restrict their innovation capacity. Strengthening links between research institutions, enterprises and support programmes is therefore essential to improving competitiveness in the region.

Businesses that innovate are more resilient to external shocks. Evidence from the COVID-19 period shows companies that had already implemented digital tools and new business models adapted more effectively to disruption, while those relying on traditional approaches experienced greater difficulties.

8.2. Innovation and market dynamics

Innovation supports economic growth and influences market dynamics by creating opportunities and shaping competition. In the European furniture industry, companies that have implemented sustainable manufacturing practices or integrated circular economy principles gain an advantage over competitors that rely solely on traditional methods. Recycling in the furniture industry remains a small segment but offers significant growth potential as demand for sustainable products continues to rise (EU Commision, 2017).

9. ANALYSIS OF IKEA'S INNOVATION STRATEGY

IKEA is an example of how continuous innovation supports entrepreneurial growth and long-term competitiveness. Founded in 1943 in Sweden, the company has expanded into the world's largest furniture retailer, operating 486 stores worldwide with revenues of approximately €45.1 billion in 2024 (IKEA, 2025). Its development has been shaped by a consistent focus on design innovation, resource efficiency and customer-oriented business practices.

9.1. Innovation in Design and Production

IKEA's approach to innovation is rooted in the idea of making well-designed and functional products accessible to a broad consumer base. The company designs furniture that is easy to assemble and transport, which lowers logistics costs and improves affordability. Through vertical integration and regional manufacturing centres it maintains control over quality and efficiency. This approach illustrates how innovation in product design and production processes supports entrepreneurial scalability.

Sustainability is a key pillar of IKEA's innovation strategy. Wood is central to the company's Scandinavian design heritage and IKEA continually explores ways to use it more efficiently. Examples include the RÖNNINGE table which uses hollow wooden legs to reduce material consumption and the FRÖSET chair which uses bent veneer layers to balance flexibility and strength. These designs illustrate how innovation in materials can reduce waste while maintaining durability.

Particle board is another important part of IKEA's circular model. In 2024 it accounted for 66% of wood-based materials used in IKEA products and is made from leftover wood and sawdust. Circularity also guides product development. The redesign of the BILLY bookcase increased the use of renewable materials and introduced fittings that make it easier to assemble and disassemble, supporting reuse and recycling (IKEA, 2025).

9.2. Innovation in Customer Experience

IKEA also innovates in the way customers interact with the brand. Its omnichannel model integrates physical stores with digital tools that support planning and purchasing. In 2024 IKEA recorded approximately 899 million store visits and digital sales represented 26% of total revenue. These developments show how innovation enhances accessibility and strengthens customer engagement (IKEA, 2025).

10. CONCLUSION

Innovation is a fundamental driver of entrepreneurship and a key factor in strengthening competitiveness and sustainable economic growth. It enhances productivity, supports technological progress and enables the creation of new value through improved products, processes and organisational practices. Research, including the 2025 Nobel Prize in Economic Sciences, confirms that innovation is a continuous process connecting knowledge, technology and enterprise, forming the foundation of long-term development.

For manufacturing sectors such as woodworking and furniture production, innovation is increasingly linked to digitalisation, material efficiency and sustainable use of renewable resources. The adoption of Industry 4.0 technologies, circular production models and improved management practices enables enterprises to raise productivity and respond to changing market and environmental expectations. These developments are particularly important for the Balkans, where many small and medium-sized enterprises face financial and technological constraints that limit their innovation capacity.

Sustained investment in research and development, education and collaboration between public institutions, research organisations and industry remain essential for strengthening innovation in the region. Such an environment allows businesses to adapt to technological change, develop new competencies and contribute to broader economic resilience and growth. Innovation should be seen as a deliberate and ongoing process that supports modern entrepreneurship. By encouraging creativity, exchanging knowledge and remaining open to technological advancement, enterprises can strengthen their competitive position and support sustainable development in an increasingly dynamic global market.

11. REFERENCES

Chesbrough, H., 2003: The Open Innovation Paradigm in Open Innovation: The New Imperative for Creating and Profiting from Technology, Harvard Business School Press, Boston, Massachusetts.

Christensen, C. M., 2016: The Innovator's Dilemma: When New Technologies Cause Great Firms to Fail, Harvard Business School Press, Boston, Massachusetts.

Červený, L.; Kunz, M.; Kučera, P., 2022: The potential of smart factories and innovative Industry 4.0 technologies in the furniture industry. Forests, 13 (12): 2171.

Filiposki, A.; Kostovska Bogoeska, G., 2024: Guide to Innovation for Small and Medium-sized Enterprises, Strengthening the capacities of small and medium-sized enterprises through improved support for innovation, MIR Foundation, Skopje.

Pirc Barčić, A.; Motik, D.; Oblak, L.; Vlosky, R., 2016: Management activity linkages to innovation deconstruction: An exploratory study of the furniture industry in Croatia. BioResources, 11 (2): 3987-4005.

Rogers, E. M., 1983: Diffusion of Innovations. Third Edition. The Free Press, A Division of Macmillan Publishing Co., Inc., New York.

Schumpeter, J., 1942: Capitalism, Socialism and Democracy. Harper & Brothers, New York.

***European Investment Bank, 2025: Investment Report 2024/2025: Innovation, integration and simplification in Europe. https://www.eib.org/en/publications/20240354-investment-report-2024

***European Commission, 2017: Circular Economy in the Furniture Industry: Overview of Current Challenges and Competence Needs. https://circulareconomy.europa.eu/platform/sites/default/files/circular-economy-in-the-furniture-industry.pdf

***European Investment Bank, EIB, 2025: Innovation, digital and human capital. https://www.eib.org/en/projects/topics/innovation-digital-and-human-capital/index

***EUROSTAT, 2025: R&D expenditure. https://ec.europa.eu/eurostat/statistics-explained/index.php?title=R%26D_expenditure

***FAO, 2022: Forest products in the global bioeconomy: Enabling substitution by wood-based products and contributing to the Sustainable Development Goals, Food and Agriculture Organization of the United Nations, Rome.

***IBM, 2023: Open the Door to Open Innovation. https://www.ibm.com/thought-leadership/institute-business-value/en-us/report/open-innovation

***Inter IKEA Group (2025): Financial Summary FY24. https://www.inter.ikea.com/-/media/interikea/igi/financial-reports/fy24-financial-

reports/inter_ikea_group_financial_summary_fy24.pdf?rev=76f8481fd2e14a63a8359eeda8eefdbd&sc_lang=en

***Inter IKEA Group (2025): How we design and innovate with wood. https://www.ikea.com/global/en/our-business/sustainability/wood-design-and-innovation/

***Mckinsey & Company, 2023: Innovative Growers: A View from the Top. https://www.mckinsey.com/capabilities/strategy-and-corporate-finance/our-insights/innovative-growers-a-view-from-the-top

***Mckinsey & Company, 2023: Strategic Growth & Innovation. https://www.mckinsey.com/capabilities/strategy-and-corporate-finance/how-we-help-clients/strategic-growth-and-innovation

***OECD, 2024: Digital Economy Outlook 2024, Volume 1, Embracing the Technology Frontier. https://www.oecd.org/en/publications/oecd-digital-economy-outlook-2024-volume-1_a1689dc5-en/full-report.html

***The Royal Swedish Academy of Sciences, 2025: Scientific Background to the Sveriges Riksbank Prize in Economic Sciences in Memory of Alfred Nobel 2025, The Committee for the Prize in Economic Sciences in Memory of Alfred Nobel. https://www.nobelprize.org/uploads/2025/10/advanced-economicsciencesprize2025.pdf

***The Royal Swedish Academy of Sciences, 2025: Press release. https://www.nobelprize.org/prizes/economic-sciences/2025/press-release/

***WIPO, World Intellectual Property Organization (2025): Global Innovation Index: Innovation at a Crossroads. https://www.wipo.int/web-publications/global-innovation-index-2025/assets/80937/global-innovation-index-2025-en.pdf

Mechanical Properties and Free-Formaldehyde Content of Particleboards Made with the Addition of Dyed Wood Chips

Španić, Nikola*; Brglez, Lucija; Stanešić, Juraj

[1] Department of Wood Technology, Faculty of Forestry and Wood Technology, University of Zagreb, Zagreb, Croatia
*Corresponding author: nspanic@sumfak.unizg.hr

ABSTRACT

Modern trends in interior design are constantly looking for new possibilities of particleboards use, not only as furniture parts but also as continuously visible wall, ceiling and floor coverings. Alongside appropriate aesthetic properties, to be used in aforementioned areas, particleboards must have acceptable physical, mechanical and chemical properties, that is they must be safe to handle, process and in use. One of the possibilities for obtaining appealing aesthetic properties of such materials is wood staining or dyeing prior to their production. Exactly that approach was used in this research where wood chips were dyed prior to single-layer particleboard production and testing. The results of determination of physical and mechanical properties showed that particleboards made with the addition of dyed wood chips had similar properties to those produced from un-treated wood chips. However, it was concluded that the increase in the dyed wood chip contents did not positively affect the examined properties. This is especially noticeable at free formaldehyde contents, where higher loads results with much higher values, above those prescribed by appropriate EN standards.

Key words: particleboards, wood chip dyeing, mechanical properties, free formaldehyde content

1. INTRODUCTION

Although solid wood staining using natural pigments and dyes is known for centuries, the possibility of wood chip dyeing prior to particleboard production is almost un-researched. This does not include dyeing with natural pigments only, but also the possibility to dye wood using artificial colourants as well. There is actually only one available text on the possibility of wood chip dyeing before panel production, and that is in a patent by Thornber and Wrangham (1976) who examined the possibility of using different colours and board surface post treatment to achieve better aesthetical properties. However, in their patent application there is no data on type of dye used and authors focus mostly on board post treatments (surface sanding in order to obtain the marble effect) and resin selection which must be compatible with dyes and must be light and gasses resistant. At almost the same time in history, Kelly, Kutscha and Shuler (1975) conducted their research in which they used different types of fluorescent and non-fluorescent dyes added directly in resin prior to wood chip gluing, in order to obtain specific aesthetical properties of boards. In their research Aniline blue, Coriphosphine O and Rhodamine B dyes were used, and surface properties of boards were determined, to see whether such products could be used in industrial OSB panel production. Their results were very good, especially those obtained for Rhodamine B dye using which also the naturally darker wood species like oak and walnut could be dyed. Their work was fundamental for today's particleboard production, where exactly Rhodamine based red and green dyes are added to resin

when Type P3 (moisture resistant; green dye) or flame resistant (red dye) particleboards are being manufactured.

As there is clearly lack of data on the possibility of wood chips dyeing prior to particleboard production, as well as on the influence that dyed chips have on particleboards properties, in this research boards containing both natural and dyed particles were produced and examined. Due to the fact that the majority of wood is comprised of cellulose, as appropriate dyes ones originally intended to be used for cotton fabric dyeing were used.

2. MATERIALS AND METHODS

2.1. Materials

2.1.1. Wood chips

In this experiment a mixture of industrially prepared wood chips (particles) for inner- layers of particleboards was used. The mixture comprised of virgin softwood (e.g. alder, poplar, willow, birch and linden) and hardwood species (e.g. hornbeam, beech and oak (up to 3 %)), and was provided by Kronospan CRO Ltd.

2.1.2. Chemical components

Urea-formaldehyde (UF) resin with a dry matter content of 66 % was used in all parts of the experiment. As catalyst, 20 % aqueous solution of ammonium sulphate and as hydrophobic agent 55 % paraffin emulsion were used. UF resin and paraffin emulsion were both kindly provided by Kronospan CRO Ltd.

As a dye for wood chip staining, commercial Simplicol® textile dyes were used. Four colours were selected (red, blue, green and purple) and dyes were used without any modifications.

2.2. Methods

2.2.1. Raw materials preparation and dyeing

In order to remove the fine particles, after sampling the wood chips were sieved on a CISA RP.08 laboratory sieve shaker, keeping only the particles of size < 0.71 mm for further investigations.

Prepared wood chips were then dyed according to dye manufacturers instructions. Briefly, to a 10 L of tap water heated in a pot to 35 °C, 400 g of fixative (sodium metasilicate buffer) was added and dissolved. It took roughly 5 minutes to dissolute the fixative, after which the 200 mL of liquid colour was added to the pot, alongside 800 g of prepared wood chips (per colour). The contents in the pot were then mixed thoroughly and left undisturbed for 90 minutes, after which the liquid colour was removed and chips were washed with tap water. Dyed chips were then spread on mats and left to air dry for 3 days. The moisture content of air-dried chips ranged between 13 and 18 %, and so the wood chips were additionally dried in a Memmert laboratory drying oven UF 110 plus, to lower their moisture content down to 5-6 % prior to

particleboard manufacturing. The same process was conducted for each of the selected colours. In Figure 1, the photograph of dyed and dried chips is shown, depicting the clear vividness of dyed chips after drying.

Figure 1. Dyed and dried wood chips

2.2.2. Particleboard preparation

Single layer, Type P2, 14 mm thick particleboards were prepared from naturally coloured and dyed wood chips. Three series of boards were made - control one containing the naturally coloured chips only, series made with 5 % addition of dyed chips, and the one made with 10 % addition of dyed wood chips. The dyed chips addition is expressed as a mass percentage of a total mass of chips required for production of a single 450×470 mm sized board. Two boards per series were made, by pressing the glued particles in a hydraulic press for 7 minutes at a temperature of 155 °C and 3.5 MPa of pressure. UF resin addition was 9.5 % based on the solid contents of wood (solid contents/solid contents). Produced panels are shown in Figure 2.

Figure 2. Produced un-trimmed particleboards

(from top to bottom: board containing 10 % dyed wood chips, board containing 5 % dyed wood chips, control board)

2.2.3. Particleboard testing

After production and prior to testing particleboards of all series were conditioned at 20±2 °C and 65±5 % relative air humidity. Then physical and mechanical properties were determined alongside the free formaldehyde contents. This was done in accordance with the following EN and ISO standards:

- EN 322:1993 Wood based panels – Determination of moisture content
- EN 323:1993 Wood based panels – Determination of density
- EN 317:1993 Particleboards and fibreboards – Determination of swelling in thickness after immersion in water
- EN 310:1993 Wood-based panels – Determination of modulus of elasticity in bending and of bending strength
- EN 319:1993 Particleboards and fibreboards – Determination of tensile strength perpendicular to the plane of the board
- ISO 12460-5:2015 Wood-based panels – Determination of formaldehyde release - Part 5: Extraction method (called the perforator method)

3. RESULTS

3.1. Determination of particleboards physical and mechanical properties

The results of the particleboard testing are given in Table 1, where board series are marked as: 0 (control boards), 5 (boards containing 5 % dyed wood chips); 10 (boards containing 10 % dyed wood chips). Abbreviations IB, MOR and MOE stand for internal bond, modulus of rupture and modulus of elasticity, respectively.

Table 1. Physical and mechanical properties of produced particleboards

Property	Board series	N	Mean±STD	Median	Min	Max
Moisture content, %	0	10	5.35±0.46	5.31	4.81	6.31
	5	10	6.96±1.52	6.64	5.47	6.64
	10	10	5.44±0.39	5.42	4.87	5.42
Density, g/cm^3	0	10	0.73±0.07	0.74	0.58	0.81
	5	10	0.72±0.07	0.74	0.60	0.80
	10	10	0.75±0.08	0.74	0.64	0.88
Thickness swelling, %	0	10	21.89±4.08	21.12	17.14	29.17
	5	10	21.75±1.40	21.87	19.28	24.86
	10	10	28.69±2.59	21.75	24.23	33.73
MOR, N/mm^2	0	10	18.35±1.93	18.03	15.55	21.88
	5	10	18.61±1.97	17.93	16.16	21.73
	10	10	16.90±1.93	17.00	13.71	20.13
MOE, N/mm^2	0	10	3150.5±204.87	3108.0	2839.7	3461.1
	5	10	3243.2±495.45	3204.5	2542.1	4237.4
	10	10	3252.1±367.84	3198.5	2706.2	3872.3
IB, N/mm^2	0	10	0.58±0.10	0.60	0.41	0.72

	5	10	0.53±0.18	0.56	0.16	0.74
	10	10	0.58±0.05	0.57	0.54	0.68

The EN 312:2010 standard defines values of 11 N/mm^2,1600 N/mm^2 and 0.35 N/mm^2, as minimum requirements for MOR, MOE and IB respectively for Type P2 particleboards (boards for interior fitments, including furniture; for use in dry conditions). The same standard permits the value of ≤ 8 mg/100 g oven dry board, for the free formaldehyde content (CH_2O). As can be seen from results in Table 2, all of produced boards fulfil those requirements, but what can also be seen is that the addition of dyed wood chips have only slight influence on mechanical properties. In most cases the 5 % addition resulted with an increase of examined mechanical properties. At 10 % addition severe drop of MOR value is noticed, which, alongside the fact that the thickness swelling of this board series is rather high compared with other examined series, can be an indication that stained chips might have acted as sort of a buffer, whose presence led to incomplete resin polymerization and crosslinking. However, as IB values for board series with 10 % dyed chips addition are the same as the ones for control series, latter mentioned claim should be further investigated. The maximum values of thickness swelling of Type P2 particleboards is not prescribed by EN 312:2010 standard, but all produced board series have higher values of thickness swelling than those prescribed for Type P3 particleboards (14 %; non-load bearing boards for use in dry and humid conditions). As for the moisture content and density, all board series fit well into values given in aforementioned standard.

One fact that was observed during particleboard testing was that the colour of the dyed chips did not fade due to high temperature used at board pressing nor it was lost after 24 h soak in the water (determination of swelling in thickness), as can be seen on Figures 3 and 4. The fact that the colour of the dyed wood chips did not fade can be considered as a confirmation of the hypothesis set before the experiment, regarding the selection of the dye used for staining. More precisely, the results reveal that the colorants used for industrial dying of cotton-based fabrics are also suitable for wood chips dyeing and that the colour is heat and water persistent.

Figure 3. Particleboard samples after 24 h soak in distilled water

(from left to right: board containing 10 % dyed wood chips, board containing 5 % dyed wood chips, control board)

Figure 4. Particleboard samples after internal bond test

(from left to right: board containing 10 % dyed wood chips, board containing 5 % dyed wood chips, control board)

3.2. Free formaldehyde determination

In Table 2 the results of free formaldehyde contents are given, from which it can be seen that the increase in the dyed chip addition to raw mat furnish led to an increase in the formaldehyde contents. This is most probably due to the fact that the use of hot toluene for formaldehyde extraction, extracted also other aldehyde compounds originating most probably from the dyes used. As spectrometric analysis of obtained extracts is somewhat insensitive of other aldehydes presence, they were then shown as an increase in the free formaldehyde contents. Nonetheless, the results reveal that the use of dyed wood chips results with the increase in the free formaldehyde contents, which fits well with the results of the mechanical properties and their tendencies. In terms of comparison of obtained values with those given in standards, only control boards and those produced with 5 % dyed wood chips addition meet the requirements of the EN 312:2010 standard.

Table 2. Results of free formaldehyde determination

Property	Board series		
	0	5	10
Free formaldehyde content, mg/100 g	4.96	6.15	13.41

4. CONCLUSIONS

The following conclusions can be made, based on the obtained results:

- Colorants (dyes) intended for textile industry can successfully be used for wood chip dyeing.
- The addition of dyed wood chips to particleboard raw furnishes, in most cases resulted with an increase of mechanical properties of thus produced particleboards.
- The rise in the addition of dyed wood chips to particleboard raw furnishes, results with a significant increase of the free formaldehyde contents.
- Additional researches are needed in order to determine the influence of colour fixative containing sodium metasilicate which most probably influences the surface pH value of stained wood chips, thus governing the formation of cohesive-adhesive

bonds in produced particleboards, reflecting also on their physical and mechanical properties.

5. REFERENCES

Kelly R. A.; Kutscha N. P.; Shuler C. E., 1975: Eastern spruce flakeboard resin distribution and decorative panel evaluation. Technical Bulettin 74. University of Maine at Orono.

Thornber, W.; Wrangham, B., 1976: *Method of making colored particleboard*. United States Patent.

***EN 312, 2010: Particleboards – Specifications.

***EN 322, 1993: Wood based panels – Determination of moisture content.

***EN 323, 1993: Wood based panels – Determination of density.

***EN 317, 1993: Particleboards and fibreboards – Determination of swelling in thickness after immersion in water.

***EN 310, 1993: Wood-based panels – Determination of modulus of elasticity in bending and of bending strength.

***EN 319, 1993: Particleboards and fibreboards – Determination of tensile strength perpendicular to the plane of the board.

***ISO 12460-5, 2015: Wood-based panels – Determination of formaldehyde release - Part 5: Extraction method (called the perforator method).

Curing Kinetics of Urea-Formaldehyde Resin in the Presence of Wood and Non-Wooden Raw Materials for Particleboard Production

Španić, Nikola*; Simon, Marta; Klarić, Miljenko; Lozančić, Nikolina[1]

[1] Department of Wood Technology, Faculty of Forestry and Wood Technology, University of Zagreb, Zagreb, Croatia
*Corresponding author: nspanic@sumfak.unizg.hr

ABSTRACT

The industrial production of particleboard is increasingly looking for alternative solutions for the basic raw materials needed for boards production. The use of recycled wooden materials is already widespread, with particleboard manufacturers looking for additional non-wooden raw materials that can be used in production. However, the introduction of such materials in furnishes must be carefully planned as non-wooden lignocellulosic materials have different chemical composition and react differently with adhesives, which leads to potential problems in particleboards production. At the physicochemical level, this primarily refers to changes in curing kinetics of commonly used urea-formaldehyde (UF) resin, and thus associated changes in particleboard pressing times. In order to determine the effect that alternative raw materials have on curing kinetics of UF resin, in this research the rice husks and corn cob kernels were used alongside wood. Several mixtures of mentioned raw materials were prepared and mixed with UF resin, and their curing kinetics were determined by means of differential scanning calorimetry (DSC), following with the infrared analysis (FTIR) of cured resins. The results reveal that the introduction of non-wooden particles caused severe changes of the reaction enthalpy of the UF resin curing leading to changes in activation energy also.

Key words: curing kinetics, non-wooden raw materials, particleboard, urea-formaldehyde resin

1. INTRODUCTION

The industrial production of particleboard has occupied a significant place within the wood industry for decades, but recently it has faced numerous challenges arising from the limited availability of wood raw materials, the increase in energy prices and the increasing demands for environmental sustainability. In line with global trends of circular economy and waste reduction, panel manufacturers are increasingly turning to alternative sources of raw materials that could partially or completely replace wood in the production process. The use of recycled wood materials is already present to a significant extent in industry, but the mechanical properties of such panels are often reduced compared to panels made from wood chips, which opens up space for exploring new possibilities and materials. Special attention is paid to non-wood lignocellulosic materials, especially those originating from agricultural production, such as rice husks and corn cob kernels, which were used in this study. These materials represent readily available and currently underutilized agricultural residues that, with proper preparation and processing, can contribute to reducing dependence on wood raw materials and increasing the energy efficiency of production.

The properties of UF resin used as a binder in common particleboard production, as well as their interactions with wood are well researched. However, there is a lack of literature data

on interaction of UF resin with non-wooden lignocellulosic materials, other to those whose topic relates to physical and mechanical properties of produced panels. For instance, Scatolino *et al*. (2013) found that the addition of corn cob kernels to pine chips reduces the board density, but also leads to higher water absorption and lower thickness swelling as the corn cob kernel share in the raw material mixture rises. Similar results were obtained by Atoyebi *et al*. (2019), who mixed corn cob kernels with sugarcane leftovers to produce boards with low thickness swelling. Jabile *et al*. (2023) made a research on boards made from the mixture of wood and rice husks and concluded that the water absorption decreases with increasing the share of husks in the raw material mixture, which can be attributed to the presence of silicon that acts as a barrier to water penetration. On the other hand, da Silva César *et al*. (2017) concluded that increasing the share of adhesive can improve the mechanical properties of boards, but that an excessive share of rice husks negatively affects the adhesion between the husk particles and the adhesive, resulting in a decrease in physical properties.

The conclusions of the above studies indicate the need for further study of the interaction between non-wood lignocellulosic materials and UF resin, especially in the context of changes in curing kinetics, activation energy and reaction enthalpy. In this study, the influence of rice husks and corn cob kernels on the curing process of UF resin is investigated using differential scanning calorimetry (DSC) and Fourier transform infrared spectroscopy (FT-IR). The results will provide a deeper understanding of the physicochemical processes that occur when using alternative raw materials and serve as a basis for assessing their sustainability and potential for commercial application in the particleboard industry.

2. MATERIALS AND METHODS

2.1. Materials

2.1.1. Wood and non-wooden raw materials

In this experiment industrial mixture of wood chips, comprised of virgin softwood (e.g. alder, poplar, willow, birch and linden) and hardwood species (e.g. hornbeam, beech and oak (up to 3 %)) and recycled wooden materials (e.g. used particleboards, waste wood materials, etc.) was used. Alongside wood, two types of non-wooden lignocellulosic materials were used - milled corn cob kernels and rice husks. Milled corn cob kernels and rice husks had densities of 0.15 to 0.25 g/cm^3, and 0.1 to 0.2 g/cm^3, respectively. Both wood and non-wooden raw materials were provided by Kronospan CRO Ltd.

2.1.2. Chemical components

Urea-formaldehyde (UF) resin with a dry matter content of 66 % was used in all parts of the experiment. As catalyst, industrially prepared 30 % aqueous solution of urea-ammonium nitrate and as hydrophobic agent 46 % paraffin emulsion were used. All of the aforementioned components were kindly provided by Kronospan CRO Ltd.

2.2. Methods

2.2.1. Raw materials preparation

After sampling the wood and non-wooden raw materials were transferred to laboratory and were left for 20 days on open trays at room conditions (20±2 °C; 65±5 % relative air humidity) to reach equilibrium, after which they were milled using a Retsch ZM 200 ultra-centrifugal mill, equipped with 1 mm trapezoidal opening sieve. Prior to use milled raw materials were additionally hand sieved, keeping only the particles of size < 0.4 mm for further investigations.

2.2.2. Preparation of the adhesive and samples mixtures

In order to investigate the influence that wood and non-wooden raw materials have on curing kinetics of UF resin based adhesive mixtures, adhesives were prepared by mixing the UF resin with paraffin emulsion (0.4 % addition) and catalyst (1 % addition). The additions were made based on solid contents of resin (solid content/solid content). To prepared adhesive, milled wood and non-wooden particles were added (6.5 % based on the mass of prepared adhesive). In cases were two types of raw materials were mixed with adhesive, their addition was 1:1 (i.e. 3.25 % of wood + 3.25 % of rice husks). In total, 8 mixtures were prepared and labelled as given in Table 1.

Table 1. Test samples description

Sample	Description
A	UF resin + catalyst
B	UF resin + catalyst + paraffin emulsion
C	UF resin + catalyst + paraffin emulsion + wood
D	UF resin + catalyst + paraffin emulsion + corn cob kernels
E	UF resin + catalyst + paraffin emulsion + rice husks
F	UF resin + catalyst + paraffin emulsion + wood + corn cob kernels
G	UF resin + catalyst + paraffin emulsion + wood + rice husks

2.2.3. Differential Scanning Calorimetry (DSC)

The thermal properties of test samples were determined by differential scanning calorimetry (DSC), carried out on a Perkin Elmer DSC 6000 analyser equipped with an Intracooler SP cooling device. The analysis of samples (~ 5 mg) was done in a nitrogen (N_2) atmosphere with a flow rate of 20 mL/min. Samples were heated and cooled from 40 °C to 200 °C at a rate of 5, 10, 15 and 20 °C/min, with an isothermal step at 200 °C for 1 min. Two measurements per sample were made, and subsequent analysis of obtained data was done using Pyris, Ver. 11 software.

2.2.4. Fourier transform infrared spectroscopy (FT-IR)

Fourier transform infrared (FT-IR) spectra of curred sample mixtures were recorded on a Shimadzu FTIR 8400-S spectrometer by the KBr pellet method, in the range of 4000 - 400 cm^{-1}, with the resolution of 4 cm^{-1}. Prior to analysis, curred resin samples were milled using the IKA A10 analytical mill and sieved using a sieve with 0.2 mm openings. Three measurement were made per sample, with subsequent processing of the obtained results performed using IRSolution Ver.1.30 software.

2.2.5. Determination of activation energy (Ea)

Based on the results obtained by DSC analysis the activation energy (E_a; kJ/mol) was calculated by applying the Kissinger-Akahira-Sunose (KAS) isoconversal method. The KAS model is based on the assumption that the rate of the curing reaction at a given reaction rate depends solely on the curing temperature, but not on the heating temperature. In the KAS model (Equation 1), the degree of conversion functions (f(α) or g(α)) are not required, and if Kissinger's assumptions (Kissinger, 1957) are correct the activation energy could be obtained from the slope ($-E_a \cdot R^{-1}$)

$$\ln\left(\frac{\beta}{T^2}\right) = \ln\left(\frac{R \cdot A}{E_a \cdot g(\alpha)}\right) - \frac{E_a}{R} \cdot \frac{1}{T} \quad (1)$$

β – heating rate (K/min)
T – peak temperature (K)
A – pre-exponential factor
E_a – activation energy (kJ/mol)
R – ideal gas constant (8.314 J/mol·K)
α – extent of cure

3. RESULTS

3.1. Determination of the influence of the heating rate on the curing kinetics of UF resin

The results of the DSC analysis given in Table 2, clearly show that the increase in the heating rate from 5 to 20 °C/min caused an increase in the peak temperature of reaction, in all examined cases, indicating accelerated reaction kinetics. The addition of wood and non-wood components (samples C-G) to the adhesive, caused the peak temperature shift to slightly higher values compared to the reference mixture (sample A), which is an indication of an increased thermal stability of the system. It was also observed that the added filler act as a buffer, affecting the speed of the polymerization and causing a slight decrease of the total enthalpy. That indicates a lower degree of crosslinking of the resin, while higher heating rates contribute greatly to reaching the conversion stage and a more complete curing of the resin.

Table 2. Curing kinetics of UF resin samples

Sample	Peak temperature, Tp, K				Activation energy, Ea, kJ/mol	R^2
	5 K/min	10 K/min	15 K/min	20 K/min		
A	356.9	365.2	371.3	376.3	73.98	0.9943
B	357.4	365.3	371.1	373.9	85.06	0.9969
C	357.2	366.0	371.9	377.7	70.52	0,9926
D	358.3	365.8	370.3	373.8	93.65	0.9998
E	358.4	366.0	372.3	376,8	77.95	0.9918
F	358.0	366.9	372.7	376.9	75.92	0.9995
G	357.4	367.0	372.5	377.8	71.21	0.9979

The results of the activation energy (E_a; kJ/mol) shows that the addition of paraffin emulsion to the resin and catalyst system causes a significant increase in the energy required to initiate the curing reaction. By introducing wood and non-wood components into the system,

the values of activation energy (E_a; kJ/mol) decrease, which means that the curing process becomes more energy-efficient, except for the addition of corn cob kernels with the highest energy value. The lowest values were recorded with the addition of wood. Such results show that the filler addition can contribute to reduction of the energy required for the crosslinking reaction, which potentially could lead to reduced energy consumption in industrial particleboard manufacturing processes.

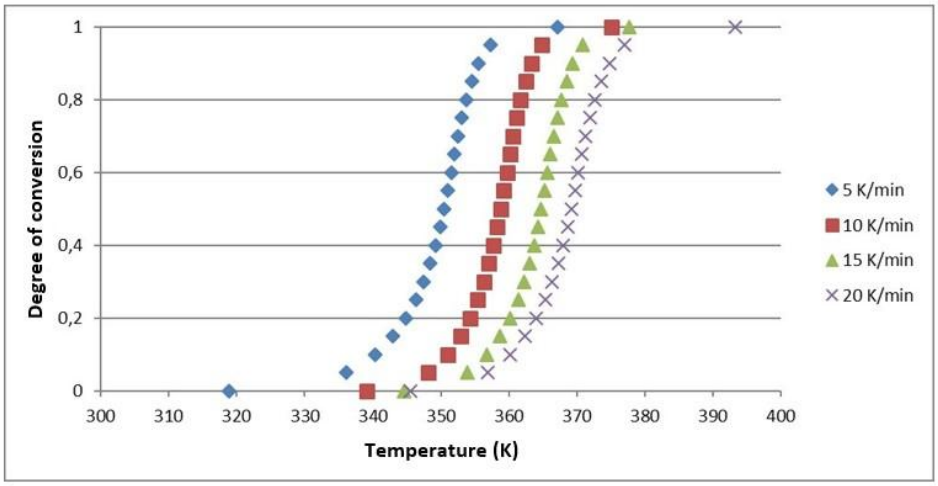

Figure 1. The relationship between the degree of conversion and the heating rate of the UF resin and catalyst mixture

In Figure 1, the heating rate dependent conversion curves are shown for catalyst cured neat UF resin (Sample A), from which can be seen that the heating rate plays a significant role on the exothermic maximum. In this case the lowest values were recorded for the samples heated at the rate of 5 °C/min and highest for the samples heated at the rate of 20 °C/min. The same tendencies were recorded for the Sample B also. However, this change when wood and non-wooden particles are added to the mixture. As can be seen from Figure 2, for a mixture of UF resin, catalyst, paraffin emulsion and wood (Sample C), the lowest values of exothermic maximum are observed for samples heated at the rate of 10 °C/min. Such tendencies are most probably due to the fact that wood's thermal conductivity and diffusivity influenced the rate at which heat is transferred to the adhesive.

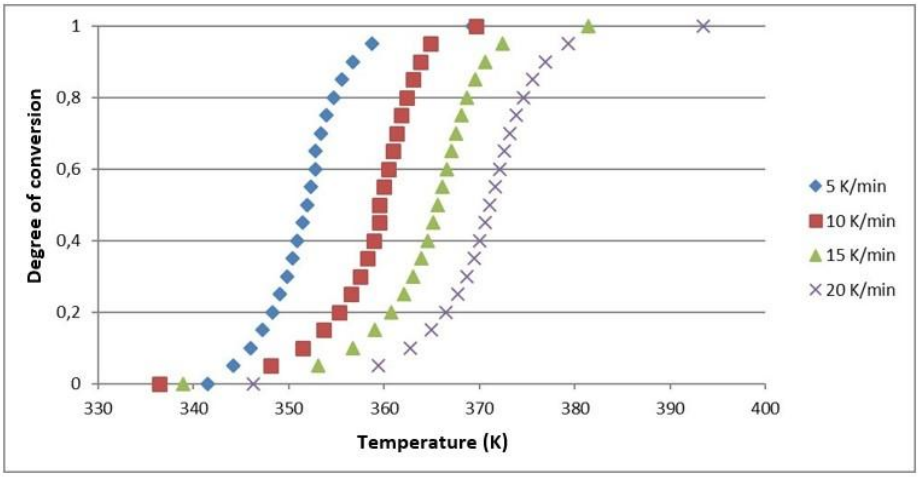

Figure 2. The relationship between the degree of conversion and the heating rate of the mixture of UF resin, catalyst, paraffin emulsion and wood

3.2. Spectrophotometric analysis of cured UF resin samples

In Figures 3 to 5 the FT-IR spectra of all analysed samples are given, sorted into 3 comparable graphical representations. The results of the FT-IR analysis can be interpreted by monitoring the intensities and positions of several characteristic bands. More precisely, those at: ≈ 3346 cm^{-1} (1) associated with the formation and stretching of the NH bonds in primary aliphatic amines of the resin; 2968 cm^{-1} (2) associated with –O–CH_3 in aliphatic amines; 1646 cm^{-1} (3) associated with the stretching of C=O bonds in primary amides (urea); 1547 cm^{-1} (4) associated with C–N stretching in secondary amines; 1384 cm^{-1} (5) associated with C–H mode in methylene and methyl groups; 1240 cm^{-1} (6) associated with stretching of C–N and N–H bonds in tertiary amides; 1138 cm^{-1} (7) associated with C–O stretching of aliphatic ester; 1037 cm^{-1} (8) associated with reductions of C–O–C bonds in formed ether bridges or C–N (NCN) stretching in methylene bonds (NCH_2N); and the ones at 777 cm^{-1} (9) associated with C=O deformation of the NCON skeleton (Myers, 1981; Jada, 1988; Zhang *et al*., 2013; Osemeahon and Barminas, 2007; Šmidriaková and Lourová, 2011).

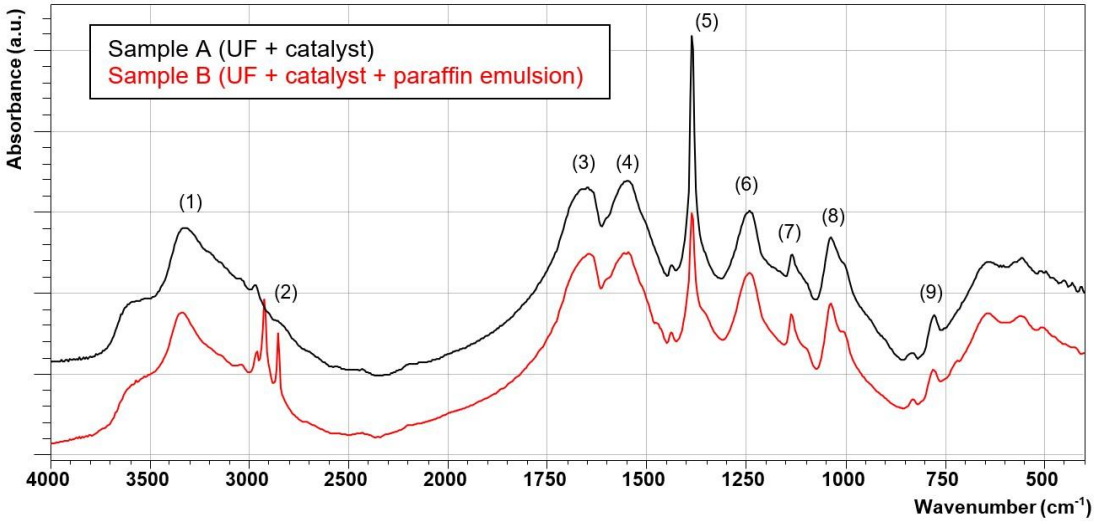

Figure 3. FT-IR spectra of UF resin cured with the addition of catalyst and paraffin emulsion

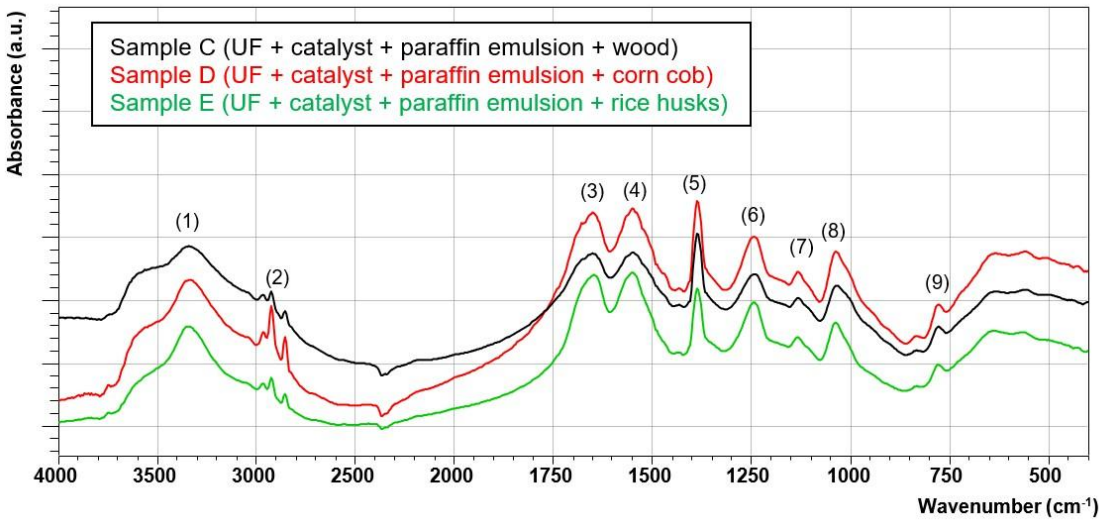

Figure 4. FT-IR spectra of UF resin cured with the addition of catalyst, paraffin emulsion, wood and non-wooden components

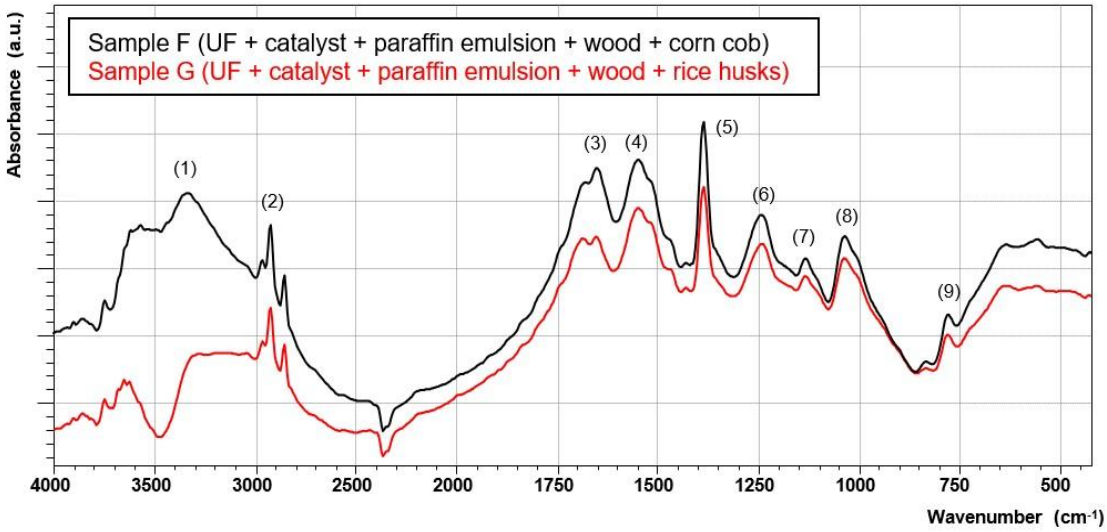

Figure 5. FT-IR spectra of UF resin cured with the addition of catalyst, paraffin emulsion and a mixture of wood and non-wooden components

The results of the FT-IR analysis showed that the addition of paraffin emulsion and natural fillers does not cause significant chemical changes in the structure of the UF resin. There are some minor differences in specific band intensities, but this can be attributed to small differences in samples size (cured adhesive shares in KBr). The only mayor difference is noticed in the FT-IR spectra of Sample F (Figure 5), where the absence of a band at ≈ 3346 cm^{-1} indicates that at curing all –OH and –NH groups have reacted and formed new methylene and ether linkages.

4. CONCLUSIONS

The following conclusions can be made, based on the obtained results:

– The heating rate significantly affects the kinetics of UF resin curing.

- Increase in the heating rate results in an increase in the peak reaction temperatures, which indicates an accelerated crosslinking process and a more intensive curing process.
- The addition of wood and non-wooden components reduces the activation energy, which leads to a more energy-efficient process.
- Although the lowest activation energy is with the addition of wood itself, the addition of non-wooden components also leads to a decrease in the activation energy and thus affects the kinetics and energy efficiency of the process, which represents a step towards a more sustainable and environmentally friendly particleboard production.
- Added components, including wood and non-wooden particles, modify the kinetics and thermal properties of the UF resin without disturbing its basic chemical structure, thereby contributing to improving the stability and sustainability of the material.

5. REFERENCES

Atoyebi, O. D.; Osueke, C. O.; Badiru, S.; Gana, A. J.; Ikpotokin, I.; Modupe, A. E.; Tegene, G. A., 2019: Evaluation of particle board from sugarcane bagasse and corn cob. International Journal of Mechanical Engineering and Technology, 10 (1): 1193-1200.

da Silva César, A. A.; Bufalino, L.; Mendes, L. M.; de Almeida Mesquita, R. G.; de Paula Protásio, T.; Mendes, R. F.; Ferreira Andrade, L. M., 2017: Transforming rice husk into a high-added value product: potential for particleboard production. Ciência Florestal, 27 (1): 303-313.

Jabile, L.; Tuyor, M. P.; Salcedo, A.; Balangao, J. K. B.; Namoco Jr., C. S., 2023: Utilization of sawdust and rice husk for particle board application. Journal of Engineering and Applied Sciences, 17 (2): 257-261.

Scatolino, M. V.; Silva, D. W.; Mendes, R. F.; Mendes, L. M., 2013: Use of maize cob for production od particleboard. Ciência e Agrotecnologia, 37 (4): 330-337.

Jada, S. S., 1988: The structure of urea-forladehyde resins. Journal of Applied Polymer Science, 35 (6): 1573-1592.

Kissinger, H. E., 1957: Reaction kinetics in differential thermal analysis. Analytical Chemistry, 29 (11): 1702-1706.

Myers, G. E., 1981: Investigation of urea-formaldehyde polymer cure by infrared. Journal of Applied Polymer Science, 26 (3): 747-763.

Osemeahon, S. A.; Barminas, J. T., 2007: Study of some physical properties of urea formaldehyde and urea proparaldehyde copolymer composite for emulsion paint formulation. International Journal of Physical Sciences, 2 (7): 169-177.

Šmidriaková, M.; Lourová, M., 2011: ATR-FTIR spectral analysis of modified UF adhesive. Annals of Warsaw University of Life Sciences – SGGW. Forestry and Wood Technology, 76: 49-53.

Zhang, J.; Wang, X.; Zhang, S.; Gao, Q.; Li, J., 2013: Effects od melamine addition stage on the performance and curing behavior of melamine-ureaformaldehyde (MUF) resin, Bioresources, 8 (4): 5500-5514.

Ergonomics of Conservation-Restoration Work: Introduction to Research into the Relationship Between Working Postures, Repetitive Tasks and the Use of Workplace Furniture and Health

Štengl, Mihael[1]; Vlaović, Zoran[2]

[1] Department of Art and Restoration, University of Dubrovnik, Dubrovnik, Croatia
[2] Institute of Furniture and Wood in Construction, University of Zagreb, Faculty of Forestry and Wood Technology, Zagreb, Croatia
*Corresponding author: mstengl@unidu.hr

ABSTRACT

This paper presents the results of an introductory part of the study on the relationship between working postures, repetitive tasks, and the use of workplace furniture and their impact on health conducted among conservators-restorers through an online survey. The objective of this study was to investigate the relationship between working postures, repetitive tasks, the use of work furniture, and the occurrence of health problems among conservators-restorers. This research was conducted through a survey of 91 respondents from Croatia and other European countries. The collected data encompassed the participants' field of specialisation, working habits, health status, and the need for and use of workplace furniture, among other factors. This paper focuses only on the analysis of the first part of the survey, which addresses the respondents' basic demographic characteristics, health status, and working habits. The results of the initial part of the survey indicate that conservators-restorers spend a substantial number of hours in awkward and static postures, and frequently engage in repetitive tasks. Such working conditions are closely associated with a high incidence of occupational diseases, including carpal tunnel syndrome and various musculoskeletal disorders. The findings highlight the necessity of improving ergonomic and occupational conditions in conservation-restoration practices, as well as the importance of greater attention to the health and well-being of professionals in this field.

Key words: conservation-restoration, ergonomics, furniture, musculoskeletal disorders

1. INTRODUCTION

Conservators-restorers (CR) play a crucial role in the preservation of cultural heritage through their expertise and professional practice. Such work requires a high level of patience and considerable time commitment and often involves repetitive tasks over extended periods (Omole *et al*., 2023) or work in unfavourable postures (Phillips et al., 2016), which may ultimately lead to long-term health problems. In this context, the present study was designed to investigate the relationship between work habits and the use of workplace furniture and their impact on the health of conservators-restorers (Langford *et al*., 2013).

This research was based on an anonymous online survey entitled "Ergonomics of Conservation-Restoration Work – A Study of the Relationship between the Use of Work Furniture, Work Postures, and Repetitive Actions and Health". The survey participants were conservator-restorers from Croatia and other European countries who engaged in conservation-restoration work on a daily basis across various specialisations.

The survey was distributed to various organisations and associations whose members are primarily involved in conservation-restoration work, including those in Austria, Croatia, Finland, France, Montenegro, Portugal, Slovenia, Spain, and Sweden.

2. MATERIAL AND METHODS

The sample frame was a person who is actively engaged in conservation-restoration work and employed in institutions or companies dedicated to the preservation and protection of cultural and historical heritage in Europe.

Based on the research objectives, a questionnaire was developed and structured to cover several key areas relevant to the work and health of conservators-restorers. The questionnaire consisted of 48 questions divided into 11 sections. It began with questions about participants' demographic characteristics and workplace context, followed by items concerning diagnosed health conditions and general health issues. Subsequent parts explored working postures and repetitive movements as well as various aspects of workplace furniture, including stools, chairs, and tables. Attention was paid to the design and arrangement of stools and chairs to the adjustability and overall suitability of work tables, such as the height and tilt of the work surface. The final section of the questionnaire was optional and included an open-ended question allowing respondents to freely share additional comments or insights.

This study used an online survey based on the procedures recommended by Dillman (2011). An online survey was conducted using Google Forms. This approach was selected because it is the most cost-effective for surveying (Dillman, 2011) and ensures data collection over a wide geographic area and low-cost data conversion (Zahs and Baker, 2007).

A total of 91 respondents participated in the study, of whom 81 % were women and 19 % were men. When grouped by age, 9 % of the participants were between 18 and 30 years, 34 % were between 31 and 40 years, 30 % were between 41 and 50 years, 21 % were between 51 and 60 years, and 6 % were over 60 years. Geographically, 62 % were from Croatia, while 38 % were from other European countries: Slovenia (11 %), Sweden (9 %), Finland (6 %), France (5 %), Austria (3 %), Montenegro (2 %), Portugal (1 %), and Spain (1 %).

The survey was conducted between January and May 2025.

3. RESULTS AND DISCUSSION

The survey was divided into two parts to present and analyse the results. The first part of the survey consisted of questions about the participants' demographic data, presence of musculoskeletal disorders, work habits, and general use of workplace furniture. The results presented here refer to the responses from the first part of the survey.

The second part of the survey, which concerns workplace furniture and its usage, is not the subject of this paper, and its results will be published in a future study by the authors.

Regarding work experience in their current job, more than three-quarters of all respondents had been employed as conservators-restorers for over 10 years, while only 12 had been in these jobs for five years or less (Figure 1).

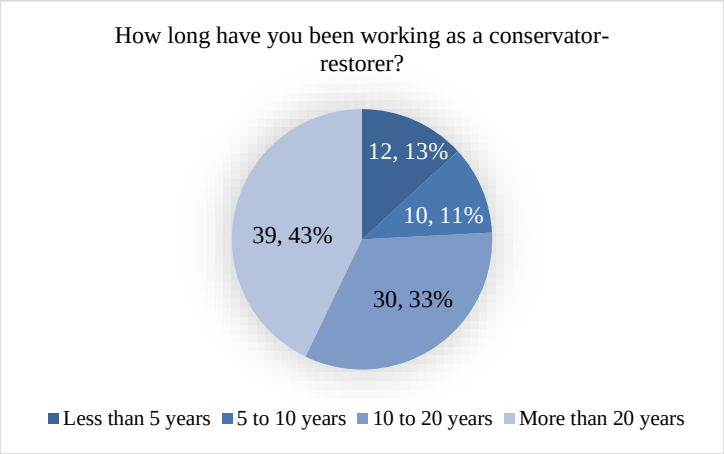

Figure 23. Answers to the question about the respondents' work period

In response to the question about the type of conservation-restoration work they primarily performed, the highest number of participants reported working on "paintings on various supports" (27), followed by "polychrome wooden sculpture" (16) and "library and archival materials, artworks on paper" (13), while other specialisations employed up to nine (9) participants (Figure 2).

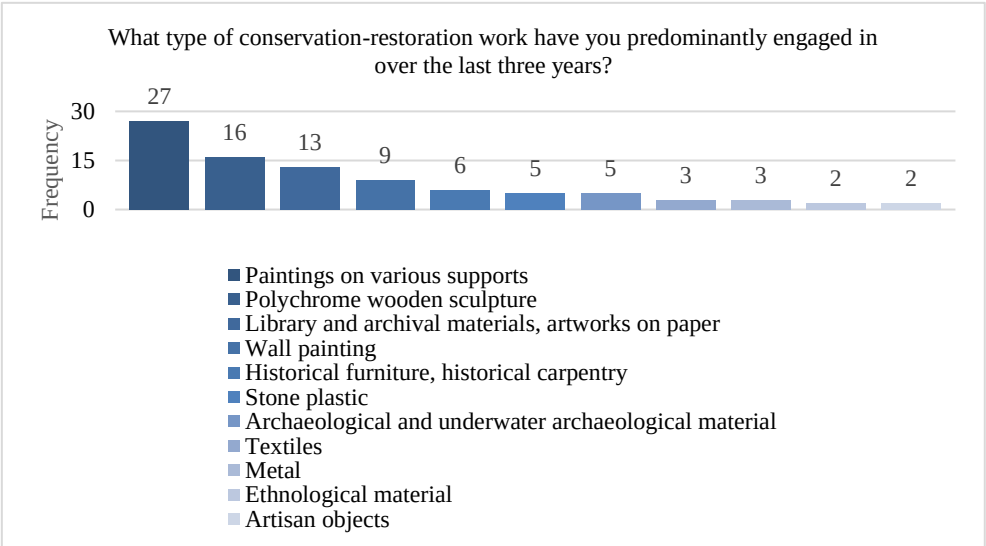

Figure 24. Answers to the question about the respondents' predominantly speciality

To the question "*Do you consider yourself a physically healthy person?*", the respondents answered affirmatively at a very high rate (80 %), while 12 % stated that they did not feel healthy but did not have medical documentation (diagnosis) confirming any issue, and 8 % reported having a confirmed health condition that may be related to the work they perform (Figure 3). It should be noted that multiple responses were provided.

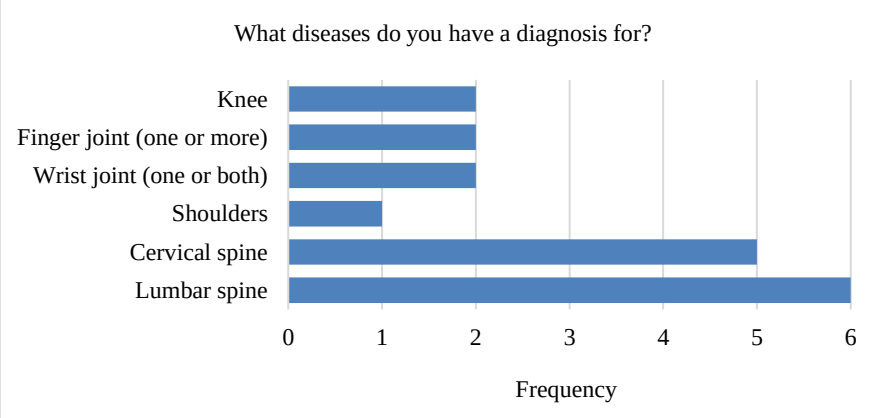

Figure 25. Answers to the question about the respondents' diagnosed diseases

The following results (Figures 4–10) apply only to 18 respondents who indicated that they had a medical diagnosis. Also, note that there were multiple answers allowed.

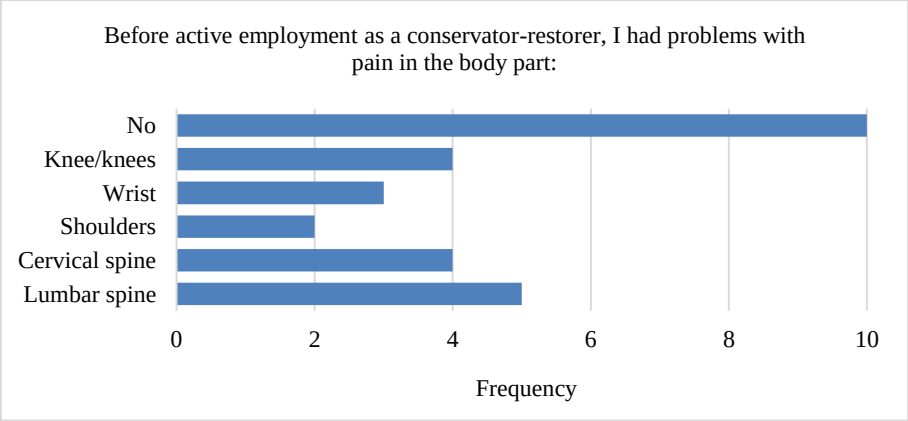

Figure 26. Answers to the question about the presence of pain before employment

In the past year, only six (6) respondents had not received any form of physical therapy for health-related conditions, whereas the others had undergone at least one of the listed types of therapy (Figure 5).

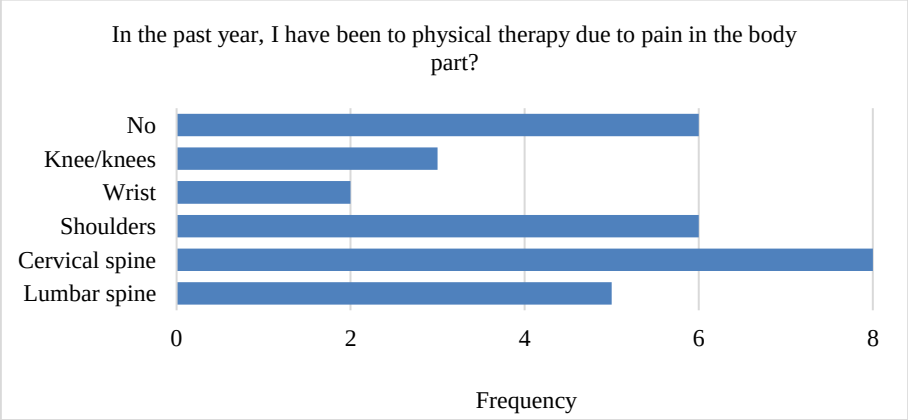

Figure 27. Responds to the question about receiving physical therapy

To the question „Due to existing or potential health problems, I request a medical check-up from my employer at least once every two years“, 13 respondents or 72 % answered negatively, and five (5) of them (28 %) answered positively.

The distribution of responses regarding respondents' belief that employers care about their health is interesting (Figure 6), as more participants believe that their employer does not care than those who believe that they do.

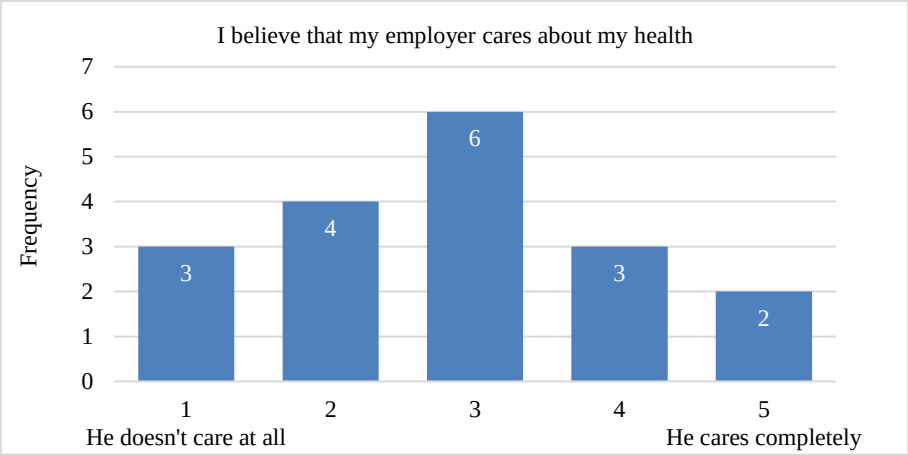

Figure 28. Answers to the question about the employer care for respondents' health

The general perception that the equipment they work with causes health problems or illnesses is illustrated by the results shown in Figure 7. However, it is noticeable that most respondents were not firmly convinced that the equipment was the source of their health issues.

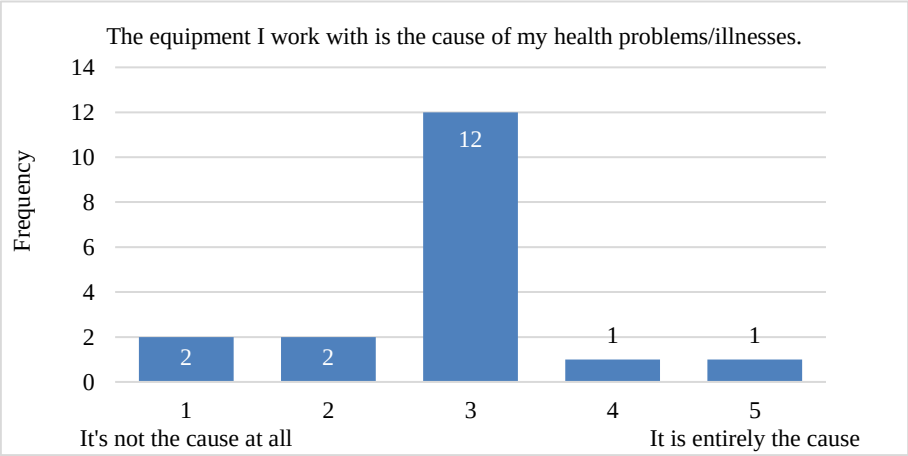

Figure 29. Answers to the question about the equipment use causes health problems

However, when it comes to the equipment that they primarily use and believe may cause health problems, the majority of respondents are convinced that there are tools, aids, and/or furniture that contribute to these issues (Figure 8).

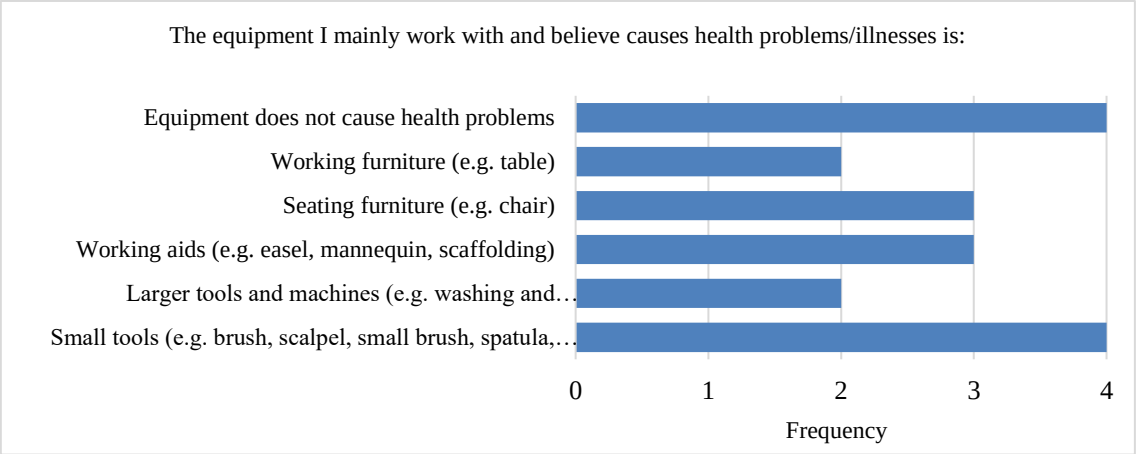

Figure 30. Responds to the question about type of working equipment causes health problems

In response to the question of whether the respondents considered the equipment they worked with to be suitable for the needs of their tasks, an undecided majority was also observed (11 participants), while a smaller group (5) believed that the equipment was appropriate for the work they performed (Figure 9).

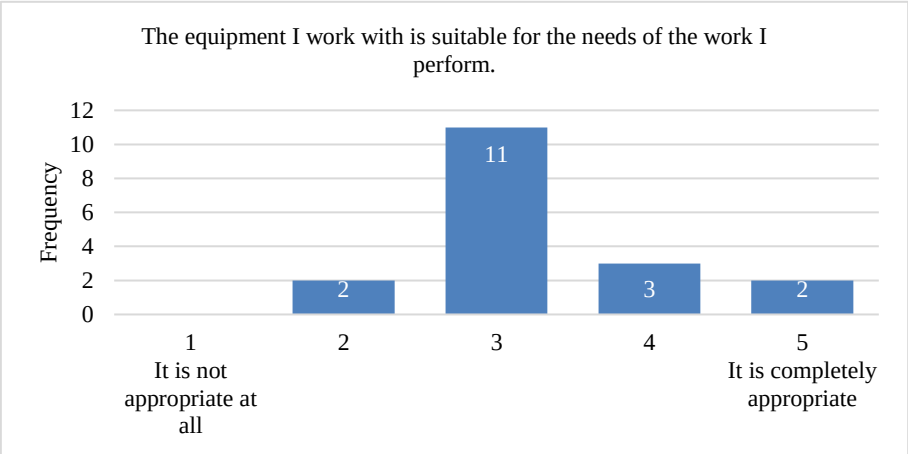

Figure 31. Answers to the question about the suitable equipment use

The following questions were available to all participants (91) and addressed work postures and repetitive actions. Participants responded using a linear scale ranging from 1 to 10. The responses are shown in Figures 10.

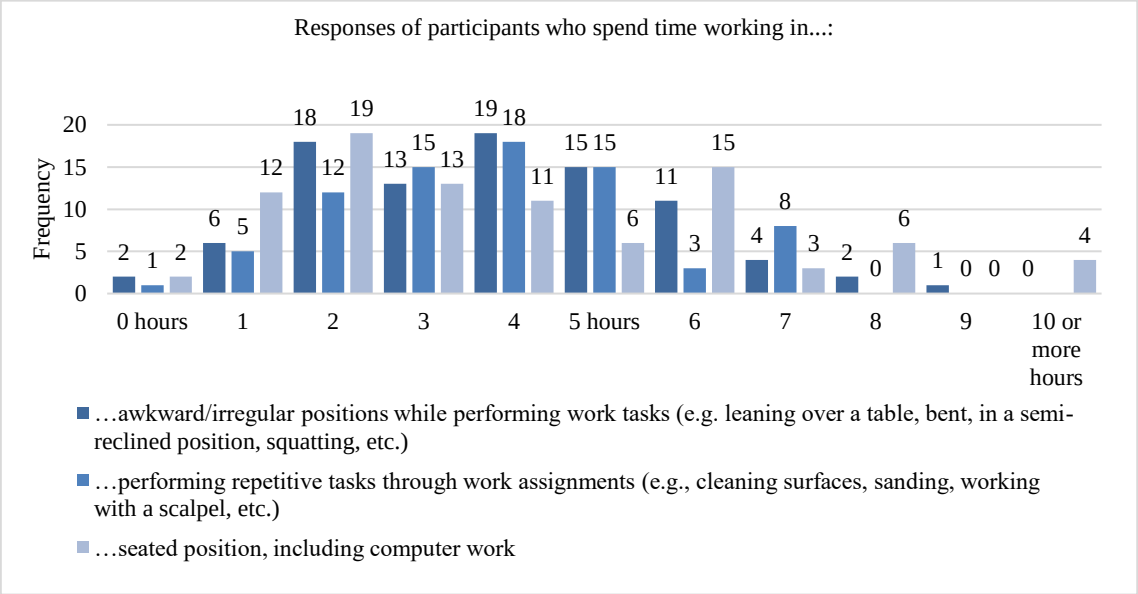

Figure 32. Responses of participants in hours during workday

The following questions were also available to all participants, and they were about their health and habits. Participants responded using a linear scale ranging from 1 to 5 and 0 to 7. The responses are shown in Figures 11 to 13. Figure 11 clearly shows that the majority of respondents take, or mostly take, regular breaks during the workday (50 participants), but a significant number of respondents do not or do not take breaks at all (29).

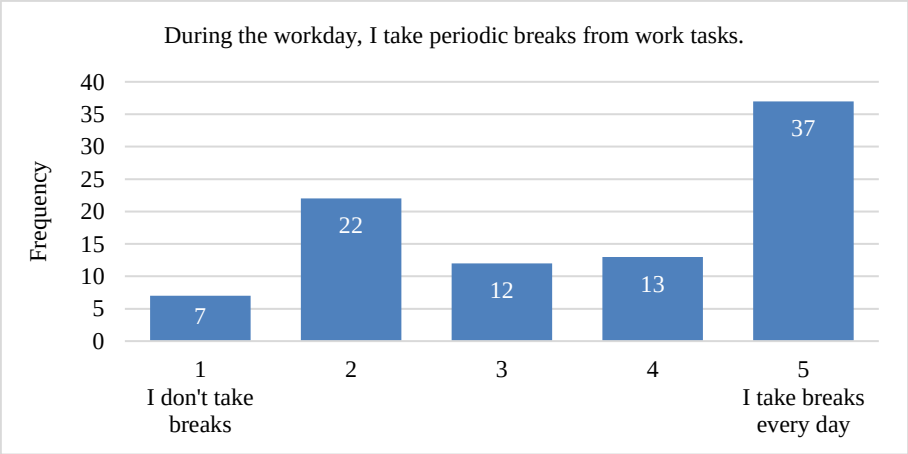

Figure 33. Answers to the question about the periodic breaks

It is also very positive and encouraging that most respondents are physically active four to seven days a week (Figure 12).

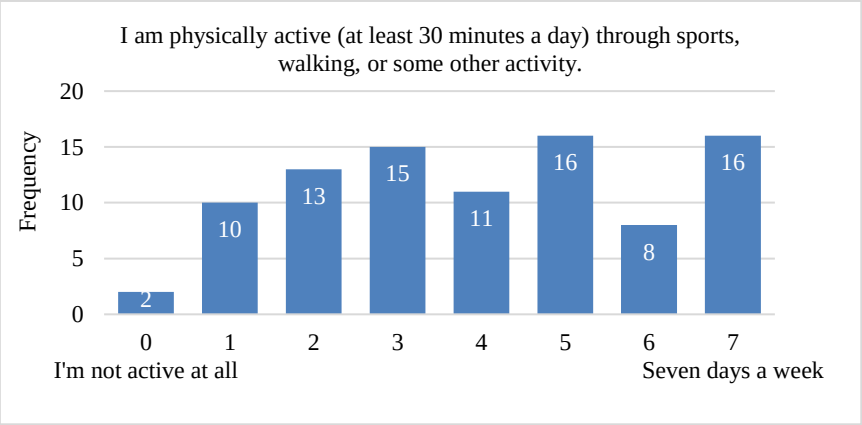

Figure 34. Answers to the question about the physical activity

It is also positive that a large number of respondents did not feel that their health had worsened over the past three years due to the nature of their work (Figure 13).

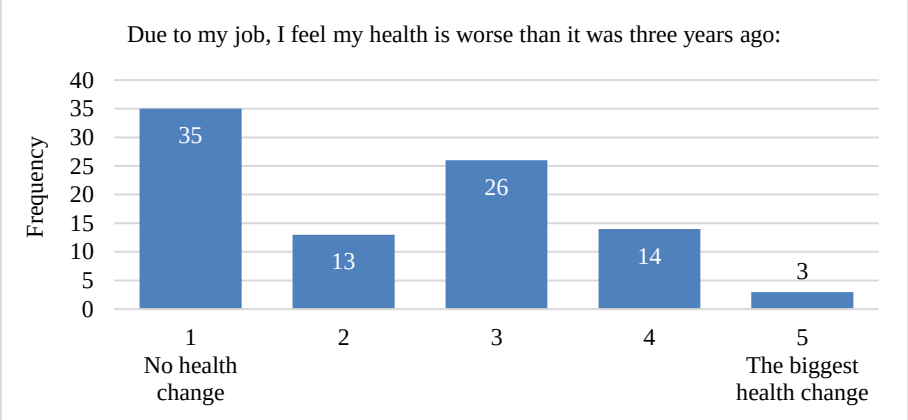

Figure 35. Answers to the question about the health due to the job

For the question about *pain experienced in particular body parts*, respondents could answer using multiple choices. Ninety-one respondents reported a high number of pain experiences, as shown in Figure 14.

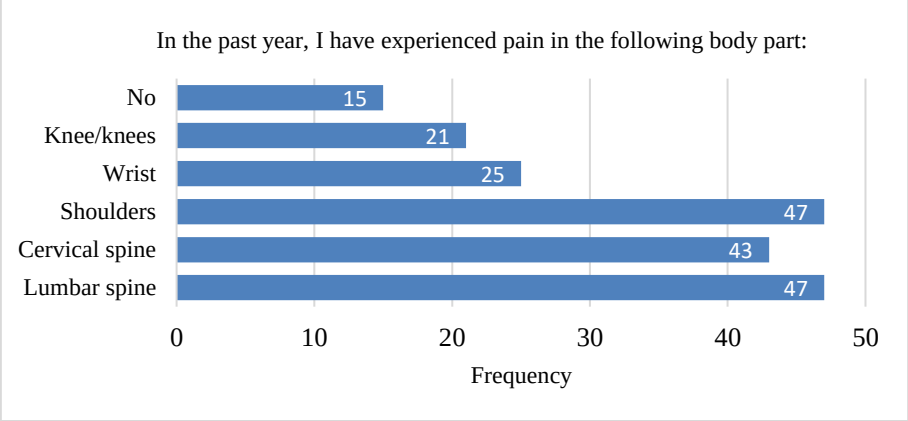

Figure 36. Answers to the question about the experienced pain

To conclude the analysis of the first part of the survey and as an introduction to its second part, respondents were asked whether they used work furniture appropriate to the type of tasks they performed daily (or frequently). Eighty respondents (88 %) answered that they use work furniture either regularly or occasionally (Figure 15).

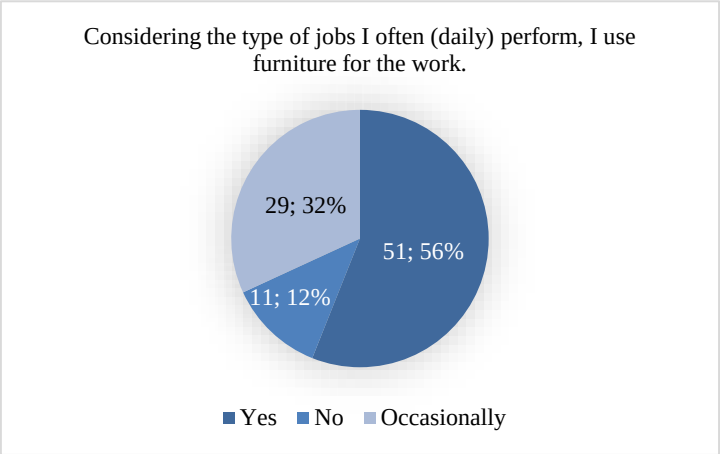

Figure 37. Answers to the question about the use of furniture

Responses to the last two questions in this part of the survey were given on a 5-point linear scale. The questions referred to the respondents' perception of whether the furniture they use is suitable for the work they perform (Figure 16) and to the type of influence (positive or negative) that this furniture has on their work (Figure 17).

From the results in Figure 16, it can be concluded that more than one-third of the respondents were undecided or unable to assess whether work furniture was appropriate for their tasks.

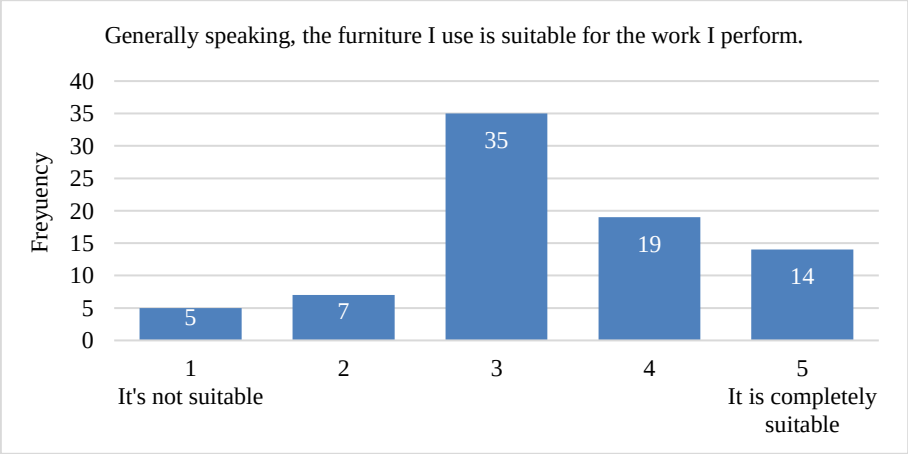

Figure 38. Answers to the question about the suitable work furniture

A similar trend was observed regarding the influence of furniture on their work, where almost one-third were undecided, but nearly 40 % believed that furniture had a positive impact on their work (Figure 17).

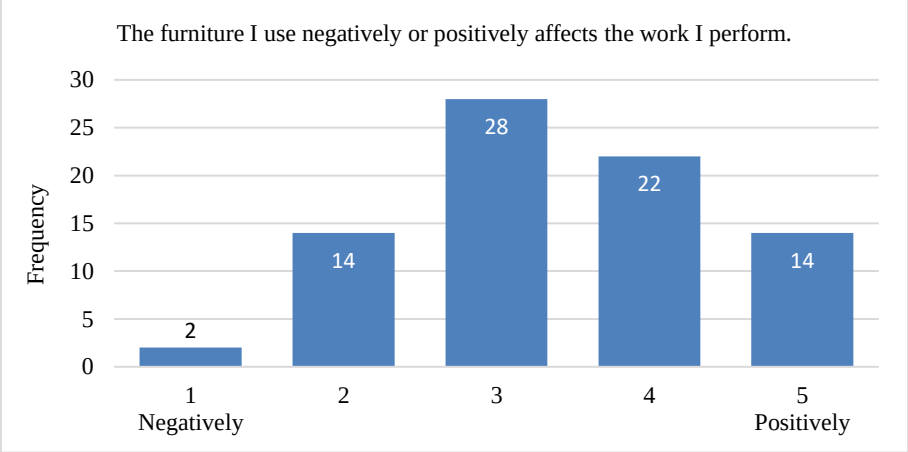

Figure 39. Answers to the question about the furniture affects the work

4. CONCLUSION

The diversity of age groups and the fact that more than 75 % of respondents had over 10 years of professional experience likely contributed to the results of this study. For the portion of respondents who did not feel healthy, the survey results suggest that most problems were related to the spine, as indicated by their responses regarding diagnosed conditions, physical therapy, and the presence of pain prior to employment. It is interesting that 80 % of respondents considered themselves healthy, although when asked about experiencing pain in any part of the body during the past year, as many as 76 respondents reported a total of 183 instances of pain. From the survey results, it can be concluded that more than three-quarters of respondents spend approximately 3 hours and 45 minutes working hours in improper working positions, and two-thirds of respondents spend more than three hours in sitting positions. This may be the reason for the large number of reported pain experiences in the past year. Three-quarters of the respondents performed repetitive tasks for an average of 3 h and 30 min daily. Combined with the fact that they take periodic breaks from work irregularly, this may negatively impact their health. Although most respondents were physically active through sports, walking, or other forms of physical activity, it can be assumed that wrist and shoulder pain results from irregularly taking periodic breaks and the large number of working hours spent performing repetitive tasks, while back pain results from prolonged sitting and working in improper positions. Almost 90 % of respondents used work furniture, and most believed that their work furniture was suitable for the work they performed and positively affected their job performance.

This paper presents the results of the first part of the survey, which addresses the respondents' basic demographic characteristics, health status, and working habits. These results will form a whole with the future results of the second part of the survey, which will aim to identify specific health risks associated with working methods, equipment, and work furniture used in this field.

5. REFERENCES

Dillman, D. A., 2011: Mail and Internet surveys: The tailored design method – 2007 Update with new Internet, visual, and mixed-mode guide. John Wiley & Sons.

Langford, M.; Beaumont, M. S.; Annett, D., 2013: Ergonomics, risk management and injury prevention in textiles conservation. Journal of the Institute of Conservation, 36 (1): 81-101. https://doi.org/10.1080/19455224.2013.774288

Omole, A. E.; Awosika, A.; Khan, A.; Adabanya, U.; Anand, N.; Patel, T.; Edmondson, C. K.; Fakoya, A. O. Millis, R. M., 2023: An Integrated Review of Carpal Tunnel Syndrome: New Insights to an Old Problem. Cureus, 15 (6): e40145. https://doi.org/10.7759/cureus.40145

Phillips, K.; Bills, J.; Gare, J., 2016: Developing modified equipment and work practices to reduce the risk of work-related musculoskeletal disorders from conservation treatment. AICCM Bulletin, 37 (1): 42-48. https://doi.org/10.1080/10344233.2016.1206289

Zahs, D.; Baker, R., 2007: Telephone and mail surveys: Advantages and disadvantages of each. Market Strategies Inc., Livonia, MI, USA.

Evaluation of Noise Emissions from a CNC Woodworking Centre under Different Cutting Conditions

Vitchev, Pavlin*; Halim, Engindzhan[1]

[1] Department "Woodworking machines", Faculty of Forestry, University of Forestry, Sofia, Bulgaria
*Corresponding author: p_vitchev@ltu.bg

ABSTRACT

This study experimentally investigates the variation of noise emission levels (L_{pA}) generated during the machining of Scots pine (*Pinus sylvestris* L.) specimens on a CNC machining center, depending on the cutting conditions. The combined effects of tool rotation speed (n), feed rate (V_f), and depth of cut (h) on noise levels were analysed. The influence of each factor on noise emission was assessed. The experimental methodology considers the background noise and the characteristics of the sound field. Specimens were processed individually using two CNC finishing spiral router cutter with identical angular and linear parameters but different cutting geometries. Graphical dependencies illustrating the correlation between the individual factors and their impact on noise levels during machine operation are presented. The results indicate that noise emission levels are significantly affected by these variables, reaching a maximum of L_{pA} = 82 dB(A) at a tool rotation speed of n = 18000 min^{-1} and a feed rate of V_f = 5 $m.min^{-1}$.

Key words: CNC machining, cutting parameters, noise generation, Scots pine (*Pinus sylvestris* L.), tool rotation speed

1. INTRODUCTION

In recent years, the modern furniture industry has witnessed a great increase in the use of CNC-controlled technological machinery. This shift has introduced new demands not only for production efficiency but also for ensuring healthy and safe working conditions. Among the critical environmental and operational challenges arising from this technological evolution is the issue of noise emissions—particularly during wood processing, where high tool rotation speeds, interaction with the material, and machine vibrations are significant sources of sound.

According to the European Directive 2003/10/EO, the upper limit for a workplace noise exposure, based on the eight-hour working day, is determined to be $L_{EX,\,8h}$ = 85 dB(A).

Noise generated during the processing of wood and wood-based materials not only poses a risk to workers' hearing but can also negatively impact the concentration, productivity, and the overall quality of the work environment. For instance, a study conducted in a wood-processing factory in Indonesia reported an average noise intensity of 97.5 dB(A), which was found to correlate with reduced concentration capacity among workers (Handoko and Elfiah, 2021).

From a technological perspective, numerous studies have demonstrated that cutting parameters, such as feed rate (V_f), depth of cut (h), and tool rotation speed (n), significantly influence noise emissions during wood machining. In longitudinal flat milling of oak and linden wood, an increase in feed rate resulted in elevated sound pressure levels: from 88.3 to 92 dB(A) for oak and from 87.1 to 89.9 dB(A) for linden (Vitchev and Halim, 2025).

Furthermore, research indicates that noise emissions during band saw cutting are affected by a combination of factors, including cutting parameters, wood species (soft or hard), and moisture content (Gholamiyan *et al*., 2022). These findings underscore the importance of optimizing machining conditions not only for productivity but also for minimizing acoustic pollution and safeguarding worker health.

Increased noise levels due to the high rotational speed of the cutting head can be compensated by changes in their structure, linear and angular parameters, or by structural changes in the machine itself (Tscheschmedjiev *et al*., 1988; Svoren, 2011; Kopecký *et al*., 2012; Gross *et al*., 2016; Dursan *et al*., 2018; Vitchev *et al*., 2018; Ruslyakov, 2021; Vitchev, 2023; Güzel and Möhring, 2025). The factors influencing the change in noise levels during the processing of wood and wood-based materials generally depend on: i) the characteristics of the processed materials (type, density, dimensions); ii) the cutting regime (cutting and feed speeds, thickness of the removed layer, cutting height); iii) the characteristics of the cutting tool (shape and number of teeth, diameter, cutting angles, type of material from which the teeth are made) (HSE, 2007; HSE, 2009; Mikal, 2016).

For the numerical investigation of sound intensity, models have been developed to predict noise emissions during wood processing. In a study utilizing artificial neural networks (ANN), it was demonstrated that factors such as cutting width, depth, and type of material can be successfully used to predict the levels of generated noise (Özşahin and Singer, 2022).

While previous research has largely concentrated on isolated aspects, such as specific wood species, individual machines, or single technological parameters, our study advances the field by adopting a more integrated approach. The present study examines the processing of specimens made from Scots pine (*Pinus sylvestris L.*) on a CNC machining centre, aiming to analyse the variations in *A*-weighted noise emission levels (L_{pA}) depending on three key technological parameters – tool rotation speed (n), feed rate (V_f), and depth of cut (h). This comprehensive perspective provides better insights into the combined influence of these parameters, contributing to a deeper understanding of noise behaviour in CNC wood machining.

2. MATERIALS AND METHODS

The experiments have been performed using CNC machining centre Rover A3.30 (Biesse, Italy) (Figure 1). The machine has overall dimensions of $L \times W \times H$ = 4900 x 2700 x 2100 mm and is installed on a concrete sound-reflecting floor with an area of 380 m², in a room with a volume of 1536 m³.

Figure 1. Wood CNC machining centre Rover A3.30 (Biesse, Italy)

The machine is equipped with three interpolated control axes, allowing stepless adjustment of the feed rate and variation of the cutting speed by changing the tool rotation frequency (*n*).

For the purpose of the study, specimens from Scots pine (*Pinus sylvestris L.*) wood, with the following characteristics: density ρ = 510 kg/m³ and moisture content of W = 12% were processed. The characteristics of the material used were determined in accordance with the standards: BDS ISO 3131 and BDS ISO 3130. The processed specimens were tangentially oriented, with the following dimensions: $l \times w \times h$ = 1000 x 50 x 50 mm.

For the processing of the experimental samples, a frontal (shank-type) spiral cutter (CMT, Italy) named *PS*-1 was used (Figure 2).

Figure 2. Cutting tool PS-1 (CMT, Italy)

The technical characteristics of the cutting tool, presented in Figure 2 is summarised in table 1, where *D* is the cutting diameter; *S* – body diameter; *L* – overall length; *I* – cutting length; *z* – number of the spiral cutting edges; n_1 – maximum rotation frequency.

Table 1. Characteristics of the cutting tool

Name	Direction of the spiral	*D* mm	*S* mm	*L* mm	*I* mm	*z*	n_1 min^{-1}
PS-1	Positive	12	12	83	35	3	18 000

The noise emission level resulting from the operation of the investigated machine is determined based on the *A*-weighted sound pressure level (L_{pA}), measured in dB(A).

The measurement point is located 1 meter away from the reference parallelepiped, corresponding to the operator's position at the machine, and is situated 1.5 meters above the sound-reflecting concrete floor (Figure 3). The processed workpieces are positioned on the machine's worktable in the area near the control panel, close to the measurement point.

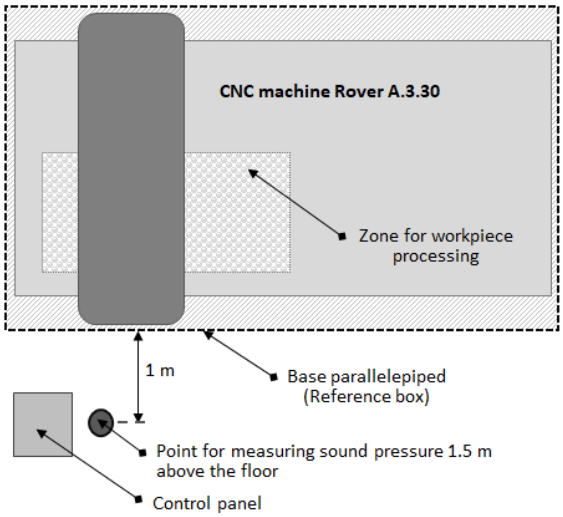

Figure 3. Diagram showing measuring point position and zone for workpiece processing

When determining the actual sound pressure level (L_{pA}), the influence of the background noise with the correction coefficient K_1 and the influence of the characteristics of the sound field with the correction coefficient K_2 were considered in the following way:

$$L_{pA} = L'_{pA} - K_1 - K_2 \quad (1)$$

Where:

L'_{pA} is the measured sound pressure level;

K_1 – the correction coefficient accounting for the influence of the background noise;

K_2 – the correction coefficient accounting for the characteristics of the sound field.

Background noise is the noise from all other internal and external sources, except the noise from the machine under study. To assess its influence, the difference (ΔL_p) between the sound pressure level from the sound source and the background noise level was calculated. In case of ΔL_p<6 dB, measurements are not recommended as the background noise will have a significant impact on the results. When $6 \leq \Delta L_p \leq 15$, it is necessary to calculate the correction coefficient K_1 which shows the influence of background noise which was calculated using the formula (2):

$$K_1 = -10lg\left(1 - 10^{-0.1\Delta L_p}\right), dB \quad (2)$$

In case of ΔL_p>15 dB the background noise does not affect the measurements as the sound pressure it generates is masked by the sound emission of the sound source. In this case $K_1 = 0$.

The correction coefficient K_2 which shows the characteristics of the sound field, depends on the volume of the room in which the measurements are made, on the sound absorption capacity of its surfaces (walls, floor, ceiling) and on the area of the measuring surface. From a practical point of view, it is most often accepted that the calculation of the correction coefficient K_2 is based on the sound absorption capacity of the room and is calculated using the formula:

$$K_2 = 10lg\left[1 + 4\frac{S}{A}\right] \quad (3)$$

where:

A is the equivalent sound absorbing area of the room, m^2;

S – the area of the measuring surface, m^2.

The equivalent sound absorption area of the room is calculated using the following formula:

$$A = \alpha . S_v \quad (4)$$

where:

α – is the sound absorption coefficient of the boundary surfaces of the test room, determined from tabulated values.;

S_v – is the total area of the boundary surfaces of the test room (walls, ceiling, and floor), expressed in square meters (m^2).

When K_2>4, the conditions for free or approximately free sound field are not fulfilled and the results of the measurements are not correct (BDS EN ISO 3744).

To investigate the combined influence of tool rotation frequency (n), feed rate (V_f), and depth of cut (h) on variations in noise emission levels, a planned three-factor experiment was conducted. In this experiment, the variable factors were adjusted at three levels: minimum, medium, and maximum (Table 2). The variation rate of the experimental factors was determined in accordance with the characteristics of the technological equipment and the material processing method. The variation between the minimum, medium, and maximum values of each investigated factor should be applied using an equal step size in order to ensure the validity and accuracy of subsequent mathematical analysis of the results.

Table 2. Values of the variable factors n, V_f, h during milling

Variable factors	Minimum value	Medium value	Maximum value
Rotation speed $n = X_1$, min^{-1}	12 000	15 000	18 000
Feed speed $V_f = X_2$, $m.min^{-1}$	2	3,5	5
Radial depth of cut $h = X_3$, mm	1	2	3

The data was statistically analysed by a specialized software Q-StatLab, which was also used to calculate the regression coefficient values of the model, the dispersion of errors and the coefficient of determination R^2.

The sound pressure level was measured with a digital sound level meter (CEL-620B1/K1 (CASELLA, UK) with built-in octave frequency filters with geometric mean frequencies from 63 Hz to 16.000 Hz and standard frequency correction characteristics *A*, *B*, *C*, according to accepted international standards which measure sound pressure levels from 20 Hz to 20 kHz. Prior to the measurements the device was calibrated by means of an acoustic calibrator of the same company with a constant sound pressure level of 114 dB, $p_0 = 2.10^{-5}$ N.m^2 at a frequency f = 180 Hz.

The experiments were carried out in accordance with BDS EN ISO 3744 and BDS ISO 7960.

3. RESULTS AND DISCUSSION

3.1. Background noise influence assessment

Based on the conducted measurements, the sound pressure levels were determined as follows:

The *A*-weighted sound pressure level resulting from the idle operation of the investigated CNC machine was 73 dB(A);

The *A*-weighted sound pressure level of the background noise was 54 dB(A).

The presented values show that the difference between the sound pressure levels of the noise source and the background noise is ΔLp > 15 dB(A). Therefore, the background noise does not influence the recorded sound pressure values generated by the machine. Consequently, the correction factor accounting for the influence of background noise has a value of $K_1 = 0$.

3.2. Determination of sound field characteristics

The machine is positioned on a concrete sound-reflecting floor in a room with dimensions $L \times W \times H = 32 \times 12 \times 4$ m. The measurement surface is located 1 meter from the reference parallelepiped and has the shape of a regular parallelepiped with an area of $S = 86.2$ m².

According to the classification of room types according to ISO 7960, the room is categorized as a *"regular cuboid room with machines or industrial space"*, with a sound absorption coefficient of the boundary surfaces $\alpha = 0.15$. After performing calculations according to equation (3), it was determined that the correction factor accounting for the characteristics of the sound field has a value of $K_2 = 2.1$.

The values of the correction factors K_1 and K_2 were subtracted from the measured sound pressure level of the machine in accordance with the relationship presented in equation (1).

3.3. Determination of the *A*-weighted sound pressure level during idle operation of the machine

In the machine's idle mode (operation without cutting), noise levels were measured in octave frequency bands with mean frequencies ranging from 125 Hz to 16.000 Hz, expressed in dB, along with the *A*-weighted sound pressure level in dB(A) for the three investigated tool rotation speeds: 12.000, 15.000, and 18.000 min^{-1}. When presenting the results in Figure 4, the correction factors K_1 and K_2 were taken into account.

The influence of the tool rotation frequency (*n)* on the variation in the generated noise level (L_p) is clearly visible from the graph. The results confirm the expectation that increasing the rotation frequency of the electrospindle, and consequently those of the cutting tool, leads to a rise in the generated noise level. This increase is attributed to the intensification of aerodynamic noise, caused by the higher swirling speed during the rotation of the cutting tool.

Regarding the frequency spectrum of the noise, it is notable that the most pronounced levels occur in the octave frequency band with a mean frequency of 4000 Hz, and this trend remains consistent across all three tool rotation speeds.

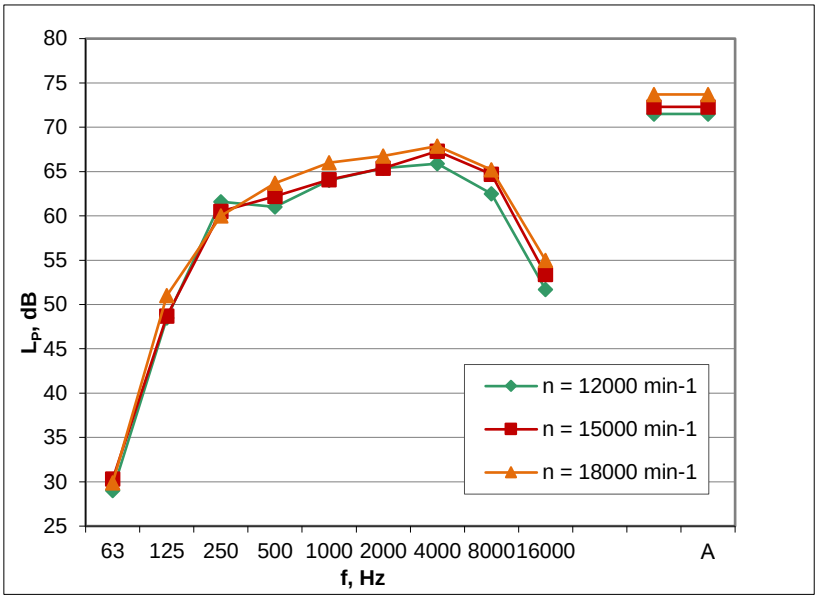

Figure 4. Noise level in octave frequency bands and A-weighted, at different rotational speeds of the cutting tool, measured during idle operation

It is well known that the human ear is most sensitive to sounds in the mid-frequency range of 1000–2000 Hz. The measured *A*-weighted sound pressure levels, expressed in dB(A), clearly indicate that the noise emission level during the machine's idle operation is well below the maximum permissible sanitary-hygienic limit of 85 dB(A).

Based on the presented methodology and the pre-established plan for conducting a three-factor experiment, the experiments were carried out using the *PS*-1 cutting tool to process Scots pine wood specimens.

Following mathematical and statistical analysis of the results using the specialized software Q-StatLab, the regression equation (5) was derived:

$$y = 81{,}89 + 0{,}7X_1 + 0{,}27X_2 + 1{,}26X_3 - 0{,}073X_1^2 + 0{,}68X_2^2 - 0{,}77X_3^2 - 0{,}25X_1X_2 - 0{,}175X_2X_3 - 0{,}4X_1X_3 \quad (5)$$

where:

y – predicted sound pressure level in coded form;

X_1 – rotation speed of the cutting tool (n) in coded form;

X_2 – feed speed (V_f) in coded form;

X_3 – radial depth of cut (h) in coded form.

The obtained values for the dispersion ratio $F = 2.859$ and the tabulated coefficient (Fisher's test) $F_T = 5.303$ show that the condition for the adequacy of the model is met and gives the confidence to analyze the derived regression equation (5). The coefficient of determination of the derived regression model is $R^2 = 0.82677$, which makes the predictability of the model reliable.

Based on the analysis of equation (5) it was predicted that when processing specimens from Scots pine wood with a cutting tool *PS*-1, the greatest influence on the noise emission level would be exerted by the rotation speed of the cutting tool $n = X_1$. This is visible by the positive value of the regression coefficient $b_1 = 0.700$, i.e. the noise emission level increases with the increase of the rotation speed of the tool (see also Figure 5 and 6). The second most important of the investigated factors was the feed speed $V_f = X_2$, with a regression coefficient $b_2 = 0.270$. The noise emission level was the least influenced by the radial depth of cut $h = X_3$, with $b_3 = 0.260$.

Our results are supported by Durcan and Burdurlu (2018) who found that increasing cutting depth and feed rate leads to higher noise levels during planing operations. In addition, Rabiei et al. (2024) conducted an empirical analysis of dust and noise pollutants in CNC wood machining. They confirmed that spindle speed, feed rate, and depth of cut significantly affect noise levels, with spindle speed being the most influential factor.

The changes in the sound pressure level depending on the rotation speed of the cutting tool (n), measured at different speed feed (V_f) is graphically presented in Figure 5.

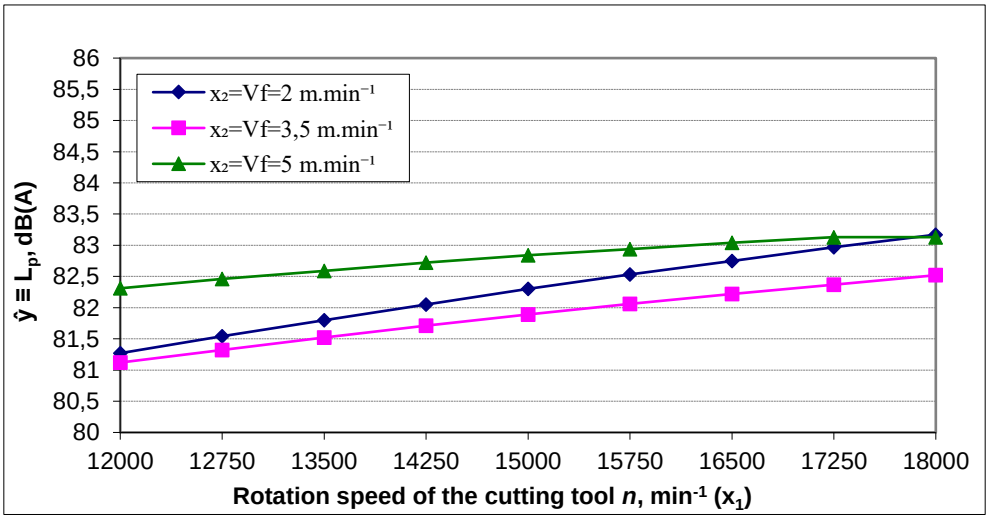

Figure 5. Influence of the rotation speed of the cutting tool PS- 1 (n) on the A-weighted sound pressure level, generated during operational mode of the machine and measure at different feed speed (V_f)

From the generated noise emission curves, it is visible that the highest noise emission level was generated at the highest feed speed $V_f = 5$ m.min^{-1}. A similar trend of increasing noise emission levels with increasing in the rotation speed of the tool was observed in the three noise curves. Based on the results, it could be concluded that the noise emission levels, measured at rotation speeds of the cutting tool 12000 min^{-1} and 18000 min^{-1}and feed speed $V_f = 5$ m.min^{-1}

change from 82.3 dB(A) to 83 dB(A), respectively. This accounts for about 30 % difference in the sound level.

Figure 6 graphically presents the changes in sound pressure level (L_p) as a function of the rotation speed of the cutting tool (n), measured at different radial depths of cut (h).

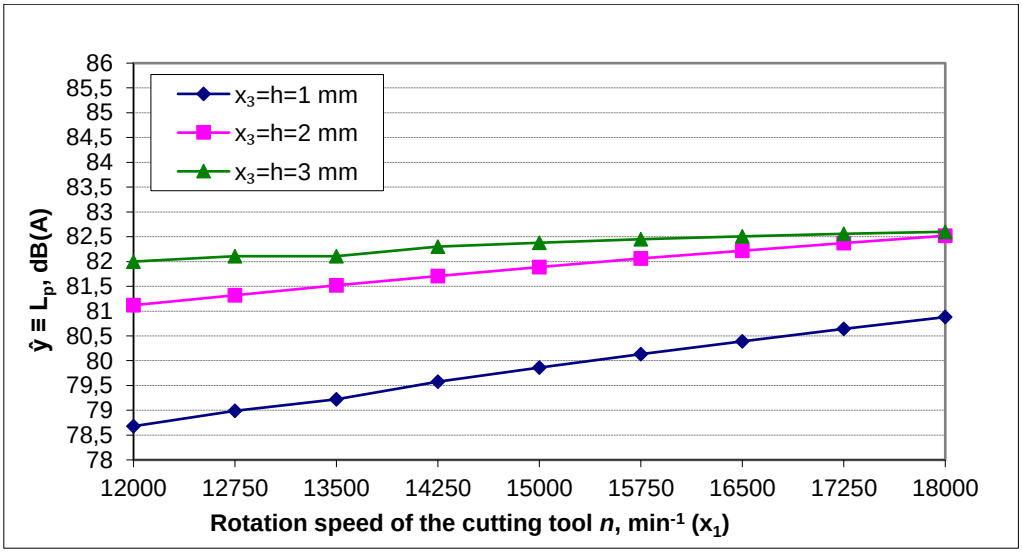

Figure 6. Influence of the rotation speed of the cutting tool PS- 1 (n) on the A-weighted sound pressure level, generated during operational mode of the machine and measured at different radial depth of cut (h)

The results confirmed the anticipated trend: an increase in rotation speed leads to a corresponding rise in sound pressure level.

Notably, the lowest radial depth of cut (h = 1 mm) consistently produced lower noise emission levels compared to h = 2 mm and h = 3 mm. Specifically, the sound pressure level increased from 78.6 dB(A) at n = 12000 min^{-1} to 81 dB(A) at n = 18000 min^{-1}, representing a difference of 2.4 dB(A).

Figure 7 depicts the variation in sound pressure levels depending both on the feed speed and the radial depth of cut.

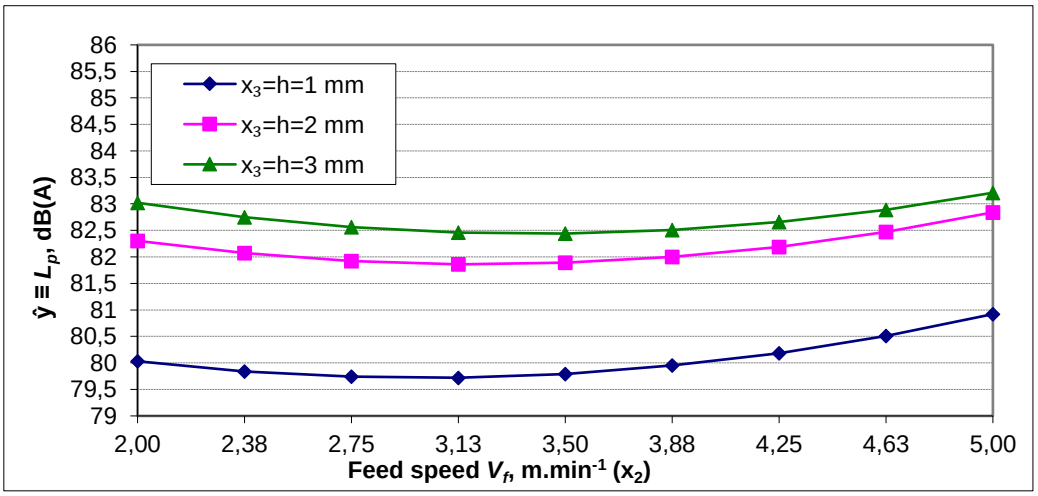

Figure 7. Influence of the feed speed on the A-weighted sound pressure level, measured at different radial depth of cut (h)

The results indicate that the feed speed (V_f,) is the second most significant factor influencing the levels of noise emissions under the tested conditions. As shown in the graph, the noise emission level increases from 80 dB(A) at V_f = 2 m/min to 83.2 dB(A) at V_f = 5 m/min. Although this represents a substantial increase, the noise level remains below the maximum permissible limit of 85 dB(A) for 8 hours/day. Under the conditions of this experiment, the lowest noise emission levels were recorded at a feed rate (V_f) between 3 and 3.5 m/min and a radial depth of cut (h) *of* 2 mm. These conditions are considered optimal for minimising noise during milling operations.

4. CONCLUSIONS AND RECOMMENDATIONS

Based on the results obtained under the different experimental conditions of this study, it could be concluded that the sound emission level does not exceed the maximum permissible occupational health and safety limit of 85 dB(A) for 8 hours/day.

When processing test specimens from Scots pine wood (*Pinus sylvestris* L.) using *PS*-1 end mill cutters (positive spiral type), the rotation speed of the tool ($n = X_1$) has the most significant influence on the noise emission level, followed by the feed speed ($V_f = X_2$), and the radial depth of cut ($h = X_3$).

To achieve lower noise emission levels during milling of specimens from Scots pine wood (*Pinus sylvestris* L.) *PS*-1 cutter, the following optimal values of the investigated factors can be recommended:

- rotation speed of the cutting tool n = 12 000 min^{-1};
- feed speed (V_f) from 2 m/min to 3.5 m/min;
- radial depth of cut h = 1 mm.

While these parameter settings are recommended for minimizing noise emission, their influence on the quality of the processed material must also be considered. Lower feed rate and radial depth of cut generally contribute to smoother surface finish and reduced risk of fiber tear-out, but they may also affect productivity compared to higher values. Conversely, increasing these two parameters can improve the productivity of the machine but may lead to rougher surfaces or dimensional inaccuracies. Future research should therefore evaluate these trade-offs to ensure that noise reduction strategies align with quality and performance requirements.

Acknowledgements: This research was financially supported by the Research Sector of the University of Forestry, Sofia, Bulgaria, under Contract No. NIS-B-1284/19.10.2023, and by the Bulgarian Ministry of Education and Science under the National Program “Young Scientists and Postdoctoral Students – 2” (2022–2025). The authors express their sincere gratitude for this support.

5. REFERENCES

Durcan, F.; Burdurlu, E., 2018: Effects of some machining parameters on noise level in planing of some wood materials. BioResources, 13 (2): 2702-2714. https://doi.org/10.15376/biores.13.2.2702-2714

Gholamiyan, H.; Gholampoor, B.; Hassanpoor Tichi, A. H., 2022: Effects of cutting parameters on the sound level and surface quality of sawn wood. BioResources, 17 (1): 1397-1410. https://doi.org/10.15376/biores.17.1.1397-1410

Gross, L.; Heisel U., 2016: Parameters influencing the noise emission of planing machines. Journal of Environmental Science and Engineering A, 5: 102-108. https://doi.org/10.17265/2162-5298/2016.02.007

Güzel, K.; Möhring, H., 2025: Approach to developing low-noise circular saw blades by determining actual required chip space volumes. Production Engineering, 19: 1119-1138. https://doi.org/10.1007/s11740-025-01362-x

Handoko, A.; Elfiah, U., 2021:The Effect Of Noise On The Level of Concentration In Wood Cutting Workers In Arjasa District, Jember District. Journal of Agromedicine and Medical Sciences, 7(2): 90. https://doi.org/10.19184/ams.v7i2.22000

Kopecký, Z.; Rousek, M.; Veselý, P.; Svoreň, J.; Karolczak, P., 2012: Effect of irregular tooth pitch on the noise level of circular saw-blade. Trieskove a Beztrieskove Obrabanie Dreva, 8 (1): 155-159.

Mika1, D.; Józwik, J., 2016: Normative measurements of noise at CNC machines work stations. Advances in Science and Technology, 30 (10): 138-143. https://doi.org/10.12913/22998624/63387

Özşahin Ş.; Singer, H., 2022: Prediction of noise emission in the machining of wood materials by means of an artificial neural networkŞükrü. New Zealand Journal of Forestry Science, 52 (11): 1179-539. https://doi.org/10.33494/nzjfs522022x92x

Rabiei, F.; Siedi, M.; Yaghoubi. S., 2024: Empirical analysis of dust and noise pollutants produced in the wood-CNC machining process. Environmental Science and Pollution Research, 31: 47584-47597.

Ruslyakov, D., 2021: Acoustic models of the main sources of noise of multi-spindle drilling woodworking machine. Akustika, 39: 4-17. https://doi.org/10.36336/akustika20213910

Svoren, J., 2011: Vplyv polohy kompenzačných drážok, medených nitov v tele pílového kotúča a nerovnomerného rozstupu zubov na kritické otáčky. Acta facultatis technicae, XVI (1): 125-132.

Tscheschmedjiev, A.; Dinkov, B.; Brezin, W. 1985: Abhangigkeit des Schalldruckpegels von der Drehzahlfrequenz rotierenden Messerwellen. Mobel und Wohnraum, 8: 245-250.

Vitchev, P.; Angelski, D.; Atanasov, D.; Mihailov, V., 2018: Study on the influence of certain factors on the sound pressure level generated during cutting with the circular saw. Proligno, 14 (4): 65-72.

Vitchev, P., 2023: Assessment of noise emission level generated by a CNC milling machine. Science Journal Innovations in Forest Industry and Engineering Design, 24 (2): 78-85.

Vitchev, P.; Halim, E., 2025: Influence of the cutting mode on the noise emission level during longitudinal-planner milling of linden and beech wood. Acta Facultatis Xylologiae Zvolen, 67 (1): 49-59. https://doi.org/10.17423/afx.2025.67.1.05

***BDS EN ISO 3744, 2010: Acoustics – Determination of sound power levels and sound energy levels of noise sources using sound pressure – Engineering methods for an essentially free field over a reflecting plane.

***BDS ISO 3130, 1999: Wood – Determination of moisture content for physical and mechanical tests.

***BDS ISO 3131, 1999: Wood – Determination of density for physical and mechanical tests.

***BDS ISO 7960, 2007: Airborne noise emitted by machine tools. Operating conditions for woodworking machines.

***Directive 2003/10/EC of the European Parliament and of the Council of 6 February 2003 on the minimum health and safety requirements regarding the exposure of workers to the risks arising from physical agents (noise) (Seventeenth individual Directive within the meaning of Article 16 (1) of Directive 89/391/EEC). https://eur-lex.europa.eu/eli/dir/2003/10/oj/eng

***EN ISO 3744, 2010: Acoustics – Determination of sound power levels and sound energy levels of noise sources using sound pressure – Engineering methods for an essentially free field over a reflecting plane.

***Health and Safety Executive (HSE), 2007: Noise at woodworking machines. Leaflet WIS13, HSE books 2007.

***Health and Safety Executive (HSE), 2009: Noise at woodworking machines, Woodworking Information Sheet No 13.

Exploring Elastic Properties of Flexible PUR and Latex Foams for Furniture

Vlaović, Zoran*; Vidoni, Nikola; Mihulja, Goran[1]

[1] Institute of Furniture and Wood in Construction, University of Zagreb Faculty of Forestry and Wood Technology, Zagreb, Croatia
*Corresponding author: zvlaovic@sumfak.unizg.hr

ABSTRACT

The problem of furniture comfort is addressed in many ways, but most often using soft polyurethane (PUR) foams or similar materials. To be a good cushioning material, a foam must exhibit good comfort and load-bearing properties. Twelve foam samples of different types, densities, and thicknesses were tested according to ISO 845:2006 and ISO 2439:2008 standards to determine their apparent core density, indentation hardness, compressive deflection coefficient, and hysteresis loss rate. The samples included conventional PUR foams, high resilience (HR) PUR foams, low resilience (visco) PUR foams, latex rubber foams, and a hybrid PUR-latex foam. Results showed that latex foam exhibited the most favourable profile, combining exceptional support with stable recovery and moderate hysteresis loss. The HR and hybrid foams also provided a strong overall performance, whereas conventional PUR foams were inconsistent, with limited support. Viscoelastic foam performed the poorest in terms of resilience and energy efficiency, confirming its role as a specialty material for pressure redistribution rather than support. The findings provide professional users (designers and manufacturers) with insights into the characteristics and qualities of different foams, facilitating their selection for use in seating and lying furniture.

Key words: elastic properties, furniture, iso 2439, latex foams, polyurethane foams

1. INTRODUCTION

Flexible polyurethane (PUR) foams are known for their ability to provide comfort, support, and durability, which are necessary qualities for use in sitting furniture and mattress applications (Obi, 2018). Owing to their versatile properties and characteristics, they have become indispensable cushioning materials, and are often the only materials used in seat or mattress construction. PUR and latex foams have eliminated the need to incorporate additional materials to achieve a certain level of comfort, which has simplified processes and reduced production costs (PFA, 2022).

In the domain of home furnishings, conventional open-cell foams, high-resilience (HR) foams, low-resilience (visco/memory) foams, and hybrid types (a combination of PUR and latex foams) are available. Latex rubber foam can be derived from natural sources, synthesised, or composed of a combination of both (PFA, 2022). This work includes research on the elastic properties of several selected PUR foams of different types (conventional, HR, and visco), one hybrid (PUR-latex), and one latex foam.

A key characteristic of flexible PUR foams is their open-cell structure. The open-cell morphology enables water vapour transport, ensuring a breathable and comfortable foam. Scarfato *et al*. (2017) shows that tested foams had similar water vapor transport due to their

open-cell structure, which could be practically important in mattress applications for moisture management.

Properties that affect the performance of PUR foam, such as density, indentation hardness (firmness), compression modulus, hysteresis, and recovery, are usually tested using ISO and other standardised methods (PFA, 2022; Scarfato *et al.*, 2017).

The comfort and support of PUR foams are defined by two basic and unavoidable properties: density and firmness (expressed numerically as IFD), which are independent parameters (Obi, 2018). Lower density foams have greater dynamic stiffness, causing discomfort due to higher resistance under dynamic loads during e.g., sitting. Higher-density foams provide better support, durability and stable seating by balancing firmness and flexibility for long-term comfort (Azmi *et al.*, 2023). Higher densities increase costs; therefore, latex foams are used in premium products and/or in combination with PUR foams (Gupta, 2007). A higher density usually means a higher compressive modulus, which ensures the usage of greater forces without deforming, which is essential for furniture and mattresses (Abdullah *et al.*, 2023; Demirel and Ergun Tuna, 2019).

PUR foams exhibit a range of mechanical behaviours under compression, which are influenced by the factors previously addressed. Performance is typically characterised by stress-strain curves, indentation force deflection (IFD), and hysteresis, which are crucial for applications ranging from automotive seating to medical pressure-relief devices (PFA, 2022; Srb and Petru, 2020). Compression set is a measure of the foam's ability to recover to its original thickness after being compressed. Higher density foams typically exhibit lower compression set values, indicating better recovery and less permanent deformation under load (Dounis and Wilkes, 1997).

Viscoelastic foams are characterised by slow recovery and high damping properties, with higher hysteresis during deformation, exhibiting broader dynamic loss angle responses, which indicate higher energy dissipation and lower resilience than HR foams. Viscoelastic foams conform closely to object shapes, providing support and comfort (Hilyard, 1994; Iyer and Srivastava, 2024). High resilience foams demonstrate consistent performance across various conditions (Dwyer, 1976). These foams exhibit a relatively narrow dynamic loss angle transition and a significant alteration in the foam storage modulus as it transitions from a glassy to a rubbery state, indicating high resilience and energy return (Hilyard, 1994). Consequently, HR foams are well suited for applications that demand durability and consistent support.

The foam thickness also affects the hysteresis and energy loss e.g., during cyclic loading and unloading. Cyclic fatigue affects foam performance through cell structure changes, impacting comfort parameters (D'Arienzo *et al.*, 2019). Thicker layers distribute loads more evenly, reducing localised stress and enhancing deformation resistance, but they may exhibit different hysteresis patterns due to their larger volume for energy absorption. Thinner foams may cause increased bottoming out due to higher interface pressures (Silva *et al.*, 2024), indicating that thickness must be carefully considered to balance stiffness and comfort.

The foam's cellular structure and the cell/wall area ratio influenced the hysteresis loss. Hilyard (1994) explained that hysteresis primarily results from the viscoelastic recovery of buckled cell elements, which is influenced by foam morphology and intermolecular linkages. Environmental factors can impact foam comfort, with weathering reducing comfort factors such

as hysteresis loss and surface firmness (D'Arienzo *et al.*, 2022). A lower hysteresis loss indicates better energy return, improving comfort and longevity (Silva *et al.*, 2024).

This paper presents the results of testing and comparing the mechanical and elastic properties of different latex and PUR foams. This study aims to provide professional users (designers and manufacturers) with insights into the characteristics and qualities of different foams and facilitate their selection for use in seating and lying furniture. The physical and elastic properties of the materials were determined using ISO 845 (ISO, 2006) and ISO 2439 (ISO, 2008) methods.

2. MATERIALS AND METHODS

This research included various flexible PUR, latex and hybrid foams from several Central European manufacturers: Plama-pur d.o.o. Slovenia, Vapeks d.o.o. Serbia, Vitafoam KFT Hungary, Eurofoam/Neveon GmbH Austria and Latexco/Novaya NV Belgium. The samples were new and had not been previously used.

2.1. Foam samples

Twelve foams of different types, densities, and thicknesses were selected for the samples in the form of square plates measuring (in mm) 390×390×thickness. Each tested sample consisted of four sub-samples (or sheets: 2 pcs. of 20 mm and 2 pcs. of 10 mm), which could be combined to form a structure of 40 mm, 50 mm and 60 mm thickness.

According to the types, the foams were flexible conventional PUR foams, high resilience PUR foams, low resilience PUR foams and latex rubber foams in standard and hybrid forms.

For the purposes of this paper, Table 1 shows the mean values of the measured densities, and detailed data on each sub-sample can be found in Vidoni (2012).

Table 9. Markings, average density and types of PUR and latex foams

Sample code	Foam manufacturer	Factory marking	Foam type	Mean sample density, kg/m^3	Standard deviation
S1	Plama-pur	PN 2534	Conventional	27.04	0.11
S2	Plama-pur	PN 3038	Conventional	28.61	0.15
S3	Vapeks	Vapen S 3534	Conventional	33.08	0.25
S4	Plama-pur	PT 4048	Conventional	35.70	0.39
S5	Vitafoam	HR 3028	High-resilience	30.09	1.01
S6	Eurofoam	HR 3536	High-resilience	36.45	0.23
S7	Eurofoam	Cellpur R 5225	High-resilience	54.20	1.07
S8	Eurofoam	Cellpur R 5235	High-resilience	54.16	0.32
S9	Eurofoam	Cellpur R 5245	High-resilience	51.32	0.41
S10	Latexco	Purlatex 60	Hybrid	57.88	0.21
S11	Latexco	Latex 65	Latex	64.96	7.47
S12	Vitafoam	Visco V 5015	Low-resilience	53.62	1.02

The samples were simply coded with the letter S and a series of ordinal numbers from 1 to 12. The samples consisted of several sheets depending on the sample thickness. The sheets (sub-samples) were not glued together. Samples with a thickness of 40 mm consisted of two sheets of 20 mm, samples with a thickness of 50 mm consisted of three sheets (20 mm+20 mm+10 mm), and samples with a thickness of 60 mm consisted of four sheets (2×20 mm+2×10 mm).

The samples were previously conditioned in laboratory climate air conditions of (23±2) °C and (50±5) % relative humidity per the requirements of ISO 845:2006 and ISO 2439:2008.

2.2. Methods

After conditioning, the samples were subjected to determining the apparent core density of cellular plastics and rubbers, according to ISO 845:2006. Four individual sheets per sample were measured and weighed on an analytical balance (Sartorius ED224S-0CE, range 0–220 g, readability 0,1 mg) and the mean sample density was calculated (Table 1).

The thickness of the sub-samples was measured using an Inspekt S device (load range 0-2 kN, LabMaster ver. 3.0.5.26; H&P MPT GmbH, Germany), using a circular indenter (diameter 200 mm) that applied a force of 4,8-5,0 N to the sub-sample (Figure 1).

The next step was to determine the indentation hardness, compressive deflection coefficient, and hysteresis loss rate of flexible cellular materials according to ISO 2439:2008 (methods B and E). The load unit used for this part of the experiment was the Inspekt S and LabMaster software.

a) b)

Figure 1. a) Device for testing the mechanical properties of foams; b) Inspekt S – pressing an indenter into the sample S8, thickness 50 mm (photo: Vlaović)

Tests were conducted on all samples with thicknesses of 40, 50, and 60 mm. For the purposes of this research, the sheets in each tested sample were not glued (due to the limited number of sheets available) when testing their different thickness combinations, and these were the only deviations from ISO 2439:2008 when performing the experiments.

A detailed description of the standardised indentation hardness test method is provided in ISO 2439:2008.

3. RESULTS AND DISCUSSION

The results presented in this chapter refer to research into the mechanical (elastic) properties of foams, in accordance with ISO 2439:2008, according to the *Method B* (hardness and compression modulus/support factor), and *Method E* (recovery/hysteresis return, compression modulus/support factor and hysteresis loss rate). The detailed measured values for both methods, for all the samples are available in Vidoni (2012).

3.1. Results of indentation hardness characteristics

Method B is the procedure described in ISO 2439 which determines the indentation hardness characteristics at 25 %, 40 % and 65 % of the initial sample thickness, maintaining each indentation for 30 seconds.

Table 2 shows measured values of standard indentation hardness on a given sample and specified sample thicknesses of 40, 50, and 60 mm.

Table 2. Values of indentation hardness HB for different sample thickness (Method B)

Sample code	HB25% N	HB40% N	HB65% N	HB25% N	HB40% N	HB65% N	HB25% N	HB40% N	HB65% N
	thickness 40 mm			thickness 50 mm			thickness 60 mm		
S1	118.3	148.4	301.7	118.5	148.4	302.5	124.5	161.3	312.0
S2	134.2	166.5	323.7	144.3	177.6	337.3	152.2	192.0	360.4
S3	105.2	140.7	267.7	113.0	151.0	283.5	120.7	162.4	301.3
S4	153.2	204.6	407.6	160.6	213.9	420.6	167.9	225.7	437.3
S5	91.1	125.7	265.5	95.7	132.2	275.6	98.6	138.8	285.5
S6	125.4	176.2	383.3	131.6	184.7	397.2	135.4	193.2	411.6
S7	87.9	120.6	271.9	88.4	122.6	274.3	89.3	125.0	277.5
S8	112.4	150.5	323.2	114.2	153.8	328.0	115.1	156.5	329.8
S9	136.1	180.0	381.4	139.7	185.7	387.2	143.0	191.9	396.6
S10	40.8	56.5	116.1	41.7	58.6	120.5	42.7	60.7	123.8
S11	43.5	80.9	255.7	40.5	76.9	242.4	39.6	75.6	235.9
S12	39.7	52.5	96.0	40.2	54.1	98.2	41.4	56.6	102.3

The results for eleven samples show a trend that with increasing the sample thickness, the hardness at 25 %, 40 %, and 65 % deformation increases slightly, except for sample S11 (Latex 65), where it decreases slightly.

Looking at the types of foams, the highest HB values were recorded for conventional PUR (S1-S4) and HR foams (S5-S9), while the lowest was recorded for low-resilience foam S12 (Visco V 5015), and only slightly higher for hybrid foam S10 (Purlatex 60).

Indentation factors (IF) are convenient means of expressing the hardness results. IFs are the ratios of the forces required to obtain the indentations of 25 % and 65 % to the force needed to obtain the indentation of 40 % (ISO 2439).

A single hardness value (e.g., HB40%) can serve as a standard reference hardness for quality control and specification, chosen because it’s roughly the middle of the working compression range, but not as a comfort reference needed for furniture.

The two foams might have the same 40 % indentation hardness, but very different indentation factors, indicating different firmness profiles or compression behaviours (PFA, 2022). A user's comfort in a mattress or seat cushion depends on how the foam feels on the surface and also deeper in the material. This can be observed in Figure 2 on the example of samples S3 and S8, or even better is the comparison of 60 mm thick samples S2 and S9, which have almost identical HB40% (192 N, Table 2), but very different compression modulus of 2.4 and 2.8, respectively.

Figure 2 shows the indentation factors (IF) of the initial softness (surface comfort, presented as a ratio of 25 %/40 %), IF of deep support (resistance to bottoming out, presented by a ratio of 65 %/40 %), and finally the compression modulus (or support factor (Sf), presented as a ratio of 65 %/25 %). Only data for the 50 mm sample thickness are shown here, since their values lie between the values for the 40 mm and 60 mm thicknesses and are very similar.

Conventional PUR foams (S1-S4) samples show uniform values, with IF 25 %/40 % between 0.7-0.8, IF 65 %/40 % around 1.9-2.0, and Sf ranging 2.3-2.6. This indicates predictable but modest support and resilience. This limited variation suggests that conventional PUR foams provide stable but basic mechanical performance, with moderate comfort and pressure distribution.

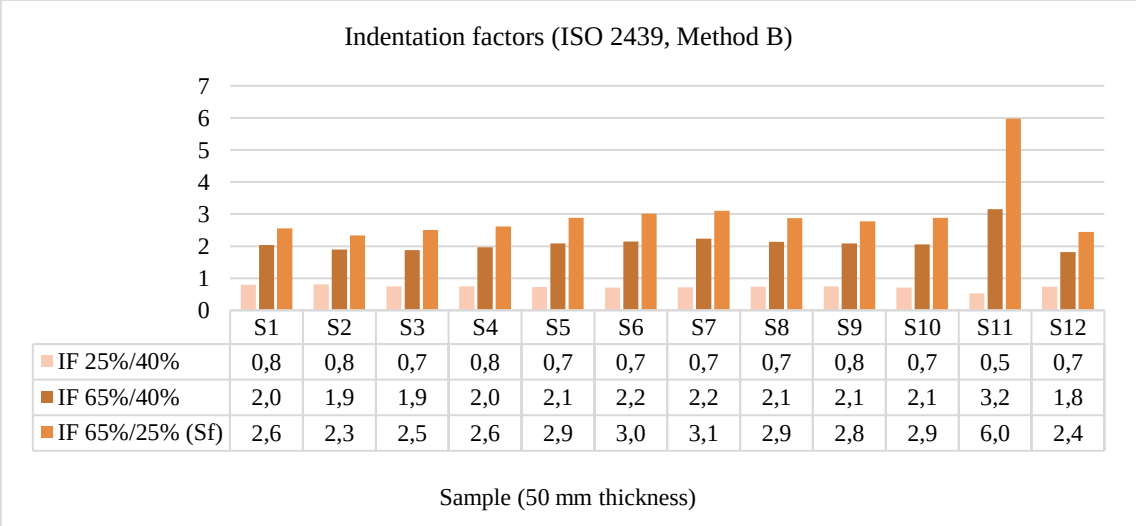

	S1	S2	S3	S4	S5	S6	S7	S8	S9	S10	S11	S12
IF 25%/40%	0,8	0,8	0,7	0,8	0,7	0,7	0,7	0,7	0,8	0,7	0,5	0,7
IF 65%/40%	2,0	1,9	1,9	2,0	2,1	2,2	2,2	2,1	2,1	2,1	3,2	1,8
IF 65%/25% (Sf)	2,6	2,3	2,5	2,6	2,9	3,0	3,1	2,9	2,8	2,9	6,0	2,4

Figure 2. Indentation factors of a 50 mm thick samples (Method B)

High resilience foams (S5-S9) compared to conventional PUR foams exhibit similar IF 25 %/40 % (0.7-0.8) but consistently higher IF 65 %/40 % (2.0-2.2) and Sf values (2.8-3.1). This reflects improved support and better capacity to accommodate load over a wider deformation range, enhancing both comfort and durability. The higher support factors highlight HR foams' suitability for long-term sitting comfort.

Hybrid PUR/latex foam (S10) presents intermediate behaviour, with IF 65%/40% of 2.3 and Sf of 2.9, aligning with HR foams. It combines resilience with moderate support, suggesting balanced comfort properties.

Latex foam (S11) stands out with an IF 65 %/40 % of 3.2, and an exceptionally high Sf (6.0), far exceeding that of other groups. This reflects very strong progressive resistance with increasing indentation, which may provide pronounced support but could also reduce perceived

softness. Its high support factor suggests excellent spinal alignment support, although potentially at the expense of immediate plushness.

Low resilience foam (S12) displays relatively low IF 25 %/40 % (0.7) and moderate IF of 65 %/40 % (1.8), with a comparatively low Sf of 2.4. This indicates a softer, conforming behaviour with limited progressive resistance, prioritizing pressure redistribution over support. Such properties are consistent with slow-recovery, body-molding characteristics.

3.2. Results of compressive deflection coefficient and hysteresis loss rate

Method E is the procedure described in ISO 2439 which determines the compressive deflection coefficient and hysteresis loss rate, which provides additional information about materials' load-bearing properties.

Recovery, often referred to as hysteresis return (Figure 3), is a measure of how well a flexible PUR foam regains its original thickness and properties after being deformed and unloaded. Recovery directly relates to the energy loss during deformation. The lower the hysteresis loss, the greater the recovery, meaning the foam "springs back" more faithfully to its original shape (PFA, 2022).

The hysteresis loss rate (Af) (Figure 4) is a measure of the energy absorbed when the foam is subjected to deformation. Kreter (1985; cited in Hilyard, 1994) defined a parameter called hysteresis loss in terms of the relative load difference between the loading and unloading indentation force deflection (IFD) curves at 25 % compression.

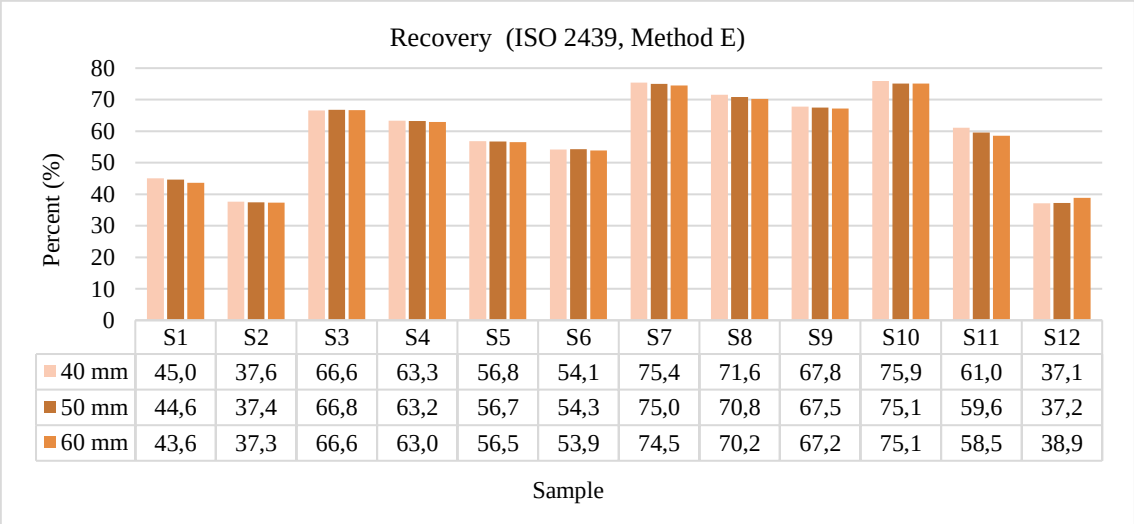

	S1	S2	S3	S4	S5	S6	S7	S8	S9	S10	S11	S12
40 mm	45,0	37,6	66,6	63,3	56,8	54,1	75,4	71,6	67,8	75,9	61,0	37,1
50 mm	44,6	37,4	66,8	63,2	56,7	54,3	75,0	70,8	67,5	75,1	59,6	37,2
60 mm	43,6	37,3	66,6	63,0	56,5	53,9	74,5	70,2	67,2	75,1	58,5	38,9

Figure 3. Recovery/hysteresis return values for different sample thickness (Method E)

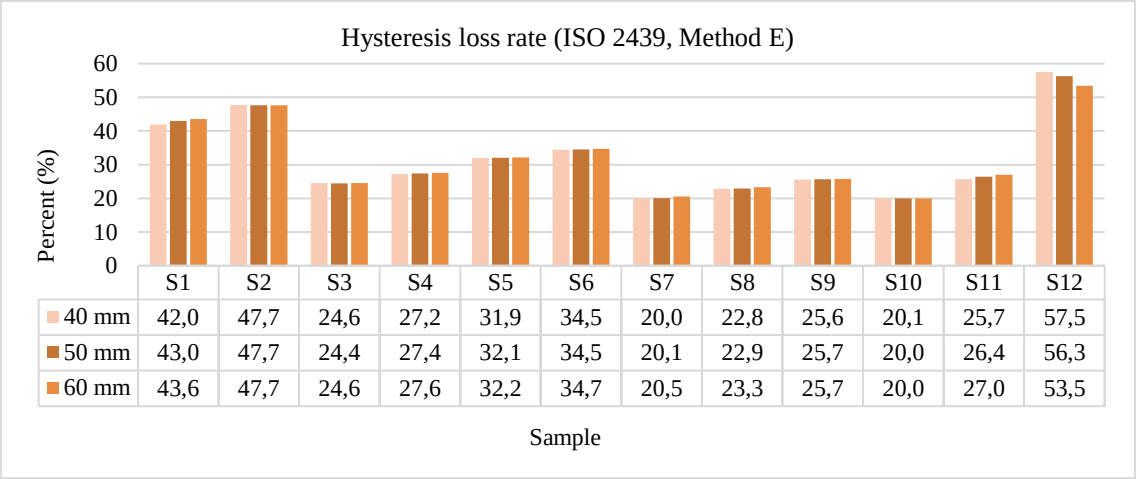

	S1	S2	S3	S4	S5	S6	S7	S8	S9	S10	S11	S12
40 mm	42,0	47,7	24,6	27,2	31,9	34,5	20,0	22,8	25,6	20,1	25,7	57,5
50 mm	43,0	47,7	24,4	27,4	32,1	34,5	20,1	22,9	25,7	20,0	26,4	56,3
60 mm	43,6	47,7	24,6	27,6	32,2	34,7	20,5	23,3	25,7	20,0	27,0	53,5

Figure 4. Hysteresis loss rate (Af) values for all sample thickness (Method E)

When the support factor (Sf) (Figure 5) is calculated from Method E measurements (Figure 6), it takes into account the ability of the foam to retain the support after being subjected to stress, which is more relevant to fatigue, durability and hysteresis effects. While Method B is best for determining initial comfort/support in new foam, Method E is more relevant for assessing long-term support, especially in applications where the foam is repeatedly stressed and expected to recover (such as mattresses, seats, or automotive foams).

The combined analysis of recovery (Figure 3), hysteresis loss (Figure 4), and support factor (Figure 5) presents apparent differences in mechanical performance across foam groups.

Conventional PUR foams show variability. While some samples (S3-S4) reach moderate recovery (63-67 %) with relatively low hysteresis loss (24-28 %), others (S1-S2) combine poor recovery with high energy dissipation, with consistently low support factors (1.8-2.3). These results underscore the limited resilience and load-bearing progression of conventional PUR.

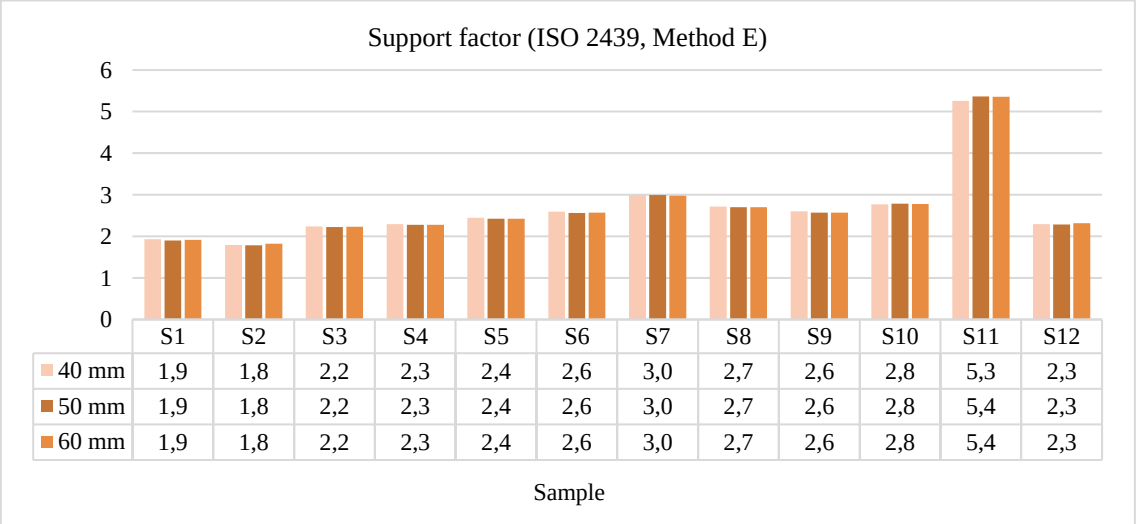

	S1	S2	S3	S4	S5	S6	S7	S8	S9	S10	S11	S12
40 mm	1,9	1,8	2,2	2,3	2,4	2,6	3,0	2,7	2,6	2,8	5,3	2,3
50 mm	1,9	1,8	2,2	2,3	2,4	2,6	3,0	2,7	2,6	2,8	5,4	2,3
60 mm	1,9	1,8	2,2	2,3	2,4	2,6	3,0	2,7	2,6	2,8	5,4	2,3

Figure 5. Support factor (Sf) values for all sample thickness (Method E)

HR foams (S5-S9) shows a more balanced performance profile, characterized by higher recovery (54-75 %), moderate hysteresis loss (20-35 %), and improved support factors (2.4-3.0). These results confirm HR foams' suitability for seating applications where resilience and

progressive firmness are required. Next one, the hybrid pur/latex foam (S10), outperforms HR foams in both recovery (75-76 %) and support factor (2.8-2.9) while maintaining low hysteresis loss (20-26 %) – indicating efficient energy return and superior comfort potential.

Latex foam (S11) shows the best overall results, with a high support factor (> 5.0), moderate recovery (58-61 %), and modest hysteresis loss (26-27 %). This combination reflects phenomenal load distribution and progressive support, making latex particularly suitable when comfort and long-term seating performance are most important. In contrast, viscoelastic foam (S12) shows the least favourable resilience characteristics, with very low recovery (37-39 %) and extremely high hysteresis loss (54-58 %), coupled with weak support factors (2.2-2.3). These values confirm "memory" foams' design intent for pressure redistribution rather than elastic responsiveness or support efficiency.

Across all properties, thickness (40-60 mm) exerts a negligible influence, reinforcing that mechanical behaviour is primarily determined by foam composition and cellular architecture rather than geometry.

A graphical representation of the IFD test measurements of different sample thicknesses are shown in Figure 6.

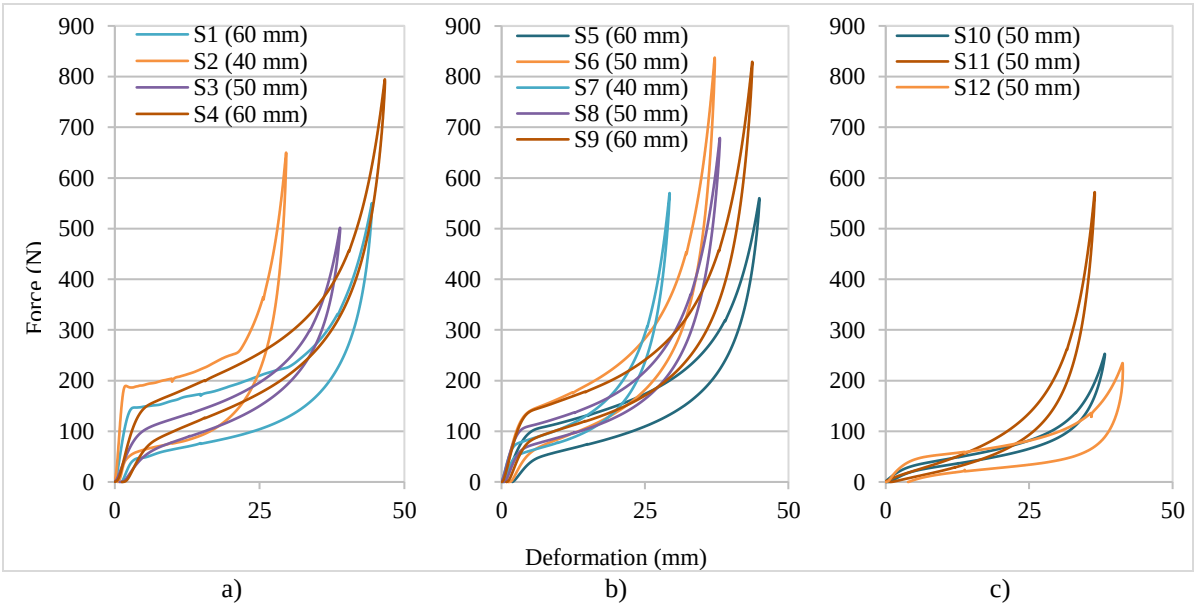

Figure 6. IFD curves (Method E) of foams: a) Conventional PUR; b) HR PUR; c) Hybrid, latex and visco PUR

4. CONCLUSIONS

Limiting ourselves to the tested samples of selected types of foams, considering their qualities, physical and mechanical properties, the following conclusions can only be guidelines and trends that have been shown in the mutual relationships of the observed materials, and not general conclusions.

Based on the results, there are clear differences between the foam groups in terms of resilience, energy dissipation, and support. Latex foam demonstrated the most favourable profile, combining exceptional support with stable recovery and moderate hysteresis loss, while the hybrid and HR foams also provided strong overall performance. Conventional PUR foams

are inconsistent, with some showing acceptable resilience, but generally limited support. Viscoelastic foam performed the poorest in terms of resilience and energy efficiency, confirming its role as a specialty material for pressure redistribution rather than support.

Foam composition, rather than thickness, is the dominant factor shaping mechanical behaviour.

For office chairs: HR and latex foams offer the best balance of resilience and progressive support, making them ideal for long-term seating comfort. Viscoelastic foams can enhance comfort when layered appropriately. Latex is extremely effective due to its high support factor, while HR foams provide strong performance with cost advantages.

For mattresses: Viscoelastic foams contribute valuable pressure redistribution but should be combined with more resilient foams, such as latex or HR, to ensure adequate support and durability. Conventional PUR foams remain less suitable for both applications (sitting and lying) due to their inconsistent mechanical behaviour.

The final selection of a particular material for a particular application on a particular product requires results based on tests that include objective and subjective methods, taking into account the feelings of real users.

Acknowledgements: The authors express their gratitude to Bernarda d.o.o. Pušćine, Croatia, for providing samples for the research.

5. REFERENCES

Abdullah, M.; Ramtani, S.; Yagoubi, N., 2023: Mechanical properties of polyurethane foam for potential application in the prevention and treatment of pressure ulcers. *Results in Engineering*, 19: 101237, https://doi.org/10.1016/j.rineng.2023.101237

Azmi, M. H.; Khairil Anas, M. R.; Nawal Aswan, A. J.; Azizan, A.; Mohd Amzar, A., 2023: The Effect of Preload, Density and Thickness on Seat Dynamic Stiffness. *Pertanika Journal of Science and Technology*, 31 (3): 1267-1278. https://doi.org/10.47836/pjst.31.3.08

D'Arienzo, L.; Incarnato, L.; Rinaldi, S.; Scarfato, P., 2019: Comfort and fatigue performance of a Soya-derived flexible PU foam for mattresses. *AIP Conference Proceedings*, 2196: 020028. https://doi.org/10.1063/1.5140301

D'Arienzo, L.; Incarnato, L.; Rinaldi, S.; Scarfato, P., 2022: Durability of a Soya-Derived Flexible PU Foam for Mattresses: Effects of Different Artificial Aging. *Macromolecular Symposia*, 405 (1): 215. https://doi.org/10.1002/masy.202100247

Demirel, S.; Ergun Tuna, B., 2019: Evaluation of the cyclic fatigue performance of polyurethane foam in different density and category. *Polymer Testing*, Elsevier, 76: 146-153. https://doi.org/10.1016/j.polymertesting.2019.03.019

Dounis, D. V.; Wilkes, G. L., 1997: Structure-property relationships of flexible polyurethane foams. *Polymer*, 38 (11): 2819-2828. https://doi.org/10.1016/S0032-3861(97)85620-0

Dwyer, F. J., 1976: A Review of Factors Affecting Durability Characteristics of Flexible Urethane Foams. *Journal of Cellular Plastics*, 12 (2): 104-113. https://doi.org/10.1177/0021955X7601200205

Gupta, R., 2007: *Polymer Foams Handbook, CWL Publishing Enterprises, Inc., Madison*, 2004, Elsevier, https://doi.org/10.1016/B978-0-7506-8069-1.X5000-4

Hilyard, N. C., 1994: Hysteresis and energy loss in flexible polyurethane foams. In: *Low Density Cellular Plastics*, Springer Netherlands, Dordrecht, pp. 226-269. https://doi.org/10.1007/978-94-011-1256-7_8

Iyer, D.; Srivastava, S., 2024: *Facile Classification of Polyurethane Foam from Post-Consumer-Use Mattresses*, Los Angeles, California, USA.

Obi, B. E., 2018: *Polymeric Foams Structure-Property-Performance*, Elsevier. https://doi.org/10.1016/C2012-0-06136-4

Scarfato, P.; Di Maio, L.; Incarnato, L., 2017: Structure and physical-mechanical properties related to comfort of flexible polyurethane foams for mattress and effects of artificial weathering. *Composites Part B: Engineering*, 109: 45-52. https://doi.org/10.1016/j.compositesb.2016.10.041

Silva, P.; Ribeiro, D.; Postolache, O.; Seabra, E.; Mendes, J., 2024: Static Factors in Sitting Comfort: Seat Foam Properties, Temperature, and Contact Pressure. *Applied Sciences*, 14: 7753. https://doi.org/10.3390/app14177753

Srb, P.; Petru, M., 2020: Numerical simulation of composite car seat cushion. *MM Science Journal*,. 2020 (2): 3932-3937. https://doi.org/10.17973/MMSJ.2020_06_2020011

Vidoni, N., 2012: *Research of Elastic Properties of Different Types of PU Foams*, Bachelor thesis (in Croatian), University of Zagreb Faculty of Forestry and Wood Technology, Croatia.

***ISO 845, 2006: Cellular Plastics and Rubbers - Determination of Apparent Density, International Organization for Standardization (ISO), Geneva, Switzerland.

***ISO 2439, 2008: Flexible Cellular Polymeric Materials - Determination of Hardness (Indentation Technique), International Organization for Standardization (ISO), Geneva, Switzerland.

***PFA, 2022: InTouch, *Bulletin Series*, Polyurethane Foam Association, Loudon, TN.

Challenges and Perspectives of Digital Transformation in the Wood Industry

Vukman, Karla*; Klarić, Kristina; Miklošić, Denis; Crnojević, Jelena; Perić, Ivana[1]

[1] Department of Production Organization, Faculty of Forestry and Wood Technology, University of Zagreb, Zagreb, Croatia

*Corresponding author: kvukman@sumfak.unizg.hr

ABSTRACT

Digital transformation is increasingly viewed not only as a technological shift but as a strategic and organizational process where digital culture and employee readiness play a central role. This paper examines the digital maturity of Croatia's wood industry, comparing survey data collected in 2025 with earlier findings. The analysis reveals changing adoption patterns, particularly regarding ERP/CRM systems, organizational culture, and the integration of sustainability. While traditional barriers such as costs and technical difficulties have diminished, ERP and CRM use has declined, indicating a selective and non-linear digitalization trajectory. The results confirm that Europe's wood industry remains 20–30 years behind more advanced sectors, with ERP systems still underutilized as efficiency drivers. Furthermore, sustainability and risk management have emerged as essential components of the digital agenda. By providing evidence from a post-transition economy, this study highlights the growing importance of digital culture, employee skills, and sustainability in shaping industrial digital transformation.

Keywords: digital transformation, wood industry, enterprise resource planning, sustainability, resistance to change

1. INTRODUCTION

Digital transformation is increasingly recognized not only as a technological shift but also as a strategic and organizational process that shapes competitiveness, culture, and sustainability (Vial, 2019; Westerman *et al*., 2014). While sectors such as automotive and electronics have adopted digital technologies rapidly, traditional industries such as wood face unique challenges: maintaining stable physical production while integrating complex digital tools (Vukman *et al.*, 2024). The European wood industry employs more than 3.1 million people and generates over €136 billion in added value (Eurostat, 2024), but still lags 20-30 years behind advanced industries in terms of digitalization (Vukman *et al.*, 2024). Digitalization in this sector is not only a question of competitiveness but also of sustainability, as it directly manages renewable resources and plays a central role in the circular economy (Jamwal *et al.*, 2021). Previous studies highlight a 'digital paradox': despite the availability of and economic justification for tools, adoption remains significantly slower compared to other sectors (Matt *et al.*, 2015; OECD, 2023). At the same time, successful transformation depends less on technology and more on strategy, organizational culture, and employee readiness (Bharadwaj *et al.*, 2013; Kane *et al.*, 2015; Sebastian *et al.*, 2020). Croatia represents a relevant case study. While progress has been made in infrastructure and e-services, SMEs remain below the EU average in adopting advanced digital tools, with pronounced rural–urban disparities (European Commission, 2024; World Bank, 2024). The wood industry, dominated by SMEs, illustrates these challenges

especially strongly: limited resources, dependence on external suppliers, and complex supply chains constrain adoption (Premkumar, 2003; Eller *et al.*, 2020).

This paper analyzes the challenges and perspectives of digital transformation in the Croatian wood industry, focusing on ERP/CRM adoption, organizational culture, and sustainability. It compares findings from two preliminary surveys (2019 and 2025) with established theoretical frameworks (Schumpeter, 1942; Porter & Heppelmann, 2014; Teece, Pisano & Shuen, 1997; Orlikowski, 2000; Leonardi, 2011). The results highlight selective and non-linear trajectories, where barriers are decreasing but ERP and CRM remain underutilized. By providing evidence from a post-transition economy, this study contributes to understanding how digital culture, employee skills, and sustainability shape transformation in traditional industries.

2. THEORETICAL BACKGROUND

Digital transformation in traditional industries combines technological, organizational, and cultural dimensions. Schumpeter's (1942) concept of creative destruction explains how innovation reshapes industries, while Porter and Heppelmann (2014) show how IoT enables smart connected products across product life cycles. The dynamic capabilities framework (Teece *et al.*, 1997; Winter, 2003) highlights sensing, seizing, and reconfiguring opportunities, which are crucial in sectors with complex physical production. From a sociotechnical perspective, transformation emerges from interactions of technology and social practices (Orlikowski, 2000; Leonardi, 2011), while Zuboff (1988) stresses that digitalization also creates new knowledge. ERP and CRM systems remain core digital tools, supporting efficiency, transparency, and customer orientation. Yet adoption in the wood industry is limited, often due to high costs, lack of sector-specific solutions, and SME resource constraints (Vukman *et al.*, 2024). Benefits fall into operational, managerial, and infrastructural categories (Shang & Seddon, 2002), while adoption dynamics are explained by Rogers' (2003) Diffusion of Innovation Theory and DeLone & McLean's (2003) IS Success Model.

Organizational culture is another decisive factor. Schein (2017) and Hartl & Hess (2017) emphasize agility, collaboration, and data-driven decision-making, while Klarić et al. (2024) show that education and leadership are key to embedding a digital culture. Risk management is also part of this agenda: Perić *et al.* (2025) propose fuzzy AHP–FMEA to increase resilience in digitally integrated companies.

Finally, digital transformation in the wood industry must be seen through the lens of sustainability. Elkington's (1998) triple bottom line and circular economy studies (Jamwal *et al.*, 2021; Dragomir *et al.*, 2023; Nylén *et al.*, 2025) show that digital technologies are indispensable for resource optimization and waste reduction. For SMEs, challenges are compounded by limited resources and reliance on external providers, yet flexibility in decision-making can also enable faster adaptation (Premkumar, 2003; Eller *et al.*, 2020).

3. METHODOLOGY

This study is based on two preliminary surveys conducted among Croatian wood industry companies. The first survey was carried out in 2019 (23 companies), while the second was conducted in 2025 (20 companies). The target population included SMEs from C16 (wood processing) and C31 (furniture manufacturing), with a minimum of five employees and continuous operations over the past three years. For both survey waves, the Dun & Bradstreet company database was used to identify eligible firms. The selection included all active companies in the Republic of Croatia with more than five employees classified under C16 and C31, according to the NKD classification. From this population, companies were invited to participate in the study. Data were collected through an online questionnaire distributed via SurveyMonkey, which enabled efficient administration and response tracking. The 2019 questionnaire was based on validated scales (Davis, 1989; Venkatesh *et al.*, 2003), while the 2025 version was expanded to include digital culture (Kane *et al.*, 2015; Hartl & Hess, 2017) and sustainability constructs (Jamwal *et al.*, 2021). All items were measured on 5-point Likert scales, supplemented with demographic questions. Reliability of the main constructs was satisfactory (Cronbach's $\alpha = 0.72–0.89$). The response rate in both surveys was around 40%, which aligns with expectations for B2B research in traditional industries (Cycyota & Harrison, 2006). While the small sample size and voluntary participation limit generalizability, both waves are positioned as exploratory studies that provide indicative insights into ERP/CRM adoption, barriers, and sustainability practices. Comparative analysis between 2019 and 2025 focused on ERP/CRM usage, digitalization challenges, and organizational practices. Although the survey instruments were not fully identical, conceptually comparable indicators were selected to ensure the validity of the comparison.

4. RESULTS AND DISCUSSION

4.1. ERP and CRM adoption

Survey results indicate a sharp decline in ERP and CRM implementation between 2019 and 2025 (Table 1). In 2019, 87 % of companies reported ERP use, but by 2025, only 40% retained such systems, with an average usage intensity of 2.2 on a 5-point scale (Perić *et al.*, 2019; Kremenjaš, 2019). CRM systems followed the same trajectory, dropping from 91.3% in 2019 to just 35 % in 2025. This decline suggests that digital transformation in the wood industry is not linear. Instead, SMEs are increasingly turning to modular or specialized tools such as CAD/CAM, IoT, and MES/SCADA, or face challenges in maintaining complex ERP/CRM solutions (Vukman *et al.*, 2024). Previous research highlights that customized solutions dominate in SMEs but often lack long-term sustainability (Perić *et al.*, 2019).

Table 1. ERP and CRM Adoption in Croatian Wood Industry (2019 vs. 2025)

Indicator	2019	2025
ERP adoption (%)	87.0	40.0
CRM adoption (%)	91.3	35.0
ERP usage intensity (mean, 1–5 scale)	-	2.2/5

As shown in Figure 2, the perceived barriers to digitalization decreased notably between 2019 and 2025. High implementation costs dropped from 4.0 to 3.11, lack of external support

from 4.4 to 2.74, and technical difficulties from 3.9 to 2.47. The shortage of qualified staff showed only a slight decline (3.9 to 3.21), while employee resistance, measured for the first time in 2025, was relatively low at 2.16. These results indicate progress in infrastructure, external support, and employee acceptance of digital change. However, the persistent lack of qualified personnel remains the most critical barrier, consistent with findings in SME digitalization research (Eller *et al.*, 2020).

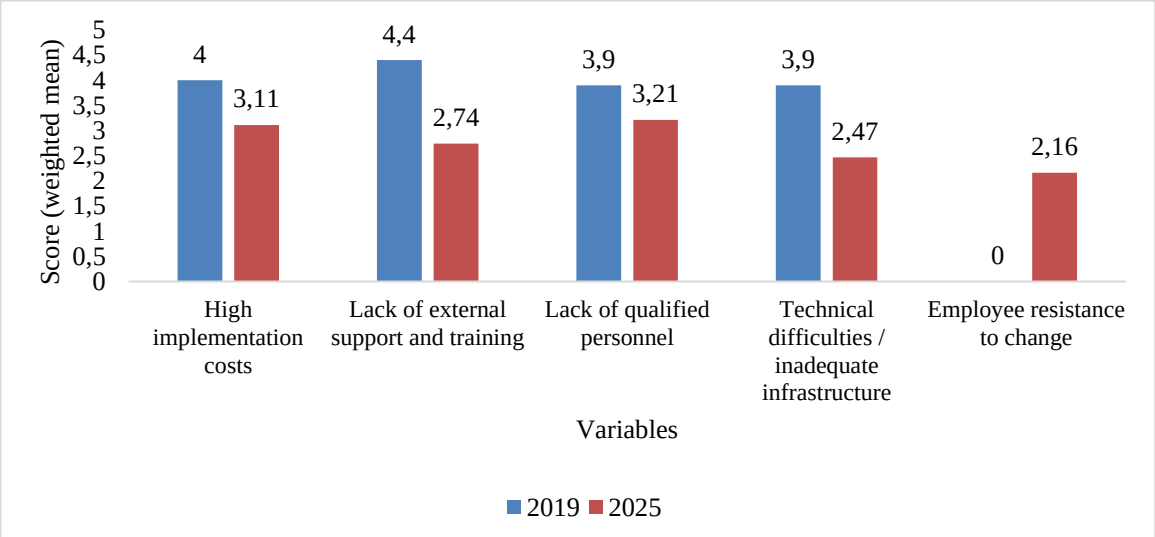

Figure 2. Perceived Barriers to Digitalization in the Wood Industry (2019 and 2025)

4.2. Digital culture and sustainability

The 2025 results indicate that employee resistance is no longer a significant obstacle (2.16/5), reflecting the effectiveness of improved change management strategies. This supports Klarić *et al.* (2024), who emphasize the role of digital culture, leadership, and employee training in transformation processes. Nevertheless, the shortage of qualified staff (3.21/5) underscores the need for systematic competence development as a prerequisite for digital maturity. Sustainability has become a recognized element of the digital agenda, aligned with Elkington's (1998) triple bottom line. However, the practical adoption of digital tools for material tracking, inventory management, and circular economy practices remains limited. Studies confirm that circularity in the wood industry requires comprehensive digital support across all stages from design to recycling (Dragomir *et al.*, 2023; Nylén *et al.*, 2025). The Croatian case indicates that sustainability is strategically acknowledged but not yet operationalized in everyday processes.

4.3. Interpretive synthesis

The findings confirm a digital paradox: although barriers such as high costs, lack of support, and technical difficulties have significantly decreased, ERP and CRM adoption have declined. This suggests a selective and non-linear trajectory of digital transformation, where SMEs prioritize modular and flexible solutions over comprehensive platforms. As emphasized by Perić *et al.* (2025), successful digital transformation requires a holistic approach that integrates technology, organizational change, competence development, and sustainability practices.

5. CONCLUSION

The comparative analysis of surveys conducted in 2019 and 2025 highlights major changes in the digitalization of the Croatian wood industry. Despite a stable company structure across both surveys (C16 wood processing and C31 furniture), ERP adoption fell from 87% to 40% of firms, with a usage intensity of only 2.2/5 in 2025, while CRM dropped from 91.3% to 35%. This confirms that digital transformation in the sector follows a non-linear and selective path, often replacing ERP/CRM with modular or specialized tools (Perić *et al.*, 2019; Vukman *et al.*, 2024).

Perceived barriers declined significantly between 2019 and 2025, with costs, technical difficulties, and a lack of external support all easing, while employee resistance (2.16) emerged as minor. Yet, the shortage of qualified staff (3.21) persists as the key limitation (Eller *et al.*, 2020). Sustainability has gained attention in line with the triple bottom line (Elkington, 1998), but remains weakly implemented in practice, confirming the need for stronger digital support to enable circular economy models (Dragomir *et al.*, 2023; Nylén *et al.*, 2025).

These preliminary findings reveal a paradox: barriers are decreasing, but adoption of key systems is falling. Progress requires systematic investment in employee competencies, better integration of ERP/CRM with modern platforms, and stronger alignment of digitalization with sustainability goals. A holistic approach that links technology, organization, and culture (Perić *et al.*, 2025) will be crucial for the competitiveness and long-term sustainability of the wood industry.

6. REFERENCES

Bharadwaj, A.; El Sawy, O.A.; Pavlou, P.A.; Venkatraman, N., 2013: Digital business strategy: Toward a next generation of insights. MIS Quarterly, 37 (2): 471-482. https://doi.org/10.25300/MISQ/2013/37:2.3

Cycyota, C. S.; Harrison, D. A., 2006: What (not) to expect when surveying executives: A meta-analysis of top manager response rates and techniques over time. Organizational Research Methods, 9 (2): 133-160. https://doi.org/10.1177/1094428105280770

Davis, F. D., 1989: Perceived usefulness, perceived ease of use, and user acceptance of information technology. MIS Quarterly, 13 (3): 319-340. https://doi.org/10.2307/249008

DeLone, W. H.; McLean, E. R., 2003: The DeLone and McLean model of information systems success: A ten-year update. Journal of Management Information Systems, 19 (4): 9-30. https://doi.org/10.1080/07421222.2003.11045748

Dragomir, M.; Tofană, S.; Dragomir, D.; Țițu, A.M.; Popescu, D., 2023: Assessing circularity in the wood industry—Methodology, tool, and results. Forests, 14: 1935. https://doi.org/10.3390/f14101935

Elkington, J., 1998: Cannibals with forks: The triple bottom line of 21st century business. New Society Publishers, Oxford.

Eller, R.; Alford, P.; Kallmünzer, A.; Peters, M., 2020: Antecedents, consequences, and challenges of small and medium-sized enterprise digitalization. Journal of Business Research, 112: 119-127. https://doi.org/10.1016/j.jbusres.2020.03.004

Hartl, E.; Hess, T., 2017: The role of cultural values for digital transformation: Insights from a Delphi study. In: Proceedings of the 23rd Americas Conference on Information Systems (AMCIS), Boston, pp. 1-10. https://core.ac.uk/download/pdf/301371796.pdf

Jamwal, A.; Agrawal, R.; Sharma, M.; Giallanza, A., 2021: Industry 4.0 technologies for manufacturing sustainability: A systematic review and future research directions. Applied Sciences, 11: 5725. https://doi.org/10.3390/app11125725

Kane, G. C.; Palmer, D.; Phillips, A. N.; Kiron, D.; Buckley, N., 2015: Strategy, not technology, drives digital transformation. MIT Sloan Management Review, 14 (1): 1-25.

Klarić, K.; Barčić, A.P.; Greger, K.; Vukman, K.; Perić, I.; Klarić, M., 2024: Striving for excellence: Deconstruction of the total quality management measuring model for Croatian furniture industry. Sustainability, 16 (24): 11236. https://doi.org/10.3390/su162411236

Kremenjaš, K., 2019: Application of integrated information systems in small and medium-sized wood-processing enterprises. Master's thesis. University of Zagreb, Faculty of Forestry and Wood Technology. https://zir.nsk.hr/islandora/object/sumfak%3A1839

Leonardi, P. M., 2011: When flexible routines meet flexible technologies: Affordance, constraint, and the imbrication of human and material agencies. MIS Quarterly, 35 (1): 147-167. https://ssrn.com/abstract=1607718

Matt, C.; Hess, T.; Benlian, A., 2015: Digital transformation strategies. Business & Information Systems Engineering, 57: 339-343. https://doi.org/10.1007/s12599-015-0401-5

Nylén, E. J.; Klitkou, A., 2025: Digital innovations in wooden construction for a circular economy. Circular Economy and Sustainability. https://doi.org/10.1007/s43615-025-00667-4

Orlikowski, W. J., 2000: Using technology and constituting structures: A practice lens for studying technology in organizations. Organization Science, 11 (4): 404-428. http://www.jstor.org/stable/2640412

Perić, I.; Klarić, K.; Pirc Barčić, A.; Vukman, K.; Sedlar, T.; Grošelj, P., 2025: Optimising risk management in wood-based manufacturing: A fuzzy AHP–FMEA framework approach. BioResources, 20 (2): 2979-3001. https://doi.org/10.15376/biores.20.2.2979-3001

Porter, M. E.; Heppelmann, J. E., 2014: How smart, connected products are transforming competition. Harvard Business Review, 92 (11): 64-88. https://eclass.aegean.gr/modules/document/file.php/TNEY202/HBR_How-Smart-Connected-Products-Are-Transforming-Competition%20copy.pdf

Premkumar, G., 2003: A meta-analysis of research on information technology implementation in small business. Journal of Organizational Computing and Electronic Commerce, 13 (2): 91-121. https://doi.org/10.1207/S15327744JOCE1302

Rogers, E. M., 2003: Diffusion of innovations (5th edition). Free Press, New York.

Schumpeter, J. A., 1942: Capitalism, socialism and democracy. Harper & Brothers, New York.

Sebastian, I. M.; Ross, J. W.; Beath, C.; Mocker, M.; Moloney, K. G.; Fonstad, N. O., 2020: How big old companies navigate digital transformation. MIS Quarterly Executive, 16 (3): 197-213. https://doi.org/10.4324/9780429286797-6

Schein, E. H., 2010: Organizational culture and leadership (4th edition). Wiley, Hoboken.

Shang, S.; Seddon, P., 2002: Assessing and managing the benefits of enterprise systems: The business manager's perspective. Information Systems Journal, 12: 271-300. https://doi.org/10.1046/j.1365-2575.2002.00132.x

Teece, D. J.; Pisano, G.; Shuen, A., 1997: Dynamic capabilities and strategic management. Strategic Management Journal, 18 (7): 509-533. https://doi.org/10.1002/(SICI)1097-0266(199708)18:7

Venkatesh, V.; Morris, M. G.; Davis, G. B.; Davis, F. D., 2003: User acceptance of information technology: Toward a unified view. MIS Quarterly, 27 (3): 425-478. https://doi.org/10.2307/30036540

Vial, G., 2019: Understanding digital transformation: A review and a research agenda. The Journal of Strategic Information Systems, 28 (2): 118-144. https://doi.org/10.1016/j.jsis.2019.01.003

Vukman, K.; Klarić, K.; Greger, K.; Perić, I., 2024: Driving efficiency and competitiveness: Trends and innovations in ERP systems for the wood industry. Forests, 15 (2): 230. https://doi.org/10.3390/f15020230

Westerman, G.; Bonnet, D.; McAfee, A., 2014: Leading digital: Turning technology into business transformation. Harvard Business Review Press, Boston.

Winter, S. G., 2003: Understanding dynamic capabilities. Strategic Management Journal, 24 (10): 991-995. https://doi.org/10.1002/smj.318

Zuboff, S., 1988: In the age of the smart machine: The future of work and power. Basic Books, New York.

***European Commission, 2024: Digital economy and society index (DESI) 2024 – Croatia. https://digital-strategy.ec.europa.eu

***Eurostat, 2024: Wood products – production and trade. https://ec.europa.eu/eurostat/statistics-explained/index.php?title=Wood_products_-_production_and_trade

***OECD, 2023: SME and entrepreneurship outlook 2023. OECD Publishing, Paris. https://doi.org/10.1787/c5ac21d0-en

***World Bank, 2024: Croatia digital diagnostic brief. https://thedocs.worldbank.org/en/doc/4b0646b73e6d49479422855d4a7a48c6-0080012024/original/Croatia-Digital-Diagnostic-Brief.pdf

Thickness Joining of Solid Wood Using Rotary Welding

Župčić, Ivica; Čatić, Matija; Đukić, Igor; Gržan, Tomislav; Hasan, Marin[1*]

[1] Department of Wood Technology, Faculty of Forestry and Wood Technology, University of Zagreb, Zagreb, Croatia
Corresponding author: mhasan@sumfak.unizg.hr

ABSTRACT

Wood welding is a relatively new technology for joining wooden elements that offers environmentally friendly joints and an alternative to classic methods such as wood gluing. There are two main methods of wood welding: vibration and rotational welding. In both methods, friction and pressure result in the formation of a welded joint. This paper examines the possibilities of thickness joining of solid wood using rotational dowel welding. Based on the results of the research, it can be concluded that the variable hole diameter significantly contributes to increasing the strength of the joint, regardless of the type of dowel. Also, samples with a smooth dowel surface achieve higher joint strengths on average compared to grooved dowel surfaces. The highest mean value of the joint strength was achieved in samples where smooth dowels were welded into holes of variable diameter and is 295.3 MPa.

Key words: rotary welding, thickness joining, dowel, solid wood

1. INTRODUCTION

Wood welding is the joining of two or more elements together without the addition of glue or other bonding agents. Wood welding is a relatively new method that first appeared in the late 20th century, and significant research into welding began in the early 2000s. The two most commonly used methods of welding solid wood and wood panels are vibration welding and rotation welding. In rotation welding, the substrate (elements) is stationary, and the dowel (wooden wedge) rotates with a displacement in the direction of its longitudinal axis. The surface of the dowel wears against the perimeter of the hole (its surface area/volume and diameter decrease, and the dowel takes the shape of a truncated cone, while the surface area of the hole increases) and the hole widens, and the surrounding cells of the dowel and the hole thicken. The result of friction on the contact surfaces is heat that "softens and melts" the wood structure (hemicellulose and lignin), and the wood fibers become intertwined due to vibration or rotation. Carbohydrates are the main component of the melt, and lignin modification occurs (Pizzi *et al*., 2006).

The strength of rotary welded joints is comparable to the strength of glued joints. Approximately 2 s after welding, the frictional force achieves a stable state. No considerable changes in frictional force and interface strength were observed and interface strength increased with normal force (Yin *et al.,* 2021). The strength of welded joints is affected by many factors such as duration of the welding process (movement of the dowel in the direction of the vertical axis per revolution), interference fit (difference between the diameter of the dowel and the hole), welding depth, rotation frequency, wood species, direction of welding (parallel or perpendicular

to the direction of the fibres), width of growth rings, welding temperature (Pizzi *et al*., 2004; Bocquet *et al*., 2007; Leban *et al*., 2008; Župčić, 2010; Župčić *et al*., 2022).

Oak and spruce elements can be joined by thickness, and the pull-out force or strength of the joint depends on the shape of the hole. The weakest results were obtained with a continuous hole diameter because the dowel tip was not welded due to a lack of melt. Passing through the oak element reduced the dowel diameter, and thus the required clearance, and dowel welding at the tip was not achieved. Between elements with a continuous hole diameter of 8 mm and samples with a variable hole diameter (6, 7, 8, and 9 mm), the pull-out force of the dowel is 2.3 times higher. The shape of the hole affects the consumption of the dowel tip, which directly affects the pull-out force or strength of the joint (Župčić *et al*., 2008).

According to Leban *et al*. (2008), the optimal welding depth is 22 mm, a slightly higher pull-out is achieved with a welding depth of 46 mm. Kanazawa *et al*. (2005) studied the pull-out forces of welded depths of 15 and 30 mm. The test results showed that the pull-out forces of the joints welded to the depth of 30 mm were twice larger than that of 15 mm.

Rotary welding of wood can be used in the manufacture of furniture and wooden supports using width, thickness and length assembly. Wood welding also finds application in floor structures and corner joints and other wood products.

The aim of the work was to determine the possibilities of thickness assembly of beech elements using rotary welding of dowels. Given the intensive wear of the dowel tip, the influence of the shape of the hole (continuous or variable diameter) and the influence of the type of dowel (smooth or profiled surface) was investigated.

2. MATERIALS AND METHODS

For research purposes, samples were made from beech (*Fagus Silvatica* L.) from plank 50 mm thick. The average density was (0.69 ± 0.03) g/cm³ (according to HRN ISO 13061-2 (2015)). After sawing and wood planing, the cross-section of the elements was 30 mm × 30 mm. The elements thus prepared were shortened to a length of 300 mm (Figure 1). Four holes were drilled on each element (64 mm was the distance between the holes), with a drill with a diameter of 6, 7, 8 and 9 mm depending on the shape of the hole. The samples were then divided into two groups according to the geometry of the hole (Figure 2). The first group of samples had holes with a variable diameter along the depth of the joint. On the upper element, a hole with a diameter of 9 mm was first drilled to a depth of 15 mm, after which drilling continued with a diameter of 8 mm to a total depth of 30 mm. On the lower element, the hole was 7 mm to a depth of 10 mm, and then the diameter was 6 mm to the end of the element. The second group of samples had a cylindrical hole with a diameter of 8 mm on both elements. The diameter of the hole was 0.06 to 0.1 mm smaller than the diameter of the drill bit, which was influenced by the elastic deformations of the wood during the drilling of the hole.

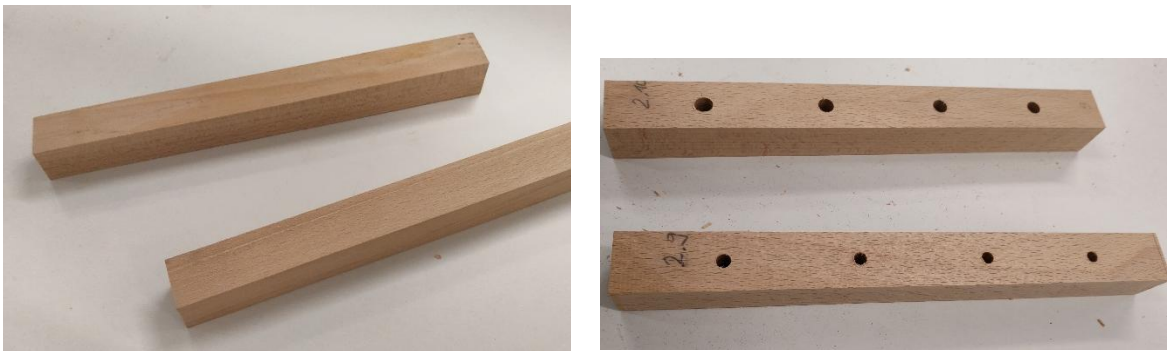

a b

Figure 1. Beech elements: a) before drilling, b) after drilling the hole

The dowels used in the study had a smooth and grooved surface. The diameter of the grooved dowels was 10.04 mm and the smooth dowels 10.02 mm. The dowels were sawn from 1000 mm long rods to a length of 120 mm, and their edges were slightly ground to make it easier to start welding.

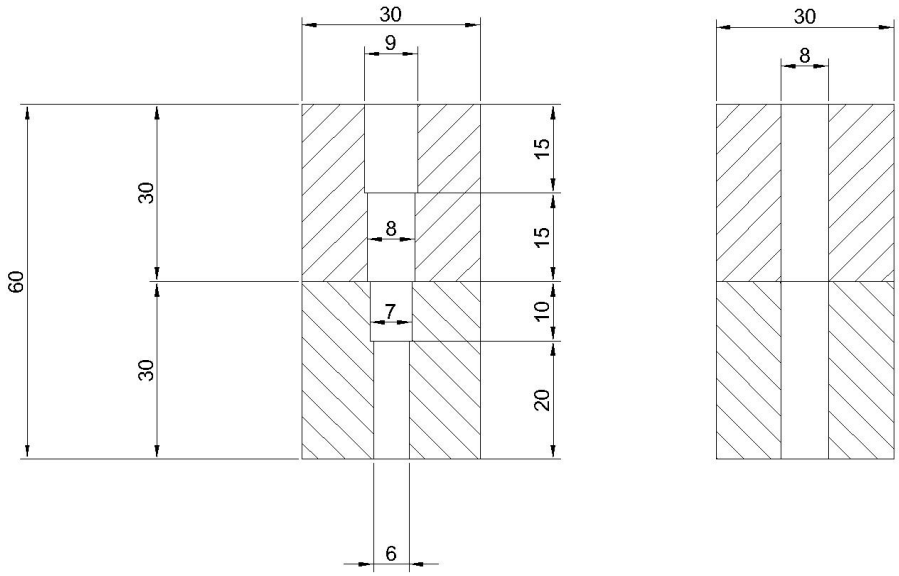

a b

Figure 2. Cross-section of two types of samples: a) with a variable diameter hole

b) with a continuous diameter hole

After preparing the elements and dowels, the samples were made using the rotational welding technique. Two elements were placed one on top of the other in thickness and the rotating dowel passed through the first element and was welded into the second element to a depth of 20 mm, so the total welding depth was 50 mm. The dowel rotated during welding at a rotational frequency of 1520 min^{-1}. A total of 80 dowels were welded (Table 1).

Table 1. List of used codes

Code	Code description	Number of welded dowels
S1	dowels with a smooth surface and a hole of constant diameter	20
S4	dowels with a smooth surface and a hole of variable diameter	20
NS1	dowels with a profiled surface and a hole of constant diameter	20
NS4	dowels with a profiled surface and a hole of variable diameter	20

After welding, the samples were sawed into four parts so that each welded dowl could be tested individually in a tensile testing machine. he samples were tested for tensile force, and with each welded sample, the core was pulled out. The tensile testing machine was set so that the sample breaks within one minute. During the test, the maximum force that occurred at the moment of failure was measured.

3. RESULTS AND DISCUSSION

According to the research conducted, beech elements can be successfully joined by thickness using welded dowels. The shape of the hole has a statistically significant influence on the strength of the joint due to wear of the dowel tip. When the dowel tip is adjusted to the diameter of the hole, there is no friction or melt forming the welded joint. The dowel passes through the first element and the dowel tip is worn down when it reaches the second element where there is no friction and therefore no welding if the hole is of continuous diameter. During the welding process, the tip of the dowel is intensively worn, and due to the rotation, the lignin is lost from the melt at the tip, and the tip of the dowel remains unwelded, which also reduces the strength of the joint (Figure 3).

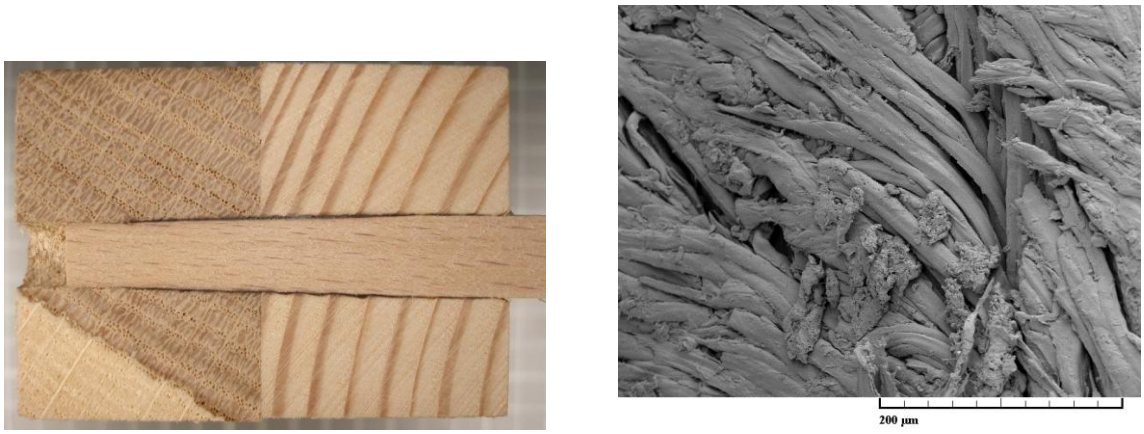

a b

Figure 3. The top of the dowls is not welded: a) due to the consumption of the dowel (Župčić et al. 2008), b) scanning electron microscopic (SEM) images of the dowel's tips so intertwined fibers of the dowel oriented in the direction of rotation welding is not achieved (Župčić, 2010)

The strength of the welded joint increases with the increase of the welding depth up to 20 mm, and then decreases towards the welding depth of 30 mm. It turns out that 20 mm is the optimal welding depth for a cylindrical hole (for researched parameters of welding), although the optimal depth also depends on the difference between the dowel and hole diameter. The

welding depth increases from 20 to 30 in the direction perpendicular to wood grain, the strength decreases by 21 %. (Župčić *et al*., 2024).

In order to avoid a reduction in the strength of the joint at a welding depth of 20 mm, a hole of variable diameter was drilled. This significantly increases the strength of the welded joint. The test results show that the geometry of the hole has a statistically significant effect on the strength of the welded joints (Figure 4). Samples with a hole of variable diameter (S4 and NS4) achieved statistically significantly higher strength values compared to those with a continuous diameter hole (S1 and NS1). The highest strength was achieved by samples S4 (295.3 MPa), while the lowest strength was recorded for samples NS1 (53.5 MPa). It was also found that dowels with a smooth surface (S1 and S4) achieve higher values of tensile strength compared to dowels with a profiled surface (NS1 and NS4). Profiled dowels have a smaller volume, i.e. less wood material due to the profile on the periphery, and they wear out faster, which affects the strength of the welded joint. The results show that the smooth surface of the dowel in combination with the variable diameter of the hole is conducive to creating the strongest welded joint. The volume of the smooth dowel is larger compared to the grooved one, so there is more material that melts and creates a melt during welding.

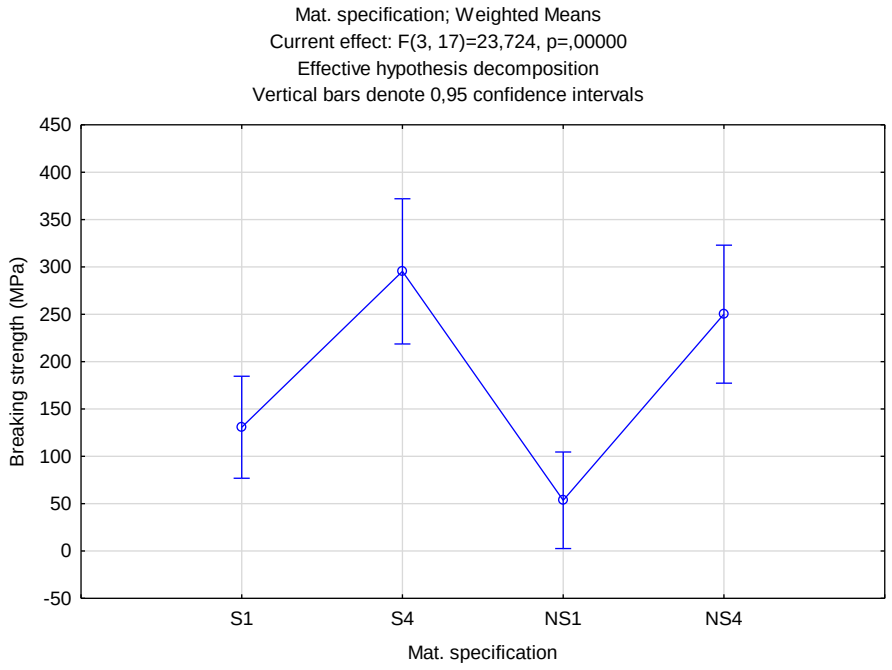

Figure 4. Influence of hole shape and dowel surface woodworking on joint strength

4. CONCLUSIONS

The factors studied that affect the strength of rotationally welded joints are the geometry of the hole (continuous or variable diameters) and the surface treatment of the dowel (smooth or profiled). Of the factors studied, the geometry of the hole has the greatest influence on the strength of the welded joint, while the influence of the profiled surface of the dowel is significantly smaller. When welding a smooth dowel into a hole with a variable diameter, the

strength of the welded joint increases by 2.3 times compared to a hole with a continuous diameter. When welding a profiled dowel into a hole with a variable diameter, the strength of the welded joint increases by 4.7 times compared to a hole with a continuous diameter.

The influence of the dowel on the strength of the welded joint is smaller compared to the shape of the hole. When welding a smooth dowel into a hole with a continuous diameter, the strength is 144 % higher compared to a profiled dowel, while when welding a profiled dowel into a hole with a variable diameter, the strength is 18% higher compared to a profiled dowel.

5. REFERENCES

Bocquet, J. F.; Pizzi, A.; Resch, L., 2007: Full-scale industrial wood floor assembly and structures by welded-through dowels. Holz als Roh- und Werkstoff, 65: 149-155. https://doi.org/10.1007/s00107-006-0170-4

Kanazawa, F.; Pizzi, A.; Properzi, M.; Delmotte, L.; Pichelin, F., 2005: Parameters influencing wood-dowel welding by high-speed rotation. Journal of Adhesion Science and Technology, 19 (12): 1025-1038. https://doi.org/10.1163/156856105774382444

Leban, J. M.; Mansouri, H. R.; Omreni, P.; Pizzi, A., 2008: Dependence of dowel welding on rotation rate. Holz als Roh- und Werkstoff, 66, 241-242. https://doi.org/10.1007/s00107-008-0228-6

Pizzi, A.; Leban, J. M.; Kanazawa, F.; Properzi, M.; Pichelin, F., 2004: Wood dowel bonding by high-speed rotation welding. Journal of Adhesion Science and Technology, 18 (11): 1263-1278. https://doi.org/10.1163/1568561041588192

Pizzi, A.; Despres, A.; Mansouri, H. R.; Leban, J. M.; Rigolet, S., 2006: Wood joints by through-dowel rotation welding: microstructure, 13c-nmr and water resistance. Journal of Adhesion Science and Technology, 20 (5) 427-436. https://doi.org/10.1163/156856106777144327

Župčić, I.; Mihulja, G.; Bogner, A.; Grbac, I.; Hrovat, B., 2008: Welding of solid wood. Drvna industrija, 59 (3): 113-119.

Župčić, I., 2010: Factors Influencing the Merging of Lathe Beech Elements by Welding Technique, Doctoral Dissertation, University of Zagreb, Faculty of Forestry, Zagreb, Croatia.

Župčić, I.; Povržení, K.; Balaško, K.; Radmanović, K., 2022: Temperatures in rotary welding of dowels in the beech wood. BioResources, 17(4): 5848-5860. https://doi.org/10.15376/biores.17.4.5848-5860

Župčić, I.; Đukić, I.; Hasan, M., 2024: Influence of depth of friction-welded dowels on the strength of rotary welded joints. BioResources, 19 (2): 3047-3059. https://doi.org/10.15376/biores.19.2.3047-3059

Yin, W.; Zheng, Y.; Lu, H.; Tian, Y., 2021: Tribological and mechanical properties of wood dowel rotation welding with different additives. Journal of Adhesion Science and Technology, 37 (3): 411-425. https://doi.org/10.1080/01694243.2021.2021682.

***HRN ISO 13061-2, 2015: Physical and mechanical properties of wood - Testing methods for smaller solid wood samples - Part 2: Determination of density for conducting physical and mechanical properties tests ISO 13061-2:2014. International Organization for Standardization, Geneva, Switzerland.